



<http://researchspace.auckland.ac.nz>

ResearchSpace@Auckland

Copyright Statement

The digital copy of this thesis is protected by the Copyright Act 1994 (New Zealand).

This thesis may be consulted by you, provided you comply with the provisions of the Act and the following conditions of use:

- Any use you make of these documents or images must be for research or private study purposes only, and you may not make them available to any other person.
- Authors control the copyright of their thesis. You will recognise the author's right to be identified as the author of this thesis, and due acknowledgement will be made to the author where appropriate.
- You will obtain the author's permission before publishing any material from their thesis.

To request permissions please use the Feedback form on our webpage.

<http://researchspace.auckland.ac.nz/feedback>

General copyright and disclaimer

In addition to the above conditions, authors give their consent for the digital copy of their work to be used subject to the conditions specified on the [Library Thesis Consent Form](#) and [Deposit Licence](#).

Note : Masters Theses

The digital copy of a masters thesis is as submitted for examination and contains no corrections. The print copy, usually available in the University Library, may contain corrections made by hand, which have been requested by the supervisor.

Cooperative Diversity for Energy Efficient Wireless Sensor Networks

Ljiljana Simić

A thesis submitted in fulfilment of the requirements for the degree of
Doctor of Philosophy in Electrical and Electronic Engineering,
The University of Auckland, 2010.

Abstract

This thesis investigates the feasibility of deploying cooperative diversity as a practical energy saving technique for extending the operational lifetime of a wireless sensor network. Wireless sensor networks consist of many resource-constrained distributed nodes, powered by small batteries which are typically never replaced. In cooperative communication a partner node overhears and repeats a source node's message to the destination receiver, where the two independently faded signals are combined. The resulting diversity benefit of achieving reliable communication at a much lower transmission energy cost reduces the energy consumption of the sensor nodes.

A novel low-complexity distributed cooperation strategy for energy-constrained wireless sensor networks is presented in this thesis. The proposed cooperation strategy is named ECO-OP in reference to the energy-conserving cooperation it facilitates among autonomous sensor nodes. ECO-OP is based on simple yet robust power allocation and partner choice heuristics which enable individual sensor nodes to independently make energy efficient cooperation decisions. The heuristics are computationally efficient and based solely on measurements of average channel path loss, making them suitable for practical implementation on resource-constrained sensor nodes. Importantly, ECO-OP thereby enables simple sensor nodes to cooperate autonomously to extend the lifetime of the wireless sensor network as a whole. To the best knowledge of the author, ECO-OP is the first distributed cooperation strategy for coordinating cooperative communication in an energy-constrained wireless network.

The behaviour and performance of network-wide cooperation using ECO-OP is analysed in three representative wireless sensor network topologies, with respect to the resulting energy conservation and network lifetime extension. Importantly, it is demonstrated that altruistic cooperation among autonomous resource-constrained sensor nodes using ECO-OP significantly extends the lifetime of the wireless sensor network as a whole. This applies to both sparse and dense networks, with both random and directed data flow. Moreover, it is shown that the low-complexity distributed ECO-OP cooperation strategy proposed in this thesis overall achieves a comparable network lifetime improvement to a computationally intensive centralised cooperation algorithm from the literature.

For my beloved grandfather, Deda Moma.

Acknowledgements

My sincerest gratitude goes to my supervisors, Dr Stevan Berber and Assoc. Prof. Kevin Sowerby, for their guidance and support throughout my PhD journey. Their generosity and wisdom have both guided and inspired me, and for this I am truly thankful.

I would like to thank the Department of Electrical and Computer Engineering for providing me with a stimulating environment and giving me every opportunity to develop my academic skills throughout the seven long yet exciting years I have spent there.

I would like to acknowledge the Tertiary Education Commission for awarding me a Bright Future Top Achiever Doctoral Scholarship.

I would also like to humbly thank all the world's great artists and scientists, who have illuminated humanity's history with their hearts and minds, for inspiring my inner world.

Big huge sparkly thanks go to my wonderful best friend Carl, whose friendship and laughter brighten every one of my days.

Most importantly, I thank from the bottom of my heart my beautiful amazing mother Jelena, for all of her love. I am incredibly blessed to be her daughter.

Contents

1	Introduction	1
1.1	Wireless Sensor Networks: The Energy-Constrained Design Paradigm	1
1.2	The Concept of Energy Efficient Cooperative Diversity	3
1.3	The Motivation and Objectives of this Thesis	6
1.4	The Structure of this Thesis	6
2	Energy Efficiency of Cooperative Diversity in Wireless Sensor Networks	11
2.1	Introduction	11
2.2	Cooperative Diversity Schemes for Wireless Sensor Networks	12
2.2.1	Cooperative Diversity Schemes Overview	12
2.2.2	Virtual-MISO	14
2.2.3	Decode-and-Forward	16
2.2.4	Adaptive Decode-and-Forward	17
2.2.5	Error Rate Expressions	19
2.3	Energy Model	19
2.3.1	Non-Cooperative Communication	22
2.3.2	Virtual-MISO	22
2.3.3	Decode-and-Forward	23
2.3.4	Adaptive Decode-and-Forward	23
2.3.5	Energy Efficiency of Cooperative Communication	24
2.4	Literature Review	26
2.4.1	Energy Efficiency of Cooperative Diversity	26
2.4.2	Power Allocation and Partner Choice for Cooperative Communication	29
2.4.2.1	Power Allocation	29
2.4.2.2	Partner Choice	31
2.4.3	Strategies for Coordinating Network-wide Cooperative Communication	34
2.5	The Contributions of this Thesis	37
2.6	Summary	39

3	Power Allocation for Energy Efficient Cooperation	41
3.1	Introduction	41
3.2	Non-Cooperative Communication	42
3.3	Ideal Cooperative Diversity	43
3.3.1	Problem Formulation	43
3.3.2	Optimum Solution	44
3.3.3	Discussion of the Optimum Solution	45
3.4	Virtual-MISO	46
3.4.1	Problem Formulation	46
3.4.2	Optimum Solution	46
3.4.3	Discussion of the Optimum Solution	48
3.5	Decode-and-Forward	49
3.5.1	Problem Formulation	49
3.5.2	Optimum Solution	49
3.5.3	Discussion of the Optimum Solution	51
3.6	Adaptive Decode-and-Forward	52
3.6.1	Problem Formulation	52
3.6.2	Optimum Solution	52
3.6.3	Discussion of the Optimum Solution	53
3.7	Summary	56
4	Partner Choice Region for Energy Efficient Cooperation	57
4.1	Introduction	57
4.2	Energy Efficiency of the Reference Cooperative System	58
4.2.1	Virtual-MISO	58
4.2.2	Decode-and-Forward	59
4.2.3	Adaptive Decode-and-Forward	60
4.2.4	Energy Efficiency Comparison of Cooperative Diversity Schemes	61
4.3	Effect of Varying the Transceiver Circuit Power	63
4.4	Effect of Varying the Source-Destination Separation	66
4.5	Effect of Varying the Channel Path Loss Exponent	70
4.6	Effect of Varying the Target Bit Error Rate	75
4.7	Most Energy Efficient Cooperative Diversity Scheme for Wireless Sensor Networks	78
4.8	Summary	79
5	Practical Energy Efficiency of Adaptive Decode-and-Forward Cooperation	81
5.1	Introduction	81

5.2	Development of the Power Allocation Heuristic	82
5.3	Energy Conservation Performance of the Power Allocation Heuristic	86
5.3.1	Energy Efficiency of the Reference Cooperative System	87
5.3.2	Effect of Varying the Transceiver Circuit Power	89
5.3.3	Effect of Varying the Source-Destination Separation	89
5.3.4	Effect of Varying the Channel Path Loss Exponent	90
5.3.5	Effect of Varying the Target Bit Error Rate	91
5.4	Discussion of the Practical Significance of the Power Allocation Heuristic	92
5.5	Summary	92
6	Partner Choice Strategies for Practical Energy Efficient Cooperation	95
6.1	Introduction	95
6.2	Best Partner Choice Problem Definition	96
6.3	Development of the Partner Choice Heuristics	97
6.3.1	First Global Knowledge Partner Choice Heuristic: GKH_1	97
6.3.2	Second Global Knowledge Partner Choice Heuristic: GKH_2	98
6.3.3	Local Knowledge Partner Choice Heuristic: LKH	99
6.4	Illustration of Partner Selection using the Partner Choice Heuristics	99
6.4.1	Regular Candidate Partner Node Placement	100
6.4.2	Random Candidate Partner Node Placement	103
6.5	Partner Ranking Performance of the Partner Choice Heuristics	105
6.5.1	Performance of the Partner Choice Heuristics as the Number of Candidate Partner Nodes is Varied	106
6.5.2	Effect of Varying the Transceiver Circuit Power	109
6.5.3	Effect of Varying the Source-Destination Separation	111
6.5.4	Effect of Varying the Channel Path Loss Exponent	113
6.5.5	Effect of Varying the Target Bit Error Rate	114
6.6	Discussion of the Practical Significance of the Partner Choice Heuristics	116
6.7	Summary	117
7	ECO-OP: A Distributed Cooperation Strategy for Energy-Constrained Wireless Sensor Networks	119
7.1	Introduction	119
7.2	The ECO-OP Cooperation Strategy	120
7.3	Overview of Investigations Analysing the Performance of ECO-OP	125
7.3.1	Investigation of Energy Conservation via Network-wide Cooperation	126
7.3.2	Investigation of Network Lifetime Extension via Network-wide Cooperation	127
7.4	Wireless Sensor Network Model and Simulation Parameters	130

7.5	Wireless Sensor Network Energy Consumption Definitions and Metrics . . .	134
7.5.1	Node Energy Consumption in a Non-Cooperative Network	135
7.5.2	Node Energy Consumption in a Cooperative Network	138
7.6	Wireless Sensor Network Lifetime Definitions and Metrics	141
7.6.1	Node Lifetime in a Non-cooperative Network	142
7.6.2	Node Lifetime in a Cooperative Network	144
7.7	Summary	149
8	Illustration of Energy Conservation via Network-wide Cooperation	151
8.1	Introduction	151
8.2	Topology A Network: Central Destination Receiver	152
8.3	Topology B Network: Remote Destination Receiver	159
8.4	Topology C Network: Node-to-Node Communication	166
8.5	Summary	172
9	Energy Conservation Performance of Network-wide Cooperation	175
9.1	Introduction	175
9.2	Topology A Network: Central Destination Receiver	176
9.3	Topology B Network: Remote Destination Receiver	182
9.4	Topology C Network: Node-to-Node Communication	187
9.5	Discussion	192
9.6	Summary	194
10	Illustration of Network Lifetime Extension via Network-wide Cooperation	197
10.1	Introduction	197
10.2	Topology A Network: Central Destination Receiver	200
10.3	Topology B Network: Remote Destination Receiver	208
10.4	Topology C Network: Node-to-Node Communication	215
10.5	Summary	222
11	Network Lifetime Extension Performance of Network-wide Cooperation	225
11.1	Introduction	225
11.2	Topology A Network: Central Destination Receiver	227
11.3	Topology B Network: Remote Destination Receiver	231
11.4	Topology C Network: Node-to-Node Communication	237
11.5	Discussion	240
11.6	Summary	242

12 Conclusions	245
A Description of the Centralised Greedy Cooperation Algorithm from the Literature	257
A.1 Introduction	257
A.2 Algorithm Description	258
A.3 Implementation Notes	261
References	263

List of Tables

2.1	Reference communication system parameters.	21
4.1	Maximum energy saving achieved for the reference system, using the vMISO, DF, and aDF cooperative diversity schemes.	62
5.1	Maximum energy saving achieved for the reference system, using optimal and heuristic power allocation for the aDF cooperative diversity scheme.	88
6.1	Performance of different partner choice rules compared to optimal partner selection, for 100 regularly placed candidate partner nodes.	103
6.2	Performance of different partner choice rules compared to optimal partner selection, for 100 randomly placed candidate partner nodes.	105
8.1	Performance of network-wide cooperation in a Topology A network of 100 regularly placed nodes, using different partner choice rules.	154
8.2	Performance of network-wide cooperation in a Topology B network of 100 regularly placed nodes, using different partner choice rules.	161
8.3	Performance of network-wide cooperation in a Topology C network of 100 regularly placed nodes, using different partner choice rules.	167
9.1	Best partner choice rule for energy-conserving ECO-OP cooperation in sparse and dense wireless sensor networks of various topology.	193
10.1	Cooperative network lifetime improvement in a Topology A network of 100 regularly placed nodes, using different cooperation strategies.	203
10.2	Cooperative network lifetime improvement in a Topology B network of 100 regularly placed nodes, using different cooperation strategies.	211
10.3	Cooperative network lifetime improvement in a Topology C network of 100 regularly placed nodes, using different cooperation strategies.	217
11.1	Best cooperation strategy for extending the lifetime of sparse and dense wireless sensor networks of various topology.	241

List of Figures

1.1	BER vs. average received SNR, for BPSK in an AWGN channel and a Rayleigh fading channel with and without diversity.	4
1.2	Illustration of cooperative diversity.	5
2.1	Classification of major cooperative diversity schemes.	12
2.2	Operation of the vMISO cooperative diversity scheme.	15
2.3	BER for BPSK in Rayleigh fading vs. average SNR at the destination receiver, for non-cooperative and cooperative communication.	16
2.4	Operation of the DF cooperative diversity scheme.	17
2.5	Operation of the aDF cooperative diversity scheme.	18
2.6	Illustration of the energy efficiency of cooperative communication vs. the source-destination separation.	25
2.7	Illustration of the geometry of a cooperative communication link.	25
3.1	Optimally energy efficient transmit power allocation for cooperative diversity with an ideal source-partner channel vs. partner location.	46
3.2	Optimally energy efficient transmit power allocation for vMISO cooperation vs. partner location.	49
3.3	Optimally energy efficient transmit power allocation for DF cooperation vs. partner location.	52
3.4	Optimally energy efficient transmit power allocation for aDF cooperation vs. partner location.	55
3.5	Probability of partner retransmitting the source's message in aDF with optimally energy efficient transmit power allocation vs. partner location.	55
4.1	Total energy savings achieved for a source node cooperating with a range of potential partners using vMISO cooperation with optimally energy efficient transmit power allocation, for the reference system.	59
4.2	Total energy savings achieved for a source node cooperating with a range of potential partners using DF cooperation with optimally energy efficient transmit power allocation, for the reference system.	60

4.3	Total energy savings achieved for a source node cooperating with a range of potential partners using aDF cooperation with optimally energy efficient transmit power allocation, for the reference system.	61
4.4	Size of the partner choice region for a given energy efficiency of vMISO, DF, and aDF cooperation, for the reference system.	62
4.5	Partner choice region boundary for energy efficient vMISO cooperation vs. transceiver circuit power consumption.	64
4.6	Partner choice region boundary for energy efficient DF cooperation vs. transceiver circuit power consumption.	64
4.7	Partner choice region boundary for energy efficient aDF cooperation vs. transceiver circuit power consumption.	65
4.8	Size of the partner choice region for a given energy efficiency of vMISO, DF, and aDF cooperation vs. transceiver circuit power consumption.	66
4.9	Maximum energy saving achieved using vMISO, DF, and aDF cooperation vs. transceiver circuit power consumption.	66
4.10	Partner choice region boundary for energy efficient vMISO cooperation vs. source-destination separation.	67
4.11	Partner choice region boundary for energy efficient DF cooperation vs. source-destination separation.	68
4.12	Partner choice region boundary for energy efficient aDF cooperation vs. source-destination separation.	68
4.13	Size of the partner choice region for a given energy efficiency of vMISO, DF, and aDF cooperation vs. source-destination separation.	70
4.14	Maximum energy saving achieved using vMISO, DF, and aDF cooperation vs. source-destination separation.	70
4.15	Partner choice region boundary for energy efficient vMISO cooperation vs. channel path loss exponent.	72
4.16	Partner choice region boundary for energy efficient DF cooperation vs. channel path loss exponent.	72
4.17	Partner choice region boundary for energy efficient aDF cooperation vs. channel path loss exponent.	73
4.18	Size of the partner choice region for a given energy efficiency of vMISO, DF, and aDF cooperation vs. channel path loss exponent.	74
4.19	Maximum energy saving achieved using vMISO, DF, and aDF cooperation vs. channel path loss exponent.	75
4.20	Partner choice region boundary for energy efficient vMISO cooperation vs. target BER.	76

4.21	Partner choice region boundary for energy efficient DF cooperation vs. target BER.	77
4.22	Partner choice region boundary for energy efficient aDF cooperation vs. target BER.	77
4.23	Size of the partner choice region for a given energy efficiency of vMISO, DF, and aDF cooperation vs. target BER.	78
4.24	Maximum energy saving achieved using vMISO, DF and aDF cooperation vs. target BER.	78
5.1	Optimally energy efficient transmit power allocation for aDF cooperation and the partial aDF power allocation solutions vs. partner location.	84
5.2	Average path loss on the source-partner and partner-destination channels vs. partner location.	85
5.3	Comparison of heuristic and optimal transmit power allocation for energy efficient aDF cooperation vs. partner location.	86
5.4	Heuristic transmit power allocation for energy efficient aDF cooperation vs. partner location.	86
5.5	Total energy savings achieved for a source node cooperating with a range of potential partners using aDF cooperation with heuristic transmit power allocation, for the reference system.	88
5.6	Size of the partner choice region for a given energy efficiency of aDF cooperation using optimal vs. heuristic power allocation, for the reference system.	88
5.7	Size of the partner choice region for a given energy efficiency of aDF cooperation using optimal and heuristic transmit power allocation vs. transceiver circuit power consumption.	89
5.8	Size of the partner choice region for a given energy efficiency of aDF cooperation using optimal and heuristic transmit power allocation vs. source-destination separation.	90
5.9	Size of the partner choice region for a given energy efficiency of aDF cooperation using optimal and heuristic transmit power allocation vs. channel path loss exponent.	91
5.10	Size of the partner choice region for a given energy efficiency of aDF cooperation using optimal and heuristic transmit power allocation vs. target BER.	91
6.1	Ranking of 100 regularly placed candidate partner nodes using different partner choice rules, for the reference system.	101

6.2	Partner node ranking using different partner choice rules vs. the optimal ranking, for 100 regularly placed candidate partner nodes.	102
6.3	Ranking of 100 randomly placed candidate partner nodes using different partner choice rules, for the reference system.	104
6.4	Partner node ranking using different partner choice rules vs. the optimal ranking, for 100 randomly placed candidate partner nodes.	105
6.5	Energy saving achieved using the 1 st ranked partner vs. number of candidate partner nodes, for different partner choice rules.	107
6.6	Variability of the energy saving achieved using the 1 st ranked partner vs. number of candidate partner nodes, for different partner choice rules. . . .	108
6.7	Correlation coefficient with the optimal partner ranking vs. number of candidate partner nodes, for different partner choice rules.	109
6.8	Energy saving achieved using the 1 st ranked partner vs. transceiver circuit power consumption, for different partner choice rules.	110
6.9	Correlation coefficient with the optimal partner ranking vs. transceiver circuit power consumption, for different partner choice rules.	110
6.10	Energy saving achieved using the 1 st ranked partner vs. source-destination separation, for different partner choice rules.	112
6.11	Correlation coefficient with the optimal partner ranking vs. source-destination separation, for different partner choice rules.	112
6.12	Energy saving achieved using the 1 st ranked partner vs. channel path loss exponent, for different partner choice rules.	114
6.13	Correlation coefficient with the optimal partner ranking vs. channel path loss exponent, for different partner choice rules.	114
6.14	Energy saving achieved using the 1 st ranked partner vs. target BER, for different partner choice rules.	115
6.15	Correlation coefficient with the optimal partner ranking vs. target BER, for different partner choice rules.	116
7.1	Flowchart describing the partner choice and power allocation method employed by a source node using the distributed ECO-OP cooperation strategy.	122
7.2	Flowchart describing the overall distributed ECO-OP cooperation strategy employed by a node in the cooperative network throughout its lifetime. . .	123
7.3	Illustration of the Topology A wireless sensor network configuration, with a central destination receiver.	131
7.4	Illustration of the Topology B wireless sensor network configuration, with a remote destination receiver.	131
7.5	Illustration of the Topology C wireless sensor network configuration, with node-to-node communication.	132

7.6	Illustration of node energy consumption in a non-cooperative network. . . .	137
7.7	Illustration of node energy consumption in a cooperative network.	140
7.8	Example of a non-cooperative Topology C network event timeline, illustrating throughout the lifetime of a node its energy consumption in acting as a destination receiver.	143
7.9	Example of a cooperative network event timeline, illustrating throughout the lifetime of a node its energy consumption in acting as a source.	145
7.10	Example of a cooperative network event timeline, illustrating throughout the lifetime of a node its energy consumption in acting as a partner.	147
7.11	Example of a cooperative Topology C network event timeline, illustrating throughout the lifetime of a node its energy consumption in acting as a destination receiver.	148
8.1	Total cooperative energy saving achieved by each source node in a Topology A network of 100 regularly placed nodes, using different partner choice rules.	153
8.2	Distribution of cooperation partner service in a Topology A network of 100 regularly placed nodes, using different partner choice rules.	155
8.3	Node energy consumption in a Topology A network of 100 regularly placed nodes, for non-cooperative communication and cooperative communication with different partner choice rules.	157
8.4	Boxplot showing the distribution of node energy consumption in a Topology A network of 100 regularly placed nodes, for non-cooperative communication and cooperative communication with different partner choice rules. . . .	158
8.5	Total cooperative energy saving achieved by each source node in a Topology B network of 100 regularly placed nodes, using different partner choice rules.	160
8.6	Distribution of cooperation partner service in a Topology B network of 100 regularly placed nodes, using different partner choice rules.	162
8.7	Node energy consumption in a Topology B network of 100 regularly placed nodes, for non-cooperative communication and cooperative communication with different partner choice rules.	163
8.8	Boxplot showing the distribution of node energy consumption in a Topology B network of 100 regularly placed nodes, for non-cooperative communication and cooperative communication with different partner choice rules. . . .	164
8.9	Total cooperative energy saving achieved by each source node in a Topology C network of 100 regularly placed nodes, using different partner choice rules.	166
8.10	Distribution of cooperation partner service in a Topology C network of 100 regularly placed nodes, using different partner choice rules.	168

8.11	Node energy consumption in a Topology C network of 100 regularly placed nodes, for non-cooperative communication and cooperative communication with different partner choice rules.	169
8.12	Boxplot showing the distribution of node energy consumption in a Topology C network of 100 regularly placed nodes, for non-cooperative communication and cooperative communication with different partner choice rules. . .	170
9.1	Average total cooperative energy saving achieved by a source node in a Topology A network vs. number of nodes in the network, using different partner choice rules.	177
9.2	Reduction in total network energy consumption achieved by cooperation in a Topology A network vs. number of nodes in the network, using different partner choice rules.	178
9.3	Distribution of node energy consumption over a Topology A network vs. number of nodes in the network, for non-cooperative communication and cooperative communication with GKH_1 and GKH_2	179
9.4	Distribution of node energy consumption over a Topology A network vs. number of nodes in the network, for non-cooperative communication and cooperative communication with LKH	180
9.5	Distribution of node energy consumption over a Topology A network vs. number of nodes in the network, for non-cooperative communication and cooperative communication with random partner choice.	180
9.6	Average total cooperative energy saving achieved by a source node in a Topology B network vs. number of nodes in the network, using different partner choice rules.	183
9.7	Reduction in total network energy consumption achieved by cooperation in a Topology B network vs. number of nodes in the network, using different partner choice rules.	184
9.8	Distribution of node energy consumption over a Topology B network vs. number of nodes in the network, for non-cooperative communication and cooperative communication with GKH_1 and GKH_2	185
9.9	Distribution of node energy consumption over a Topology B network vs. number of nodes in the network, for non-cooperative communication and cooperative communication with LKH	185
9.10	Distribution of node energy consumption over a Topology B network vs. number of nodes in the network, for non-cooperative communication and cooperative communication with random partner choice.	186

9.11	Average total cooperative energy saving achieved by a source node in a Topology C network vs. number of nodes in the network, using different partner choice rules.	188
9.12	Reduction in total network energy consumption achieved by cooperation in a Topology C network vs. number of nodes in the network, using different partner choice rules.	189
9.13	Distribution of node energy consumption over a Topology C network vs. number of nodes in the network, for non-cooperative communication and cooperative communication with GKH_1 and GKH_2	189
9.14	Distribution of node energy consumption over a Topology C network vs. number of nodes in the network, for non-cooperative communication and cooperative communication with LKH	190
9.15	Distribution of node energy consumption over a Topology C network vs. number of nodes in the network, for non-cooperative communication and cooperative communication with random partner choice.	190
10.1	Node lifetime in a Topology A network of 100 regularly placed nodes, using non-cooperative communication and cooperative communication with different cooperation strategies.	201
10.2	Node lifetime vs. number of node deaths since network activation for a Topology A network of 100 regularly placed nodes, using non-cooperative communication and cooperative communication with different cooperation strategies.	202
10.3	x^{th} node lifetime improvement factor vs. x for a Topology A network of 100 regularly placed nodes, using non-cooperative communication and cooperative communication with different cooperation strategies.	202
10.4	Average distribution of cooperation partner service throughout the lifetime of a Topology A network of 100 regularly placed nodes, using different cooperation strategies.	205
10.5	Distribution of cooperation partner selection in a Topology A network of 100 regularly placed nodes, using different cooperation strategies.	207
10.6	Node lifetime in a Topology B network of 100 regularly placed nodes, using non-cooperative communication and cooperative communication with different cooperation strategies.	209
10.7	Node lifetime vs. number of node deaths since network activation for a Topology B network of 100 regularly placed nodes, using non-cooperative communication and cooperative communication with different cooperation strategies.	210

10.8	x^{th} node lifetime improvement factor vs. x for a Topology B network of 100 regularly placed nodes, using non-cooperative communication and cooperative communication with different cooperation strategies.	210
10.9	Average distribution of cooperation partner service throughout the lifetime of a Topology B network of 100 regularly placed nodes, using different cooperation strategies.	212
10.10	Distribution of cooperation partner selection in a Topology B network of 100 regularly placed nodes, using different cooperation strategies.	213
10.11	Node lifetime in a Topology C network of 100 regularly placed nodes, using non-cooperative communication and cooperative communication with different cooperation strategies.	216
10.12	Node lifetime vs. number of node deaths since network activation for a Topology C network of 100 regularly placed nodes, using non-cooperative communication and cooperative communication with different cooperation strategies.	217
10.13	x^{th} node lifetime improvement factor vs. x for a Topology C network of 100 regularly placed nodes, using non-cooperative communication and cooperative communication with different cooperation strategies.	217
10.14	Average distribution of cooperation partner service throughout the lifetime of a Topology C network of 100 regularly placed nodes, using different cooperation strategies.	219
10.15	Distribution of cooperation partner selection in a Topology C network of 100 regularly placed nodes, using different cooperation strategies.	221
11.1	Node lifetime vs. number of node deaths since network activation for a Topology A network, using non-cooperative communication and cooperative communication with different cooperation strategies.	228
11.2	Average network lifetime improvement factor vs. number of nodes in the network, for a Topology A network using different cooperation strategies. .	230
11.3	Node lifetime vs. number of node deaths since network activation for a Topology B network, using non-cooperative communication and cooperative communication with different cooperation strategies.	232
11.4	Average network lifetime improvement factor vs. number of nodes in the network, for a Topology B network using different cooperation strategies. .	235
11.5	Node lifetime vs. number of node deaths since network activation for a Topology C network, using non-cooperative communication and cooperative communication with different cooperation strategies.	238
11.6	Average network lifetime improvement factor vs. number of nodes in the network, for a Topology C network using different cooperation strategies. .	239

A.1 Flowchart describing the centralised greedy cooperation algorithm proposed in [18].	260
---	-----

Glossary

Abbreviations

aDF	adaptive decode-and-forward
AF	amplify-and-forward
AWGN	additive white Gaussian noise
BER	bit error rate
BLER	block error rate
BPSK	binary phase shift keying
CRC	cyclic redundancy check
CSI	channel state information
DF	decode-and-forward
DSTC	distributed space-time coding
LAN	local area network
LEACH	low-energy adaptive clustering hierarchy
MISO	multiple-input-single-output
MRC	maximum ratio combining
RF	radio frequency
SER	symbol error rate
SNR	signal to noise ratio
TDMA	time division multiple access
vMISO	virtual-MISO

Symbols

B	message block size (in bits)
BER_{coop_aDF}	BER of aDF cooperative diversity system
BER_{coop_DF}	BER of DF cooperative diversity system
BER_{coop_vMISO}	BER of vMISO cooperative diversity system
BER_{full_coop}	BER of full second-order diversity system
BER_{non_coop}	BER of non-cooperative communication
BER_{s-p}	BER on source-partner channel (in vMISO and DF)
$BLER_{s-p}$	BLER on source-partner channel (in aDF)
d	transmission distance
d_{p-d}	partner-destination separation
d_{s-d}	source-destination separation
d_{s-p}	source-partner separation
E_b	required energy per bit at the receiver for target BER
$E_{battery}$	initial battery energy of a sensor node
E_{coop_aDF}	total energy consumption per bit of aDF cooperative communication link
E_{coop_DF}	total energy consumption per bit of DF cooperative communication link
$E_{coop_NETWORK}$	total energy per bit consumed by a cooperative network of M nodes
E_{coop_node}	total energy per bit consumed by an individual node in a cooperative network
$\bar{E}_{coop_node(x)}$	average total energy per bit (averaged over the x^{th} node's lifetime) consumed by the x^{th} node in a cooperative network
E_{coop_vMISO}	total energy consumption per bit of vMISO cooperative communication link

$E_{non-coop}$	total energy consumption per bit of non-cooperative communication link
$E_{non-coop-NETWORK}$	total energy per bit consumed by a non-cooperative network of M nodes
$E_{non-coop-node}$	total energy per bit consumed by an individual node in a non-cooperative network
$\bar{E}_{non-coop-node(x)}$	average total energy per bit (averaged over the x^{th} node's lifetime) consumed by the x^{th} node in a non-cooperative network
$E_{saving-coop-total}$	total energy saving achieved by cooperative communication (energy efficiency of individual cooperative link)
E_{tx-p}	transmit energy per bit of the cooperating partner
$E_{tx-p-heuristic-aDF}$	heuristic power allocation for the aDF partner-destination transmission
$E_{tx-p-opt-aDF}$	optimally energy efficient power allocation for the aDF partner-destination transmission
$E_{tx-p-opt-DF}$	optimally energy efficient power allocation for the DF partner-destination transmission
$E_{tx-p-opt-vMISO}$	optimally energy efficient power allocation for the vMISO partner-destination transmission
E_{tx-s}	transmit energy per bit of the cooperating source
$E_{tx-s-heuristic-aDF}$	heuristic power allocation for the aDF source-destination transmission
$E_{tx-s-non-coop}$	transmit energy per bit of the non-cooperating source
$E_{tx-s-opt-aDF}$	optimally energy efficient power allocation for the aDF source-destination transmission
$E_{tx-s-opt-DF}$	optimally energy efficient power allocation for the DF source-destination transmission
$E_{tx-s-opt-non-coop}$	optimally energy efficient power allocation for the non-cooperative source-destination transmission

$E_{tx_s_opt_vMISO}$	optimally energy efficient power allocation for the vMISO source-destination transmission
E_{tx_s-p}	transmit energy per bit of the source-partner communication in vMISO
$E_{tx_s-p_opt_vMISO}$	optimally energy efficient power allocation for the vMISO source-partner transmission
$E_{tx_TOTAL_coop_aDF}$	total transmit energy consumption per bit of aDF cooperative communication link
$E_{tx_TOTAL_coop_DF}$	total transmit energy consumption per bit of DF cooperative communication link
$E_{tx_TOTAL_coop_ideal}$	total transmit energy consumption per bit of cooperative communication link with an ideal source-partner channel
$E_{tx_TOTAL_coop_vMISO}$	total transmit energy consumption per bit of vMISO cooperative communication link
$E_{tx_TOTAL_heuristic_aDF}$	total transmit energy consumption per bit of aDF cooperative communication link using heuristic power allocation
GKH_1	first global knowledge partner choice heuristic (presented in this thesis)
GKH_2	second global knowledge partner choice heuristic (presented in this thesis)
k	channel path loss exponent
L	channel path loss
LKH	local knowledge partner choice heuristic (presented in this thesis)
L_{p-d}	path loss on partner-destination channel
L_{ref}	reference path loss at 1 m
L_{s-d}	path loss on source-destination channel
L_{s-p}	path loss on source-partner channel
M	number of nodes in the wireless sensor network

N	number of candidate partner nodes
N_0	Gaussian noise power spectral density
p_b	target end-to-end BER
P_{CCT-rx}	receiver circuit power consumption
P_{CCT-tx}	transmitter circuit power consumption (excluding power amplifiers)
P_{PA}	power consumption of RF power amplifiers
$P_{PA-partner-coop}$	transmission power of the cooperating partner
$P_{PA-source-coop}$	transmission power of the cooperating source
$P_{PA-source-non-coop}$	transmission power of the non-cooperating source
P_{PA-s-p}	transmission power of the source-partner communication in vMISO
p_{s-p}	target source-partner BER (in vMISO and DF)
Q	number simulation runs used to obtain a simulation result for randomly deployed networks
R_b	bit rate
SNR_{p-d}	average SNR on partner-destination channel
SNR_{s-d}	average SNR on source-destination channel
SNR_{s-p}	average SNR on source-partner channel
$T_{coop-node(x)}$	x^{th} node lifetime in a cooperative network
$T_{non-coop-node(x)}$	x^{th} node lifetime in a non-cooperative network
x	order in which sensor nodes die in a wireless sensor network of M nodes (number of node deaths since network activation)
η	drain efficiency of RF power amplifier
ξ	peak-to-average ratio of modulation scheme

Chapter 1

Introduction

1.1 Wireless Sensor Networks: The Energy-Constrained Design Paradigm

Wireless sensor networks are a key emerging technology of the 21st century. These networks consist of many small wireless sensor nodes which are densely deployed either inside or very close to the phenomenon to be observed. Each sensor node has integrated sensing, computation, and communication capability. Importantly, wireless communication enables collaboration among the individual nodes to achieve distributed sensing of the physical, biological, or environmental phenomenon of interest [1].

Wireless sensor networks have a multitude of diverse applications including environmental control, habitat monitoring, disaster relief, precision agriculture, intelligent buildings, logistics, and machine monitoring [1, 2]. For example, nodes with humidity and soil composition sensors can be deployed over a cultivated field to enable precise irrigation and fertilising in agriculture; nodes with chemical sensors can provide efficient distributed sampling of pollutant levels to monitor and improve air or water quality; and nodes with vibration and pressure sensors can be attached to hard-to-reach areas of industrial machinery to provide continuous machine surveillance and enable preventative maintenance [2]. These examples illustrate the widespread potential of wireless sensor networks to provide substantial economic benefit while contributing to sustainable solutions of the environmental and technological challenges of the 21st century.

The major advantage of wireless sensor networks compared with traditional wired sensing technology is the ability to unobtrusively deploy simpler but numerous sensors very close to the field or object to be observed and then leave them to operate unattended for a long time, often in remote or inaccessible regions [2]. However, the goal of achieving robust yet cost-effective distributed sensing over a long period of time gives rise to a multitude

of stringent design constraints for wireless sensor networks. The typical constraints and characteristics of wireless sensor nodes include [1–4]:

- **small size** - nodes must be relatively small to enable unobtrusive and convenient deployment;
- **low cost** - each node should have very low production cost to ensure the economic viability of deploying a large number of sensor nodes;
- **energy-constrained** - nodes are powered by a limited power source in the form of small non-replenishable batteries;
- **low-complexity hardware** - nodes must be inherently simple, due to size, cost, and energy constraints;
- **resource-constrained** - individual nodes are limited in computational capacity and memory, due to size, cost, and complexity constraints;
- **self-organising** - nodes must operate autonomously, since a wireless sensor network is composed of a large number of nodes without a central controlling agent.

Importantly, this represents a shift in the communication system design paradigm of wireless sensor networks compared with that of traditional infrastructure-based wireless communication systems such as cellular networks. The primary goal of a cellular network is achieving bandwidth efficiency¹ and the provision of a high quality of service (QoS) to the mobile users by a central base station which has an unlimited power supply and high computational capacity [1]. By contrast, sensor nodes must self-organise (due to the absence of a central controlling agent) but are individually constrained in terms of complexity and computational capacity. This necessitates the development of **scalable**, **distributed**, and **computationally efficient** communication algorithms suitable for practical implementation on sensor nodes.

Moreover, sensor nodes are highly energy-constrained and the operational lifetime² of a wireless sensor network is directly related to node battery lifetime. Therefore, reducing node energy consumption is of utmost importance in wireless sensor network design.

¹This is not to say that efficient spectrum utilisation is irrelevant for wireless sensor networks; rather, achieving high bandwidth efficiency is not a primary design constraint because wireless sensor networks typically have low data rates [2]. Namely, since nodes only periodically report measured sensor data (as in the application examples given above), wireless sensor networks typically have modest bandwidth requirements.

²In general, the operational or useful lifetime of a wireless sensor network is the time from network activation until the network is no longer considered to be functional [5]. However, what constitutes a functional network varies from application to application and has been defined in various ways in the literature. The precise definition used in this thesis is given in Chapter 7.

However, achieving reliable communication in the wireless environment is highly energy-intensive due to signal attenuation (path loss) and variability (fading). The communication energy cost thus typically dominates the total energy consumption of a wireless sensor node (which additionally consists of the sensing and data processing energy expenditure) [2]. Consequently, energy efficient wireless communication is one of the most central concerns in wireless sensor network design.

The purpose of this thesis is to investigate a communication technique called *cooperative diversity* for improving the energy efficiency of communication in a wireless sensor network, thereby conserving nodes' battery energy and prolonging the network's useful lifetime.

1.2 The Concept of Energy Efficient Cooperative Diversity

Wireless communication is typically severely impaired by the phenomenon of signal fading, which is due to multipath propagation of radio signals [6]. The long term average received signal strength decreases logarithmically with transmission distance due to attenuation or path loss. However, the multipath fading nature of the wireless channel additionally results in large variations in the instantaneous power of the received signal over a relatively short time. Consequently, the signal to noise ratio (SNR) at the receiver randomly fluctuates and can dramatically decrease as a result of a sudden decline in received signal power; this is referred to as a *deep fade* [7]. If the received signal SNR is too low, the receiver cannot reliably decode the message sent by the transmitter. Thus fading greatly increases the average SNR required to achieve a given target reliability of communication, as quantified by the average probability of bit error (or bit error rate, BER) at the receiver. This is illustrated in Fig. 1.1, which shows that the BER performance of a digital communication system in a wireless Rayleigh³ fading channel (top curve) is significantly worse than in the additive white Gaussian noise (AWGN) channel without fading (bottom curve).

The performance of communication in a wireless fading channel can be greatly improved by employing *diversity* techniques. Diversity involves providing multiple copies of the transmitted signal at the receiver. If these multiple signals undergo independent

³The Rayleigh fading channel model is a well-known statistical model of the (frequency non-selective) multipath wireless channel. The relationship between the baseband received signal r and the transmitted signal s is given by $r = \alpha s + n$, where the channel gain α is a zero-mean complex Gaussian random variable and n represents the additive white Gaussian noise (AWGN) at the receiver. The magnitude of the channel gain, $|\alpha|$, is a Rayleigh random variable. The envelope of the received signal thus follows a Rayleigh distribution. The theoretical background of this model of the wireless propagation environment is readily available in standard wireless communication textbooks, e.g. [6, 8, 9].

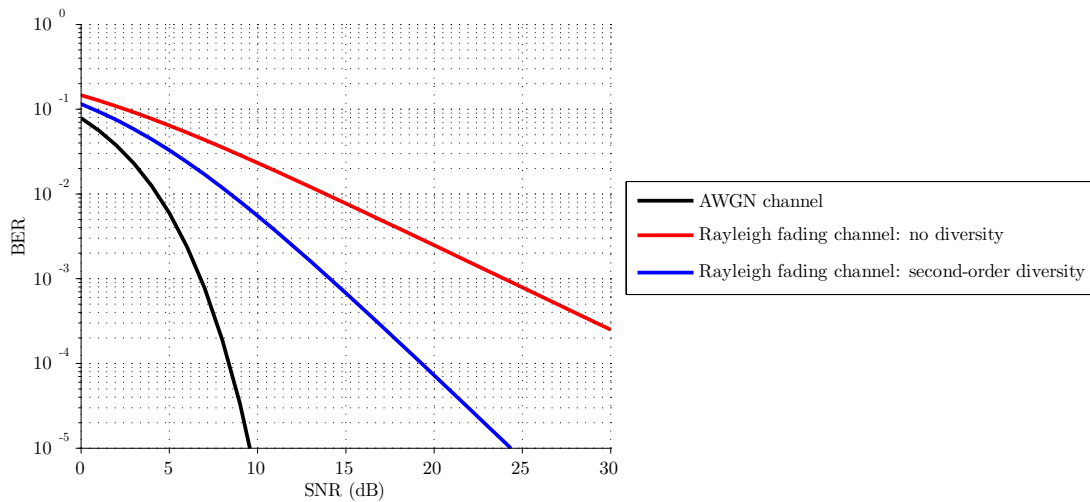


Figure 1.1: BER performance vs. average received SNR, for a digital communication system employing BPSK (binary phase shift keying) modulation operating in an AWGN channel and a Rayleigh fading channel with and without diversity.

fading, it is much less likely that all copies will be in a deep fade simultaneously. This means that the receiver can decode the transmitted signal from the received signals much more reliably by combining the received signal replicas. The number of signal replicas provided to the receiver is known as the *diversity order* [10]. The BER performance of a second order diversity communication system is shown in Fig. 1.1 (middle curve), clearly demonstrating that diversity greatly improves the performance of communication in a wireless fading channel. This performance improvement is typically quantified by the *diversity gain*, which is given by the slope of the BER vs. SNR curve at high SNRs (on a logarithmic scale) [7]. As demonstrated by Fig. 1.1, at high SNRs the BER of a communication system operating in a Rayleigh fading channel with no diversity is inversely proportional to the SNR at the receiver, whereas with second order diversity the BER is inversely proportional to the square of the SNR. This means that a diversity gain of two is achieved when two copies of the transmitted signal are combined at the receiver⁴.

Therefore, diversity greatly reduces the average SNR required to achieve a target BER at the receiver, which translates into a proportionately lower transmission energy cost. The diversity benefit of achieving reliable communication at a much lower transmission energy cost is very desirable in energy-constrained wireless sensor networks. Spatial diversity is a well-known diversity technique which uses multiple transmit or receive antennas to provide the replicas of the transmitted signal at the receiver. If there is sufficient physical separation between the antennas (at least half the wavelength), signals corre-

⁴In general, the maximum possible diversity gain is equal to the diversity order, i.e. the maximum diversity gain of M is achieved when M independently faded copies of the signal are combined at the receiver. The maximum diversity gain is achieved if the received signal copies are combined using optimal maximum ratio combining (MRC) using coherent detection, where the receiver has knowledge of the channel gains of each diversity branch [7].

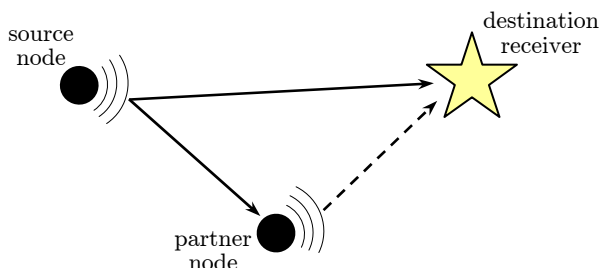


Figure 1.2: Illustration of cooperative diversity. The signals transmitted by the cooperating source and partner nodes undergo independent fading in the wireless channel, resulting in diversity gains when these two independent copies of the source’s original message are combined at the destination receiver.

sponding to each antenna experience independent uncorrelated fading [7]. However, the small size and low complexity requirements of individual sensor nodes preclude the direct implementation of multiple antenna arrays.

Recent work on cooperative transmit diversity techniques [11–15] has shown that spatial diversity gains are possible without the need for a physical antenna array at the transmitter. Instead, spatial diversity is achieved via cooperative antenna sharing among individual transmitters. Several single-antenna transmitters cooperate to send multiple copies of the message to the receiver over independently faded paths, thus forming a virtual distributed antenna array which results in cooperative diversity gains. The basic concept of cooperative diversity is illustrated in Fig. 1.2. In cooperative communication, a partner node overhears and repeats the source node’s transmission to the destination receiver. The destination receiver then combines these two independent signal copies to decode the source’s original message. Owing to the resulting diversity gain, the combined transmission energy of the cooperating source and partner nodes is substantially lower than the transmission energy of a non-cooperating source node communicating directly with the destination receiver (i.e. for the same reliability of communication). Therefore, cooperative diversity can be applied to wireless sensor networks to reduce the energy consumption of sensor nodes.

Cooperative communication is an intuitively pleasing concept for wireless sensor networks, where individual nodes inherently work towards a common goal. Furthermore, although individual sensor nodes are simple and have limited capability, they are numerous; cooperation recognizes this “strength in numbers” as an important asset which can be exploited to the network’s advantage. Therefore, using a partner node’s battery energy to improve the energy efficiency of wireless communication for another node is an apt way of better utilising the combined resources of the network.

1.3 The Motivation and Objectives of this Thesis

The concept of using cooperative diversity as a technique for improving the energy efficiency of wireless communication has previously been validated in the literature [16, 17]. However, in order to actually exploit this energy saving potential of cooperative communication in energy-constrained wireless networks, it is crucial to determine: when cooperation is beneficial and when it is not; how to select the best cooperation partner out of a set of candidate nodes; and how to best allocate transmit power to the cooperating source and partner nodes. Importantly, for a practical deployment of energy efficient cooperative communication to be feasible in a wireless sensor network, resource-constrained sensor nodes must make these cooperation decisions autonomously. Therefore, a distributed low-complexity strategy for coordinating cooperative communication among the sensor nodes is essential.

The overall goal of this thesis is to examine the feasibility of deploying cooperative diversity as a practical energy saving technique for extending the useful lifetime of a wireless sensor network. To this end, the major objectives of this thesis are to:

1. Determine the most suitable cooperative diversity scheme for practical deployment in an energy-constrained wireless sensor network;
2. Investigate the problems of transmit power allocation and partner choice for optimally energy efficient cooperative communication subject to maintaining a target communication reliability;
3. Develop a robust and effective cooperation strategy for extending the lifetime of a distributed wireless sensor network by facilitating energy efficient cooperation among its resource-constrained sensor nodes;
4. Analyse the performance and impact of network-wide cooperation among altruistic independently-acting sensor nodes, with respect to improving the energy efficiency and extending the lifetime of the wireless sensor network as a whole.

1.4 The Structure of this Thesis

This thesis is structured as follows. Chapter 2 presents the background material underlying the work presented in the remainder of the thesis. The original research presented in Chapters 3-11 of this thesis is organised into two major parts. The first, in Chapters 3-6, is concerned with the energy efficiency of an *individual* cooperative communication link, consisting of one source node communicating its message to the destination receiver by cooperating with a partner node. The second, in Chapters 8-11, is concerned with

network-wide cooperative communication among many distributed autonomous sensor nodes, where multiple cooperative links co-exist in the wireless sensor network and individual sensor nodes may take on the role of both source and partner node. Chapter 7 is the link between these two major parts of the thesis; the power allocation and partner choice heuristics developed in Chapters 5 and 6 for maximising the energy efficiency of an individual cooperative link serve as the basis for a novel network-wide cooperation strategy for energy-constrained wireless sensor networks, which is presented in Chapter 7 and subsequently thoroughly analysed in Chapters 8-11. Chapter 12 concludes the thesis. A detailed overview of the individual chapters of this thesis is presented below.

Chapter 2 presents background material which provides the foundation for the original research presented in Chapters 3-11 of this thesis. Following a brief overview of the major cooperative diversity schemes proposed in the literature, the three schemes considered in this thesis are introduced and their BER performance is specified. The energy model of wireless communication adopted throughout this thesis is also presented, and the energy efficiency of cooperative communication is defined and illustrated. The literature relevant to this thesis is then reviewed, thereby placing the original research presented in this thesis in the context of previous research. The original contributions of this thesis are highlighted at the end of Chapter 2.

Chapter 3 investigates the problem of optimally energy efficient transmit power allocation for the three major cooperative diversity schemes of interest to this thesis. The transmit power allocation which minimises the total energy consumption of the cooperative communication link, subject to a bit error rate constraint, is determined for each scheme. The nature of each optimum power allocation solution is analysed by illustrating it in terms of network geometry for a fixed source node and destination receiver and a range of potential partner locations.

Chapter 4 investigates the total communication energy savings achieved by each of the three cooperative diversity schemes considered in this thesis using the optimal transmit power allocation developed in Chapter 3. The energy savings achieved by cooperation are illustrated in terms of network geometry for a source node cooperating with a range of potential partners. By examining the resulting partner choice region, the problem of best partner choice for energy efficient cooperation is studied and basic proximity-based partner choice rules are proposed for each scheme. Moreover, the partner choice region is used as a tool for predicting each scheme's robustness as a practical energy saving technique in a randomly deployed wireless sensor network with a wide range of potential partner locations. The energy efficiency of the three candidate cooperative diversity schemes is thoroughly compared by examining each scheme's partner choice region as several key system parameters are varied. This analysis is used to determine the best scheme to practically deploy in an energy-constrained wireless sensor network.

Chapter 5 presents the development of a simple yet near-optimal power allocation heuristic for energy efficient cooperation, suitable for practical implementation on a resource-constrained sensor node. The development of the proposed heuristic is informed by the insight gained from examining the nature of the optimal transmit power allocation solution and the corresponding energy efficient partner choice region in Chapters 3 and 4 respectively.

Chapter 6 presents the development of several simple yet robust partner choice heuristics for energy efficient cooperation. The power allocation heuristic developed in Chapter 5 serves as the foundation for developing these partner choice heuristics. The proposed partner choice strategies are computationally efficient and based solely on measurements of average channel path loss, enabling resource-constrained sensor nodes to independently make energy efficient cooperation decisions.

Chapter 7 presents ECO-OP, a novel low-complexity distributed cooperation strategy for extending the lifetime of an energy-constrained wireless sensor network. ECO-OP enables simple sensor nodes to cooperate autonomously, being based on the power allocation and partner choice heuristics developed in Chapters 5 and 6. Chapter 7 also presents an overview of the investigations in Chapters 8-11 which thoroughly analyse the behaviour and performance of the proposed ECO-OP cooperation strategy. The node energy consumption and network lifetime definitions, wireless sensor network model, and simulation parameters employed in generating and analysing the simulation results of network-wide cooperative communication in Chapters 8-11 are also presented.

Chapters 8 and 9 investigate the energy conservation performance of network-wide cooperation using ECO-OP, in order to evaluate the effectiveness of ECO-OP as an energy saving technique for wireless sensor networks. To this end, the analysis in Chapters 8 and 9 examines the resulting distribution of cooperation partner service and individual node energy consumption over the network, as well as the reduction in the total network energy expenditure achieved by cooperation. In Chapter 8 the fundamental behaviour of ECO-OP is illustrated in three representative wireless sensor network topologies. In Chapter 9 the typical energy conservation performance of ECO-OP is analysed for each network topology, by considering randomly deployed networks of various node density.

Chapters 10 and 11 investigate the long-term benefit of network-wide cooperation using ECO-OP, in order to evaluate the validity of ECO-OP as an effective technique for extending the lifetime of a wireless sensor network. To this end, the analysis in Chapters 10 and 11 examines the average distribution of cooperation partner service and selection throughout the lifetime of the network, the resulting distribution of individual node lifetimes across the network, and the cooperative network lifetime improvement achieved. In Chapter 10 the fundamental long-term behaviour of ECO-OP is illustrated throughout the lifetime of the wireless sensor network, for three representative wireless sensor

network topologies. In Chapter 11 the typical network lifetime extension performance of ECO-OP is analysed for each network topology, by considering randomly deployed networks of various node density. Additionally, throughout Chapters 10 and 11 the behaviour and performance of the distributed ECO-OP cooperation strategy proposed in this thesis is compared against that of a centralised cooperation algorithm from the literature [18]. **Appendix A** contains details of this algorithm and its implementation in generating the simulation results presented in this thesis.

Chapter 12 concludes this thesis by summarising the research presented in the previous chapters, highlighting key analysis results, and suggesting future research directions.

Chapter 2

Energy Efficiency of Cooperative Diversity in Wireless Sensor Networks

2.1 Introduction

In Chapter 1 cooperative diversity was identified as a promising technique for improving the energy efficiency of wireless communication in an energy-constrained wireless sensor network. The overall goal of this thesis is to examine the feasibility of deploying cooperative diversity as a practical energy saving technique for extending the useful lifetime of a wireless sensor network. This chapter presents the background material underlying the investigation of energy efficient cooperative communication presented in the remainder of this thesis. Moreover, a review of the existing literature relevant to the aims of this thesis is presented in this chapter. Having thereby placed this thesis in the context of previous work, this chapter concludes by highlighting the original contributions of this thesis.

Firstly, an overview of the major cooperative diversity schemes proposed in the literature is presented in Section 2.2. The selection of three major cooperative diversity schemes for analysis in the remainder of this thesis is discussed. These three schemes are chosen as feasible candidates for practical deployment in wireless sensor networks, and their operation and BER performance are specified in Section 2.2. Secondly, the energy model of wireless communication employed throughout this thesis is presented in Section 2.3, where the energy efficiency of cooperative communication is also defined and illustrated. Finally, a literature review is presented in Section 2.4 and the original contributions of this thesis are summarised in Section 2.5.

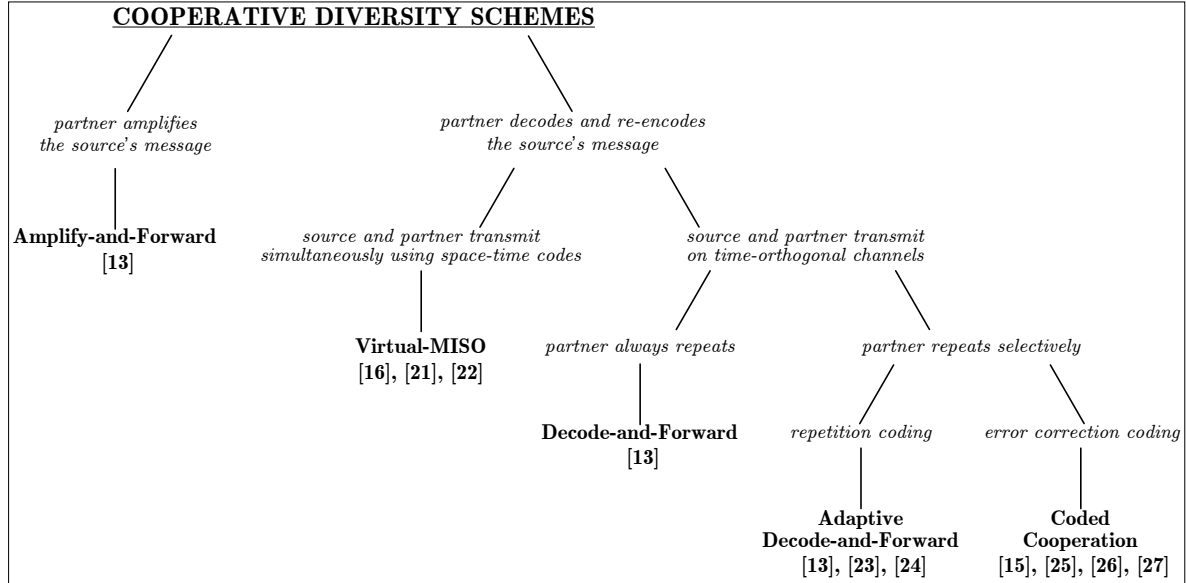


Figure 2.1: Classification of major cooperative diversity schemes from the literature based on salient characteristics.

2.2 Cooperative Diversity Schemes for Wireless Sensor Networks

2.2.1 Cooperative Diversity Schemes Overview

The major cooperative diversity schemes proposed in the literature may be classified into two broad categories according to the forwarding strategy of the partner node, as shown in Fig. 2.1. The first category comprises *amplify-and-forward* schemes, where the partner acts as an analog repeater and forwards an amplified version of the noisy message signal received from the source. The second category comprises *regenerate-and-forward* schemes, where the partner decodes and re-encodes the source's message before forwarding it to the destination receiver. Since the focus of this thesis is the investigation of cooperative diversity as a practical energy saving technique for wireless sensor networks, only schemes which would be straightforward to integrate into a conventional communication system are of interest. This excludes the amplify-and-forward (AF) [13] scheme, which would in practice require nontrivial modification of the wireless sensor node transceivers [14, 19, 20]. By contrast, the regenerate-and-forward partner forwarding strategy is straightforward to practically implement. Therefore, only the second category of schemes in Fig. 2.1 is of interest to this thesis.

Cooperative diversity schemes in the regenerate-and-forward category may be further classified based on how the source and partner nodes cooperatively transmit to the destination receiver. The source and partner nodes may form a virtual antenna array and simultaneously transmit to the destination using space-time diversity codes. These

schemes are referred to as distributed space-time coding (DSTC) [21] or virtual-MISO (multiple-input-single-output¹) [16, 22] in the literature. Alternatively, the source and partner nodes may transmit on time-orthogonal channels, similar to conventional relaying. The decode-and-forward [13] cooperative diversity scheme is the simplest example of this, where the partner node simply overhears and repeats the source's transmission to the destination. The partner node always forwards the source's message in decode-and-forward, potentially leading to error propagation which degrades the scheme's BER performance. Adaptive decode-and-forward [13, 23, 24] schemes have been proposed to mitigate the effects of error propagation. In adaptive decode-and-forward, the source's message is forwarded only if the partner had decoded it correctly. The partner typically makes its forwarding decision based on a CRC (cyclic redundancy check) or an SNR threshold applied to the message received from the source.

Whereas decode-and-forward and adaptive decode-and-forward employ repetition coding at the partner node, cooperative diversity schemes which incorporate error correction coding (such as convolutional or turbo codes) have also been proposed [15, 25–27]. In coded cooperation schemes the partner node constructs a different codeword to that received from the source, thereby providing incremental redundancy to the receiver. By avoiding repetition coding, these schemes achieve a coding gain which improves the BER performance of cooperative communication. However, this performance improvement comes at the expense of increased transceiver and processing complexity. In practice, coded cooperative diversity schemes would be prohibitively computationally intensive for resource-constrained wireless sensor nodes and are thus not considered in this thesis.

Other notable cooperative diversity schemes not shown in Fig. 2.1 include cooperative beamforming [28] and selection cooperative diversity [29]. These schemes are also not investigated in this thesis due to practical implementation concerns. Distributed beamforming requires the cooperating nodes to precisely co-phase their transmissions so that they combine constructively at the destination receiver. Given that the precise synchronisation required to achieve this beamforming effect is challenging even for a traditional physical antenna array, cooperative beamforming would be very difficult to practically implement in a distributed wireless sensor network [30]. In selection cooperative diversity candidate partner nodes compete to forward the source's message in a distributed contention process based on instantaneous channel quality. It was shown in [29] that selection cooperative diversity achieves a diversity order of $(n + 1)$ if only the best partner node from a set of n candidate partner nodes is chosen to cooperate with the source. This is an improvement over traditional cooperative diversity schemes such as DSTC, where n partner nodes would need to actively participate in the cooperative transmission to

¹Here *multiple-input-single-output* refers to a diversity communication system with multiple transmit antennas and one receive antenna.

achieve the same diversity order. However, practically implementing selection cooperative diversity in a wireless sensor network would entail substantial signalling overhead, as each candidate partner node would need to acquire knowledge of the instantaneous channel conditions to the source and destination receiver on a per-message basis.

The three major cooperative diversity schemes in Fig. 2.1 which are feasible candidates for wireless sensor networks will be considered in this thesis: virtual-MISO [16], decode-and-forward [13], and adaptive decode-and-forward [23]. A cooperative communication link consisting of a source node, destination receiver, and a single partner node is considered throughout this thesis. The BER performance of cooperative communication can be further improved if multiple partner nodes cooperate with the source node (since the diversity gain is proportional to the number of independently faded signals received by the destination). However, employing multiple cooperation partners gives rise to many implementation issues which can outweigh the diversity benefits, including the increased difficulty of synchronising and coordinating transmissions from multiple nodes and increased receiver complexity [19, 31–33]. Therefore, the analysis in this thesis only considers cooperation with a single partner node per source node, in accordance with the low-complexity constraints of wireless sensor networks.

In the following sections the three major cooperative diversity schemes of interest to this thesis are described in more detail and their BER performance is characterised. It is assumed throughout this thesis that the source-partner, partner-destination, and source-destination communication channels are independent flat (frequency non-selective) Rayleigh slow fading channels.

2.2.2 Virtual-MISO

In the virtual-MISO (vMISO) cooperative diversity scheme, the source and partner nodes act as elements of a virtual antenna array and cooperate by simultaneously transmitting the source's message to the destination receiver using space-time diversity codes [16]. This cooperative transmission is preceded by a dedicated source to partner transmission, whereby the partner node obtains knowledge of the source's message. The destination receiver combines the independently faded signals received from the source and partner in order to decode the source's message. The basic operation of vMISO is illustrated in Fig. 2.2.

In vMISO the partner node always transmits the message it received from the source, ignorant of whether it had decoded the message correctly. Thus the partner transmits an erroneous signal to the destination with probability BER_{s-p} , the BER of the preliminary source to partner transmission. This error propagation results in a very high BER at the destination, which may be roughly approximated as $BER_{error-propagation} \approx 1/2$ [23]. It follows that the overall end-to-end BER of the vMISO cooperative system, $BER_{coop-vMISO}$,

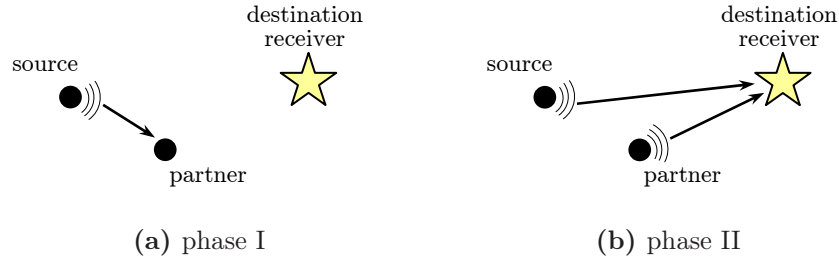


Figure 2.2: Operation of the vMISO cooperative diversity scheme: (a) in the first phase, the source node transmits its message to the partner node; (b) in the second phase, the source and partner simultaneously transmit the source's message to the destination receiver (using space-time diversity codes). The destination receiver combines the source and partner's transmissions from the second phase to decode the source's original message.

is given by ((4) in [23])

$$BER_{coop-vMISO} = (1 - BER_{s-p})BER_{full-coop} + BER_{s-p}BER_{error-propagation}, \quad (2.1)$$

where $BER_{full-coop}$ is the BER of the (full second order) cooperative diversity transmission of the source and partner to the destination.

It is evident from (2.1) that BER_{s-p} must be arbitrarily low to avoid significant error propagation and ensure that the second term in (2.1) is negligible. Accordingly, the target source-partner BER p_{s-p} is assumed to be one order lower than the target end-to-end BER of the cooperative system p_b in the subsequent analysis presented in this thesis (i.e. $p_{s-p} = p_b \times 10^{-1}$). Thus the overall end-to-end BER of the vMISO cooperative system may be re-expressed as

$$BER_{coop-vMISO} \approx BER_{full-coop}, \text{ subject to } BER_{s-p} \leq p_{s-p}. \quad (2.2)$$

It should be noted that setting the target source-partner BER to $p_{s-p} = p_b \times 10^{-1}$ translates into a less than 5% error margin between (2.1) and (2.2). In general, the target BER_{s-p} should be low enough to avoid significant error propagation at the partner node (so that the target end-to-end BER is p_b is achieved), but not so low that only nodes in the immediate vicinity of the source node are considered to be reliable cooperation partners.

The theoretical BER curve of a vMISO cooperative diversity system ($BER_{full-coop}$) is shown in Fig. 2.3, alongside that of a non-cooperative system ($BER_{non-coop}$)². It is clear from Fig. 2.3 that employing cooperative diversity reduces the total transmission energy required for a given reliability of communication.

²The theoretical BER expressions for a BPSK system in Rayleigh fading with no diversity and full second order diversity with optimal combining [8] were employed in generating the $BER_{non-coop}$ and $BER_{full-coop}$ curves in Fig. 2.3, respectively.

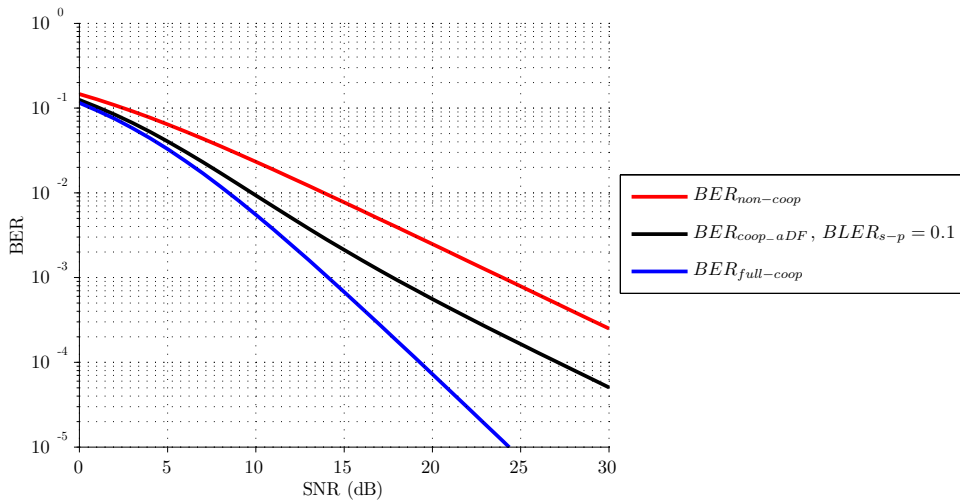


Figure 2.3: BER performance of BPSK in Rayleigh fading vs. average received SNR at the destination receiver, for non-cooperative and cooperative communication.

2.2.3 Decode-and-Forward

In contrast to vMISO, the decode-and-forward (DF) cooperative diversity scheme [13] takes advantage of the broadcast nature of the wireless channel, whereby the partner node overhears and repeats the source's original transmission to the destination receiver. Thus by avoiding an explicit source to partner transmission, DF may potentially result in greater energy savings compared to vMISO. Furthermore, since the source and partner do not simultaneously transmit to the destination, DF does not require the strict synchronization among the cooperating nodes which is essential for the proper operation of space-time coding in vMISO. This is highly advantageous in a distributed wireless sensor network where it would be difficult to achieve such precise synchronization [34]. The destination receiver combines the independently faded signals received from the source and partner in order to decode the source's message. The basic operation of DF is illustrated in Fig. 2.4.

As in vMISO the partner node always transmits the message it received from the source using DF, ignorant of whether it had decoded the message correctly. Namely, the partner node in DF always repeats the message it overheard from the source. Therefore, the transmission power of the source's original message to the destination must be high enough for the partner to reliably overhear it. Consequently, as in vMISO, the constraint of $BER_{s-p} \leq p_{s-p}$ is imposed, with $p_{s-p} = p_b \times 10^{-1}$. Therefore the overall end-to-end BER of the DF cooperative system, $BER_{coop-DF}$, is identical to that of vMISO,

$$BER_{coop-DF} \approx BER_{full-coop}, \text{ subject to } BER_{s-p} \leq p_{s-p}. \quad (2.3)$$

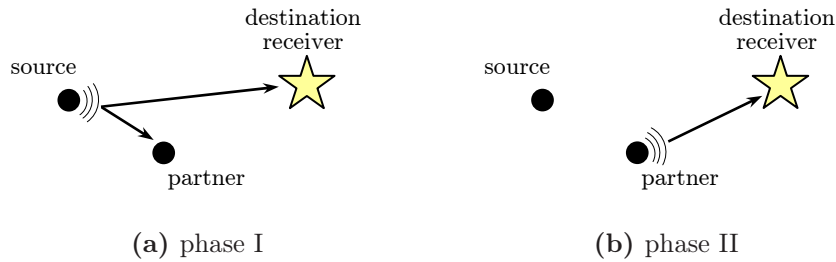


Figure 2.4: Operation of the DF cooperative diversity scheme: (a) in the first phase, the source node transmits its message to the destination receiver and the partner node; (b) in the second phase, the partner retransmits the source’s message to the destination receiver. The destination receiver combines the source’s transmission from the first phase and the partner’s transmission from the second phase to decode the source’s original message.

2.2.4 Adaptive Decode-and-Forward

The adaptive decode-and-forward (aDF) cooperative diversity scheme [23] is an adaptive variant of DF and operates as follows. In the first phase, the source’s transmission to the destination is also received and decoded by the partner, as in DF. In the second phase, there are two possible cases regarding the partner’s participation in the cooperative transmission. If the partner decodes the source’s message correctly, as determined by a CRC, it forwards it to the destination. Otherwise, if the partner does not decode the source’s message correctly, it does not retransmit and the destination only receives the source’s original transmission³. Thus in the first case, the destination receiver combines the independently faded signals received from the source and partner in order to decode the source’s message. In the second case, the destination directly decodes the signal received from the source. The basic operation of aDF is illustrated in Fig. 2.5.

Assuming the CRC always detects an erroneous message at the partner node, the probability of the partner not retransmitting is given by $BLER_{s-p}$, the BLER (block error rate) on the source-partner channel. The overall end-to-end BER of the aDF cooperative system, $BER_{coop-aDF}$, may be expressed as the weighted sum of the BERs of the two cooperative cases ([35], (6) in [24])

$$BER_{coop-aDF} = BLER_{s-p}BER_{non-coop} + (1 - BLER_{s-p})BER_{full-coop}, \quad (2.4)$$

where $BER_{non-coop}$ is the BER of the source to destination non-cooperative transmission. It should be noted that the bit error rate formulation in (2.4) is also equivalent to (3)

³It should be noted that the adaptive decode-and-forward scheme is also referred to as *selection decode-and-forward* in the literature. However, in selection decode-and-forward, as proposed in [13], the source repeats its message to the destination if the partner has decided not to forward it. In simple adaptive decode-and-forward, as proposed in [23] and assumed in this thesis, the source has no knowledge of the partner’s forwarding decision and thus never repeats its message in lieu of the partner.

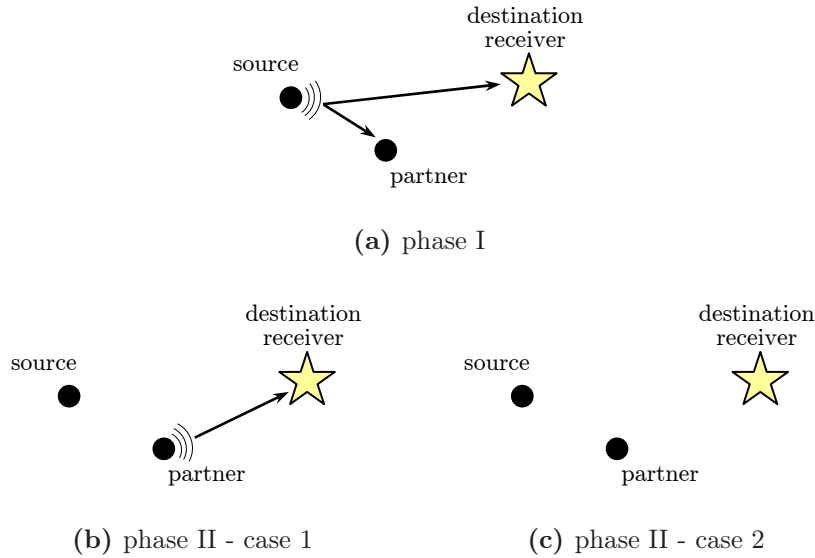


Figure 2.5: Operation of the aDF cooperative diversity scheme: (a) in the first phase, the source node transmits its message to the destination receiver and the partner node; in the second phase, (b) if the partner has decoded the source's message correctly it retransmits it to the destination receiver, (c) otherwise the partner node does not retransmit. If the latter case occurs, the destination receiver only decodes the message it received from the source in the first phase. Otherwise, the destination receiver combines the source's transmission from the first phase and the partner's transmission from the second phase to decode the source's original message.

in [23], except that in this thesis it is assumed that the partner makes its forwarding decisions based on a CRC test, rather than an SNR threshold as in [23].

As illustrated in Fig. 2.3, the BER performance of aDF with a blocked source-partner channel ($BLER_{s-p}=1$) is equivalent to that of a non-cooperative system, namely $BER_{non-coop}$. Conversely, an ideal source-partner channel ($BLER_{s-p}=0$) enables full cooperation whereby second order diversity is achieved at the destination receiver, with $BER_{coop-aDF}=BER_{full-coop}$. Finally, for $BLER_{s-p}=0.1$, the BER performance of aDF is shown to be a weighted combination of these two extreme cooperative cases, as indicated by (2.4). Fig. 2.3 demonstrates that a significant reduction in total transmission energy is achieved by aDF even when the source-partner channel is non-ideal (i.e. $BLER_{s-p}=0.1$). This flexibility suggests that aDF is a practically suitable scheme for randomly deployed wireless sensor networks, capable of extracting energy saving benefit from cooperation with a variety of (potentially non-ideal) partners.

2.2.5 Error Rate Expressions

It is assumed throughout this thesis that uncoded BPSK modulation⁴ is employed on all communication links and that the destination receiver employs optimal MRC diversity combining of the cooperative transmissions from the source and partner. The error rates $BER_{non-coop}$, $BER_{full-coop}$, BER_{s-p} , and $BLER_{s-p}$ may then be expressed as

$$BER_{non-coop} \approx \frac{1}{4SNR_{s-d}}, \quad (2.5)$$

$$BER_{full-coop} \approx \frac{3}{16SNR_{s-d}SNR_{p-d}}, \quad (2.6)$$

$$BER_{s-p} \approx \frac{1}{4SNR_{s-p}}, \quad (2.7)$$

$$BLER_{s-p} \approx \frac{K}{SNR_{s-p}}, \quad (2.8)$$

where SNR_{s-d} , SNR_{p-d} , and SNR_{s-p} are the average SNRs on the source-destination, partner-destination, and source-partner channel, respectively. The high-SNR BER approximations [8] in (2.5)-(2.7) are employed in this thesis as the exact BER expressions are cumbersome and make subsequent mathematical analysis very difficult⁵. Moreover, a closed-form expression does not exist for the exact BLER of BPSK in Rayleigh fading [36] and hence the high-SNR approximation in (2.8) is adopted instead. For a message block size of $B = 100$ bits, $K \approx 3.2$ [35] provides a good approximation to the numerically generated BLER curve in [36].

2.3 Energy Model

The energy model adopted in this thesis is based on that proposed by Cui *et al.* in [16,37] for a short range wireless communication system such as a wireless sensor network. The total energy consumption of wireless communication is assumed to consist of two dominant components: the transmission energy cost and the transceiver circuit energy consumption. Thus the total average power consumption of a short range wireless communication system may be expressed as

⁴The assumption of uncoded BPSK modulation is adopted in this thesis for the sake of simplicity. The energy efficiency of cooperative diversity using various other modulation and coding schemes may be analysed in the same manner, by adopting the appropriate error rate expressions in (2.5)-(2.8). It should be noted that such an analysis would yield the same trends as reported in this thesis for the basic case of uncoded BPSK modulation (albeit with slightly different numerical results).

⁵It should also be noted that using these high-SNR error rate approximations at worst has the effect of requiring a higher than necessary transmit power allocation to achieve the target BER at the destination receiver. This in turn simply results in a conservative estimate of the partner choice region for energy efficient cooperation in Chapter 4.

$$P_{total} = P_{PA} + P_{CCT}, \quad (2.9)$$

where P_{PA} represents the total power consumption of the RF (radio frequency) power amplifiers and P_{CCT} represents the total power consumption of all other transceiver circuit blocks [16, 37].

The power consumption of the power amplifiers P_{PA} is directly proportional to the transmit power P_{out} and may be defined as

$$P_{PA} = \frac{\xi}{\eta} P_{out}, \quad (2.10)$$

where η is the drain efficiency of the RF power amplifier and ξ is the peak-to-average ratio, which is dependent on the modulation scheme used [37]. The transmit power may be expressed as

$$P_{out} = LE_b R_b, \quad (2.11)$$

where E_b is the required energy per bit at the receiver for a target BER p_b , R_b is the bit rate, and L is the channel path loss and may be calculated according to the log-distance path loss model,

$$L = d^k L_{ref}, \quad (2.12)$$

where d is the transmission distance, k is the channel path loss exponent, and L_{ref} is the reference path loss at a reference distance of 1m [6]. It should be noted that the value of E_b is obtained from the average SNR $\frac{E_b}{N_0}$ at the receiver⁶ required to achieve the target BER p_b , where N_0 is the Gaussian noise power spectral density. To remain consistent with [16], the reference parameter values $\eta=0.35$, $\xi=1$, $R_b=10$ kb/s, $p_b=10^{-3}$, $N_0=-171$ dBm/Hz, $L_{ref}=10^9$ ($\equiv 90$ dB) and $k=3.5$ are adopted in this thesis⁷. The complete set of reference communication system parameters employed throughout this thesis is listed in Table 2.1 for convenience.

⁶The *instantaneous* received SNR in a Rayleigh fading channel is given by $\left(|\alpha|^2 \frac{E_b}{N_0}\right)$ [8], where $|\alpha|$ is the Rayleigh-distributed magnitude of the channel gain α (which is a zero-mean complex Gaussian random variable). The *average* received SNR is given by $\left(E[|\alpha|^2] \frac{E_b}{N_0}\right)$ [8], where $E[|\alpha|^2]$ is the mean of the exponentially-distributed random variable $|\alpha|^2$. In this thesis, it is assumed that $E[|\alpha|^2] = 1$ (i.e. the channel gain α is assumed to have unit variance). Therefore, the average SNR at the receiver is defined as $\frac{E_b}{N_0}$, and the average channel power is represented separately by the channel path loss L .

⁷It should be noted that $k=3.5$ is assumed in this thesis as a more realistic value than the free-space path loss exponent of $k=2$ employed in [16]. Moreover, $L_{ref} \equiv 90$ dB is assumed in this thesis based on equation (1) in [16] and the parameters quoted in Table I of [16] for a radio operating in the 2.5 GHz ISM band, except that it is assumed that sensor nodes are equipped with omnidirectional antennas, so that the transmitter and receiver antenna gains are set to $G_t = G_r = 0$ dBi, instead of 5 dBi as in [16].

Table 2.1: Reference communication system parameters.

Parameter	Symbol	Reference system value
target end-to-end BER	p_b	10^{-3}
target source-partner BER	p_{s-p}	10^{-4}
bit rate	R_b	10 kb/s
noise power spectral density	N_0	-171 dBm/Hz
drain efficiency of RF power amplifier	η	0.35
peak-to-average ratio of modulation	ξ	1
channel path loss exponent	k	3.5
reference path loss at 1 m	L_{ref}	10^9 ($\equiv 90$ dB)
transmitter circuit power consumption	P_{CCT_tx}	98.2 mW
receiver circuit power consumption	P_{CCT_rx}	109.5 mW
source-destination transmission distance	d_{s-d}	30 m

The transceiver circuit power consumption P_{CCT} may be defined as the sum of P_{CCT_tx} and P_{CCT_rx} , the total power consumed in the transmitter and receiver circuit blocks, respectively. The transceiver circuit power consumption model presented in [16, 37] is based on a generic low-IF radio architecture, and takes into account the power consumed by the D/A converter, the mixer, the active filters, and the frequency synthesizer at the transmitter, and the power consumed by the low noise amplifier, the mixer, the active filters, the intermediate frequency amplifier, and the A/D converter at the receiver. The reference transceiver circuit power consumption parameters of $P_{CCT_tx}=98.2$ mW and $P_{CCT_rx}=109.5$ mW for a radio operating in the 2.5 GHz ISM (industrial, scientific, and medical) band are adopted in this thesis in order to remain consistent with [16, 37], as shown in Table 2.1.

It is important to note that the power consumption of all transmitter and receiver circuit blocks is intentionally grouped in this thesis under the two parameters P_{CCT_tx} and P_{CCT_rx} , in order to retain a simple and robust energy model. Thus, although the reference transceiver parameters from [16, 37] are adopted, a different radio hardware architecture could be easily considered by simply changing the value of P_{CCT_tx} and P_{CCT_rx} to reflect the corresponding circuit parameters. It should also be noted that the energy consumption of baseband processing is intentionally excluded from the energy model adopted in this thesis for the sake of simplicity. Moreover, the energy consumption of baseband signal processing blocks is minor relative to that of the RF circuit blocks, assuming no advanced signal processing techniques such as iterative decoding are employed [37]. Nevertheless, the overhead of baseband processing could be easily incorporated into the energy model by augmenting the values of P_{CCT_tx} and P_{CCT_rx} assumed in the analysis. Similarly, it would be straightforward to incorporate the energy consumption of diversity combining at the destination receiver, which is also omitted from the energy model adopted in this

thesis for the sake of simplicity. As discussed in Section 2.4.1, it has been previously shown in the literature [17] that diversity combining simply represents an additional (and relatively minor) energy overhead of cooperative diversity.

2.3.1 Non-Cooperative Communication

The energy consumption of non-cooperative communication between a source node and its destination receiver consists of the transmission energy cost of the source's communication with the destination, the transmitter circuit energy consumption of the source, and the receiver circuit energy consumption of the destination. It follows the total energy consumption per bit using non-cooperative communication may be expressed as

$$E_{non-coop} = \left(P_{PA_source_non-coop} + P_{CCT_tx} + P_{CCT_rx} \right) / R_b, \quad (2.13)$$

where $P_{PA_source_non-coop}$ represents the transmission power of the source.

2.3.2 Virtual-MISO

The energy consumption of cooperative communication using vMISO consists of the energy cost of the preliminary source to partner communication and the space-time coded source and partner cooperative communication to the destination. The source to partner communication in the first phase of vMISO is a non-cooperative transmission, and the associated energy consumption consists of the transmission energy cost of the source's communication with the partner, the transmitter circuit energy consumption of the source, and the receiver circuit energy consumption of the partner. The energy consumption of the cooperative communication to the destination in the second phase of vMISO consists of the transmission energy consumption of the source and the partner, the transmitter circuit energy consumption of the source and the partner, and the receiver circuit energy consumption of the destination. Therefore, the total energy consumption per bit using vMISO cooperative communication may be expressed as [16]

$$E_{coop_vMISO} = \left(\begin{array}{l} P_{PA_s-p} + P_{PA_source_coop} + P_{PA_partner_coop} \\ 3P_{CCT_tx} + 2P_{CCT_rx} \end{array} \right) / R_b, \quad (2.14)$$

where P_{PA_s-p} represents the power of the source's (non-cooperative) transmission to the partner, and $P_{PA_source_coop}$ and $P_{PA_partner_coop}$ represent the transmission power of the cooperating source and partner respectively.

2.3.3 Decode-and-Forward

The energy consumption of cooperative communication using DF is the sum of the energy cost of the source's communication with the destination (overheard by the partner) and the partner's communication with the destination. The energy consumption of the source's transmission in the first phase of DF consists of the transmission energy consumption of the source, the transmitter circuit energy consumption of the source, and the receiver circuit energy consumption of the partner and the destination. The energy consumption of the partner's transmission in the second phase of DF consists of the transmission energy consumption of the partner, the transmitter circuit energy consumption of the partner, and the receiver circuit energy consumption of the destination. Therefore, the total energy consumption per bit using DF cooperative communication may be expressed as [38]

$$E_{coop-DF} = \left(\frac{P_{PA-source-coop} + P_{PA-partner-coop+}}{2P_{CCT-tx} + 3P_{CCT-rx}} \right) / R_b. \quad (2.15)$$

2.3.4 Adaptive Decode-and-Forward

The communication energy consumption of aDF consists of the energy cost of the source to destination communication and, whenever the partner can decode the source's transmission correctly, the partner to destination communication. As with DF, the energy consumption of the source's transmission in the first phase of aDF consists of the transmission energy consumption of the source, the transmitter circuit energy consumption of the source, and the receiver circuit energy consumption of the partner and the destination. As discussed in Section 2.2.4, in aDF the partner retransmits the source's message with probability $(1 - BLE R_{s-p})$. Therefore, the energy consumption of the second phase of aDF is on average equal to the energy consumption of the partner's transmission in the second phase of DF (consisting of the transmission energy consumption of the partner, the transmitter circuit energy consumption of the partner, and the receiver circuit energy consumption of the destination), multiplied by the probability of the partner forwarding the source's message. Therefore, the total energy consumption per bit using aDF cooperative communication may be expressed as [35]

$$E_{coop-aDF} = \left(\frac{P_{PA-source-coop} + (1 - BLE R_{s-p})P_{PA-partner-coop+}}{(2 - BLE R_{s-p})P_{CCT-tx} + (3 - BLE R_{s-p})P_{CCT-rx}} \right) / R_b. \quad (2.16)$$

2.3.5 Energy Efficiency of Cooperative Communication

In this thesis the energy efficiency of cooperative communication is defined as the percentage energy saving achieved by cooperating,

$$E_{\text{saving-coop-total}} = \frac{100 \times (E_{\text{non-coop}} - E_{\text{coop}})}{E_{\text{non-coop}}}, \quad (2.17)$$

where $E_{\text{non-coop}}$ is given by (2.13) and E_{coop} is given by (2.14)-(2.16) for vMISO, DF, and aDF respectively. Comparing (2.13) with (2.14)-(2.16), it is apparent that a positive $E_{\text{saving-coop-total}}$ is obtained only once the reduction in the total transmission energy due to cooperative diversity is greater than the overhead of the increased circuit energy consumption of cooperation. Whereas circuit energy is a fixed overhead, it is evident from (2.12) that transmission energy is a function of transmission distance. Therefore, cooperation becomes energy efficient beyond a threshold source-destination separation [16, 17, 38].

This is illustrated in Fig 2.6, which shows the total energy saving achieved by cooperative communication as the source-destination separation d_{s-d} is increased. For the purposes of illustration, vMISO cooperation is assumed in generating Fig 2.6, however it is important to note that the curve shown in Fig 2.6 is representative of the energy efficiency of a cooperative diversity scheme in general. It is assumed that the source and partner are separated by 1m and equidistant from the destination receiver (i.e. the source-partner separation $d_{s-p}=1$ m and the partner-destination separation $d_{p-d}=d_{s-d}$). The geometry of the cooperative communication link is illustrated in Fig. 2.7. It should also be noted that the reference communication system parameters in Table 2.1 and optimum power allocation (as developed in Chapter 3) were assumed in generating Fig 2.6.

Fig 2.6 shows that the energy saving achieved via cooperative communication increases with an increasing source-destination separation, as the circuit energy overhead of cooperation becomes less significant overall. Importantly, Fig 2.6 clearly demonstrates that cooperative communication only becomes worthwhile beyond the threshold source-destination separation of around 12 m. Non-cooperative communication is more energy efficient for source-destination separations below this threshold, since the increase in circuit consumption due to cooperation exceeds the transmission energy reduction obtained via cooperative diversity. Moreover, Fig 2.6 shows that very significant energy savings are achieved past the break-even threshold source-destination transmission distance. For example, cooperation reduces the energy cost of communication by over 50% for a source 17 m away from the destination receiver and by over 83% for a source 30 m away. Therefore, provided the source-destination transmission range is beyond a certain threshold, cooperative communication has the potential to dramatically reduce the total energy cost of wireless communication in a sensor network.

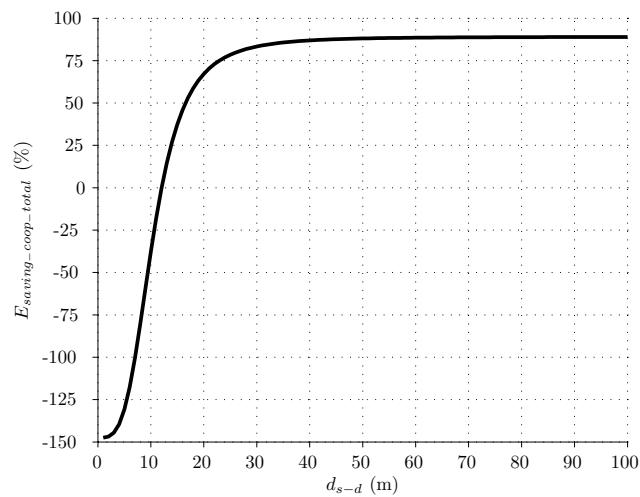


Figure 2.6: Illustration of the energy efficiency of cooperative communication vs. the source-destination separation. It is assumed that the source and partner are separated by 1 m and equidistant from the destination receiver, and that vMISO with optimal power allocation (as developed in Chapter 3) is employed.

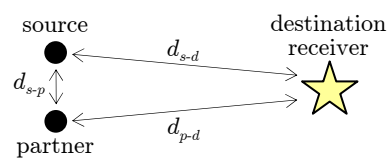


Figure 2.7: Illustration of the geometry of a cooperative communication link.

2.4 Literature Review

A vast number of publications have appeared in the literature dealing with various aspects of cooperative communication in the relatively short time since cooperative diversity was introduced into the mainstream research literature by [11, 12, 14, 21] less than a decade ago. The literature review presented in this section will thus only discuss the subset of the existing literature on cooperative communication which is most relevant to the aims of this thesis. Accordingly, this literature review focuses on the four main areas of interest to this thesis: (i) the energy efficiency of cooperative diversity, (ii) optimal power allocation for cooperative communication, (iii) best partner choice for cooperative communication, and (iv) strategies for coordinating network-wide cooperative communication. The literature relating to the first area is reviewed in Section 2.4.1, thereby providing an account of the fundamental research on the energy efficiency of cooperative communication on which the work in this thesis is founded. The literature relevant to the remaining three areas is reviewed in Sections 2.4.2 and 2.4.3, thereby placing the original research presented in Chapters 3-11 of this thesis in the context of previous research.

2.4.1 Energy Efficiency of Cooperative Diversity

The energy efficiency of cooperative communication in a wireless sensor network was first investigated in [16]. The energy efficiency of the vMISO cooperative diversity scheme was considered within a clustered wireless sensor network scenario, whereby neighbouring sensor nodes cooperate to transmit information to a remote destination receiver. The analysis in [16] employed the energy model proposed in [37], which considers the transmission energy cost and the transceiver circuit energy consumption as the two dominant components of the total energy consumption of a short-range communication system such as a wireless sensor network; this fundamental energy model has been adopted in this thesis, as discussed in Section 2.3. It was shown in [16] that although cooperative diversity reduces the transmission energy cost of wireless communication, it results in an increased circuit energy overhead by involving an additional transceiver by way of the partner. Importantly, it was demonstrated that if the source-destination transmission distance is large enough, cooperative communication can significantly reduce the total energy cost of wireless communication. This fundamental result has been discussed and illustrated in Section 2.3.5.

The work in [16] was extended in [17] by considering the impact of the additional energy overhead of channel estimation. Namely, the source and partner must transmit training bits for CSI (channel state information) acquisition at the destination receiver to enable coherent combining of the space-time coded cooperative transmission, which further increases the total energy cost of cooperation compared to non-cooperative com-

munication. The key finding of [16] was confirmed in [17], showing that cooperation results in a more energy-efficient communication system beyond a threshold source-destination transmission distance, even when all significant energy overheads are taken into account. The study in [17] also investigated the impact of varying the value of the path loss exponent k from 2 to 4, showing that the break-even threshold transmission distance for energy efficient cooperation is lower for higher values of k (which are more realistic than the free-space path loss exponent of $k=2$ considered in [16]).

In [39,40] energy efficient cooperative communication was studied within the context of a wireless sensor network operating under the LEACH (low-energy adaptive clustering hierarchy) networking protocol [41]. These studies incorporate vMISO cooperative diversity into the clustered wireless sensor network architecture, whereby a cluster-head node cooperates with nodes which are members of its own cluster to transmit information to a remote destination receiver [39] or the cluster-head of another cluster in the network [40]. It was demonstrated in [39,40] that cooperative LEACH results in a substantial improvement in network lifetime compared with traditional LEACH, even when all the overheads of cooperative communication are taken into account. Moreover, it was shown in [39] that increasing the number of cooperation partners in the cluster overall results in a greater network lifetime improvement but also increases the threshold source-destination transmission distance for energy efficient cooperation.

The energy efficiency of clustered cooperation in a wireless sensor network was further investigated in [42], where a random number of relay⁸ nodes cooperate to facilitate inter-cluster communication using an adaptive version of the vMISO cooperative diversity scheme (a CRC test is employed at the candidate relay nodes, as in aDF, to determine which nodes participate in the space-time coded cooperative transmission). It was shown that the energy efficiency of cooperative communication may decrease with a larger number of relay nodes, due to the increased circuit energy overhead of multiple relay nodes participating in the cooperative transmission. The analysis in [42] thereby confirmed the result from [39] that a greater number of cooperation partners is only worthwhile provided a sufficiently large inter-cluster (i.e. source-destination) transmission distance. The impact of varying the target packet error rate for the inter-cluster communication was also investigated in [42], indicating that a greater number of relays in a cluster is preferable for a more strict target packet error rate.

It is important to note that all of the studies in [16,17,39,40,42] only investigated the special case of cooperation within a clustered network architecture, whereby neighbouring source and partner nodes (typically separated by a distance of 1 m) cooperate to transmit information to a remote destination receiver. In this thesis, the more general case of a

⁸The terms *partner* and *relay* are used interchangeably in this literature review, reflecting their usage in the literature to refer to the node that cooperates with the source node to help communicate its message to the destination receiver.

randomly deployed wireless sensor network is investigated instead, whereby a source node may select a cooperation partner which is not necessarily a neighbouring node. An aspect of this research was presented in [38], wherein it was shown that the source-destination transmission distance must be at least comparable to the source-partner separation to ensure energy efficient vMISO and DF cooperation. Independently from [42], the case of multiple cooperation partners was also considered in [38], showing that although the maximum energy efficiency of cooperation increases with the number of cooperation partners so does the break-even threshold source-destination transmission distance due to the associated increased circuit energy overhead.

In [28] the energy efficiency of cooperative beamforming was investigated, whereby the source broadcasts data to a set of relays, some of which cooperatively beamform to forward the source's message to the destination. The main contribution of [28] is the analysis of the energy overhead of the relays obtaining knowledge of CSI (which is necessary for weighting the relays' transmit signals so they add up coherently at the destination receiver) and its impact on the optimal number and set of participating relays for energy efficient cooperation. It was shown that the energy cost of training and feedback of CSI is significant and results in a trade-off between decreasing the transmission energy cost by employing more relays and decreasing the energy overhead of CSI acquisition by employing fewer relays. It should be noted that the analysis in [28] assumed a long-range transmission system and thus adopted an energy model that did not consider the circuit energy overhead of cooperative communication, unlike the studies in [16, 17, 39, 40, 42]. Nonetheless, the investigation in [28] confirmed that cooperative communication only becomes energy efficient once the transmission energy reduction due to cooperative diversity exceeds any significant energy overheads of cooperation.

Another interesting but distinct line of research is the literature on the energy efficiency of cooperative broadcasts in wireless networks [43–45]. These works are based on the technique of opportunistic large arrays (OLA) which facilitates energy efficient information flooding in the network; the nodes in the OLA together retransmit a message broadcast by the originating source node or another OLA, without explicit coordination but in response to received energy, whereby nodes receiving a broadcast message from an OLA superimpose the signals received from all nodes that previously transmitted in order to benefit from diversity. Lastly, it is also interesting to mention the study in [46], which presents a game-theoretic analysis of the impact of node selfishness on the energy efficiency of a multi-hop network employing DF relaying. Within the game-theoretic incentive policy considered, the results in [46] indicate that in a large network it is sufficient for a very small proportion of nodes to be altruistic relay nodes to ensure full cooperation among all nodes in the network.

2.4.2 Power Allocation and Partner Choice for Cooperative Communication

The literature reviewed in the previous section addressed the elementary question of whether cooperative diversity is a viable energy saving technique for energy-constrained wireless networks. These studies demonstrated that cooperation can significantly improve the energy efficiency of wireless communication, even when the associated energy overheads are taken into account. However, in order to fully exploit the benefits of cooperative communication two further questions must be addressed: (1) how to best allocate transmit power to the cooperating source and partner nodes - *the power allocation problem*, and (2) how to select the best partner out of a set of candidate nodes - *the partner choice problem*, such that cooperation gain is maximised. The existing literature on power allocation and partner choice for cooperative communication is reviewed in this section; the original research addressing the problems of power allocation and partner choice for energy efficient cooperation in a wireless sensor network presented in Chapters 3-6 of this thesis is thereby placed in the context of previous research.

2.4.2.1 Power Allocation

The majority of the power allocation methods for cooperative diversity techniques proposed in the literature are designed to optimally distribute a fixed total transmit power between the cooperating source and partner nodes in order to improve the reliability of communication (which may be quantified in terms of outage probability, received SNR, or error rate). For example, in [47,48] the optimal transmit power allocation which minimises the outage probability of the source-destination communication link was investigated for cooperative diversity systems with multiple relay nodes; a simple near-optimal solution based on knowledge of average channel gains was proposed for the DF scheme in [47], whereas in [48] closed-form optimum power allocation solutions were derived for the AF, DF, and vMISO schemes in the high SNR regime. Similarly, the transmit power allocation which maximises the received SNR at the destination was considered in [49] for the AF and DF cooperative diversity schemes, whereas the studies in [50,51] investigated the optimum power allocation which minimises the symbol error rate (SER) for the aDF cooperative diversity scheme.

However, the problem of optimal power allocation for energy efficient cooperation, which is of interest in this thesis, is distinct from those considered in [47–51]. Rather than distributing a fixed transmit power to improve communication reliability, the aim of optimal power allocation for energy efficient cooperation is instead to determine the transmit power allocation which minimises the total energy consumption of cooperative communication, subject to maintaining a fixed target communication reliability. The

problem of optimal power allocation for energy efficient cooperation subject to a target error rate constraint, which is of interest in this thesis, was recently addressed in the studies presented in [33, 42].

In [42] the transmit power allocation which minimises the total communication energy consumption of an adaptive vMISO cooperative diversity scheme was investigated subject to a packet error rate (PER) constraint. However, the analysis presented in [42] is restricted to the specialised case of a clustered cooperative link geometry (whereby the neighbouring source and partner nodes are assumed to be equidistant from the destination receiver). By contrast, in this thesis the power allocation problem is investigated under the assumption of a general cooperative link geometry, such that the source and partner nodes may experience dissimilar average channel path loss to the destination. The analysis in this thesis is thus applicable both to the general case of a randomly deployed wireless sensor network and the specialised case of a clustered architecture.

In [33] the transmit power allocation which minimises the sum of the source and partner transmit energies was investigated for the AF and aDF⁹ cooperative diversity schemes subject to a BER constraint. The work in [33] thus considers a very similar research question to that addressed by the original research on power allocation for energy efficient cooperation presented in Chapters 3 and 5 of this thesis (and published independently in [35]). However, the power allocation problem for energy efficient cooperation was investigated in [33] under the restrictive assumption of reciprocal cooperation, whereby source nodes are paired and must serve as each other's cooperation partners¹⁰. By contrast, in this thesis the more general case of non-reciprocal cooperation is investigated, whereby a node is not obliged to serve as the cooperation partner for its own partner node.

Importantly, the power allocation solutions presented in [33, 42] were obtained via a numerical search¹¹. It would be prohibitively computationally expensive for a resource-constrained sensor node to perform such a search, rendering the power allocation solutions in [33, 42] practically infeasible for distributed wireless sensor networks. One of the goals of this thesis is to develop computationally efficient transmit power allocation strategies which enable simple sensor nodes to cooperate autonomously to improve the energy efficiency of the wireless sensor network.

Aside from the investigations in [33, 42], which are most relevant to the research questions addressed by this thesis, various other forms of the energy efficient power allocation problem have also been considered in [32, 52, 53]. In [32] power allocation was investigated

⁹A variant of the aDF cooperative diversity scheme based on quadrature signalling proposed in [24] was considered in [33].

¹⁰Moreover, due to implementation concerns associated with the aDF variant proposed in [24], the aDF power allocation solution presented in [33] was based on the additional constraint that a node must use the same transmit power whether it is acting as the source or as the partner.

¹¹Specifically, the power allocation solution proposed in [33] for the aDF cooperative diversity scheme was obtained by numerically solving a 5th order polynomial.

for an AF wireless relay system where multiple source nodes in the network communicate with their destination receiver with the help of a relay; power allocation problems based on several criteria, including minimising the maximum transmit power over all sources nodes in the network, were formulated as geometric programming problems and solved numerically. The minimum transmit power allocation problem for AF was also investigated in [52], where the power allocation strategy that minimises the total relay power was derived for an AF cooperative link consisting of one source and destination pair helped by multiple relays. The energy efficiency of AF and DF with optimal transmit power allocation was compared in [53], wherein the energy required for transmitting one information bit was approximated with respect to the spectral efficiency. Whereas the work in [32, 52, 53] is largely based on computationally intensive and centralised power control, the focus of this thesis is the development of distributed and computationally efficient power allocation solutions. Moreover, as discussed in Section 2.2, the AF cooperative diversity scheme is not considered in this thesis due to practical implementation concerns.

2.4.2.2 Partner Choice

One of the first investigations of the partner choice problem for cooperative communication appearing in the literature was published in [54]. The problem of selecting a candidate partner to obtain the maximum improvement in communication reliability (quantified in terms of error rate reduction) was considered for a single cooperative link employing the coded cooperation diversity scheme proposed in [26]. The partner choice problem was examined in terms of network geometry via the *user cooperative region*, which was defined as the locations of candidate partners with whom cooperation is beneficial for a given source node (i.e. yields a reliability improvement). It was shown that it is solely the quality¹² of the source-destination and partner-destination communication channels which determines whether cooperation with a given partner node is beneficial, although the quality of the source-partner link influences the extent of cooperation gain achieved. In other words, the boundary of the user cooperative region for reliability-improving coded cooperation was shown to be a circle centered around the destination. Importantly, the concept of user cooperative region proposed in [54] will be used in Chapters 4 and 5 of this thesis as a tool for evaluating how beneficial cooperation is given different candidate partners and studying the problem of best partner choice for energy efficient cooperation. The alternative term *partner choice region* will be adopted in this thesis to refer to the

¹²The *quality* of the channel informally refers to the average received SNR, which is determined by the transmit power (assumed in [54] to be fixed and identical for the source and partner nodes) and the average channel path loss (which is mapped to network distances using a formula analogous to 2.12).

network region wherein the partner node may be located to yield a given positive energy efficiency of cooperation for a fixed source and destination pair.

Whereas the analysis in [54] considered a single cooperative link, the problem of allocating partners for a network of nodes was investigated in [55] for the coded cooperation scheme proposed in [15]. Assuming that each node helps n other nodes, the problem of selecting which source nodes a given partner node should help was addressed. A distributed fixed priority protocol was proposed for enabling individual partner nodes to decide which source nodes to cooperate with, assuming the nodes have no knowledge of network channel state information (i.e. no location or average channel path loss information). It was shown that the proposed fixed priority protocol guarantees a diversity order of $(n + 1)$ for all transmissions across the network. A centralised greedy node selection algorithm which minimises the average node outage probability across the network given full network channel information was also proposed, showing that the centralised algorithm achieves a significantly higher cooperative gain compared to the fixed priority protocol.

Since the early studies in [54, 55], numerous further publications have addressed various other forms of the partner choice problem for cooperative communication. However, as with power allocation, the majority of the literature on partner choice focuses on investigating partner selection which maximises the improvement in communication reliability via cooperation. For example, a relay placement algorithm which minimises the average probability of error was proposed in [56] for the AF and DF cooperative diversity schemes. The problem of selecting multiple relay nodes for a source-destination AF cooperative link was investigated in [57] with the aim of maximising the received SNR at the destination; the optimal multiple relay selection strategy was obtained via an exhaustive search and several suboptimal linear complexity multiple relay selection strategies were proposed. An information-theoretic analysis of the multiple relay selection problem for maximising system throughput was presented in [31] for a variant of the DF cooperative diversity scheme, where two relay selection algorithms were proposed based on proximity to rate-maximising locations. In [51] the power allocation and relay selection problems were jointly investigated for the aDF cooperative diversity scheme with the aim of minimising the SER, where the optimal relay is chosen using instantaneous channel state information about the source-relay and relay-destination channels.

The partner choice problem for energy efficient cooperation subject to a target error rate constraint, which is of interest in this thesis, has previously been addressed by Mahinthan *et al.* in [19, 33]. Specifically, these studies considered the problem of optimally grouping nodes in a network into cooperating pairs such that the overall transmit energy consumption over the network is minimised. This partner matching problem for energy efficient reciprocal cooperation was investigated for the DF and aDF cooperative diversity

schemes in [19] and for the AF and aDF¹³ cooperative diversity schemes in [33] (wherein it was considered jointly with the power allocation problem, as discussed in Section 2.4.2.1). The optimization problem of selecting pairs of cooperating nodes was formulated as the problem of weighted matching on a graph in [19, 33], which can be solved using the optimal maximum weighted (MW) matching algorithm in polynomial time. Two suboptimal Worst-Link-First (WLF) matching algorithms were also proposed, whose complexity is one order lower than the MW matching algorithm. The WLF matching algorithms give the nodes with the worse link quality (and thus higher non-cooperative energy consumption) a higher priority to select their partners. The suboptimal WLF matching algorithm proposed in [19] uses the energy saved by reciprocal cooperation between a pair of users as the matching weights, whereas the near-optimal WLF matching algorithm proposed in [33] uses the maximum energy consumed by either node in the reciprocal cooperation pair as the matching weights.

The work in [19, 33] thus considers a similar research question to that addressed by the original research on partner choice for energy efficient cooperation presented in Chapters 4 and 6 of this thesis (and published independently in [35, 58]). The key distinction between [19, 33] and the work presented in this thesis is the restrictive assumption of reciprocal cooperation, which is essential to the work in [19, 33]. By contrast, the more general case of non-reciprocal cooperation is considered in this thesis, whereby a node is not obliged to serve as the cooperation partner for its own partner node. The reciprocal cooperation assumption also restricts the number of source nodes served by any given partner node to one, motivating the matching algorithms proposed in [19, 33]. Importantly, it is straightforward to show that enforcing reciprocal cooperation is suboptimal from the point of view of minimising network-wide transmit energy consumption. Let us define a given source node's preferred partner choice to be the candidate partner node with whom cooperation minimises the total transmit energy per bit consumed on the source-partner-destination cooperative communication link. It follows that allowing each source node to select its preferred partner necessarily minimises the total transmit energy consumption over the network. A reciprocal cooperation arrangement would only result in the optimally energy efficient network-wide partner allocation if each pair of nodes were each other's preferred partner choice; however this is generally not the case, as was indeed observed in [33]. Consequently, a more flexible arrangement is assumed in this thesis instead, where nodes are altruistic in the sense that a given node may serve as cooperation partner to none, one, or multiple other nodes (regardless of whether that node receives cooperation help itself). Such a non-symmetrical cooperation arrangement is advantageous from the point of view of energy conservation for a wireless sensor network, where

¹³A variant of the aDF cooperative diversity scheme based on quadrature signalling proposed in [24] was considered in [19, 33].

the overall energy efficiency of the network takes precedence over per-node fairness. For example, a partner node located close to the destination receiver has an inherent energy advantage and can afford to serve as the preferred cooperation partner of multiple source nodes located far from the destination, thereby maximising network-wide energy efficiency while redistributing the combined energy resource of the network¹⁴; enforcing reciprocal cooperation as in [19, 33] does not allow such an arrangement.

Furthermore, the network-wide partner matching algorithms developed in [19, 33] are centralised and based on an explicit calculation of the energy associated with each potential cooperative transmission. This means that the partner choice solutions proposed in [19, 33] would be prohibitively computationally expensive for practical implementation in a wireless sensor network¹⁵. One of the goals of this thesis is to develop distributed and computationally efficient partner selection strategies which enable simple sensor nodes to cooperate autonomously to improve the energy efficiency of the wireless sensor network. Moreover, the partner choice region for energy efficient reciprocal cooperation was illustrated in [19, 33], demonstrating that the best reciprocal cooperation pairing was distinct from each individual node's preferred partner choice [33]. However, the use of this insight in the development of the proposed partner selection solutions was limited to motivating a different matching weight for the WLF algorithm in [33] compared with that in [19]. By contrast, in this thesis the partner choice region for energy efficient cooperation is examined in order to gain insight into the partner choice problem and thus inform the development of simple distributed cooperation strategies.

Several other forms of the energy efficient partner selection problem have also been considered in the literature, for example in [28, 59, 60]. However, these studies are not directly relevant to the research questions addressed by this thesis and are thus omitted from this literature review.

2.4.3 Strategies for Coordinating Network-wide Cooperative Communication

The literature reviewed in the previous section addressed the problem of optimal resource allocation for fully exploiting the potential benefits of cooperative communication; specifically, the problem of interest to this thesis is that of optimal transmit power allocation

¹⁴Notwithstanding this, allowing a single node to serve as cooperation partner to multiple source nodes creates the issue of potentially overburdening a very popular partner node, causing it to prematurely deplete its batteries to the detriment of the network's operational lifetime; this issue will be thoroughly investigated in the analysis presented in Chapters 8-11 of this thesis.

¹⁵The analysis in [19, 33] assumed infrastructure-based wireless networks such as a cellular network or wireless LAN (local area network), where the computational complexity of the proposed WLF matching algorithms would be acceptable. However, the low-complexity requirement for a distributed wireless sensor network is much more stringent, where nodes are highly resource and energy constrained compared to a base station in an infrastructure-based network.

and best partner choice to maximise the energy efficiency of cooperative communication. However, the majority of the studies reviewed in the previous section solely considered the performance of an individual cooperative communication link. In order to practically deploy cooperative communication in an energy-constrained wireless network, these two essential functions of partner selection and power control must be integrated into a robust strategy for coordinating network-wide cooperation among the network's nodes. Moreover, in a resource-constrained wireless sensor network, a simple cooperation strategy which enables individual sensor nodes to autonomously make energy efficient cooperation decisions is essential.

The ultimate goal of this thesis is to develop a distributed low-complexity cooperation strategy to extend the lifetime of a wireless sensor network by facilitating energy-conserving network-wide cooperation among its sensor nodes. Whereas a number of studies have previously investigated the problem of coordinating network-wide cooperation to improve the reliability of communication in a wireless LAN or cellular network [61–65], the problem of developing a network-wide cooperation strategy for an energy-constrained wireless network has been largely unaddressed in the existing literature. The few studies [18, 33, 66] which have considered some form of this research question are discussed in the remainder of this section, thus placing the original research presented in Chapters 7-11 of this thesis in the context of previous literature.

A centralised greedy cooperation algorithm was proposed in [18] for maximising the minimum node lifetime in an energy-constrained wireless network using cooperative communication, whereby a central controller performs a computationally intensive offline greedy search to allocate cooperation partners and transmit power for each node in the network. The algorithm in [18] iteratively allocates a partner node to each source node in the network by maximising the minimum node lifetime at each step, whereby transmission power is allocated to the cooperating source and partner nodes such that their projected lifetimes are equalised. However, the proposed cooperation algorithm is centralised and thus unsuitable for a distributed wireless sensor network. Importantly, the algorithm is also prohibitively computationally expensive for practical deployment in a resource-constrained wireless sensor network. By contrast, the goal of this thesis is to develop a distributed low-complexity network-wide cooperation strategy which enables resource-constrained sensor nodes to cooperate autonomously to extend the operational lifetime of the wireless sensor network. Nonetheless, the work published in [18] is the most similar in the existing literature to the original research on network-wide cooperation for extending wireless sensor network lifetime presented in Chapters 7-11 of this thesis (and published independently in [67, 68]). Consequently, the cooperation algorithm proposed in [18] will serve as a benchmark in Chapters 10 and 11 for evaluating the effectiveness

of the novel cooperation strategy presented in Chapter 7 of this thesis as a technique for extending the lifetime of a wireless sensor network¹⁶.

As discussed in Sections 2.4.2.1 and 2.4.2.2, the work in [33] is the most closely related in the existing literature to the original research on power allocation and partner choice strategies for energy efficient cooperation presented in this thesis. As [33] proposed a network-wide partner grouping algorithm along with a power allocation solution, it could likewise be considered to be a strategy for coordinating network-wide cooperation in an energy-constrained wireless network, as [18]. However, a direct comparison will not be presented between the power allocation and partner choice strategy proposed in [33] and the novel cooperation strategy developed in this thesis, due to the restrictive assumption of reciprocal cooperation underlying the work in [33]. The centralised cooperation algorithm proposed in [18], which allows non-reciprocal cooperation, thus serves as a better benchmark in this thesis. Moreover, the cooperation strategy in [33] was developed with the aim of minimising the total energy per transmission, which is similar to the design approach underlying the cooperation strategy proposed in this thesis. By contrast, the cooperation algorithm from [18] seeks to explicitly maximise network lifetime. Therefore, a comparison of the cooperation strategy developed in this thesis against that of [18] also offers valuable and interesting insight into the behaviour and performance of two fundamentally distinct approaches to coordinating cooperative communication in an energy-constrained wireless network.

In another line of research, a novel energy efficient selective single-relay cooperative diversity scheme (analogous to [29]) was proposed in [66]; for each message transmitted by the source, candidate relay nodes compete in a distributed contention process based on instantaneous channel quality and an explicit calculation of the energy consumption associated with the potential cooperative transmission. Two power control strategies to be employed by the candidate relay nodes were also proposed with the aim of (i) minimising the total transmit energy consumption per message, and (ii) maximising the minimum residual energy among all nodes in the network, subject to supporting a target data rate. As the cooperative diversity scheme proposed in [66] incorporates both a distributed relay selection protocol and a power allocation solution, it could also be considered to be a distributed strategy for coordinating network-wide cooperation. However, this scheme requires each candidate relay to acquire knowledge of instantaneous channel quality on a per-message basis and explicitly compute the power allocation and total transmit energy consumption of the potential cooperative transmission for the source node in order to participate in the distributed relay contention process. Importantly, the significant signalling

¹⁶Appendix A contains a detailed description of the algorithm proposed in [18] and notes regarding its implementation in generating the simulation results presented in Chapters 10 and 11 of this thesis.

and computational overhead involved with reselecting the relay on a per-message basis in this manner is highly undesirable in a resource-constrained wireless sensor network.

2.5 The Contributions of this Thesis

The original contributions of this thesis are presented in Chapters 3-11; aspects of this research have been published in [35, 38, 58, 67, 68]. The major contributions of this thesis may be summarised as follows:

- **Investigation of the optimal power allocation problem for energy efficient vMISO, DF, and aDF cooperation in Chapter 3.** The power allocation problem for energy efficient cooperation subject to a bit error rate constraint has not been studied previously in the literature for a general (non-clustered) cooperative link geometry and the general case of non-reciprocal cooperation.
- **Investigation of the partner choice region for energy efficient vMISO, DF, and aDF cooperation in Chapter 4.** The partner choice region is used as a tool for evaluating the energy conservation performance of each cooperative diversity scheme and predicting its robustness as a practical energy saving technique in a randomly deployed wireless sensor network with a wide range of potential partner locations. The partner choice region for achieving a given total communication energy saving for the general case of non-reciprocal cooperation has not been previously examined in the literature.
- **Comparison of the energy efficiency of three major cooperative diversity schemes to determine the best scheme to practically deploy in an energy-constrained wireless sensor network in Chapter 4.** The energy efficiency of vMISO, DF, and aDF cooperation is thoroughly compared across a wide range of communication system settings and cooperative link configurations, by examining each scheme's partner choice region as several key system parameters are varied. The results demonstrate that aDF is significantly superior to vMISO and DF. A thorough evaluation of the energy efficiency of major cooperative diversity schemes suitable for practical deployment in wireless sensor networks is absent from the existing literature.
- **Development of a simple yet near-optimal power allocation heuristic for energy efficient aDF cooperation in Chapter 5.** The proposed heuristic consists of two straightforward formulae suitable for practical implementation on a resource-constrained sensor node. By contrast, the power allocation solutions pro-

posed in the previous literature were obtained via a numerical search and are practically infeasible for sensor nodes.

- **Development of several distributed and simple partner choice heuristics for energy efficient aDF cooperation in Chapter 6.** The proposed heuristics are computationally efficient and based solely on measurements of average channel path loss, enabling resource-constrained sensor nodes to independently make cooperation decisions which conserve overall network energy. By contrast, only centralised partner matching algorithms which are prohibitively computationally expensive have been proposed in the existing literature.
- **Development of ECO-OP, a novel low-complexity distributed cooperation strategy for energy-constrained wireless sensor networks in Chapter 7.** ECO-OP is based on the power allocation and partner choice heuristics developed in Chapters 5 and 6, thereby enabling simple sensor nodes to cooperate autonomously to extend the lifetime of the wireless sensor network as a whole. To the best knowledge of the author, ECO-OP is the first distributed cooperation strategy for coordinating cooperative communication in an energy-constrained wireless network. Moreover, ECO-OP is a computationally efficient cooperation strategy with low signalling overhead and is thus suitable for practical implementation on resource-constrained sensor nodes.
- **Analysis of the behaviour and performance of network-wide cooperation using ECO-OP in three representative wireless sensor network topologies with respect to the resulting energy conservation in Chapters 8 and 9 and network lifetime extension in Chapters 10 and 11.** The analysis in Chapters 8 and 9 demonstrates that the distributed cooperation decisions made by individual nodes using ECO-OP constitute an effective network-wide cooperation strategy for reducing a wireless sensor network's energy consumption. The analysis of the long-term behaviour of ECO-OP in Chapters 10 and 11 serves to show that altruistic cooperation among autonomous resource-constrained sensor nodes using ECO-OP always significantly extends the lifetime of the wireless sensor network as a whole. This applies to both sparse and dense networks, with both random and directed data flow.
- **Comparison of ECO-OP with the centralised greedy cooperation algorithm from the literature [18] in Chapters 10 and 11.** The characteristic long-term behaviour and performance of these two fundamentally distinct approaches to coordinating cooperative communication in an energy-constrained wireless network are illustrated and analysed. Importantly, it is demonstrated that the

low-complexity distributed ECO-OP cooperation strategy proposed in this thesis overall achieves a comparable network lifetime improvement to the computationally intensive centralised cooperation algorithm from the literature.

2.6 Summary

In this chapter fundamental background material regarding the energy efficiency of cooperative diversity in wireless sensor networks has been presented. Following an overview of the major cooperative diversity schemes proposed in the literature, three cooperative diversity schemes (vMISO, DF, and aDF) which are feasible candidates for practical deployment in wireless sensor networks have been identified. The BER expressions characterising the performance of these three cooperative diversity schemes in a wireless Rayleigh fading channel have been specified.

The energy model of wireless communication employed throughout this thesis has also been presented. The total energy consumption of wireless communication is assumed to consist of two dominant components: the transmission energy cost and the transceiver circuit energy consumption. The total energy consumption per bit over the cooperative communication link has been characterised for each cooperative diversity scheme of interest to this thesis, by considering the energy consumed by the source, partner, and destination receiver. The energy efficiency of cooperative communication has been defined as the percentage energy saving achieved over the communication link via cooperation.

Importantly, it has been shown that a positive cooperative energy saving is obtained only once the reduction in the total transmission energy due to cooperative diversity is greater than the overhead of the increased circuit energy consumption of cooperation. Whereas circuit energy is a fixed overhead, transmission energy is a function of transmission distance. Thus cooperative communication becomes energy efficient beyond a threshold source-destination separation. Importantly, it has also been demonstrated that very significant energy savings are achieved by cooperation as the source-destination separation is increased past this break-even transmission distance. Therefore, provided the source-destination transmission range is beyond a certain threshold, cooperative communication has the potential to significantly reduce the total energy cost of wireless communication in a sensor network.

Finally, a literature review has been presented in this chapter, focusing on the central areas of interest to this thesis: the energy efficiency of cooperative diversity, optimal power allocation and partner choice for cooperative communication, and strategies for coordinating network-wide cooperative communication. The major original contributions of this thesis, presented in Chapters 3-11, have also been highlighted in this chapter.

The energy model and BER performance of cooperative communication presented in this chapter form the basis for the analysis presented in Chapter 3, where the problem of optimal transmit power allocation for energy efficient vMISO, DF, and aDF cooperation is investigated. The energy efficiency of these three candidate cooperative diversity schemes will then be thoroughly compared in Chapter 4, in order to determine which is the best scheme to practically deploy in an energy-constrained wireless sensor network.

Chapter 3

Power Allocation for Energy Efficient Cooperation

3.1 Introduction

In this chapter the optimally energy efficient allocation of transmission power is determined for the three major cooperative diversity schemes considered in this thesis: vMISO, DF, and aDF. The concept of applying cooperative diversity to wireless sensor networks to increase the energy efficiency of wireless communication was introduced in Chapter 2. This energy efficiency improvement is achieved via the reduction in the total transmission energy required for reliable communication resulting from cooperative diversity. Thus the proper allocation of transmit power to the cooperating source and partner nodes is crucial for fully exploiting the energy saving potential of cooperative communication. The optimal allocation of transmit power¹ to the cooperating source and its partner is defined to be that which minimises the overall energy consumed by the cooperative communication system, while achieving reliable communication.

The power allocation solution for a non-cooperative communication system is firstly presented in Section 3.2 to serve as a basis for comparison. Secondly, the power allocation solution for an ideal cooperative diversity system with a perfect source-partner channel is presented in Section 3.3 to establish the upper limit of the transmission energy reduction achievable via cooperation. Finally, the problem of transmit power allocation for optimally energy efficient vMISO, DF, and aDF cooperation is studied in Sections 3.4, 3.5, and 3.6, respectively. Throughout the chapter these power allocation solutions are illustrated in terms of network geometry for a fixed source node and destination receiver and a range of potential partner locations, using (2.12) to map the path loss values L_{s-d} , L_{s-p} , and L_{p-d}

¹It should be noted that although this thesis refers to the problem of transmit power allocation, the optimal allocation of transmit energy per bit rather than power is studied in this chapter, as the (arbitrary) bit rate R_b is fixed in the analysis.

to transmission distances d_{s-d} , d_{s-p} , and d_{p-d} respectively. This facilitates an analysis and comparison of the nature of the power allocation solution for each cooperative diversity scheme. It should be noted that this analysis is based on the set of reference cooperative system parameters employed throughout this thesis and listed in Table 2.1.

The power allocation solutions developed in this chapter are used in Chapter 4 to investigate the total energy savings achieved by the three cooperative diversity schemes via the partner choice region for energy efficient cooperation. The analysis in Chapter 4 thus ultimately enables a through comparison of vMISO, DF, and aDF across a wide range of network configurations to determine which is the best scheme to practically deploy in an energy-constrained wireless sensor network.

3.2 Non-Cooperative Communication

The problem of transmit power allocation for optimally energy efficient non-cooperative communication may be formally expressed as the constrained minimisation problem

$$\underset{E_{tx-s-non-coop}}{\operatorname{argmin}} \{E_{non-coop}\}, \text{ subject to } BER_{non-coop} \leq p_b, \quad (3.1)$$

where $E_{non-coop}$ is given by (2.13) and $BER_{non-coop}$ is given by (2.5). The transmit energy per bit of the non-cooperating source, $E_{tx-s-non-coop}$, may be expressed as

$$E_{tx-s-non-coop} = \frac{\eta}{\xi} P_{PA-source-non-coop} / R_b. \quad (3.2)$$

The objective function and constraint in (3.1) may be expressed explicitly in terms of the decision variable $E_{tx-s-non-coop}$ as

$$E_{non-coop} = \frac{\xi}{\eta} E_{tx-s-non-coop} + \left(P_{CCT-tx} + P_{CCT-rx} \right) / R_b, \quad (3.3)$$

$$BER_{non-coop} \approx \frac{N_0 L_{s-d}}{4 E_{tx-s-non-coop}}, \quad (3.4)$$

where SNR_{s-d} is related to $E_{tx-s-non-coop}$ using (2.11) and (3.2),

$$SNR_{s-d} = \frac{E_{tx-s-non-coop}}{N_0 L_{s-d}}. \quad (3.5)$$

It is then straightforward to show that the optimally energy efficient transmit power allocation for a non-cooperative communication system, $E_{tx-s-opt-non-coop}$, is given by

$$E_{tx-s-opt-non-coop} = \frac{N_0 L_{s-d}}{4 p_b}. \quad (3.6)$$

For the reference system parameters adopted in this thesis (Table 2.1), the transmit energy per bit for non-cooperative source-destination communication equates to around $294\mu\text{J}$.

3.3 Ideal Cooperative Diversity

A finite amount of transmission energy must be spent for the information exchange between the source and partner in all practical cooperative diversity schemes. This source-partner transmission energy represents an overhead of cooperation and thus decreases the energy savings otherwise achieved via spatial diversity gains. Therefore, the transmit power allocation solution for a cooperative diversity system with a perfect source-partner channel² is presented in this section in order to establish the upper limit of the transmission energy reduction achievable via cooperation. For convenience, this hypothetical scheme is referred to as “ideal cooperative diversity” in this chapter. This solution will also be employed in analysing the nature of the power allocation solutions for vMISO, DF, and aDF presented in the subsequent sections.

3.3.1 Problem Formulation

The problem of transmit power allocation for optimally energy efficient cooperative communication with a perfect source-partner channel (i.e. ideal cooperative diversity) may be formulated as the constrained minimisation problem

$$\underset{E_{tx-s}, E_{tx-p}}{\operatorname{argmin}} \{E_{coop-ideal}\}, \text{ subject to } BER_{coop-ideal} \leq p_b, \quad (3.7)$$

where $BER_{coop-ideal}$ is given by (2.6) and $E_{coop-ideal}$ is defined as

$$E_{coop-ideal} = \left(P_{PA-source-coop} + P_{PA-partner-coop} \right) / R_b, \quad (3.8)$$

where $P_{PA-source-coop}$ and $P_{PA-partner-coop}$ represent the transmission power of the cooperating source and partner respectively. It should be noted that the transceiver circuit energy overhead of practical cooperation has been deliberately excluded in defining $E_{coop-ideal}$ since it is not relevant in considering the transmit power allocation of ideal cooperative diversity. Finally, the cooperative transmit energies per bit of the source and partner, E_{tx-s} and E_{tx-p} respectively, may be expressed as

$$E_{tx-s} = \frac{\eta}{\xi} P_{PA-source-coop} / R_b, \quad (3.9)$$

²It is assumed that there is no signal attenuation due to path loss on the “perfect” source-partner channel (i.e. $L_{s-p} = 0$).

$$E_{tx-p} = \frac{\eta}{\xi} P_{PA-partner-coop} / R_b. \quad (3.10)$$

3.3.2 Optimum Solution

The objective function and constraint in (3.7) may be expressed explicitly in terms of the decision variables E_{tx-s} and E_{tx-p} as follows. Substituting (3.9), (3.10) into (3.8), $E_{coop-ideal}$ may be restated as

$$E_{coop-ideal} = \frac{\xi}{\eta} (E_{tx-s} + E_{tx-p}) . \quad (3.11)$$

Furthermore, SNR_{s-d} and SNR_{p-d} may be related to E_{tx-s} and E_{tx-p} using (2.11) and (3.9) and (3.10) respectively,

$$SNR_{s-d} = \frac{E_{tx-s}}{N_0 L_{s-d}}, \quad (3.12)$$

$$SNR_{p-d} = \frac{E_{tx-p}}{N_0 L_{p-d}}. \quad (3.13)$$

Substituting (3.12) and (3.13) into (2.6), $BER_{coop-ideal}$ may be restated as

$$BER_{coop-ideal} = \frac{3N_0^2 L_{s-d} L_{p-d}}{16E_{tx-s} E_{tx-p}}. \quad (3.14)$$

Thus E_{tx-p} may be expressed as a function of E_{tx-s} and the $BER_{coop-ideal}$ constraint in (3.7) by rearranging (3.14):

$$E_{tx-p} = \frac{3N_0^2 L_{s-d} L_{p-d}}{16p_b E_{tx-s}}. \quad (3.15)$$

Finally, by substituting (3.11), (3.14), (3.15) into (3.7), the ideal cooperative diversity optimal power allocation problem may be stated as

$$\operatorname{argmin}_{E_{tx-s}} \left\{ \frac{\xi}{\eta} \left(E_{tx-s} + \frac{3N_0^2 L_{s-d} L_{p-d}}{16p_b E_{tx-s}} \right) \right\} . \quad (3.16)$$

Equation (3.16) is solved for the optimally energy efficient power allocation for the source-destination transmission, $E_{tx-s-opt-ideal}$, by differentiating the objective function with respect to E_{tx-s} and setting it to zero, giving

$$E_{tx-s-opt-ideal} = \sqrt{\frac{3N_0^2 L_{s-d} L_{p-d}}{16p_b}}. \quad (3.17)$$

The optimally energy efficient power allocation for the partner-destination transmission, $E_{tx-p-opt-ideal}$, is then obtained by substituting (3.17) into (3.15), giving

$$E_{tx_p_opt_ideal} = \sqrt{\frac{3N_0^2 L_{s-d} L_{p-d}}{16p_b}}. \quad (3.18)$$

Comparing (3.17) and (3.18), it is interesting to note that equal transmit power allocation is optimal for energy efficient ideal cooperative diversity. The total transmit energy consumption of ideal cooperative diversity may thus be expressed as

$$E_{tx_TOTAL_coop_ideal} = 2\sqrt{\frac{3N_0^2 L_{s-d} L_{p-d}}{16p_b}}. \quad (3.19)$$

3.3.3 Discussion of the Optimum Solution

The power allocation solution for ideal cooperative diversity is illustrated alongside that of non-cooperative communication in Fig. 3.1 for the reference system given in Table 2.1 for a range of partner node locations. A one-dimensional³ cooperative communication link configuration is considered, with the partner node being located somewhere on the straight line passing through the source node and the destination receiver. The partner's location is specified in Fig. 3.1 in terms of its distance from the destination receiver, normalised by the source-destination separation (e. g. the partner and source are co-located when $d_{p-d}/d_{s-d} = 1$). Fig. 3.1 demonstrates that ideal cooperative diversity yields the highest reduction in total transmit energy the closer the partner is to the destination receiver (i.e. $d_{p-d}/d_{s-d} \rightarrow 0$); this follows from (3.19) which shows that $E_{tx_TOTAL_coop_ideal}$ approaches zero as $L_{p-d} \rightarrow 0$. Secondly, Fig. 3.1 shows that ideal cooperative diversity is energy efficient provided the partner-destination separation is less than about 3.5 times that of the source-destination separation (i.e. $|d_{p-d}/d_{s-d}| < 3.5$), which corresponds to the condition of $E_{tx_TOTAL_coop_ideal} < E_{tx_s_opt_non-coop}$. Substituting (2.12) into (3.6) and (3.19), this condition indicates that the maximum partner-destination separation for energy efficient ideal cooperative diversity is given by

$$d_{p-d_MAX} = \sqrt[k]{\frac{1}{12p_b}} (d_{s-d}), \quad (3.20)$$

which confirms that $d_{p-d_MAX}/d_{s-d} \approx 3.5$ for the reference system parameters of $k=3.5$ and $p_b=10^{-3}$.

³It should be noted that the special case of a one-dimensional cooperative link configuration is considered here solely for ease of demonstration; the general case of a two-dimensional cooperative link geometry will be considered in subsequent chapters of this thesis.

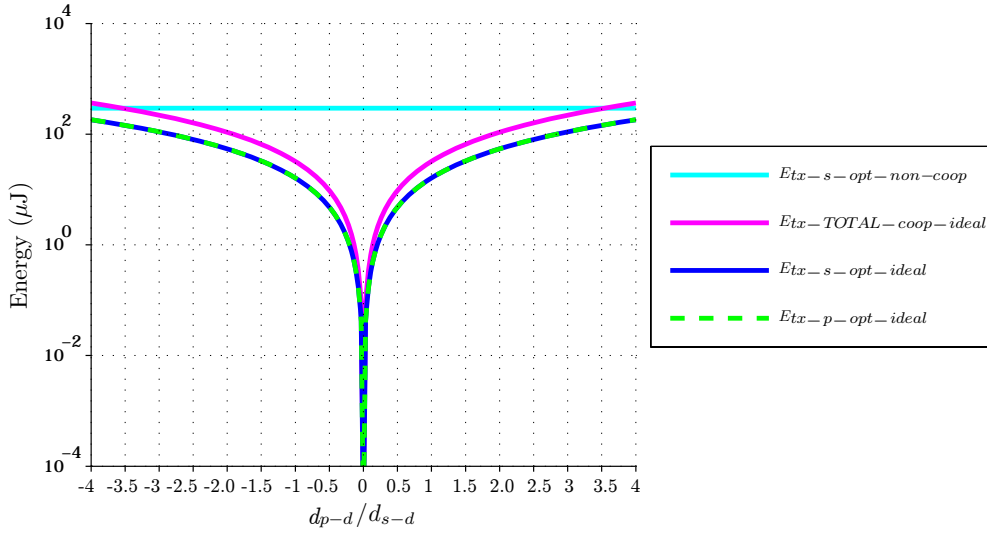


Figure 3.1: Optimally energy efficient transmit power allocation solution for ideal cooperative diversity (with an ideal source-partner channel) vs. partner location.

3.4 Virtual-MISO

3.4.1 Problem Formulation

The problem of transmit power allocation for optimally energy efficient vMISO cooperation may be formulated as the constrained minimisation problem

$$\underset{E_{tx_{s-p}}, E_{tx_{s}}, E_{tx_{p}}}{\operatorname{argmin}} \{E_{coop_vMISO}\}, \text{ subject to } BER_{coop_vMISO} \leq p_b, \quad (3.21)$$

where E_{coop_vMISO} is given by (2.14) and BER_{coop_vMISO} is given by (2.2). The transmit energy per bit of the source for its preliminary communication with the partner, $E_{tx_{s-p}}$, may be expressed as

$$E_{tx_{s-p}} = \frac{\eta}{\xi} P_{PA_{s-p}} / R_b, \quad (3.22)$$

3.4.2 Optimum Solution

The objective function and constraint in (3.21) may be expressed explicitly in terms of the decision variables $E_{tx_{s-p}}$, $E_{tx_{s}}$, and $E_{tx_{p}}$ as follows. Substituting (3.9), (3.10), and (3.22) into (2.14), E_{coop_vMISO} may be restated as

$$E_{coop_vMISO} = \frac{\xi}{\eta} (E_{tx_{s-p}} + E_{tx_{s}} + E_{tx_{p}}) + (3P_{CCT_tx} + 2P_{CCT_rx}) / R_b. \quad (3.23)$$

Using (2.11) and (3.22) SNR_{s-p} may be related to $E_{tx_{s-p}}$ as

$$SNR_{s-p} = \frac{E_{tx_{s-p}}}{N_0 L_{s-p}}, \quad (3.24)$$

whereas SNR_{s-d} and SNR_{p-d} are related to E_{tx-s} and E_{tx-p} as given by (3.12) and (3.13) respectively. Substituting (2.6), (2.7), (3.12), (3.13), and (3.24) into (2.2), $BER_{coop-vMISO}$ may be restated as

$$BER_{coop-vMISO} = \frac{3N_0^2 L_{s-d} L_{p-d}}{16E_{tx-s} E_{tx-p}}, \text{ subject to } E_{tx-s-p} \geq \frac{N_0 L_{s-p}}{4p_{s-p}}. \quad (3.25)$$

As in ideal cooperative diversity, E_{tx-p} is related to E_{tx-s} and the $BER_{coop-vMISO}$ constraint as given by (3.15). Finally, by substituting (3.23), (3.25), (3.15) into (3.21), the vMISO optimal power allocation problem may be stated as

$$\begin{aligned} \underset{E_{tx-s-p}, E_{tx-s}}{\operatorname{argmin}} \left\{ \frac{\xi}{\eta} \left(E_{tx-s-p} + E_{tx-s} + \frac{3N_0^2 L_{s-d} L_{p-d}}{16p_b E_{tx-s}} \right) + (3P_{CCT-tx} + 2P_{CCT-rx}) / R_b \right\}, \\ \text{subject to } E_{tx-s-p} \geq \frac{N_0 L_{s-p}}{4p_{s-p}}, \end{aligned} \quad (3.26)$$

Solving (3.26) for the optimally energy efficient power allocation for the vMISO source-destination transmission, $E_{tx-s-opt-vMISO}$, and the vMISO partner-destination transmission, $E_{tx-p-opt-vMISO}$, results in the identical power allocation to that derived for ideal cooperative diversity, giving

$$E_{tx-s-opt-vMISO} = \sqrt{\frac{3N_0^2 L_{s-d} L_{p-d}}{16p_b}}, \quad (3.27)$$

$$E_{tx-p-opt-vMISO} = \sqrt{\frac{3N_0^2 L_{s-d} L_{p-d}}{16p_b}}. \quad (3.28)$$

Finally, the optimally energy efficient power allocation for the preliminary source-partner transmission in vMISO, $E_{tx-s-p-opt-vMISO}$, is obtained by satisfying the constraint in (3.26), giving

$$E_{tx-s-p-opt-vMISO} = \frac{N_0 L_{s-p}}{4p_{s-p}}. \quad (3.29)$$

Therefore, combining (3.27), (3.28), and (3.29), the total transmit energy consumption of vMISO cooperation may be expressed as

$$E_{tx-TOTAL-coop-vMISO} = 2\sqrt{\frac{3N_0^2 L_{s-d} L_{p-d}}{16p_b}} + \frac{N_0 L_{s-p}}{4p_{s-p}}. \quad (3.30)$$

3.4.3 Discussion of the Optimum Solution

The power allocation solution for the vMISO cooperative diversity scheme is illustrated in Fig. 3.2 for the reference system given in Table 2.1 for a range of partner node locations. The non-cooperative communication and ideal cooperative diversity power allocation solutions are also shown in Fig. 3.2 for comparison. As in Fig. 3.1, a one-dimensional cooperative link geometry is considered, with the partner node being located somewhere on the straight line passing through the source node and the destination receiver.

Fig. 3.2 clearly demonstrates that the information exchange between the source and the partner accounts for the most significant transmit energy consumption in vMISO. Thus Fig. 3.2 shows that vMISO yields a reduction in the total transmit energy expenditure provided the source-partner separation is less than about half the source-destination separation (i.e. $|(d_{s-d} - d_{p-d})/d_{s-d}| < 0.5$), which corresponds to the condition of $E_{tx_TOTAL_coop_vMISO} < E_{tx_s_opt_non-coop}$, with $E_{tx_TOTAL_coop_vMISO} \approx E_{tx_s-p_opt_vMISO}$. Substituting (2.12) into (3.6) and (3.29), this condition indicates that the maximum source-partner separation for energy efficient vMISO cooperation⁴ is given by

$$d_{s-p_MAX} = \sqrt[k]{\frac{p_{s-p}}{p_b}} (d_{s-d}), \quad (3.31)$$

which confirms that $d_{s-p_MAX}/d_{s-d} \approx 0.5$ for the reference system parameters of $k=3.5$, $p_b=10^{-3}$, and $p_{s-p}=10^{-4}$. Therefore, the non-ideal source-partner channel limits the energy efficiency of vMISO cooperation such that only a very restricted range of partner node locations close to the source node are beneficial.

Furthermore, Fig. 3.2 demonstrates that the highest energy efficiency of vMISO cooperation corresponds to the partner node being very close to the source node (i.e. $d_{p-d}/d_{s-d} \approx 1$), when the source-partner transmit energy consumption is very small. Under this condition, the total transmit energy of vMISO cooperation may be approximated by the sum of the cooperative transmit energy of the source and partner, which is equivalent to the total transmit energy of ideal cooperative diversity given by (3.19).

⁴Only the transmit energy consumption is considered here. This is equivalent to assuming that the transceiver circuit energy consumption is negligible.

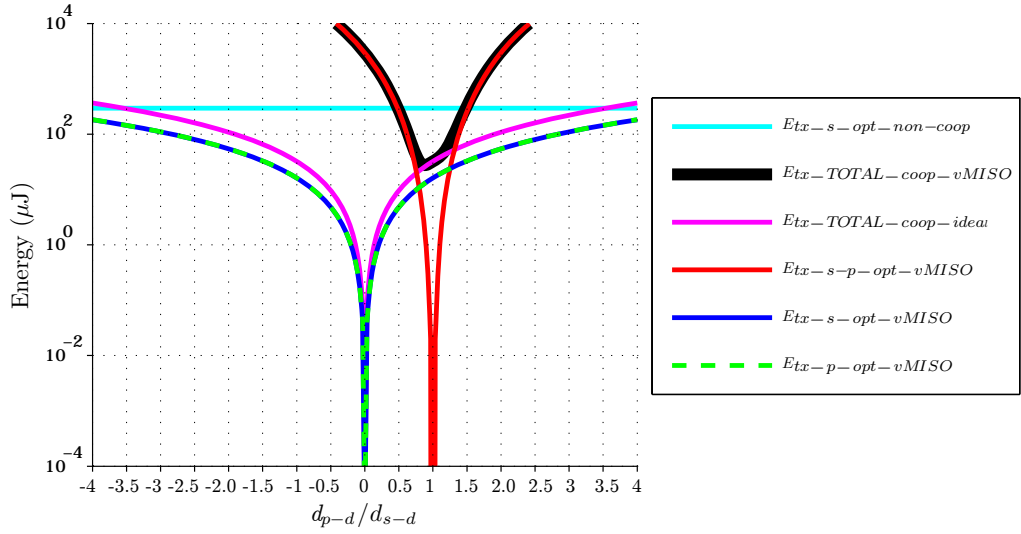


Figure 3.2: Optimally energy efficient transmit power allocation solution for vMISO cooperation vs. partner location.

3.5 Decode-and-Forward

3.5.1 Problem Formulation

The problem of transmit power allocation for optimally energy efficient DF cooperation may be formulated as the constrained minimisation problem

$$\underset{E_{tx-s}, E_{tx-p}}{\operatorname{argmin}} \{E_{coop-DF}\}, \text{ subject to } BER_{coop-DF} \leq p_b, \quad (3.32)$$

where $E_{coop-DF}$ is given by (2.15) and $BER_{coop-DF}$ is given by (2.3).

3.5.2 Optimum Solution

The objective function and constraint in (3.32) may be expressed explicitly in terms of the decision variables E_{tx-s} and E_{tx-p} as follows. Substituting (3.9), (3.10) into (2.15), $E_{coop-DF}$ may be re-expressed as

$$E_{coop-DF} = \frac{\xi}{\eta} (E_{tx-s} + E_{tx-p}) + (2P_{CCT-tx} + 3P_{CCT-rx}) / R_b. \quad (3.33)$$

Using (2.11) and (3.9) SNR_{s-p} in DF may be related to E_{tx-s} ,

$$SNR_{s-p} = \frac{E_{tx-s}}{N_0 L_{s-p}}, \quad (3.34)$$

whereas SNR_{s-d} and SNR_{p-d} are related to E_{tx-s} and E_{tx-p} as given by (3.12) and (3.13) respectively. Similarly to (3.25), $BER_{coop-DF}$ may be restated as

$$BER_{coop-DF} = \frac{3N_0^2 L_{s-d} L_{p-d}}{16E_{tx-s} E_{tx-p}}, \text{ subject to } E_{tx-s} \geq \frac{N_0 L_{s-p}}{4p_{s-p}}. \quad (3.35)$$

As in vMISO, E_{tx-p} is related to E_{tx-s} and the $BER_{coop-DF}$ constraint as given by (3.15). Finally, by substituting (3.33), (3.35), (3.15) into (3.32), the DF optimal power allocation problem may be stated as

$$\begin{aligned} \underset{E_{tx-s}}{\operatorname{argmin}} \left\{ \frac{\xi}{\eta} \left(E_{tx-s} + \frac{3N_0^2 L_{s-d} L_{p-d}}{16p_b E_{tx-s}} \right) + (2P_{CCT-tx} + 3P_{CCT-rx}) / R_b \right\}, \\ \text{subject to } E_{tx-s} \geq \frac{N_0 L_{s-p}}{4p_{s-p}}, \end{aligned} \quad (3.36)$$

Equation (3.36) is solved as follows. Differentiating the objective function with respect to E_{tx-s} and setting it to zero gives

$$E_{tx-s} = \sqrt{\frac{3N_0^2 L_{s-d} L_{p-d}}{16p_b}}. \quad (3.37)$$

However, the E_{tx-s} constraint in (3.36) must also be satisfied. Thus the optimally energy efficient power allocation for the DF source-destination transmission, $E_{tx-s-opt-DF}$, is given by

$$E_{tx-s-opt-DF} = \max \left\{ \sqrt{\frac{3N_0^2 L_{s-d} L_{p-d}}{16p_b}}, \frac{N_0 L_{s-p}}{4p_{s-p}} \right\}. \quad (3.38)$$

The optimally energy efficient power allocation for the DF partner-destination transmission, $E_{tx-p-opt-DF}$, can then be obtained by substituting (3.38) into (3.15), giving

$$E_{tx-p-opt-DF} = \frac{3N_0^2 L_{s-d} L_{p-d}}{16p_b E_{tx-s-opt-DF}}. \quad (3.39)$$

Therefore, combining (3.38) and (3.39), the total transmit energy consumption of DF cooperation may be expressed as

$$E_{tx-TOTAL-coop-DF} = \begin{cases} 2\sqrt{\frac{3N_0^2 L_{s-d} L_{p-d}}{16p_b}} & , \text{ if } L_{s-p} < \left(p_{s-p} \sqrt{\frac{3L_{s-d} L_{p-d}}{p_b}} \right) \\ \frac{N_0 L_{s-p}}{4p_{s-p}} + \frac{3p_{s-p} N_0 L_{s-d} L_{p-d}}{4p_b L_{s-p}} & , \text{ otherwise.} \end{cases} \quad (3.40)$$

3.5.3 Discussion of the Optimum Solution

The power allocation solution for the DF cooperative diversity scheme is illustrated in Fig. 3.3 for the reference system given in Table 2.1 for a range of partner node locations. The non-cooperative communication and ideal cooperative diversity power allocation solutions are also shown in Fig. 3.3 for comparison. As in Fig. 3.1, a one-dimensional cooperative link geometry is considered, with the partner node being located somewhere on the straight line passing through the source node and the destination receiver.

Comparing Fig. 3.3 and Fig. 3.2 reveals that the DF source transmit power allocation is very similar to the vMISO source-partner transmit power allocation. This indicates that the DF source power consumption is dominated by ensuring a good source-partner channel. Moreover, the total transmission energy consumption of DF cooperation may be approximated to the dominant energy expenditure associated with the source-partner transmission. Thus, like vMISO, DF cooperation only results in a reduction of the transmit energy consumption for a very limited range of partner node locations close to the source node. The maximum source-partner separation for energy efficient DF cooperation is thus also given by (3.31). Fig. 3.3 also demonstrates that, as for vMISO, for a good source-partner channel (i.e. $d_{p-d}/d_{s-d} \approx 1$) the total transmit energy of DF cooperation may be approximated by the sum of the cooperative transmit energy of the source and partner, which is equivalent to the total transmit energy of ideal cooperative diversity given by (3.19).

Finally, the energy advantage of DF avoiding an explicit source-partner transmission is evident in comparing the DF source power allocation in Fig. 3.3 with the total vMISO source power allocation in Fig. 3.2. It can also be observed from Figs. 3.2 and 3.3 that the transmit energy expenditure of the partner node in DF is generally much lower than for vMISO for a given partner location. This reveals a further energy advantage of DF over vMISO resulting from replacing the separate source-partner and source-destination transmissions in vMISO by a single broadcast message in DF.

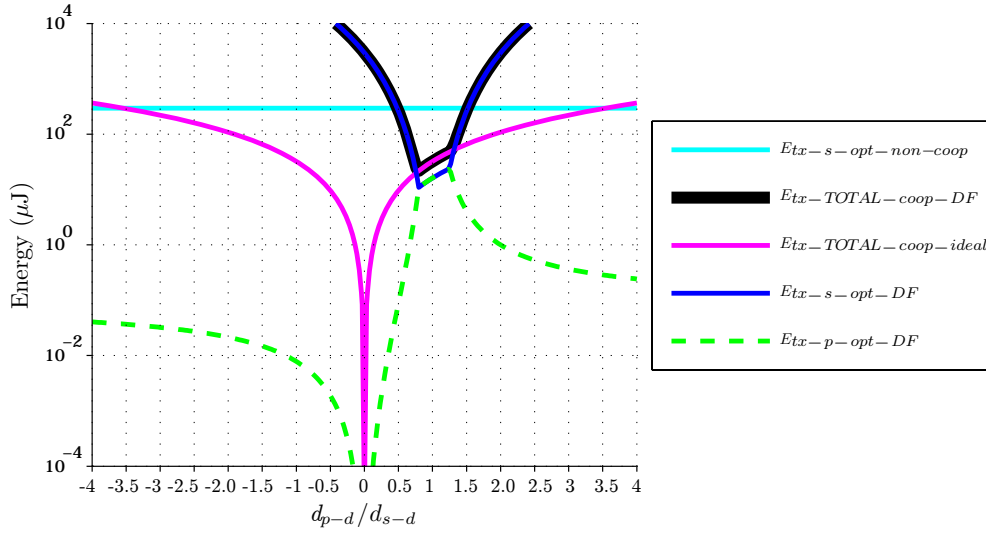


Figure 3.3: Optimally energy efficient transmit power allocation solution for DF cooperation vs. partner location.

3.6 Adaptive Decode-and-Forward

3.6.1 Problem Formulation

The problem of transmit power allocation for optimally energy efficient aDF cooperation may be formulated as the constrained minimisation problem

$$\underset{E_{tx-s}, E_{tx-p}}{\operatorname{argmin}} \{E_{coop-aDF}\}, \text{ subject to } BER_{coop-aDF} \leq p_b, \quad (3.41)$$

where $E_{coop-aDF}$ is given by (2.16) and $BER_{coop-aDF}$ is given by (2.4).

3.6.2 Optimum Solution

The objective function and constraint in (3.41) may be expressed explicitly in terms of the decision variables E_{tx-s} and E_{tx-p} as follows. In aDF, SNR_{s-p} , SNR_{s-d} , and SNR_{p-d} are related to E_{tx-s} and E_{tx-p} as given by (3.34), (3.12) and (3.13), respectively. Substituting (3.9), (3.10), (2.8), (3.34) into (2.16), $E_{coop-aDF}$ may be re-expressed as

$$E_{coop-aDF} = \frac{\xi}{\eta} E_{tx-s} + \frac{\xi}{\eta} \left(1 - \frac{KN_0 L_{s-p}}{E_{tx-s}}\right) E_{tx-p} + \left(2 - \frac{KN_0 L_{s-p}}{E_{tx-s}}\right) \frac{P_{CCT-tx}}{R_b} + \left(3 - \frac{KN_0 L_{s-p}}{E_{tx-s}}\right) \frac{P_{CCT-rx}}{R_b}. \quad (3.42)$$

Similarly, substituting (2.5), (2.6), (2.8), (3.12), (3.13), (3.34) into (2.4), $BER_{coop-aDF}$ may be restated as

$$BER_{coop-aDF} = \frac{KN_0^2 L_{s-d} L_{s-p}}{4E_{tx-s}^2} + \left(1 - \frac{KN_0 L_{s-p}}{E_{tx-s}}\right) \frac{3N_0^2 L_{s-d} L_{p-d}}{16E_{tx-s} E_{tx-p}}. \quad (3.43)$$

Thus E_{tx-p} may be expressed as a function of E_{tx-s} and the $BER_{coop-aDF}$ constraint in (3.41) by rearranging (3.43):

$$E_{tx-p} = \frac{\left(1 - \frac{KN_0 L_{s-p}}{E_{tx-s}}\right) 3N_0^2 L_{s-d} L_{p-d}}{16E_{tx-s} \left(p_b - \frac{KN_0^2 L_{s-d} L_{s-p}}{4E_{tx-s}^2}\right)}. \quad (3.44)$$

Finally, by substituting (3.42), (3.44) into (3.41), the aDF optimal power allocation problem may be stated as

$$\underset{E_{tx-s}}{\operatorname{argmin}} \left\{ \begin{array}{l} \frac{\xi}{\eta} E_{tx-s} + \frac{\xi}{\eta} \frac{\left(1 - \frac{KN_0 L_{s-p}}{E_{tx-s}}\right)^2 3N_0^2 L_{s-d} L_{p-d}}{16E_{tx-s} \left(p_b - \frac{KN_0^2 L_{s-d} L_{s-p}}{4E_{tx-s}^2}\right)} + \\ \left(2 - \frac{KN_0 L_{s-p}}{E_{tx-s}}\right) \frac{P_{CCT-tx}}{R_b} + \left(3 - \frac{KN_0 L_{s-p}}{E_{tx-s}}\right) \frac{P_{CCT-rx}}{R_b} \end{array} \right\}. \quad (3.45)$$

It is evident from (3.45) that the aDF energy efficient power allocation problem is non-linear with respect to the decision variable E_{tx-s} . Thus in the absence of a straightforward analytical solution, a numerical search is employed to solve (3.45) for $E_{tx-s-opt-aDF}$, the optimally energy efficient power allocation for the aDF source-destination transmission. The optimally energy efficient power allocation for the aDF partner-destination transmission, $E_{tx-p-opt-aDF}$, is then given by (3.44) with $E_{tx-s} = E_{tx-s-opt-aDF}$. Finally, it follows that the total transmit energy consumption of aDF cooperation may be expressed as

$$E_{tx-TOTAL-coop-aDF} = E_{tx-s-opt-aDF} + \left(1 - \frac{KN_0 L_{s-p}}{E_{tx-s-opt-aDF}}\right) E_{tx-p-opt-aDF} \quad (3.46)$$

3.6.3 Discussion of the Optimum Solution

The search-based optimum solution for the aDF source and partner power allocation is illustrated in Fig. 3.4 for the reference system given in Table 2.1 for a range of partner node locations. Additionally, Fig. 3.5 shows the corresponding probability of the partner retransmitting the source's message (having successfully decoded it), $(1 - BLER_{s-p})$, which represents the quality of the source-partner channel. The non-cooperative communication

and ideal cooperative diversity power allocation solutions are also shown in Fig. 3.4 for comparison. As in Fig. 3.1, a one-dimensional cooperative link geometry is considered, with the partner node being located somewhere on the straight line passing through the source node and the destination receiver.

Fig. 3.4 shows that the optimal total transmit energy for aDF is lowest when the partner is located roughly midway between the source and the destination (i.e. $d_{p-d}/d_{s-d} \approx 0.5$), and generally increases the further away the partner is from the source-destination link. This suggests that optimal transmit power allocation for aDF must achieve a balance between ensuring a good source-partner channel and a good partner-destination channel. Namely, aDF transmit energy consumption is not solely dominated by the source-partner channel as in vMISO and DF. Fig. 3.1 also demonstrates that, as for vMISO and DF, the total transmit energy of aDF cooperation is closely approximated by the total transmit energy of ideal cooperative diversity given by (3.19) for a good source-partner channel. A good source-partner channel corresponds to a high probability of the partner retransmitting the source's message; Fig. 3.5 confirms that $(1 - BLER_{s-p}) \approx 1$ for $0.5 \lesssim (d_{p-d}/d_{s-d}) \lesssim 1.5$.

Importantly, it is clear from Fig.3.4 that aDF cooperation achieves a reduction in total transmit energy consumption for a much wider range of partner node locations than vMISO and DF (i.e. $-2.5 < ((d_{p-d})/d_{s-d}) < 3.5$). This is a reflection of the adaptivity of the aDF scheme, whereby the partner node only retransmits the packets it overheard correctly from the source, making cooperation beneficial despite a non-ideal source-partner channel. Moreover, Fig. 3.4 indicates that the energy efficiency of aDF cooperation is limited both by the partner-destination channel (with the maximum partner-destination separation being $3.5d_{s-d}$, as given by (3.20)) and by the source-partner channel (with the maximum source-partner separation being $3.5d_{s-d}$, which corresponds to $(1 - BLER_{s-p}) = 0$ for $(d_{p-d}/d_{s-d}) < -2.5$ in Fig. 3.5). This is further evidence that the partner-destination and source-partner links are equally important factors in determining the energy efficiency of aDF cooperation.

Finally, Fig. 3.4 shows that the source transmit energy dominates the total aDF power allocation. Fig. 3.4 also demonstrates that the average partner transmit energy consumption, given by $((1 - BLER_{s-p}) E_{tx-p-opt-aDF})$, generally increases the further away the partner is from the destination, unless there is a low probability of re-transmission. Namely, a partner node located far from the source node re-transmits infrequently and thus consumes less transmit energy on average.

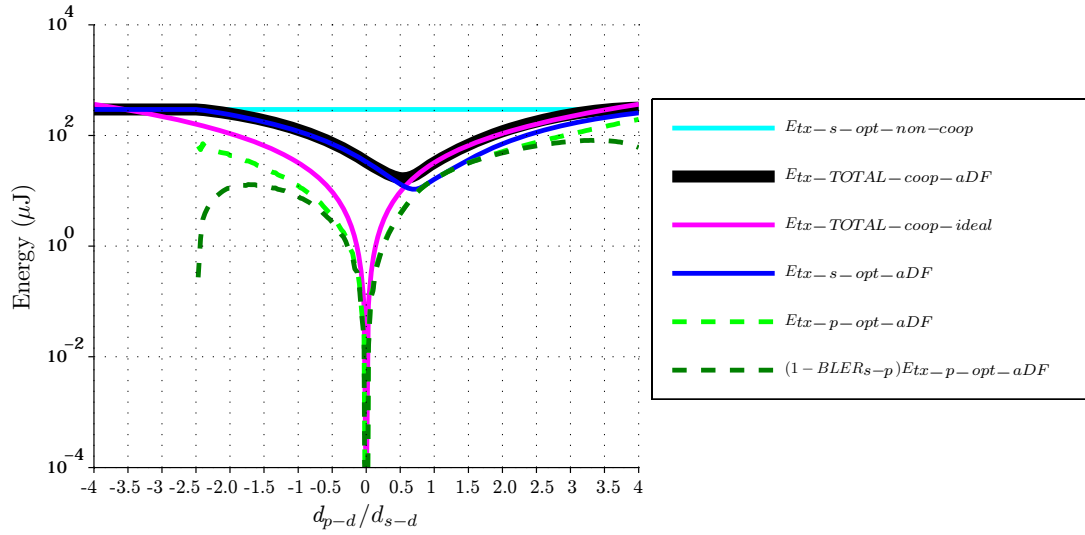


Figure 3.4: Optimally energy efficient transmit power allocation for aDF cooperation vs. partner location.

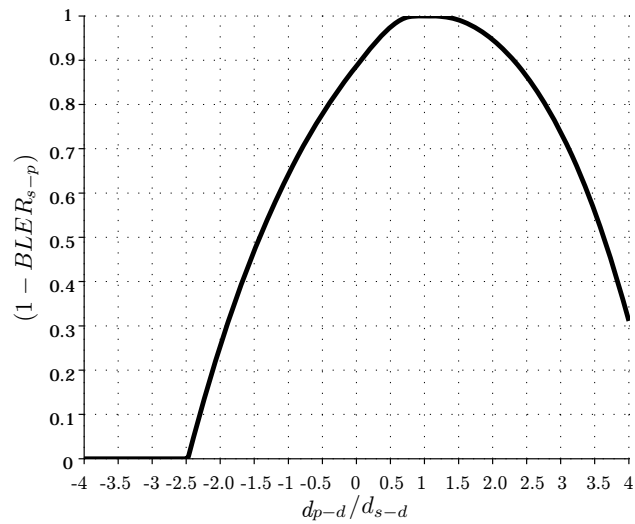


Figure 3.5: Probability of partner retransmitting the source's message in aDF with optimally energy efficient transmit power allocation vs. partner location.

3.7 Summary

In this chapter the problem of transmit power allocation for optimally energy efficient vMISO, DF, and aDF cooperation has been studied. The proper allocation of transmission power to the cooperating source and partner nodes is essential for fully exploiting the energy saving potential of cooperative communication. Analytical expressions for the optimally energy efficient transmit power allocation have been derived for vMISO and DF cooperation. It has been shown that the optimal power allocation problem for aDF cooperation is non-linear, necessitating the use of a numerical search to obtain the optimal solution.

The nature of the optimum power allocation solution for each cooperative diversity scheme has been illustrated in terms of network geometry for a reference cooperative system with a range of potential partner locations. The analysis in this chapter has shown that the information exchange between the source and the partner dominates the transmit energy consumption of vMISO and DF cooperation. Thus the non-ideal source-partner channel limits the energy efficiency of vMISO and DF cooperation such that only a very restricted range of partner node locations close to the source node are beneficial. By contrast, the analysis of the search-based aDF power allocation solution has revealed that aDF achieves the highest reduction in total transmit energy when the partner is located roughly midway between the source and the destination. This suggests that the optimal transmit power allocation for aDF must achieve a balance between ensuring a good source-partner channel and a good partner-destination channel. Therefore, the source-partner and partner-destination links are both equally important factors in determining the energy efficiency of aDF cooperation.

Importantly, a comparison of the power allocation solutions for the three schemes has demonstrated that aDF cooperation achieves a reduction in total transmit energy consumption for a much wider range of partner node locations than vMISO and DF. This advantage is a reflection of the adaptivity of the aDF scheme, whereby the partner node only retransmits the packets it overheard correctly from the source, making cooperation beneficial despite a non-ideal source-partner channel (unlike in vMISO and DF).

The power allocation solutions for vMISO, DF, and aDF cooperation developed in this chapter form the basis for the analysis presented in Chapter 4, where the total energy savings achieved by the three cooperative diversity schemes are investigated via the partner choice region for energy efficient cooperation.

Chapter 4

Partner Choice Region for Energy Efficient Cooperation

4.1 Introduction

This chapter presents the total communication energy savings achieved by the vMISO, DF, and aDF cooperative diversity schemes using the optimal allocation of transmit power developed in Chapter 3. The performance of the three schemes is compared across a wide range of network configurations by considering the energy savings achieved for a source node cooperating with a range of potential partners¹. The schemes' energy conservation performance is thus examined in terms of the partner choice region for energy efficient cooperation.

The partner choice region² is defined as the network region wherein the partner node may be located to yield a positive $E_{\text{saving-coop-total}}$ (as defined by (2.17)). It is desirable for the partner choice region to be as large as possible and to chiefly represent areas of high cooperative energy saving; this means that cooperation would yield substantial energy savings for a wide range of candidate partner node locations. Such robustness and flexibility are very important for enabling practical implementation of cooperative diversity in randomly deployed wireless sensor networks. The partner choice region is thus a very useful tool for evaluating how beneficial cooperation might be in practice. Furthermore, by examining the partner choice region, the problem of best partner choice for energy efficient cooperation is studied.

In Section 4.2 the partner choice region for energy efficient vMISO, DF, and aDF cooperation is presented and analysed for a reference system. This investigation leads to

¹Equation (2.12) is used to map the path loss values L_{s-d} , L_{s-p} , and L_{p-d} to transmission distances d_{s-d} , d_{s-p} , and d_{p-d} respectively.

²The concept of partner choice region as a tool for evaluating how beneficial cooperation is with different candidate partners was originally proposed in [54] as the “user cooperative region” for coded cooperation deployed to improve communication reliability.

basic strategies for selecting the best cooperation partner from among a set of candidate partner nodes such that $E_{saving-coop-total}$ is maximised using each scheme. The impact of various system parameters on the partner choice region for energy efficient vMISO, DF, and aDF cooperation is then investigated in Sections 4.3-4.6. The energy efficiency of cooperation is thus extensively evaluated for a wide range of communication system configurations. Moreover, this analysis facilitates a thorough comparison of the energy conservation performance of the three cooperative diversity schemes across a wide range of network configurations and system parameters. The results of this investigation are examined in Section 4.7 to determine which is the best scheme to practically deploy in an energy-constrained wireless sensor network.

4.2 Energy Efficiency of the Reference Cooperative System

The analysis in this chapter is based on the set of reference cooperative system parameters employed throughout this thesis and listed in Table 2.1. This section presents and compares the partner choice region for energy efficient vMISO, DF, and aDF cooperation using optimal power allocation for this reference system. In subsequent sections, the impact of several key system parameters on the energy efficiency of cooperation is investigated by considering the performance of the reference system when one parameter at a time is varied. It should be noted that in this section, for ease of comparison, the partner choice region is illustrated in terms of network geometry using the same scale for all three schemes. However, in subsequent sections various scales are used in the partner choice region plots in order to display sufficient detail.

4.2.1 Virtual-MISO

The contour graph in Fig. 4.1 shows the total energy savings resulting from vMISO cooperation for a range of partner locations³ using optimal transmit power allocation, as given by (3.27)-(3.29). The maximum energy saving achieved by vMISO cooperation over all considered partner locations is 84.9%. The higher the cooperative energy savings achieved, the smaller the radius of the corresponding contour in Fig. 4.1. Thus the partner choice region is smaller for a higher energy efficiency of cooperation. Moreover, it is evident from Fig. 4.1 that the closer a potential partner is to the source node, the higher the energy saving obtained from cooperating with that partner. Therefore,

³Throughout this chapter, the candidate partner node locations considered are on a uniform $1\text{ m} \times 1\text{ m}$ grid covering the network area (i.e. a candidate partner node is placed every 1 m in the x-direction and every 1 m in the y-direction from the destination receiver located at the origin).

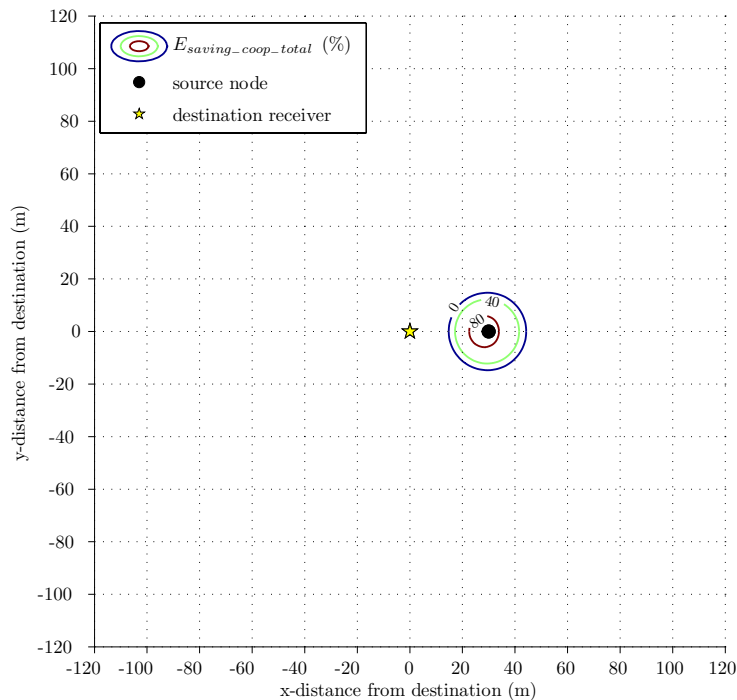


Figure 4.1: Total energy savings (2.17) achieved for a source node cooperating with a range of potential partners using vMISO cooperation with optimally energy efficient transmit power allocation (given by (3.27)-(3.29)), for the reference system specified in Table 2.1.

the source-partner channel is the dominant factor in determining the energy efficiency of vMISO cooperation. This observation suggests a simple rule for choosing the best cooperation partner for energy efficient vMISO cooperation: “*select the partner node which is located closest to the source*”. Lastly, Fig. 4.1 shows that the radius of the partner choice region boundary⁴ for energy efficient vMISO cooperation ($E_{saving_coop_total}=0\%$ contour) is roughly half of the source-destination separation. In other words, vMISO cooperation is energy efficient for a restricted set of partner locations close to the source node.

4.2.2 Decode-and-Forward

The total energy savings resulting from DF cooperation with optimal transmit power allocation, as given by (3.38) and (3.39), are shown in Fig. 4.2 for a range of partner locations. In general, the closer the partner node is to the source, the higher the energy saving obtained from DF cooperation, as for vMISO. Thus the basic rule for choosing the best cooperation partner for vMISO also holds for DF cooperation: “*select the partner node which is located closest to the source*”. However, comparing the size of the partner choice region for the same cooperative energy saving in Fig. 4.1 and Fig. 4.2 reveals a slight energy efficiency advantage of DF over vMISO. The maximum energy saving achieved

⁴It should be noted that the size of the partner choice region in Fig. 4.1 would further decrease if the BER constraint imposed on the source-partner channel were to be tightened (see Section 2.2.2).

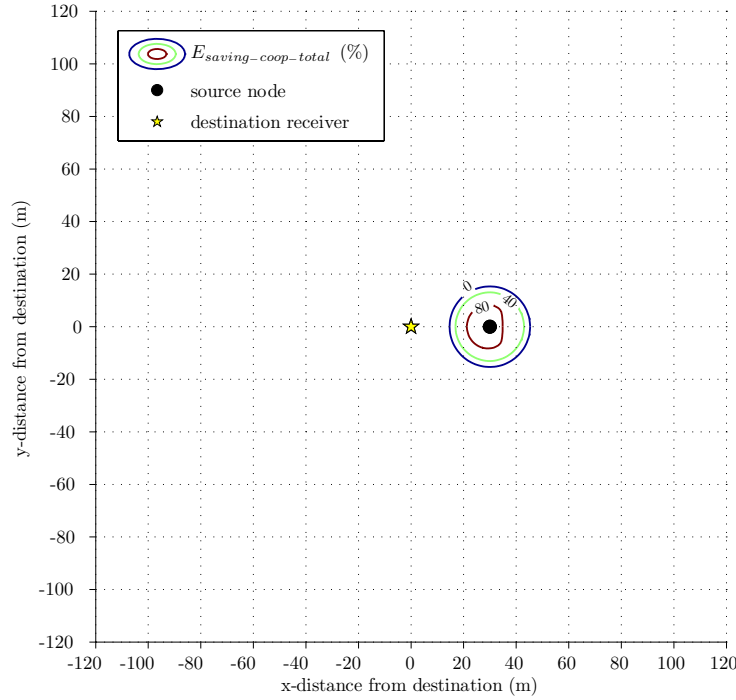


Figure 4.2: Total energy savings (2.17) achieved for a source node cooperating with a range of potential partners using DF cooperation with optimally energy efficient transmit power allocation (given by (3.38), (3.39)), for the reference system specified in Table 2.1.

over all considered partner locations using DF cooperation is also slightly higher than for vMISO, being 86.7%. This energy efficiency advantage of DF is a due to the additional transmission energy consumption of the explicit source to partner communication in vMISO, which is avoided in DF.

4.2.3 Adaptive Decode-and-Forward

An exhaustive search is used to obtain the optimally energy efficient transmit power allocation for aDF cooperation, as discussed in Chapter 3. The resulting energy savings are shown in Fig. 4.3 for a range of partner locations. The contours in Fig. 4.3 are centered about midway between the source and destination. This suggests that the partner-destination and source-partner links are equally important factors in determining the energy efficiency of aDF cooperation (in contrast to vMISO and DF). This is a reflection of the adaptivity of the aDF scheme, whereby a given partner node only retransmits the packets it overheard correctly from the source. These results suggest the following strategy for choosing the best cooperation partner for energy efficient aDF cooperation: “select the partner node which is located closest to the midway point between the source and the destination”. The maximum energy saving achieved by aDF cooperation over all considered partner locations is 88.4%, which is slightly higher than for DF and vMISO. Importantly, aDF achieves significantly higher energy savings than DF and vMISO over

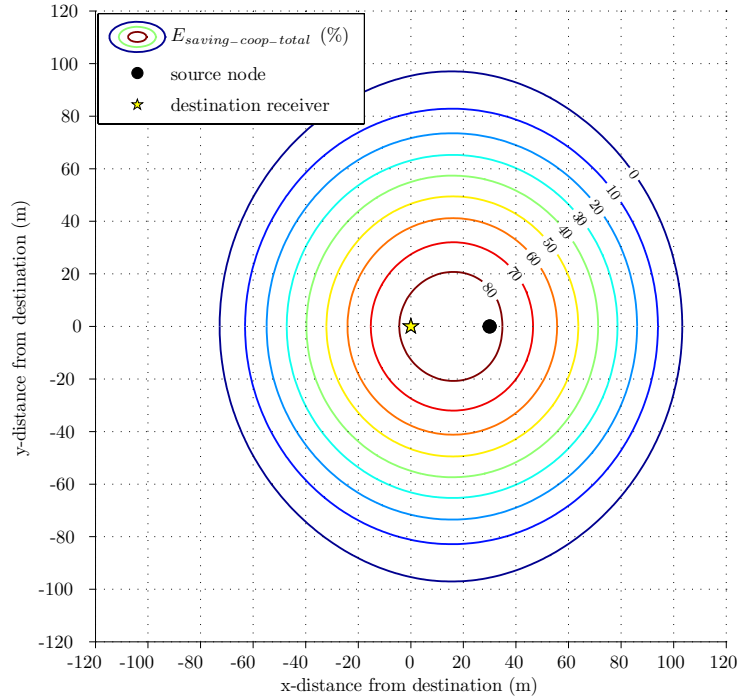


Figure 4.3: Total energy savings (2.17) achieved for a source node cooperating with a range of potential partners using aDF cooperation with optimally energy efficient transmit power allocation (solution obtained via numerical search), for the reference system specified in Table 2.1.

a wide range of partner locations, as demonstrated by a comparison of Fig. 4.3 with Figs. 4.1 and 4.2. Whereas the diameter of the partner choice region boundary for energy efficient cooperation (0% contour) is roughly equal to d_{s-d} for vMISO or DF, it is 6 times that for aDF. In fact, it is observed that the diameter of the 80% energy saving contour for aDF cooperation is slightly larger than the diameter of the 0% energy saving contour for DF or vMISO cooperation. Such a large energy efficiency advantage is due to the adaptive nature of aDF, which enables significant energy savings to be achieved despite a non-ideal source-partner channel.

4.2.4 Energy Efficiency Comparison of Cooperative Diversity Schemes

In this section the energy conservation performance of vMISO, DF and aDF cooperation is evaluated using two measures of merit. These two measures are employed throughout the remainder of this chapter to explicitly compare the three cooperative diversity schemes for a range of different system configurations. Firstly, Table 4.1 summarises the maximum energy saving achieved for the reference system over all considered partner locations using the vMISO, DF and aDF cooperative diversity schemes. This metric represents the limit of how well a cooperative diversity scheme can perform if the best possible cooperation

Table 4.1: Comparison of the maximum energy saving achieved over all considered partner locations using the vMISO, DF, and aDF cooperative diversity schemes for the reference system specified in Table 2.1.

Cooperative diversity scheme	Maximum energy saving (%)
vMISO	84.9
DF	86.7
aDF	88.4

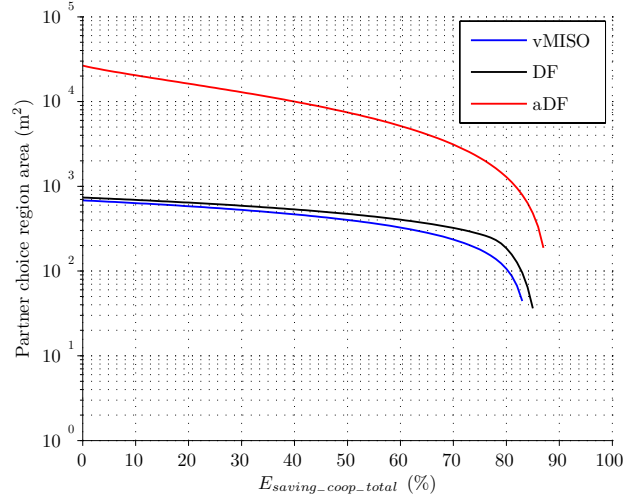


Figure 4.4: Comparison of the size of the partner choice region for a given energy efficiency of vMISO, DF, and aDF cooperation for the reference system specified in Table 2.1.

partner location is chosen. Secondly, Fig. 4.4 presents the area of the partner choice region for a given minimum energy efficiency of vMISO, DF and aDF cooperation for the reference system. This metric enables a quantitative comparison of the size of the partner choice region for a given energy efficiency of cooperation shown in Figs. 4.1, 4.2, and 4.3. It is calculated by estimating the network area enclosed by the contour line representing the corresponding energy efficiency of cooperation. As discussed previously, a larger partner choice region area equates to better performance of cooperation as a practical energy saving technique.

Table 4.1 shows that aDF results in a slightly higher (1.7%) maximum energy efficiency of cooperation than DF, which in turn yields a maximum energy saving 1.8% higher than vMISO. This reveals a slight energy efficiency advantage of aDF over DF and vMISO given the ideal case of selecting a cooperation partner located at the corresponding optimum location. Furthermore, the results in Fig. 4.4 show that the area of the partner choice region for any given energy efficiency of cooperation is consistently larger for DF than vMISO. Specifically, the size of the DF partner choice region is between 1.08 to 2.16 times larger than that of vMISO, with the discrepancy between the two schemes increasing for a higher energy efficiency of cooperation. Importantly, Fig. 4.4 also shows that aDF consistently achieves a substantial energy efficiency advantage over DF and vMISO. Specifically,

the area of the aDF partner choice region for any given energy efficiency of cooperation is between 6.9 and 36 times larger than that of DF, with the discrepancy between the two schemes generally decreasing for a higher energy efficiency of cooperation. This significant energy efficiency advantage of aDF clearly demonstrates the scheme's superior robustness and flexibility as a practical energy saving technique.

4.3 Effect of Varying the Transceiver Circuit Power

In this section the effect of varying the transceiver circuit power consumption on the energy efficiency of vMISO, DF, and aDF cooperation is investigated. The energy savings achieved via cooperation for a range of partner node locations are calculated for the reference communication system specified in Table 2.1 with $P_{CCT_tx}=P_{CCT_rx}=\{0 \text{ W}, 10 \text{ mW}, 100 \text{ mW}, 1 \text{ W}\}$. It should be noted that $P_{CCT_tx}=P_{CCT_rx}=100 \text{ mW}$ is roughly equal to the reference system setting of $P_{CCT_tx}=98.2 \text{ mW}$, $P_{CCT_rx}=109.5 \text{ mW}$.

The corresponding partner choice region boundary ($E_{saving_coop_total}=0\%$) for energy efficient vMISO, DF, and aDF cooperation is illustrated in Figs. 4.5, 4.6, and 4.7, respectively. These results demonstrate that the size of the partner choice region decreases with increasing transceiver circuit power consumption for all three schemes. The case with $P_{CCT_tx}=P_{CCT_rx}=0 \text{ W}$ is equivalent to purely considering the transmission energy savings achieved by cooperation. As discussed in Chapter 2, increased circuit energy consumption is an overhead of cooperative communication. Thus a non-zero circuit power consumption decreases the total cooperative energy saving achieved by cooperation, as illustrated by the decreasing size of the partner choice region for a higher circuit power consumption in Figs. 4.5, 4.6, and 4.7.

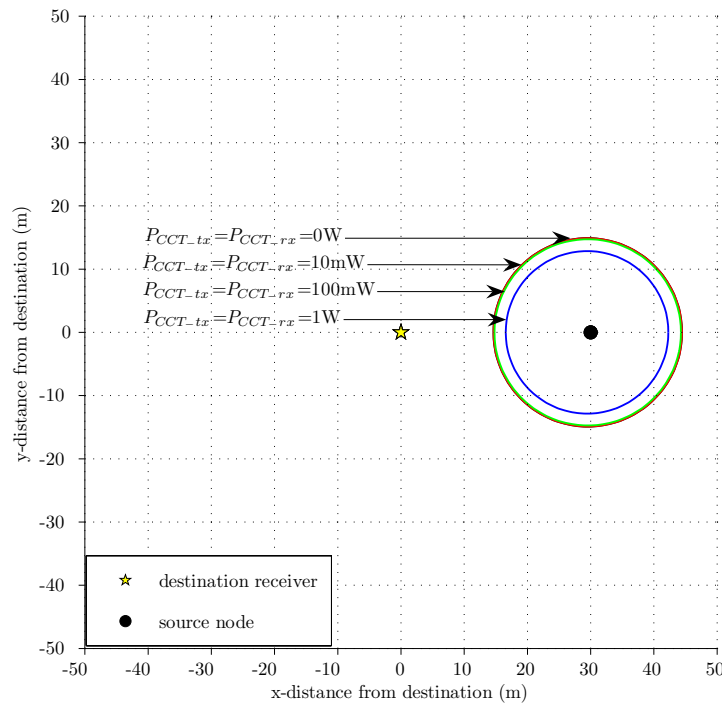


Figure 4.5: Partner choice region boundary ($E_{saving_coop_total}=0\%$) for energy efficient vMISO cooperation vs. the transceiver circuit power consumption.

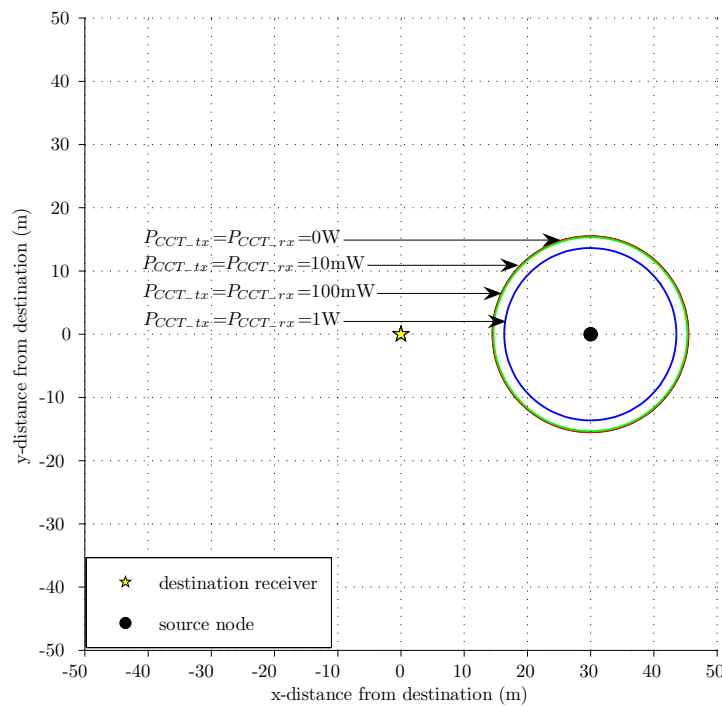


Figure 4.6: Partner choice region boundary ($E_{saving_coop_total}=0\%$) for energy efficient DF cooperation vs. the transceiver circuit power consumption.

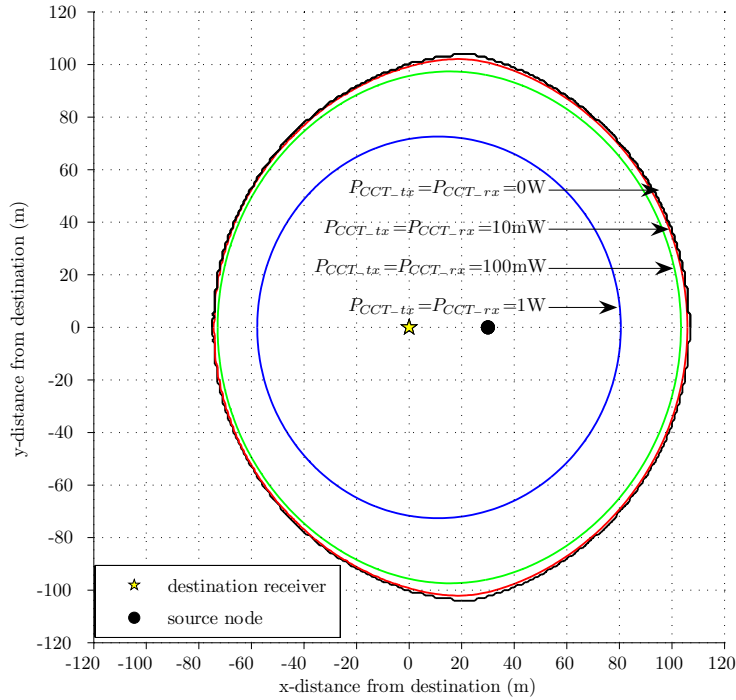


Figure 4.7: Partner choice region boundary ($E_{saving_coop_total}=0\%$) for energy efficient aDF cooperation vs. the transceiver circuit power consumption.

The energy conservation performance of the three schemes for different values of transceiver circuit power consumption is further quantified in Fig. 4.8 in terms of the area of the partner choice region for a given minimum energy efficiency of cooperation. Fig. 4.8 confirms that a larger circuit power consumption corresponds to a smaller partner choice region for achieving any given energy efficiency of cooperation. Furthermore, Fig. 4.8 shows that DF maintains a slight energy efficiency advantage over vMISO for all considered values of transceiver circuit power consumption. Specifically, the area of the DF partner choice region for a given energy efficiency of cooperation is between 1.08 and 3.07 times larger than that of vMISO. Fig. 4.8 also shows that aDF consistently achieves a significant energy efficiency advantage over DF and vMISO. Specifically, the area of the aDF partner choice region for a given energy efficiency of cooperation is between 6.8 and 38 times larger than that of DF.

Lastly, Fig. 4.9 shows that the maximum energy efficiency of cooperation achieved over all considered partner locations decreases with an increasing transceiver circuit power consumption. Without the overhead of circuit energy ($P_{CCT_tx}=P_{CCT_rx}=0$ W), cooperation yields a maximum energy saving of 90.61%, 92.59%, and 94.27% using vMISO, DF, and aDF respectively. As the transceiver circuit power consumption overhead increases, the maximum energy efficiency of cooperation achieved also decreases proportionally. Fig. 4.9 furthermore demonstrates that aDF consistently results in a slightly higher maximum energy efficiency of cooperation than DF, which in turn yields a slightly higher maximum energy saving than vMISO.

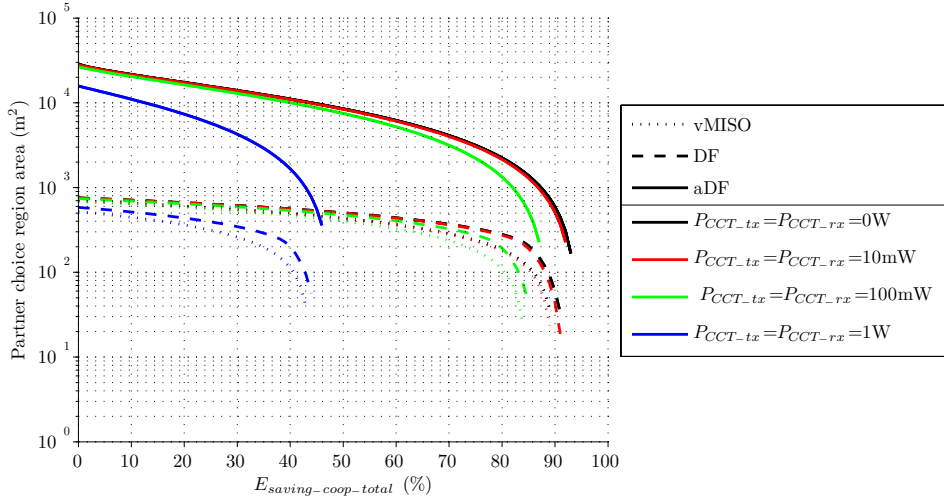


Figure 4.8: Comparison of the size of the partner choice region for a given energy efficiency of vMISO, DF, and aDF cooperation vs. the transceiver circuit power consumption.

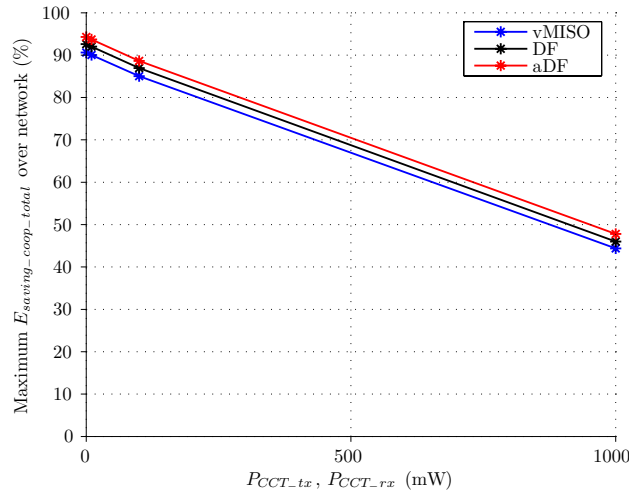


Figure 4.9: Maximum energy saving achieved over all considered partner node locations via vMISO, DF, and aDF cooperation vs. the transceiver circuit power consumption.

4.4 Effect of Varying the Source-Destination Separation

Separation

In this section the effect of varying the source-destination separation, d_{s-d} , on the energy efficiency of vMISO, DF, and aDF cooperation is investigated. The energy savings achieved via cooperation for a range of partner node locations are calculated for the reference communication system specified in Table 2.1 with $d_{s-d} = \{15 \text{ m}, 20 \text{ m}, 30 \text{ m}, 40 \text{ m}, 50 \text{ m}, 60 \text{ m}, 70 \text{ m}, 80 \text{ m}, 90 \text{ m}, 100 \text{ m}\}$.

The corresponding partner choice region boundary ($E_{\text{saving-coop-total}} = 0\%$) for energy efficient vMISO, DF, and aDF cooperation is illustrated in Figs. 4.10, 4.11, and 4.12,

respectively. These results demonstrate that the size of the partner choice region increases with increasing source-destination separation for all three schemes. A larger source-destination separation requires a higher non-cooperative transmission energy to achieve the target BER, as indicated by (3.6). Thus the corresponding maximum total cooperative transmission energy that still results in an energy saving is also higher. Accordingly, a greater range of partner locations results in energy efficient cooperation. In vMISO and DF, the total cooperative transmission energy increases with increasing source-partner separation (as shown by Figs. 3.2 and 3.3). This is consistent with the increasing permissible source-partner separation for energy efficient cooperation observed in Figs. 4.10 and 4.11 for an increasing source-destination separation. It follows that the partner choice region boundaries for vMISO and DF cooperation are roughly circles centered around the source node. By contrast, in aDF the total cooperative transmission energy increases the further away the partner is from both the source and the destination (as shown by Fig. 3.4). This corresponds to the partner choice region boundaries for aDF cooperation shown in Fig. 4.12 being centered roughly midway between the source node and the destination receiver, with a larger permissible distance of the partner node from this point for an increasing source-destination separation.

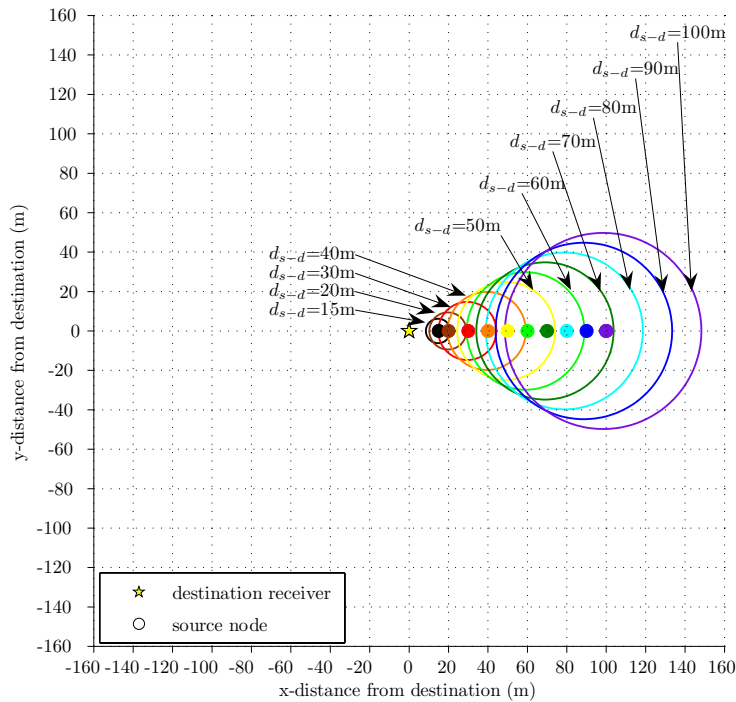


Figure 4.10: Partner choice region boundary ($E_{saving_coop_total}=0\%$) for energy efficient vMISO cooperation vs. the source-destination separation.

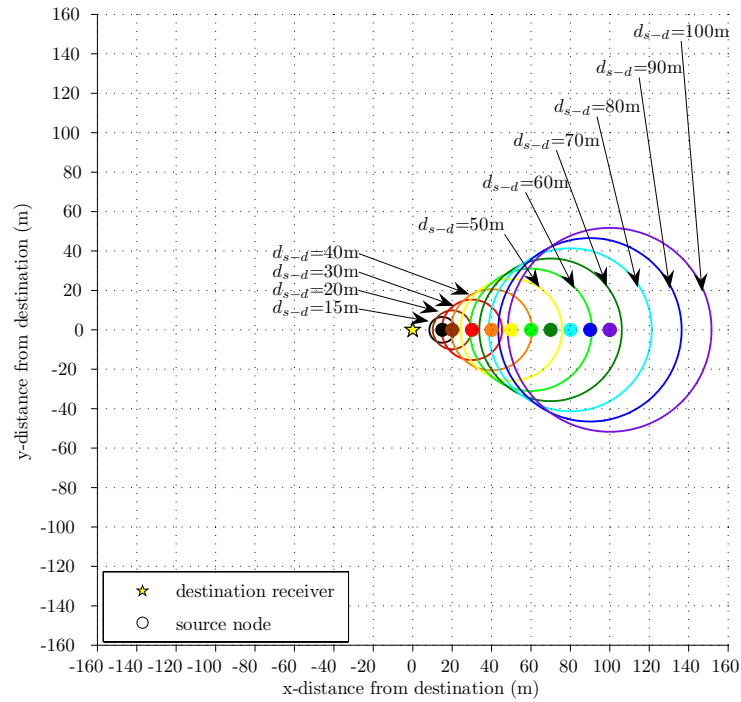


Figure 4.11: Partner choice region boundary ($E_{saving_coop_total}=0\%$) for energy efficient DF cooperation vs. the source-destination separation.

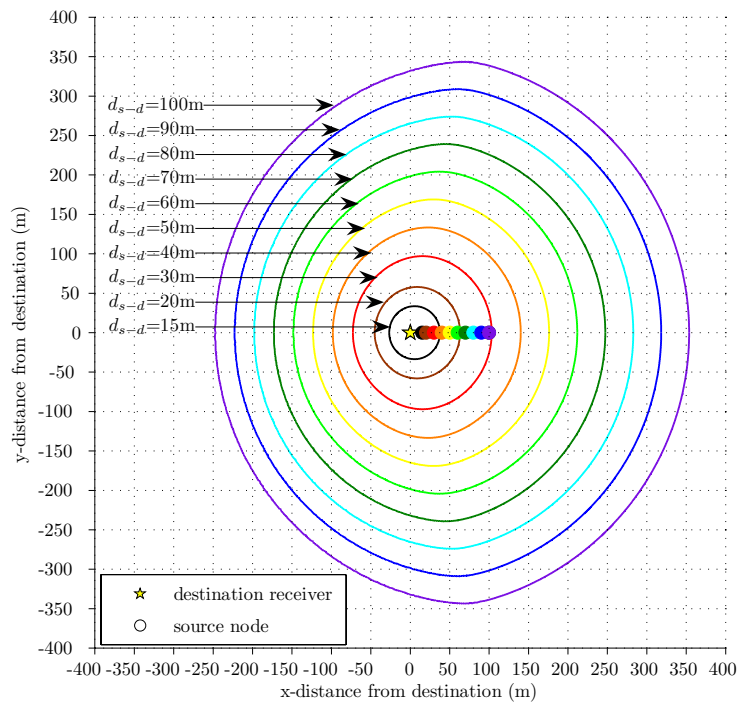


Figure 4.12: Partner choice region boundary ($E_{saving_coop_total}=0\%$) for energy efficient aDF cooperation vs. the source-destination separation.

The energy conservation performance of the three schemes for different values of source-destination separation is further quantified in Fig. 4.13 in terms of the area of the partner choice region for a given minimum energy efficiency of cooperation. Fig. 4.13

shows that a larger source-destination separation corresponds to a larger partner choice region for achieving any given energy efficiency of cooperation. Furthermore, Fig. 4.13 demonstrates that DF maintains a slight energy efficiency advantage over vMISO for all considered values of the source-destination separation. Specifically, the area of the DF partner choice region for a given energy efficiency of cooperation is between 1.08 and 2.9 times larger than that of vMISO. Importantly, Fig. 4.13 also clearly demonstrates that aDF consistently achieves a significant energy efficiency advantage over DF and vMISO. Specifically, the area of the aDF partner choice region for a given energy efficiency of cooperation is between 6.7 and 37.6 times larger than that of DF.

Finally, Fig. 4.14 shows that the maximum energy efficiency of cooperation achieved over all considered partner locations increases with an increasing source-destination separation, ranging from around 39% for $d_{s-d}=15$ m to around 92% $d_{s-d}=100$ m. This is due to the fact that the fixed circuit energy overhead of cooperation becomes less dominant overall as the transmission energy increases with transmission distance, resulting in a higher total cooperative energy saving. As discussed in Chapter 2, it follows that cooperative communication is only energy efficient beyond a threshold source-destination separation. In order to illustrate this, the maximum energy efficiency of cooperation achieved for source-destination separations less than 15m is also shown⁵ in Fig. 4.14. Fig. 4.14 thus confirms that cooperative communication is energy efficient only if the source-destination separation is larger than around 12 m (assuming the reference system parameters); otherwise, the increase in circuit consumption due to cooperation exceeds the transmission energy reduction obtained via cooperative diversity, and a negative cooperative energy saving results. Fig. 4.14 also shows that aDF results a slightly higher (up to 2%) maximum energy efficiency of cooperation than DF, which in turn yields a maximum energy saving up to 1.9% higher than vMISO.

⁵Namely, the maximum energy efficiency for $d_{s-d}<15$ m was obtained by calculating the energy savings achieved via cooperation for $d_{s-d}=\{11\text{ m}, 12\text{ m}, 13\text{ m}, 14\text{ m}\}$, for the reference system and a range of partner node locations.

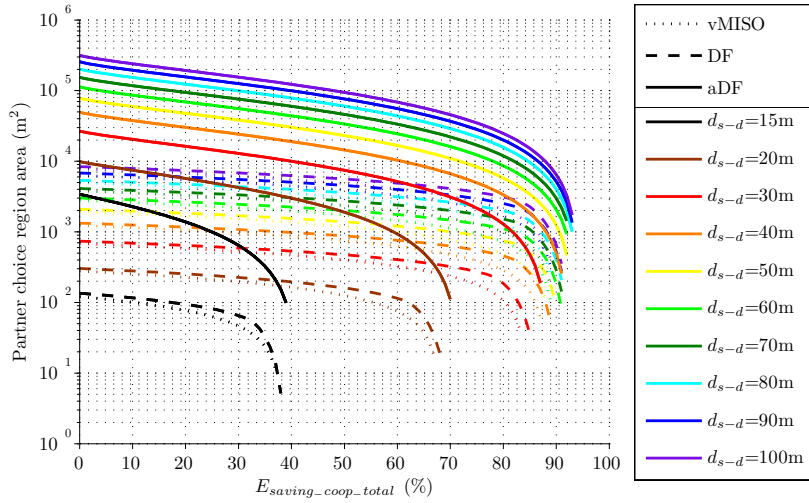


Figure 4.13: Comparison of the size of the partner choice region for a given energy efficiency of vMISO, DF, and aDF cooperation vs. the source-destination separation.

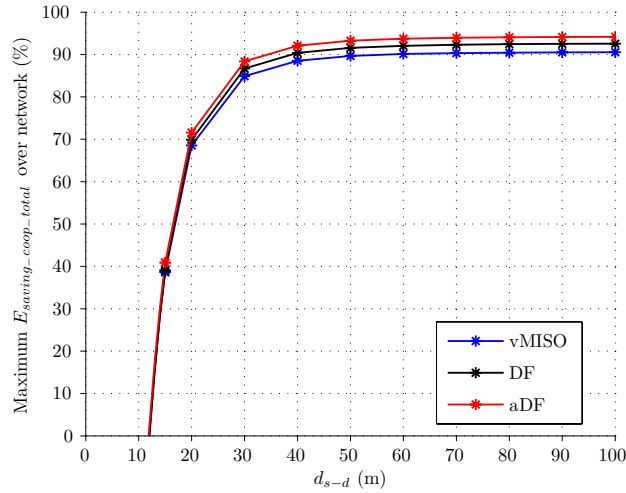


Figure 4.14: Maximum energy saving achieved over all considered partner node locations via vMISO, DF, and aDF cooperation vs. the source-destination separation.

4.5 Effect of Varying the Channel Path Loss Exponent

In this section the effect of varying the channel path loss exponent, k , on the energy efficiency of vMISO, DF, and aDF cooperation is investigated. The channel path loss exponent characterises the propagation environment by determining how transmission distance is mapped to average channel path loss, as given by (2.12). The energy savings achieved via cooperation for a range of partner node locations are calculated for the reference communication system specified in Table 2.1 with $k = \{3, 3.5, 4, 5, 6, 7, 8, 9, 10\}$. The corresponding partner choice region boundary ($E_{saving_coop_total} = 0\%$) for energy

efficient vMISO, DF, and aDF cooperation is illustrated in Figs. 4.15, 4.16, and 4.17, respectively.

Figs. 4.15 and 4.16 show that the size of the partner choice region boundary for vMISO and DF cooperation increases as the channel path loss exponent is increased. As discussed in Chapter 3, the source-partner channel is the limiting factor in the energy efficiency of vMISO and DF cooperation. Namely, for the purpose of considering the partner choice region boundary, the total transmission energy consumption of vMISO and DF cooperation may be approximated to the dominant energy expenditure associated with the source-partner transmission (given by (3.29)). The maximum source-partner separation for energy efficient vMISO and DF cooperation is therefore approximated by (3.31). Since the condition $p_{s-p} < p_b$ must be imposed to prevent error propagation in vMISO and DF cooperation⁶, for a fixed source-destination separation (3.31) shows that $d_{s-p-MAX}$ increases as k is increased. This is consistent with the larger permissible source-partner separation for energy efficient cooperation generally observed in Figs. 4.15 and 4.16 for a larger value of k . However, it is also interesting to observe from Figs. 4.15 and 4.16 that for high values of k the right hand side of the partner choice region boundary moves increasingly closer to the source node. This demonstrates the increasing influence of the partner-destination channel on the energy efficiency of vMISO and DF cooperation as k is increased. As demonstrated in Chapter 3, the overall transmission energy for vMISO and DF cooperation may be approximated by the cooperative transmission energy of the source and partner, given by (3.19), when the source-partner transmission energy is not dominant. Substituting (2.12) into (3.19) indicates that the transmission energy required for the cooperative transmission in vMISO and DF is proportional to $(d_{p-d})^{\frac{k}{2}}$. It follows that a smaller maximum partner-destination separation for energy efficient vMISO and DF cooperation is observed in Figs. 4.15 and 4.16 for high values of k .

Fig. 4.17 demonstrates that the size of the partner choice region boundary for aDF cooperation decreases as the channel path loss exponent is increased. This is contrary to the trend observed for vMISO and DF cooperation. Fig. 4.17 also shows that the partner choice region boundaries are centered midway between the source and the destination. This indicates that the maximum allowable source-partner separation and partner-destination separation for energy efficient cooperation both decrease as k is increased. These results further support the observation made in Chapter 3 that optimally energy efficient aDF cooperation appears to achieve a balance between ensuring a good source-partner channel and good partner-destination channel. As k is increased a fixed channel quality (as measured by the average channel path loss, given by (2.12)) corresponds to a smaller transmission distance. It follows that smaller permissible source-partner

⁶This condition is defined and discussed in Chapter 2.

and partner-destination separations for energy efficient aDF cooperation are observed in Fig. 4.17 for a larger channel path loss exponent.

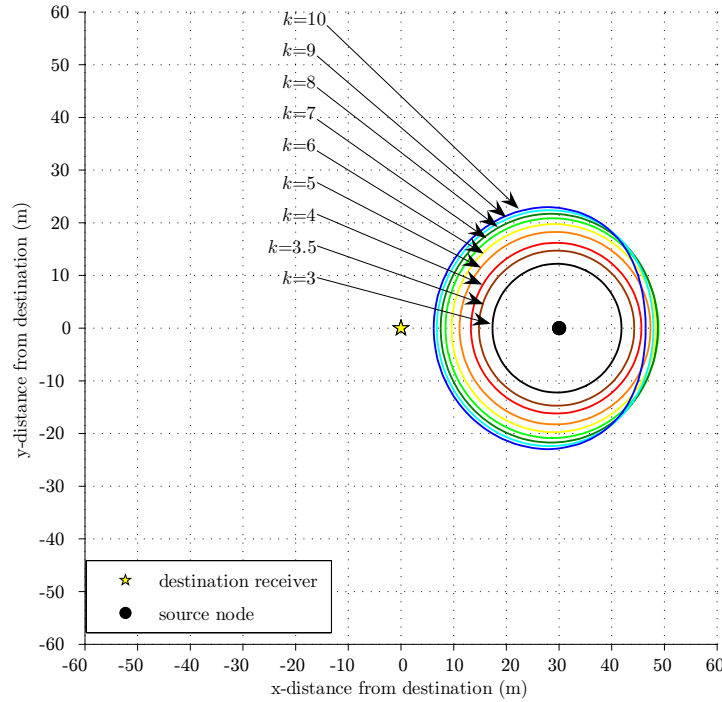


Figure 4.15: Partner choice region boundary ($E_{saving_coop_total}=0\%$) for energy efficient vMISO cooperation vs. the channel path loss exponent.

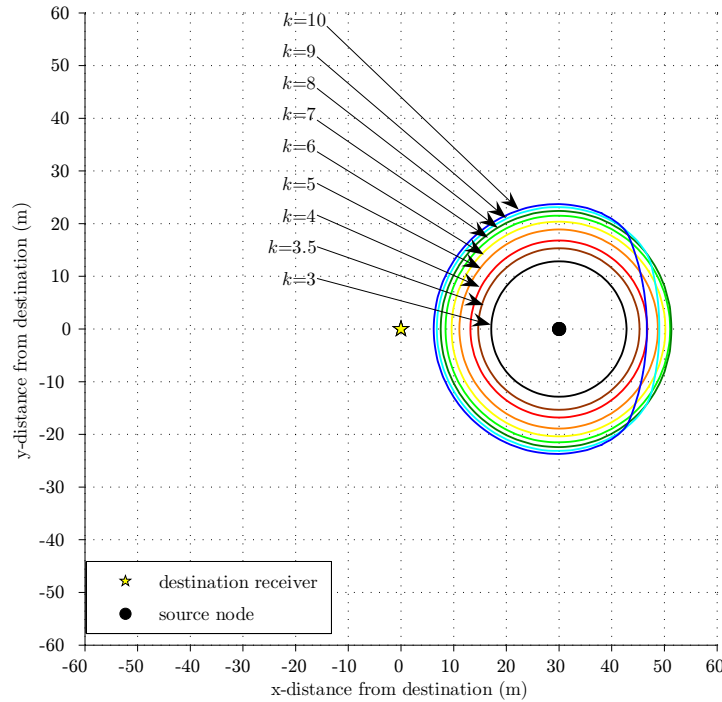


Figure 4.16: Partner choice region boundary ($E_{saving_coop_total}=0\%$) for energy efficient DF cooperation vs. the channel path loss exponent.

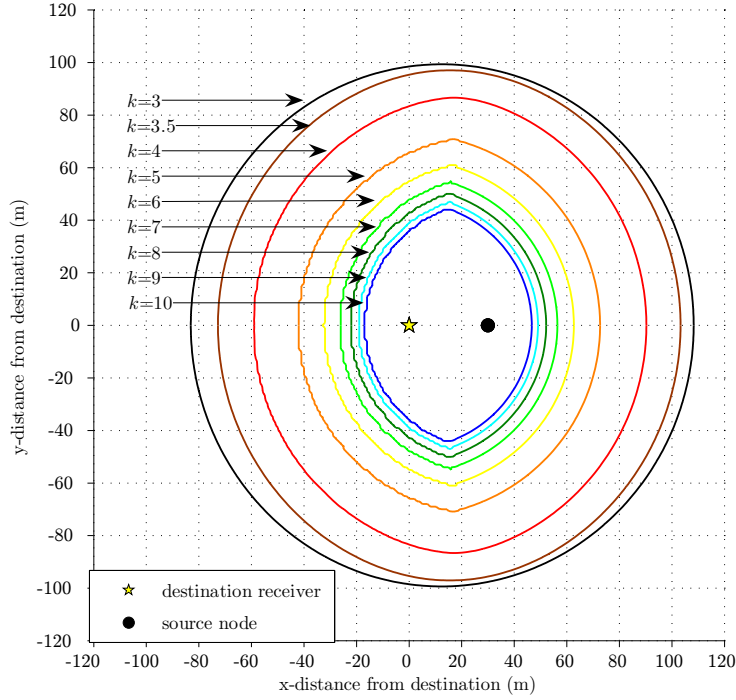


Figure 4.17: Partner choice region boundary ($E_{saving_coop_total}=0\%$) for energy efficient aDF cooperation vs. the channel path loss exponent.

The energy conservation performance of the three schemes for different values of channel path loss exponent is further quantified in Fig. 4.18 in terms of the area of the partner choice region for a given minimum energy efficiency of cooperation. Fig. 4.18 shows that a larger value of k in general corresponds to a larger partner choice region for achieving a given energy efficiency of VMISO and DF cooperation. Fig. 4.13 also shows that for aDF cooperation a larger value of k corresponds to a smaller partner choice region for values of low to moderate energy efficiency. These results are consistent with the partner choice region boundary trend observed as k is varied in Figs. 4.15, 4.16, and 4.17. However, Fig. 4.18 also shows that a larger value of k corresponds to a larger partner choice region for achieving a high energy efficiency of aDF cooperation. This is due to the fact that the transmit energy reduction achieved by cooperative diversity for a given partner location increases as k is increased. Substituting (2.12) into (3.6) and (3.19), this transmit energy reduction may be expressed in terms of k as

$$\frac{E_{tx_non_coop}}{E_{tx_TOTAL_coop_ideal}} = \frac{1}{2\sqrt{3}p_b} \left(\frac{d_{s-d}}{d_{p-d}} \right)^{\frac{k}{2}}. \quad (4.1)$$

Since $d_{p-d} < d_{s-d}$ for a high energy efficiency of aDF cooperation (as shown by Fig. 4.3), increasing k results in a greater reduction of transmit energy due to cooperative diversity. Fig. 4.18 also demonstrates that DF maintains a slight energy efficiency advantage over vMISO for all considered values of k . Specifically, the area of the DF partner choice region for a given energy efficiency of cooperation is between 1.06 and 2.3 times larger than that

of vMISO. Importantly, Fig. 4.18 also clearly demonstrates that aDF consistently achieves a significant energy efficiency advantage over DF and vMISO. Specifically, the area of the aDF partner choice region for a given energy efficiency of cooperation is between 2.1 and 57.6 times larger than that of DF.

Finally, Fig. 4.19 shows that the maximum energy efficiency of vMISO, DF, and aDF cooperation achieved over all considered partner locations increases with an increasing channel path loss exponent, ranging from around 63% to around 99.3%. This trend is due to the increase in transmit energy savings as k is increased indicated by (4.1). Furthermore, the fixed circuit energy overhead of cooperation becomes less dominant overall as the absolute transmission energy increases with k , resulting in a higher total cooperative energy saving. Fig. 4.19 also shows that the maximum energy efficiency of vMISO is slightly (up to 0.9%) lower than that of DF, which in turn achieves a marginally lower (up to 1.7%) maximum energy efficiency than aDF.

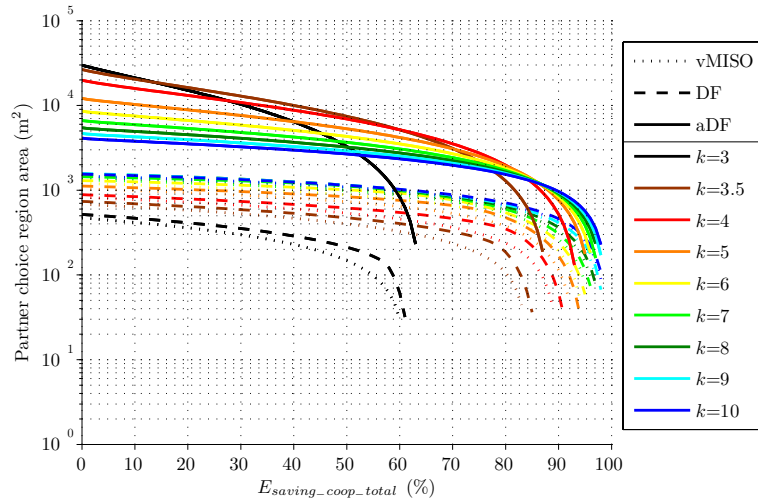


Figure 4.18: Comparison of the size of the partner choice region for a given energy efficiency of vMISO, DF, and aDF cooperation vs. the channel path loss exponent.

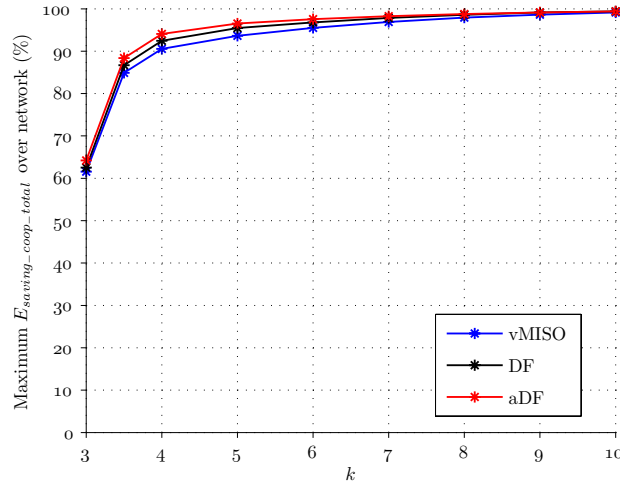


Figure 4.19: Maximum energy saving achieved over all considered partner node locations via vMISO, DF, and aDF cooperation vs. the channel path loss exponent.

4.6 Effect of Varying the Target Bit Error Rate

In this section the effect of varying the target end-to-end BER, p_b , on the energy efficiency of vMISO, DF, and aDF cooperation is investigated. The energy savings achieved via cooperation for a range of partner node locations are calculated for the reference communication system specified in Table 2.1 with $p_b = \{10^{-2}, 10^{-3}, 10^{-4}, 10^{-5}, 10^{-6}\}$. It should be noted that for vMISO and DF, the target source-partner BER p_{s-p} is set to $p_{s-p} = p_b \times 10^{-1}$ (to maintain a low approximation error in (2.2), (2.3) and avoid error propagation at the partner node, as discussed in Chapter 2).

The corresponding partner choice region boundary ($E_{savings-coop-total} = 0\%$) for energy efficient vMISO, DF, and aDF cooperation is illustrated in Figs. 4.20, 4.21, and 4.22, respectively. These results demonstrate that the size of the partner choice region increases as the target BER is decreased for all three schemes. As shown in Fig. 2.3, the lower the target BER, the higher the SNR gain due to cooperative diversity. This translates into cooperation achieving a greater reduction in transmission energy for a lower target BER, as evidenced by (4.1). Consequently, a greater range of partner locations results in energy efficient cooperation. However, whereas this effect is very pronounced in aDF, in vMISO and DF it is offset by an increasingly tight source-partner BER constraint p_{s-p} . As a result, the increase in the size of the partner choice region boundary in Figs. 4.21 and 4.22 for vMISO and DF cooperation becomes marginal as p_b is decreased.

The energy conservation performance of the three schemes for different values of the target end-to-end BER is further quantified in Fig. 4.23 in terms of the area of the partner choice region for a given minimum energy efficiency of cooperation. Fig. 4.23 shows that a lower target BER corresponds to a larger partner choice region for achieving any given energy efficiency of cooperation. Furthermore, Fig. 4.23 demonstrates that DF maintains

a slight energy efficiency advantage over vMISO for all considered values of p_b . Specifically, the area of the DF partner choice region for a given energy efficiency of cooperation is between 1.002 and 33 times larger than that of vMISO. Importantly, Fig. 4.23 also clearly demonstrates that aDF consistently achieves a significant energy efficiency advantage over DF and vMISO. Specifically, the area of the aDF partner choice region for a given energy efficiency of cooperation is between 5.7 and 2302 times larger than that of DF. The discrepancy between aDF and the other two schemes grows as p_b is decreased, which is consistent with the trends exhibited in Figs. 4.22, 4.21, and 4.20.

Finally, Fig. 4.24 shows that the maximum energy efficiency of cooperation achieved over all considered partner locations increases with a decreasing target BER, ranging from around 33.5% to around 99.7%. This is due to the greater transmission energy savings achieved for a lower p_b , as indicated by (4.1). Moreover, the absolute transmission energy increases as p_b is decreased and thus the fixed circuit energy overhead of cooperation becomes less dominant. This also contributes to the higher total cooperative energy savings observed in Fig. 4.24 for lower values of p_b . Fig. 4.24 additionally shows that aDF results a slightly higher (up to 3.6%) maximum energy efficiency of cooperation than DF, which in turn yields a maximum energy saving up to 4.45% higher than vMISO.

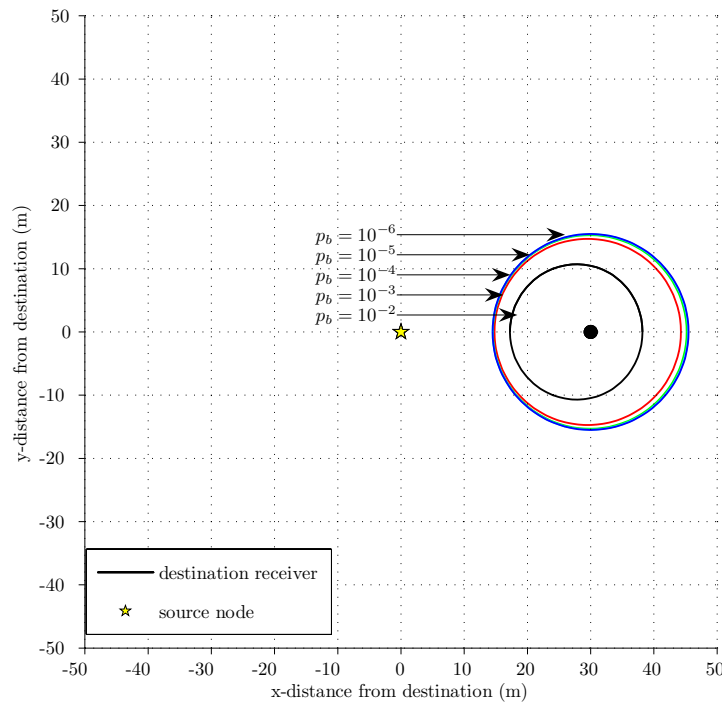


Figure 4.20: Partner choice region boundary ($E_{saving_coop_total}=0\%$) for energy efficient vMISO cooperation vs. the target BER.

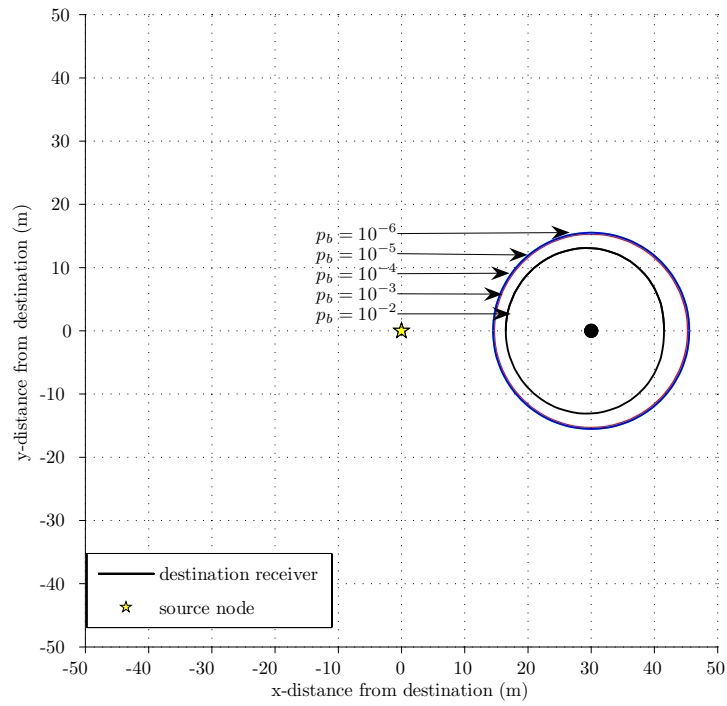


Figure 4.21: Partner choice region boundary ($E_{saving_coop_total}=0\%$) for energy efficient DF cooperation vs. the target BER.

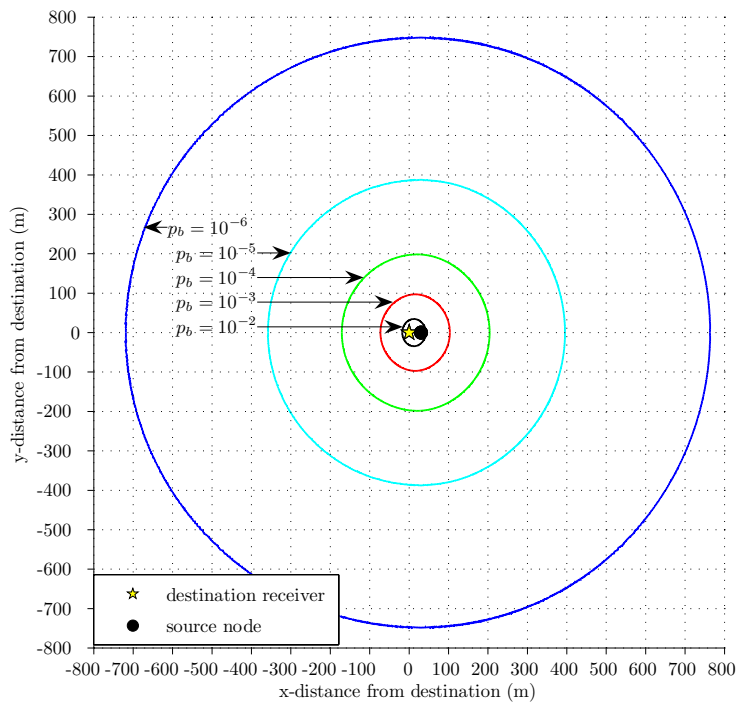


Figure 4.22: Partner choice region boundary ($E_{saving_coop_total}=0\%$) for energy efficient aDF cooperation vs. the target BER.

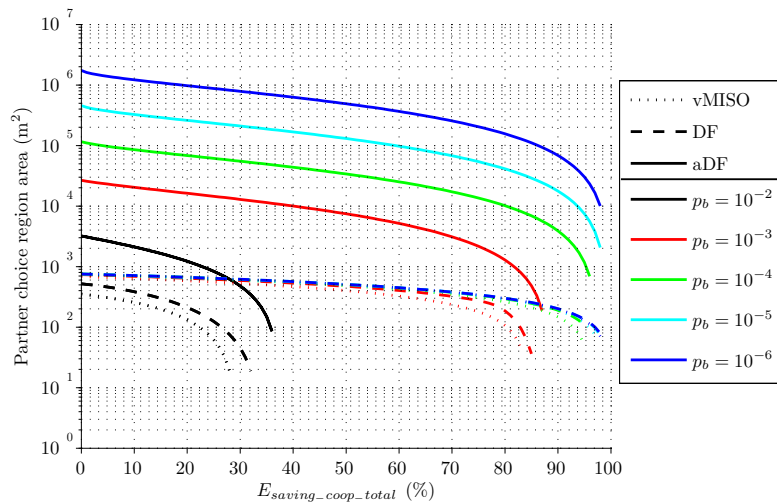


Figure 4.23: Comparison of the size of the partner choice region for a given energy efficiency of vMISO, DF, and aDF cooperation vs. the target BER.

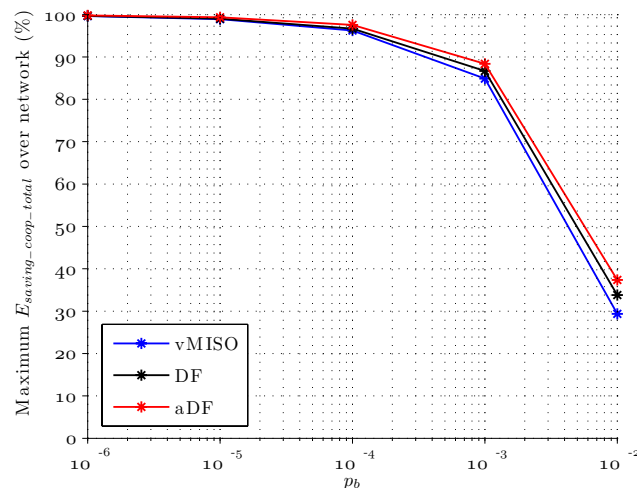


Figure 4.24: Maximum energy saving achieved over all considered partner node locations via vMISO, DF and aDF cooperation vs. the target BER.

4.7 Most Energy Efficient Cooperative Diversity Scheme for Wireless Sensor Networks

The energy efficiency of vMISO, DF and aDF cooperation has been thoroughly analysed in the preceding sections under a wide range of network configurations and various system parameter settings. The performance of the schemes has been quantified and compared in terms of the maximum energy efficiency of cooperation achieved and the partner choice region size for a given energy efficiency of cooperation. These results have consistently shown the energy conservation performance of DF to be slightly superior to vMISO. Additionally, as discussed in Chapter 2, practical deployment of vMISO would not be entirely

straightforward in a wireless sensor network due to the requirement of strict synchronisation between cooperating sensor nodes. By contrast, DF has a low implementation complexity. It may thus be concluded that the DF cooperative diversity scheme is overall superior to vMISO as a practical energy saving technique for wireless sensor networks. Importantly, the results presented in this chapter have also consistently demonstrated that the energy conservation performance of aDF is significantly superior to vMISO and DF. Additionally, being a variant of DF, aDF is straightforward to practically implement. Therefore, it may be concluded that aDF is the best cooperative diversity scheme to practically deploy in an energy-constrained wireless sensor network. Consequently, the remainder of this thesis solely considers the aDF cooperative diversity scheme.

It is interesting to note that the relatively small partner choice region centered around the source node exhibited by vMISO and DF cooperation implies that these schemes would only be energy efficient in sufficiently dense networks (where a partner node is likely to be found within this restricted region). By contrast, the significantly larger aDF partner choice region centered midway between the source and destination receiver indicates that aDF cooperation could yield substantial energy savings even in a sparse wireless sensor network. This is particularly important in terms of the long-term energy efficiency of cooperation, with the average network density diminishing over time as sensor nodes deplete their batteries. Similarly, these results also suggest that clustered cooperation, as proposed in [39, 40, 42], is not the most energy efficient way to deploy cooperation in a wireless sensor network. Clustered cooperation typically incorporates vMISO cooperative diversity into a clustered network architecture (such as LEACH [41]) whereby so-called cluster-head nodes cooperate with nodes which are members of their own cluster to communicate with a remote destination receiver. The results presented in this chapter indicate that it would be more beneficial to instead deploy aDF cooperation whereby cluster-heads are permitted to cooperate with other cluster-heads (or other network nodes which are not necessarily members of the cluster-head node's own cluster).

4.8 Summary

In this chapter the energy conservation performance of the vMISO, DF, and aDF cooperative diversity schemes has been analysed in terms of the partner choice region for energy efficient cooperation. The partner choice region has been employed as a tool for evaluating how well different cooperative diversity schemes would perform as practical energy saving techniques; a large partner choice region is indicative of a robust and flexible scheme suitable for deployment in energy-constrained wireless sensor networks. Furthermore, by examining the partner choice region, basic proximity-based strategies have been proposed for selecting the best cooperation partner from among a set of candidate nodes.

The energy efficiency of cooperation has been extensively evaluated by investigating the impact of various system parameters on the partner choice region. The analysis has shown that the size of the partner choice region for all three schemes increases as the transceiver circuit power consumption is decreased, the source-destination separation is increased, and the target BER is decreased. Similarly, the results have demonstrated that the maximum energy efficiency of cooperation achieved over all considered partner locations increases for all three schemes as the transceiver circuit power consumption is decreased, the source-destination separation is increased, and the target BER is decreased. As the channel path loss exponent is increased, the size of the partner choice region for vMISO and DF increases, whereas it generally decreases for aDF cooperation. However, the maximum energy efficiency of cooperation achieved over all considered partner locations increases as the channel path loss exponent is increased for all three schemes.

Importantly, this analysis has enabled a thorough comparison of the energy conservation performance of the three cooperative diversity schemes across a wide range of network configurations and system parameters. The results presented in this chapter have consistently demonstrated that the energy conservation performance of aDF is significantly superior to vMISO and DF. This significant energy efficiency advantage of aDF clearly demonstrates the scheme's superior robustness and flexibility as a practical energy saving technique. Additionally, being a variant of DF, aDF is straightforward to practically implement. Therefore, it has been concluded that aDF is the best cooperative diversity scheme to deploy in an energy-constrained wireless sensor network. Accordingly, the subsequent chapters solely consider the aDF cooperative diversity scheme.

Chapter 5

Practical Energy Efficiency of Adaptive Decode-and-Forward Cooperation

5.1 Introduction

In Chapter 4 it was concluded that aDF is the most suitable cooperative diversity scheme to deploy in energy-constrained wireless sensor networks due to its superior energy efficiency and low implementation complexity. However, the aDF energy saving results presented in Chapter 4 are based on optimum transmit power allocation obtained via numerical search. In practice, such a search is prohibitively computationally expensive, especially if it is to be performed by a simple sensor node. In this chapter a simple power allocation heuristic is developed which enables sensor nodes to autonomously determine a near-optimally energy efficient allocation of transmit power for aDF cooperation.

The heuristic is developed and illustrated in Section 5.2. The validity of the heuristic is investigated in Section 5.3 via the partner choice region for energy efficient cooperation across a wide range of network configurations and system parameter settings. The practical energy efficiency of aDF cooperation is thus thoroughly examined in this chapter. In Section 5.4 the practical significance of the proposed power allocation heuristics is discussed.

The power allocation heuristic developed in this chapter (together with the partner choice heuristics developed in Chapter 6) forms the basis of a simple and practical cooperation strategy for energy-constrained wireless sensor networks which is presented in Chapter 7 and analysed in Chapters 8-11.

5.2 Development of the Power Allocation Heuristic

In Chapter 3 it was shown that the optimal power allocation for energy efficient aDF cooperation appears to be the result of the combined influence of the source-partner and partner-destination channels. Based on this observation, a power allocation heuristic for aDF is formulated in this section by considering the individual impact of the two channels to account for the resulting overall optimum solution.

Firstly, let us limit our consideration to the impact of the partner-destination channel on the optimal aDF power allocation problem in (3.45) by assuming an ideal source-partner channel (i. e. letting $L_{s-p} \rightarrow 0$). Taking into account this assumption, the objective function given by (3.42) and the BER constraint given by (3.43) may be re-stated as:

$$\lim_{L_{s-p} \rightarrow 0} E_{coop-aDF} = \frac{\xi}{\eta} E_{tx-s} + E_{tx-p}, \quad (5.1)$$

$$\lim_{L_{s-p} \rightarrow 0} BER_{coop-aDF} = \frac{3N_0^2 L_{s-d} L_{p-d}}{16E_{tx-s} E_{tx-p}}. \quad (5.2)$$

The aDF power allocation optimisation problem assuming an ideal source-partner channel may then be expressed as

$$\operatorname{argmin}_{E_{tx-s}, E_{tx-p}} \left\{ \frac{\xi}{\eta} E_{tx-s} + E_{tx-p} \right\}, \text{ subject to } \frac{3N_0^2 L_{s-d} L_{p-d}}{16E_{tx-s} E_{tx-p}} \leq p_b, \quad (5.3)$$

which is identical to the ideal cooperative diversity power allocation problem solved in Chapter 3. Thus the optimally energy efficient power allocation for the source and partner transmissions in aDF with an ideal source-partner channel are given by

$$E_{tx-s-opt-aDF}(L_{s-p} \rightarrow 0) = \sqrt{\frac{3N_0^2 L_{s-d} L_{p-d}}{16p_b}}, \quad (5.4)$$

$$E_{tx-p-opt-aDF}(L_{s-p} \rightarrow 0) = \sqrt{\frac{3N_0^2 L_{s-d} L_{p-d}}{16p_b}}. \quad (5.5)$$

The total transmit energy consumption of aDF cooperative diversity with an ideal source-partner channel may thus be expressed as

$$E_{tx-TOTAL-coop-aDF}(L_{s-p} \rightarrow 0) = 2\sqrt{\frac{3N_0^2 L_{s-d} L_{p-d}}{16p_b}}. \quad (5.6)$$

Secondly, let us limit our consideration to the impact of the source-partner channel on the optimal aDF power allocation problem in (3.45) by assuming an ideal partner-

destination channel (i. e. letting $L_{p-d} \rightarrow 0$). Taking into account this assumption, the objective function in (3.42) and BER constraint in (3.43) may be re-stated as:

$$\lim_{L_{p-d} \rightarrow 0} E_{coop-aDF} = \frac{\xi}{\eta} E_{tx-s} + (2 - BLE R_{s-p}) \frac{P_{CCT-tx}}{R_b} + (3 - BLE R_{s-p}) \frac{P_{CCT-rx}}{R_b}, \quad (5.7)$$

$$\lim_{L_{p-d} \rightarrow 0} BER_{coop-aDF} = \frac{K N_0^2 L_{s-d} L_{s-p}}{4 E_{tx-s}^2}. \quad (5.8)$$

The aDF power allocation optimisation problem assuming an ideal partner-destination channel may then be expressed as

$$\underset{E_{tx-s}}{\operatorname{argmin}} \left\{ \frac{\xi}{\eta} E_{tx-s} + (2 - BLE R_{s-p}) \frac{P_{CCT-tx}}{R_b} + (3 - BLE R_{s-p}) \frac{P_{CCT-rx}}{R_b} \right\} \quad (5.9)$$

, subject to $E_{tx-s} \geq \sqrt{\frac{K N_0^2 L_{s-d} L_{s-p}}{4 p_b}}$.

The first term in the objective function in (5.9) is minimised when $E_{tx-s} = 0$. The last two terms representing the circuit energy cost of cooperation are also minimised when $E_{tx-s} \rightarrow 0$ such that $BLE R_{s-p} \rightarrow 1$ (this corresponds to the partner node never re-transmitting the source's message). However, the E_{tx-s} constraint in (5.9) must also be satisfied in order to achieve the target BER p_b . Thus the optimally energy efficient power allocation for the aDF source transmission with an ideal partner-destination channel is given by

$$E_{tx-s-opt-aDF}(L_{p-d} \rightarrow 0) = \sqrt{\frac{K N_0^2 L_{s-d} L_{s-p}}{4 p_b}}. \quad (5.10)$$

Moreover, it is obvious that no power is required for the partner-destination transmission if the partner-destination channel is assumed to be ideal. Namely, the optimally energy efficient power allocation for the aDF partner-destination transmissions with an ideal partner-destination channel is given by

$$E_{tx-p-opt-aDF}(L_{p-d} \rightarrow 0) = 0. \quad (5.11)$$

The total transmit energy consumption of aDF cooperative diversity with an ideal partner-destination channel may thus be expressed as

$$E_{tx-TOTAL-coop-aDF}(L_{p-d} \rightarrow 0) = \sqrt{\frac{K N_0^2 L_{s-d} L_{s-p}}{4 p_b}}. \quad (5.12)$$

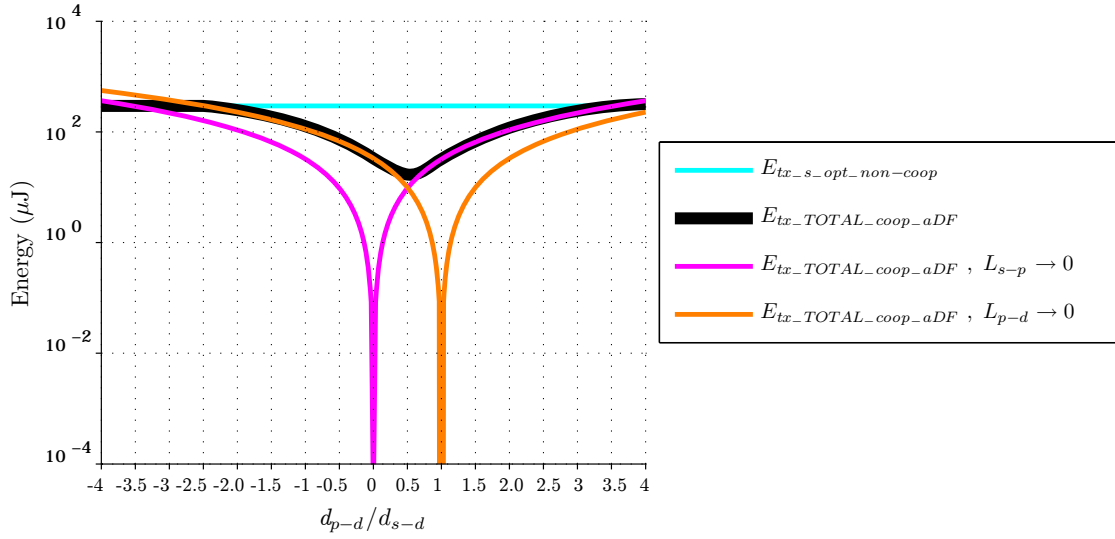


Figure 5.1: Optimally energy efficient transmit power allocation for aDF cooperation (obtained via numerical search) and the partial aDF power allocation solutions (given by (5.6) and (5.12)) vs. partner location.

The power allocation solutions given by (5.6) and (5.12) are illustrated in Fig. 5.1 for the reference system given in Table 2.1 for a range of partner node locations¹. The non-cooperative communication power allocation solution (given by (3.6)) and the optimal aDF power allocation solution (obtained via numerical search in Chapter 3) are also included in Fig. 5.1 for comparison. Importantly, Fig. 5.1 demonstrates that (5.6) and (5.12) together provide a good approximation to the optimal aDF power allocation obtained via numerical search in Chapter 3. Namely, $E_{tx_TOTAL_coop_aDF}$ is approximated by (5.6) when the source-partner channel is dominant (i.e. for $x_{p-d}/d_{s-d} < 0.5$, as shown by Fig. 5.2), and by (5.12) when the partner-destination channel is dominant (i.e. for $x_{p-d}/d_{s-d} > 0.5$, as shown by Fig. 5.2).

In view of this finding, a power allocation heuristic for aDF is proposed in this chapter is based on the conjecture that superimposing the solutions to the two independent sub-problems in (5.3) and (5.9) results in a very good approximation to the optimum solution of the full optimisation problem in (3.45). Thus the power allocation heuristic for energy efficient aDF cooperation is formulated as

$$E_{tx_s_heuristic_aDF} = \sqrt{\frac{3N_0^2 L_{s-d} L_{p-d}}{16p_b}} + \sqrt{\frac{KN_0^2 L_{s-d} L_{s-p}}{4p_b}}, \quad (5.13)$$

where $E_{tx_s_heuristic_aDF}$ gives the power allocation for the aDF source to destination transmission. The power allocation for the aDF partner to destination transmission,

¹As in Chapter 3, a one-dimensional cooperative link configuration is considered for ease of demonstration, with the partner node being located somewhere on the horizontal line passing through the source node and the destination receiver. The partner's location is specified in terms of its x-distance from the destination receiver, normalised by the source-destination separation.

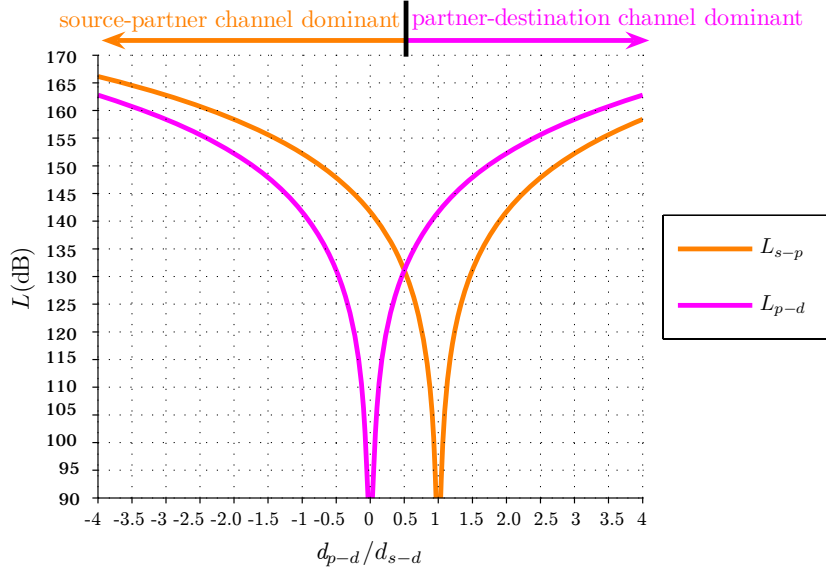


Figure 5.2: Quality of the source-partner and partner-destination channels (in terms of average path loss) vs. partner location. The source-partner channel path loss is dominant for $x_{p-d}/d_{s-d} < 0.5$, whereas the partner-destination channel path loss is dominant for $x_{p-d}/d_{s-d} > 0.5$.

$E_{tx_p_heuristic_aDF}$, is then obtained by substituting (5.13) into (3.44) to satisfy the BER constraint in (3.41):

$$E_{tx_p_heuristic_aDF} = \frac{\left(1 - \frac{KN_0 L_{s-p}}{E_{tx_s_heuristic_aDF}}\right) 3N_0^2 L_{s-d} L_{p-d}}{16E_{tx_s_heuristic_aDF} \left(p_b - \frac{KN_0^2 L_{s-d} L_{s-p}}{4E_{tx_s_heuristic_aDF}^2}\right)}. \quad (5.14)$$

It follows that the total transmit energy consumption of aDF cooperation using the heuristic power allocation may be expressed as

$$E_{tx_TOTAL_heuristic_aDF} = E_{tx_s_heuristic_aDF} + \left(1 - \frac{KN_0 L_{s-p}}{E_{tx_s_heuristic_aDF}}\right) E_{tx_p_heuristic_aDF} \quad (5.15)$$

The heuristic aDF power allocation given by (5.15) is shown in Fig. 5.3 alongside the optimal aDF power allocation solution (obtained via numerical search in Chapter 3) for the reference cooperative system and a range of partner node locations. Additionally, the constituent parts of the heuristic power allocation solution are shown in Fig. 5.4 for completeness. Importantly, Fig. 5.3 confirms that the heuristic aDF power allocation $E_{tx_TOTAL_heuristic_aDF}$ provides a very good approximation to the optimal aDF power

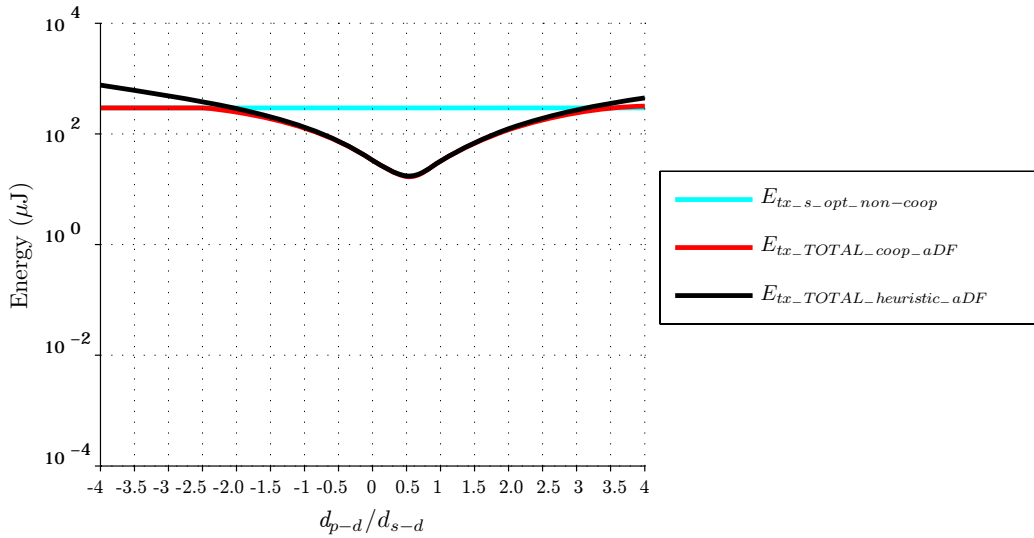


Figure 5.3: Comparison of heuristic transmit power allocation (given by (5.15)) and optimal transmit power allocation (obtained via numerical search) for energy efficient aDF cooperation vs. partner location.

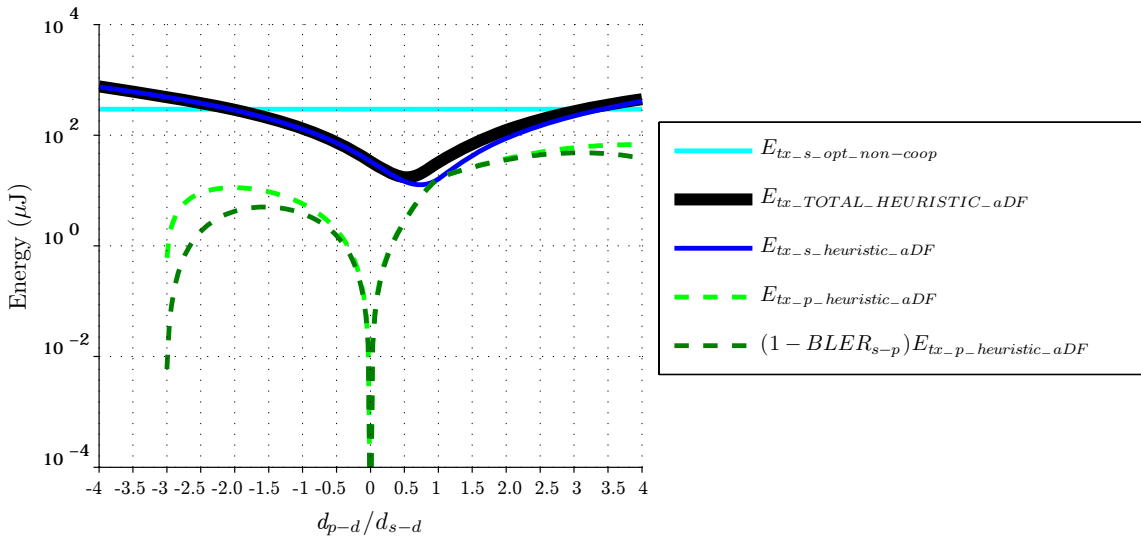


Figure 5.4: Heuristic transmit power allocation for energy efficient aDF cooperation (given by (5.13), (5.14)) vs. partner location.

allocation $E_{tx_TOTAL_coop_aDF}$. This suggests that the aDF power allocation heuristic proposed in this chapter is near-optimal with respect to maximising the energy efficiency of aDF cooperation.

5.3 Energy Conservation Performance of the Power Allocation Heuristic

In this section the energy conservation performance of the aDF power allocation heuristic is evaluated and compared to that of aDF with optimal power allocation presented in

Chapter 4. Namely, the practical energy efficiency of aDF cooperation is examined in terms of the partner choice region for energy efficient cooperation. The impact of various system parameters on the heuristic's performance is also analysed in order to demonstrate the validity of the heuristic across a wide range of communication system configurations. As in Chapter 4, the energy conservation performance is quantified in terms two key metrics²: the area of the partner choice region for a given minimum energy efficiency of cooperation and the maximum energy saving achieved over all considered partner node locations.

5.3.1 Energy Efficiency of the Reference Cooperative System

The total energy savings resulting from aDF cooperation using the power allocation heuristic in (5.13) and (5.14) are shown in Fig. 5.5 for a range of partner locations³ for the reference cooperative system given in Table 2.1. Comparing Fig. 5.5 with Fig. 4.3, it is evident that the proposed power allocation heuristic overall provides a very good approximation to the optimum aDF power allocation obtained via numerical search. The heuristic power allocation prescribes a somewhat smaller partner choice region than the search-based optimum allocation for energy savings of less than 50%. Importantly, the heuristic power allocation results in virtually the same partner choice region for high cooperative energy savings as optimum power allocation. This is confirmed by Fig. 5.6 which shows that the area of the partner choice region for any given energy efficiency of aDF cooperation is only slightly larger for optimal compared with heuristic power allocation. Specifically, the size of the aDF partner choice region with optimal power allocation is only between 1.04 and 1.43 times larger that of aDF using the power allocation heuristic, with the discrepancy between the two power allocation methods diminishing for a higher energy efficiency of cooperation. Finally, Table 5.1 shows that the maximum energy efficiency of aDF cooperation with heuristic power allocation is only marginally lower (0.2%) than that achieved with optimum power allocation. This reveals that the power allocation heuristic developed in this chapter results in near-optimally energy efficient aDF cooperation given the ideal case of selecting a cooperation partner located at the corresponding best location.

²The significance of these metrics is discussed in Section 4.2.4.

³As in Chapter 4, the candidate partner node locations considered are on a uniform 1m×1m grid covering the network area (i.e. a candidate partner node is placed every 1m in the x-direction and every 1m in the y-direction from the destination receiver located at the origin).

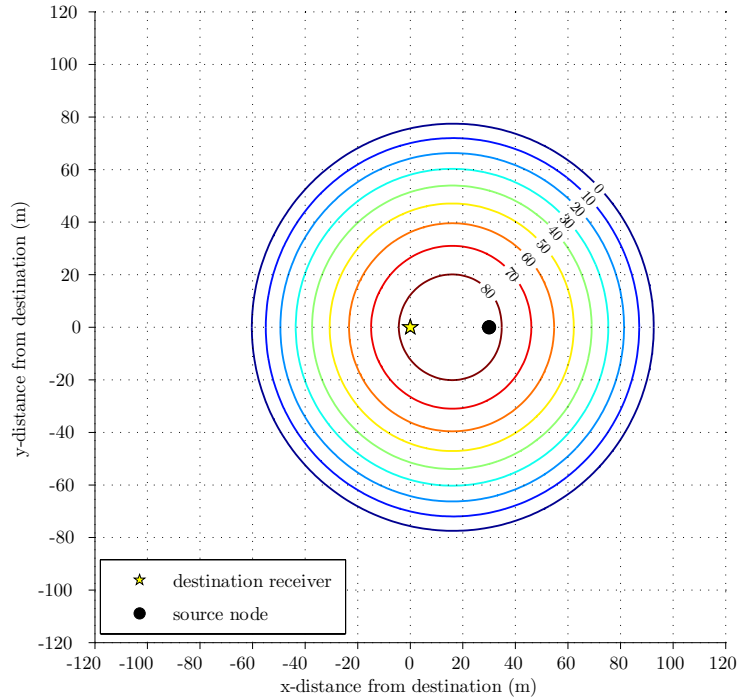


Figure 5.5: Total energy savings (2.17) achieved for a source node cooperating with a range of potential partners using aDF cooperation with heuristic transmit power allocation (given by (5.13), (5.14)), for the reference system specified in Table 2.1.

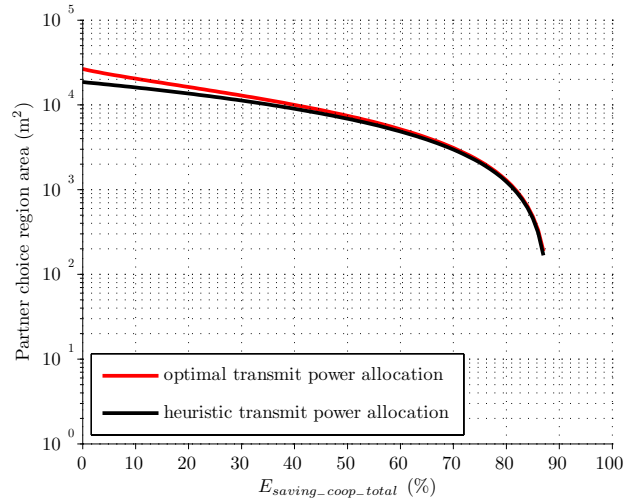


Figure 5.6: Size of the partner choice region for a given energy efficiency of aDF cooperation using optimal vs. heuristic power allocation, for the reference system.

Table 5.1: Comparison of the maximum energy saving achieved over all considered partner locations using optimal and heuristic power allocation for the aDF cooperative diversity scheme, for the reference system specified in Table 2.1.

Power allocation method	Maximum energy saving (%)
Optimum (search-based)	88.4
Heuristic (given by (5.13), (5.14))	88.2

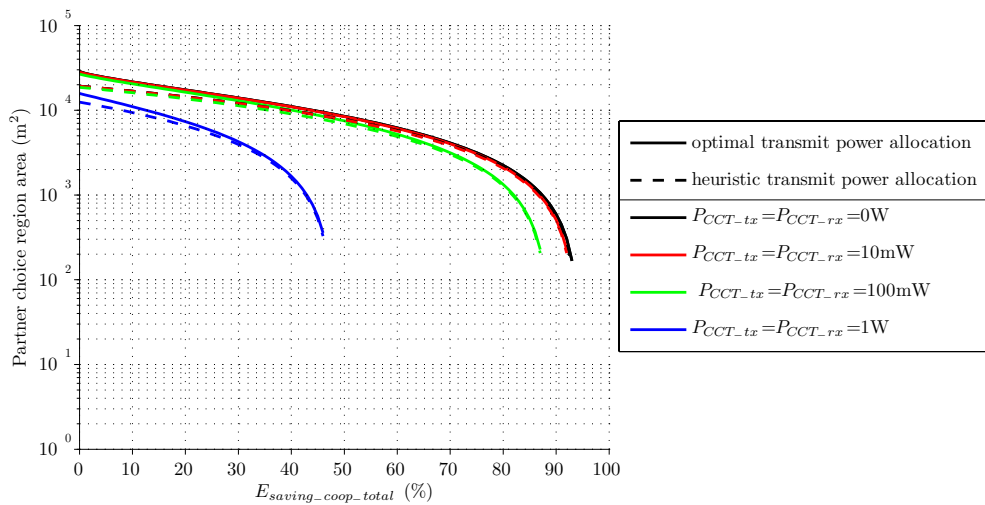


Figure 5.7: Comparison of the size of the partner choice region for a given energy efficiency of aDF cooperation using optimal and heuristic transmit power allocation vs. the transceiver circuit power consumption.

5.3.2 Effect of Varying the Transceiver Circuit Power

The energy conservation performance of aDF cooperation using optimal and heuristic power allocation for different values of the transceiver circuit power consumption ($P_{CCT_tx} = P_{CCT_rx} = \{0 \text{ W}, 10 \text{ mW}, 100 \text{ mW}, 1 \text{ W}\}$) is quantified in Fig. 5.7 in terms of the area of the partner choice region for a given minimum energy efficiency of cooperation. Fig. 5.7 demonstrates that heuristic power allocation achieves a very similar energy efficiency as optimal power allocation for all considered values of the transceiver circuit power consumption. Specifically, the area of the partner choice region for a given energy efficiency of cooperation using aDF with optimal power allocation is only between 1.03 and 1.49 times larger than that resulting from aDF with heuristic power allocation. Moreover, heuristic power allocation yields virtually the same maximum energy efficiency of cooperation as optimal power allocation (shown in Fig. 4.8) for all considered values of the transceiver circuit power consumption. Specifically, the discrepancy between the two power allocation methods ranges from 0.16% to 0.17%.

5.3.3 Effect of Varying the Source-Destination Separation

The energy conservation performance of aDF cooperation using optimal and heuristic power allocation for different values of the source-destination separation ($d_{s-d} = \{15 \text{ m}, 20 \text{ m}, 30 \text{ m}, 40 \text{ m}, 50 \text{ m}, 60 \text{ m}, 70 \text{ m}, 80 \text{ m}, 90 \text{ m}, 100 \text{ m}\}$) is quantified in Fig. 5.8 in terms of the area of the partner choice region for a given minimum energy efficiency of cooperation. Fig. 5.8 demonstrates that heuristic power allocation achieves a very similar energy efficiency as optimal power allocation for all considered values of the source-destination

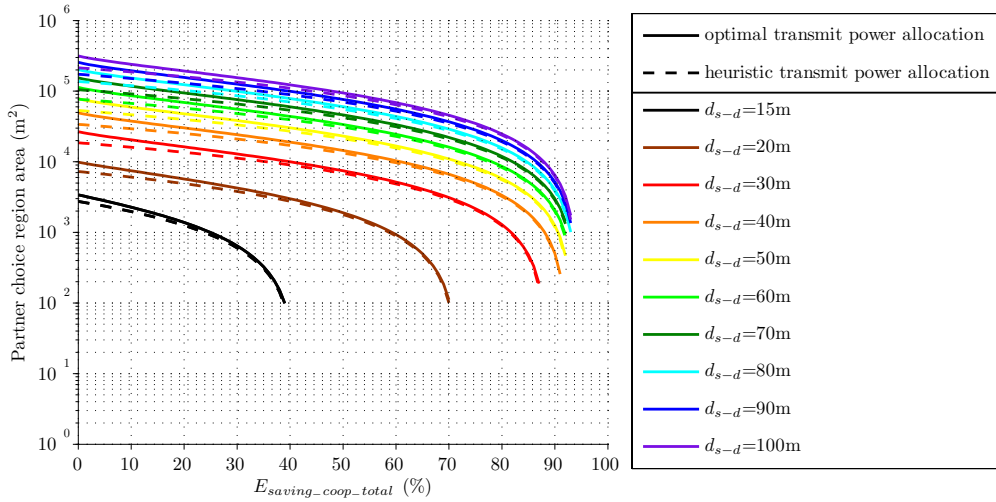


Figure 5.8: Comparison of the size of the partner choice region for a given energy efficiency of aDF cooperation using optimal and heuristic transmit power allocation vs. the source-destination separation.

separation. Specifically, the area of the partner choice region for a given energy efficiency of cooperation using aDF with optimal power allocation is only between 1.03 and 1.47 times larger than that resulting from aDF with heuristic power allocation. Furthermore, heuristic power allocation yields virtually the same maximum energy efficiency of cooperation as optimal power allocation (shown in Fig. 4.13) for all considered values of the source-destination separation (the discrepancy between the two power allocation methods ranges from 0.16% to 0.17%).

5.3.4 Effect of Varying the Channel Path Loss Exponent

The energy conservation performance of aDF cooperation using optimal and heuristic power allocation for different values of the channel path loss exponent ($k = \{3, 3.5, 4, 5, 6, 7, 8, 9, 10\}$) is quantified in Fig. 5.9 in terms of the area of the partner choice region for a given minimum energy efficiency of cooperation. Fig. 5.9 shows that the area of the partner choice region for a given energy efficiency of cooperation using aDF with optimal power allocation is only between 1.006 and 1.43 times larger than that resulting from aDF with heuristic power allocation. Therefore heuristic power allocation achieves a very similar energy efficiency as optimal power allocation for all considered values of the channel path loss exponent. Additionally, heuristic power allocation yields virtually the same maximum energy efficiency of cooperation as optimal power allocation (shown in Fig. 4.18) for all considered values of the channel path loss exponent, with the discrepancy between the two power allocation methods ranging from 0.02% to 0.2%.

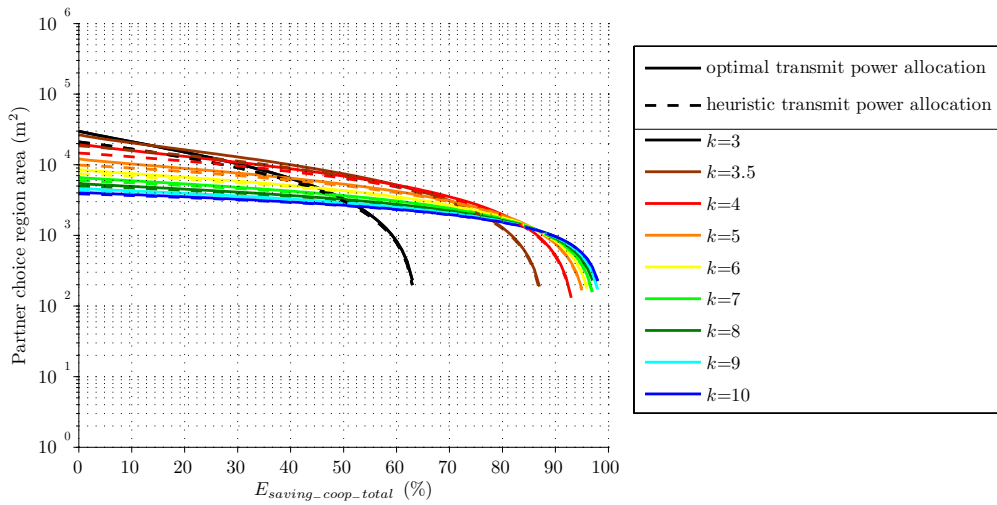


Figure 5.9: Comparison of the size of the partner choice region for a given energy efficiency of aDF cooperation using optimal and heuristic transmit power allocation vs. the channel path loss exponent.

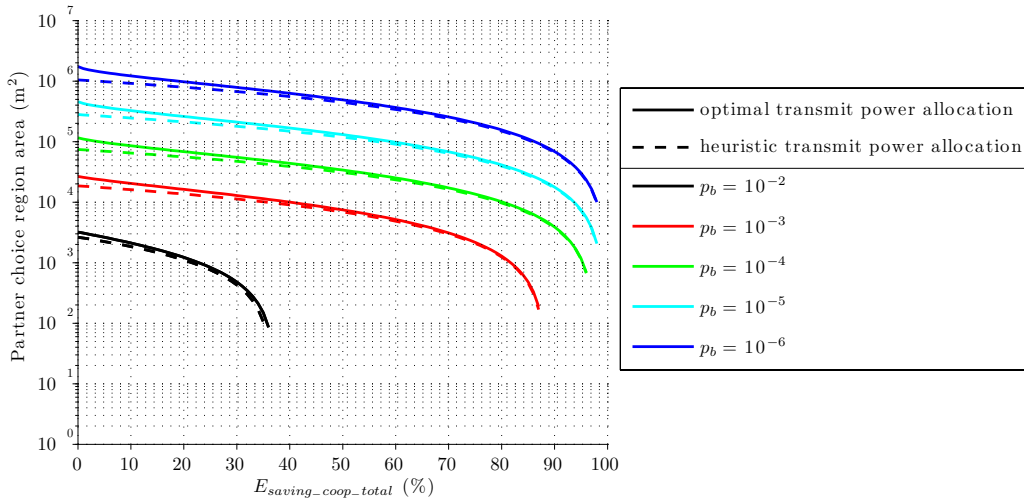


Figure 5.10: Comparison of the size of the partner choice region for a given energy efficiency of aDF cooperation using optimal and heuristic transmit power allocation vs. the target BER.

5.3.5 Effect of Varying the Target Bit Error Rate

The energy conservation performance of aDF cooperation using optimal and heuristic power allocation for different values of the target BER ($p_b = \{10^{-2}, 10^{-3}, 10^{-4}, 10^{-5}, 10^{-6}\}$) is quantified in Fig. 5.10 in terms of the area of the partner choice region for a given minimum energy efficiency of cooperation. Fig. 5.10 shows that the area of the partner choice region for a given energy efficiency of cooperation using aDF with optimal power allocation is only between 1.03 and 1.67 times larger than that resulting from aDF with heuristic power allocation. Therefore heuristic power allocation achieves a very similar energy efficiency as optimal power allocation for all considered values of the target BER.

Moreover, heuristic power allocation yields virtually the same maximum energy efficiency of cooperation as optimal power allocation (shown in Fig. 4.23) for all considered values of the target BER, with the discrepancy between the two power allocation methods ranging from 0.005% to 0.71%.

5.4 Discussion of the Practical Significance of the Power Allocation Heuristic

The analysis presented in the preceding sections has consistently shown that the proposed aDF power allocation heuristic achieves a very similar energy efficiency of cooperation as the optimal power allocation across a wide range of network configurations and system parameter settings. Importantly, the heuristic consists of two straightforward formulae that can be easily and autonomously computed by a sensor node. By contrast, the computationally intensive search required to determine the optimal aDF power allocation would be infeasible for a simple sensor node to perform. Therefore, the proposed power allocation heuristic is a simple and practical yet near-optimal power allocation strategy for energy efficient aDF cooperation in a resource-constrained wireless network.

Moreover, aside from enabling practical implementation of energy efficient aDF cooperation, the heuristic developed in this chapter provides an important insight into the nature of the power allocation solution for aDF. Namely, the development and analysis of the heuristic presented in this chapter has clearly demonstrated that the source-partner and partner-destination channels are equally important factors in determining the energy efficiency of aDF cooperation. Firstly, this result is significant because it contributes important knowledge towards developing robust partner selection strategies for practical aDF cooperation in Chapter 6. Secondly, this result enables a power allocation heuristic to be derived for aDF cooperation with various modulation and coding schemes, using the exact same method as was employed for the case of uncoded BPSK modulation in this chapter.

5.5 Summary

In this chapter a power allocation heuristic for practical energy efficient aDF cooperation has been proposed. The heuristic has been developed by considering the individual impact of the source-partner and partner-destination channels on the power allocation for optimally energy efficient aDF cooperation. It has been shown that the heuristic aDF power allocation, obtained by superimposing the solutions to these two independent sub-problems, results in a very good approximation to the optimal aDF power allocation obtained via numerical search.

The energy conservation performance of the proposed aDF power allocation heuristic has been analysed in terms of the partner choice region for energy efficient cooperation. The practical energy efficiency of aDF cooperation has thereby been evaluated across a wide range of communication system configurations. The results of this investigation have consistently demonstrated that the aDF power allocation heuristic proposed in this chapter is near-optimal with respect to maximising the energy efficiency of aDF cooperation. Importantly, this near-optimal heuristic consists of two simple formulae that can be easily and autonomously computed by sensor nodes. By contrast, a search must be performed to obtain the optimal aDF power allocation, which is prohibitively computationally expensive for resource-constrained sensor nodes.

Therefore, the proposed power allocation heuristic is a simple and practical yet near-optimal power allocation strategy for energy efficient aDF cooperation in a resource-constrained wireless network. In Chapter 6 the power allocation heuristic developed in this chapter serves as the foundation for developing several robust partner choice strategies for practical aDF cooperation. Together these power allocation and partner choice heuristics constitute the core of the distributed cooperation strategy for energy-constrained wireless networks proposed in this thesis, which is presented and analysed in Chapters 7- 11.

Chapter 6

Partner Choice Strategies for Practical Energy Efficient Cooperation

6.1 Introduction

For practical deployment of cooperative communication to be feasible in a wireless sensor network, sensor nodes must be able to make energy efficient cooperation decisions independently. In Chapter 5 a simple yet near-optimal power allocation heuristic was proposed for practical energy efficient aDF cooperation. This heuristic enables sensor nodes to autonomously determine the best allocation of transmit power for cooperation. The other crucial aspect of practical cooperation is the selection of the most beneficial cooperation partner out of a set of several potential partner nodes available in the network. This problem of best partner choice was previously examined in this thesis in Chapter 4, where the partner choice region for energy efficient cooperation was investigated.

In practice it would be infeasible for a resource-constrained sensor node to select its cooperation partner by explicitly calculating the actual energy saving expected from each candidate partner node. Instead, a simple and robust partner selection strategy is required to enable practical distributed cooperation among sensor nodes. In this chapter, several computationally efficient partner choice heuristics are developed based on either global or local knowledge of average path loss values in the network. These are practical partner selection strategies which can be autonomously implemented by resource-constrained sensor nodes to obtain significant cooperative energy savings.

In Section 6.2 the best partner choice problem is formally defined. Three different partner choice heuristics of varying computational complexity are developed in Section 6.3 and their partner selection performance is illustrated in Section 6.4. The validity of the proposed partner choice heuristics is thoroughly evaluated across a wide range of communication system configurations in Section 6.5 by comparing their partner ranking performance against that of optimal partner selection. Moreover, by comparing the performance of the

three heuristics, the trade-off between heuristic complexity and performance is examined throughout the chapter. In Section 6.6 the practical significance of the proposed partner choice heuristics is discussed.

The partner choice heuristics developed in this chapter (together with the power allocation heuristic developed in Chapter 5) form the basis of the distributed cooperation strategy for energy-constrained wireless networks proposed in this thesis, which is presented and analysed in Chapters 7-11.

6.2 Best Partner Choice Problem Definition

The best cooperation partner out of a set of N candidate partner nodes is defined to be the partner with whom cooperating yields the highest energy saving. The problem of selecting the best cooperation partner for energy efficient aDF cooperation may thus be formally expressed as

$$\operatorname{argmax}_{L_{s-p(i)}, L_{p(i)-d}} \{E_{\text{saving-coop-total}}(L_{s-p(i)}, L_{p(i)-d})\}, i \in \{1, 2, \dots, N\}, \quad (6.1)$$

where $L_{s-p(i)}$ and $L_{p(i)-d}$ are the channel path loss values associated with the i^{th} candidate partner node in the set of N candidate partners and $E_{\text{saving-coop-total}}$ is given by (2.17). It is assumed that transmit power allocation is based on the near-optimally energy efficient power allocation heuristic developed in Chapter 5. Namely, E_{coop} in (2.17) is given by substituting (5.13) and (5.14) into (3.42).

Substituting (5.13) and (5.14) into (6.1) it is evident that the optimisation problem in (6.1) is non-linear with respect to the decision variables $L_{s-p(i)}$ and $L_{p(i)-d}$; thus a search-based method must be used to find the optimum solution. The solution to this partner choice problem has been illustrated in terms of network geometry in Fig. 5.5 of Chapter 5, which shows the energy savings achieved from cooperation using the power allocation heuristic in (5.13), (5.14) for a range of potential partner node locations (assuming the reference system parameters in Table 2.1). The partner choice problem has also been thoroughly investigated in terms of the partner choice region for energy efficient cooperation in Chapter 4 for the case of optimal aDF power allocation.

The analysis in Chapters 4 and 5 has demonstrated that the optimally energy efficient partner node location for aDF cooperation is about midway between the source and the destination. Based on this observation, a basic strategy for choosing the best cooperation partner for energy efficient aDF cooperation was formulated in Chapter 4. However, this preliminary heuristic only predicts the optimal partner location and is not designed to correctly differentiate between two non-ideal candidate partner nodes. Moreover, such a location-based partner selection rule requires a source node to have knowledge of its own

location relative to the destination receiver as well as the location of candidate partner nodes (both relative to the source node and the destination receiver). This is highly undesirable for nodes in the infrastructure-less wireless sensor network, where localisation is a non-trivial problem. However, whereas sensor nodes have to infer network distances, they can directly measure received signal strength. Thus the partner choice heuristics developed in the following section are based on knowledge of average path loss values in the network.

6.3 Development of the Partner Choice Heuristics

For a fixed source node and destination receiver, the maximisation problem in (6.1) may be re-expressed as the equivalent minimisation problem,

$$\underset{L_{s-p(i)}, L_{p(i)-d}}{\operatorname{argmin}} \quad \{E_{coop-aDF}(L_{s-p(i)}, L_{p(i)-d})\}, \quad i \in \{1, 2, \dots, N\}, \quad (6.2)$$

where $E_{coop-aDF}$ is given by (3.42) wherein E_{tx-s} and E_{tx-p} are functions of L_{s-p} and L_{p-d} as given by (5.13) and (5.14).

The expression for $E_{coop-aDF}$ may be simplified by only considering the dominant terms¹ in (3.42) which are dependent on the decision variables L_{s-p} and L_{p-d} , giving

$$E_{coop-aDF} \approx E_{tx-s} + \left(1 - \frac{KN_0 L_{s-p}}{E_{tx-s}}\right) E_{tx-p}, \quad (6.3)$$

which is equivalent to $E_{tx-TOTAL-heuristic-aDF}$ in (5.15). It was observed in Chapter 3 that the source transmit energy dominates the total aDF power allocation. This is also clearly demonstrated by Fig 5.4 in Chapter 5, which shows that the $E_{tx-TOTAL-heuristic-aDF}$ curve is very similar to that of $E_{tx-s-heuristic-aDF}$. It follows that $E_{coop-aDF}$ may be roughly approximated as

$$E_{coop-aDF} \approx E_{tx-s}. \quad (6.4)$$

Furthermore, the fundamental relationship between E_{tx-s} and L_{s-p} and L_{p-d} in (5.13) may be expressed as

$$E_{tx-s} \propto \sqrt{L_{s-p}} + \sqrt{L_{p-d}}. \quad (6.5)$$

6.3.1 First Global Knowledge Partner Choice Heuristic: GKH_1

Substituting (6.4), (6.5) into (6.2), the first partner choice heuristic is formulated as

¹Namely, $P_{CCT-tx}=P_{CCT-rx}=0$ is assumed for the purpose of formulating the partner choice heuristics, since circuit energy consumption is an unavoidable overhead of cooperation.

$$GKH_1 = \underset{L_{s-p(i)}, L_{p(i)-d}}{\operatorname{argmin}} \left\{ \sqrt{L_{s-p(i)}} + \sqrt{L_{p(i)-d}} \right\}, i \in \{1, 2, \dots, N\}. \quad (6.6)$$

Thus a source node selects its partner using GKH_1 by computing the partner rating metric $\left\{ \sqrt{L_{s-p}} + \sqrt{L_{p-d}} \right\}$ for all N candidate partner nodes and selecting the partner with the lowest partner rating metric result. It should be noted that since GKH_1 requires full information about each candidate partner node, $\{L_{s-p(i)}, L_{p(i)-d}\}, i \in \{1, 2, \dots, N\}$, the source must have global knowledge of network path losses in order to perform partner selection using this partner choice heuristic.

The partner location which minimises the GKH_1 partner rating metric is midway between the source and the destination receiver. This can be easily demonstrated by considering a one-dimensional cooperative network configuration, with the partner node being located somewhere on the horizontal line passing through the source node and the destination receiver², such that $d_{s-p} = d_{s-d} - d_{p-d}$. Using (2.12) to map path loss to distance, the GKH_1 minimisation problem in (6.6) may be re-expressed as: $\min \left\{ L_{ref}^{\frac{k}{2}} (d_{s-d} - d_{p-d})^{\frac{k}{2}} + L_{ref}^{\frac{k}{2}} d_{p-d}^{\frac{k}{2}} \right\}$. It can then be solved by setting the derivative of the objective function to zero to give the optimal GKH_1 partner location as $d_{p-d} = \frac{d_{s-d}}{2}$. Therefore, GKH_1 will select the partner located³ at $d_{p-d} = d_{s-p} = \frac{d_{s-d}}{2}$, which has been shown to be the near-optimal partner location for energy efficient aDF cooperation in Chapters 4 and 5.

6.3.2 Second Global Knowledge Partner Choice Heuristic: GKH_2

The second partner choice heuristic is formulated by simplifying GKH_1 to construct the simplest partner rating metric possible using full information about each candidate partner node,

$$GKH_2 = \underset{L_{s-p(i)}, L_{p(i)-d}}{\operatorname{argmin}} \left\{ \max \left\{ L_{s-p(i)}, L_{p(i)-d} \right\} \right\}, i \in \{1, 2, \dots, N\}, \quad (6.7)$$

Thus the best partner is chosen using GKH_2 based solely on the dominant path loss associated with each candidate partner node. In other words, GKH_2 judges each candidate partner node based on the poorer quality channel of the two channels (source-partner and partner-destination) associated with that partner node. Whereas GKH_1 requires a calculation to generate the partner rating metric, GKH_2 produces the metric via a comparison

²The one-dimensional cooperative network geometry in fact minimises both d_{s-p} and d_{p-d} for a given d_{s-d} .

³Provided a candidate partner node exists at this exact location.

of the two path loss values associated with each candidate partner node, thereby further reducing the computational burden of partner choice.

As for GKH_1 , the partner location which minimises the GKH_2 partner rating metric is midway between the source and the destination receiver. Again considering a one-dimensional cooperative network configuration such that $d_{s-p} = d_{s-d} - d_{p-d}$, the GKH_2 minimisation problem in (6.7) may be re-expressed as: $\min \left\{ \max \left\{ L_{ref}^k (d_{s-d} - d_{p-d})^k, L_{ref}^k d_{p-d}^k \right\} \right\}$. This objective function is minimised when $L_{ref}^k (d_{s-d} - d_{p-d})^k = L_{ref}^k d_{p-d}^k$, giving the optimal GKH_2 partner location as $d_{p-d} = \frac{d_{s-d}}{2}$. Therefore, GKH_2 will also select the partner at the near-optimally energy efficient location of $d_{p-d} = d_{s-p} = \frac{d_{s-d}}{2}$.

6.3.3 Local Knowledge Partner Choice Heuristic: LKH

The last partner choice heuristic is formulated by modifying GKH_2 such that partner selection is made solely on the basis of partial information about each candidate partner node, $\{L_{s-p(i)}\}$, $i \in \{1, 2, \dots, N\}$,

$$LKH = \underset{L_{s-p(i)}}{\operatorname{argmin}} \{L_{s-p(i)}\}, i \in \{1, 2, \dots, N\}. \quad (6.8)$$

Importantly, LKH only requires the source to have local knowledge of network path losses, thereby enabling simple sensor nodes to cooperate autonomously in a fully distributed and scalable manner. By contrast, GKH_1 and GKH_2 entail a higher organisational and signalling overhead since full average channel state information must be exchanged among the nodes in the network. Moreover, LKH has the lowest complexity of all three proposed partner choice heuristics, since it directly uses the L_{s-p} measurement as the partner rating metric. However, the LKH partner rating metric is minimised when the partner node is co-located with the source node. Therefore, LKH will select the partner located at $d_{s-p} = 0$, $d_{p-d} = d_{s-d}$, which is clearly suboptimal.

6.4 Illustration of Partner Selection using the Partner Choice Heuristics

In this section the performance of the partner choice heuristics GKH_1 , GKH_2 , and LKH is illustrated by considering the ranking of $N=100$ candidate partner nodes in a 100 m by 100 m network area according to the partner rating metric of each heuristic. The source node is located 30 m away from the destination receiver which is at the centre of the network area and the reference cooperative system parameters specified in

Table 2.1 are assumed. The candidate partner node rankings using the proposed heuristics are compared against the optimal partner ranking, which is obtained by directly using $E_{saving_coop_total}$ as the partner rating metric⁴, as defined by (6.1). For comparison, random partner selection is also presented alongside the proposed heuristics and optimal partner selection.

It should be noted that all candidate partner nodes that result in $E_{saving_coop_total} \leq 0\%$ are ranked last-equal using optimal partner selection, since these nodes are all unsuitable cooperation partners. By contrast, when ranking partners using the proposed partner choice heuristics the source node is ignorant of the actual $E_{saving_coop_total}$ associated with each node, and thus the heuristics differentiate between these equally unsuitable partner nodes. It should also be noted that if m nodes have the same partner rating metric result they will be given the same n^{th} -equal ranking (for all partner choice rules). Namely, assuming there were $(n - 1)$ higher-ranked nodes in the candidate partner set, these m nodes will be ranked n^{th} -equal and the next best node(s) would be ranked $(n + m)^{th}$. For example, if there were two nodes which were considered third-equal best partners in a set of 5 candidate partner nodes, the sorted node rankings would be $\{1, 2, 3, 3, 5\}$.

6.4.1 Regular Candidate Partner Node Placement

Fig. 6.1 shows the ranking of $N=100$ candidate partner nodes regularly placed over the 100 m by 100 m network area using the proposed partner choice heuristics, alongside optimal and random partner selection. Fig. 6.1 demonstrates that GKH_1 and GKH_2 select as the best partner the two nodes which are located closest to the midway point between the source and the destination, as does optimal partner selection. Importantly, Fig. 6.1 illustrates that GKH_1 overall results in a virtually identical partner ranking as optimal partner selection. There is a slightly greater discrepancy between the optimal partner ranking and that given by the lower-complexity global knowledge heuristic GKH_2 in Fig. 6.1. For example, GKH_2 ranks as 3rd-equal the nodes which yield the 7th and 8th highest energy saving. Nevertheless, the partner ranking given by GKH_2 is very similar overall to the optimal ranking. By contrast, there is a clear overall difference between the optimal partner ranking and that given by the local knowledge heuristic LKH . Since LKH ranks highest the partner nodes closest to the source node, it selects as the best partner the two nodes which in fact yield only the 5th highest energy saving. Finally, random partner choice picks (in this simulation) the partner node which is ranked 49th by optimal partner selection.

The candidate partner rankings given by the different partner choice rules are plotted against the optimal partner ranking in Fig. 6.2. This scatter plot explicitly shows

⁴Obviously, the higher the $E_{saving_coop_total}$ associated with a given partner node, the higher ranked that partner is.

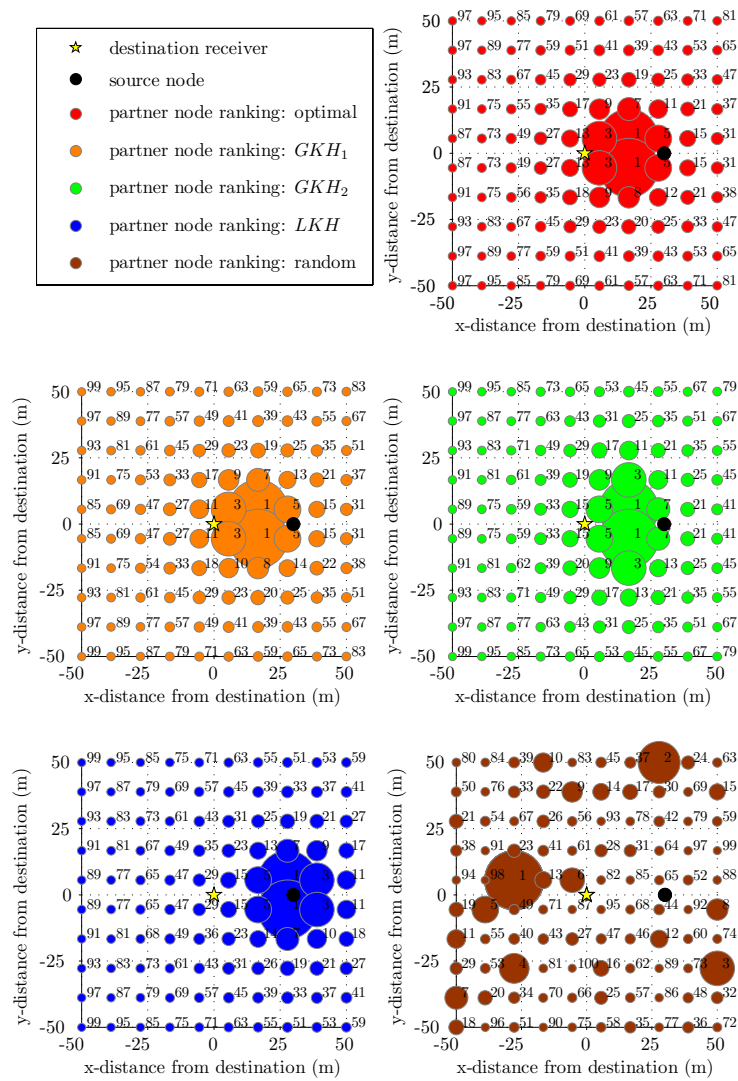


Figure 6.1: Ranking of $N=100$ candidate partner nodes regularly placed over a 100 m by 100 m network area, for different partner choice rules and the reference system specified in Table 2.1. The size of the partner node is inversely proportional to its ranking (each node is also marked with its partner ranking).

the degree of relationship between the proposed partner choice heuristics and optimal partner selection (representing the actual $E_{saving-coop-total}$ associated with each node). Fig. 6.2 clearly demonstrates the trade-off between heuristic complexity and partner selection performance: GKH_1 follows optimal partner choice very closely, GKH_2 deviates from optimal partner choice somewhat, and LKH deviates from optimal partner choice noticeably. Nevertheless, there is a clear correlation between optimal partner selection and all three proposed partner choice heuristics. By contrast, there is no correlation between random and optimal partner choice.

The degree of relationship between the partner ranking obtained using a given partner choice rule and the optimal ranking illustrated by the scatter plot in Fig. 6.2 may be quantified using the correlation coefficient. In general, the correlation coefficient, r , is a

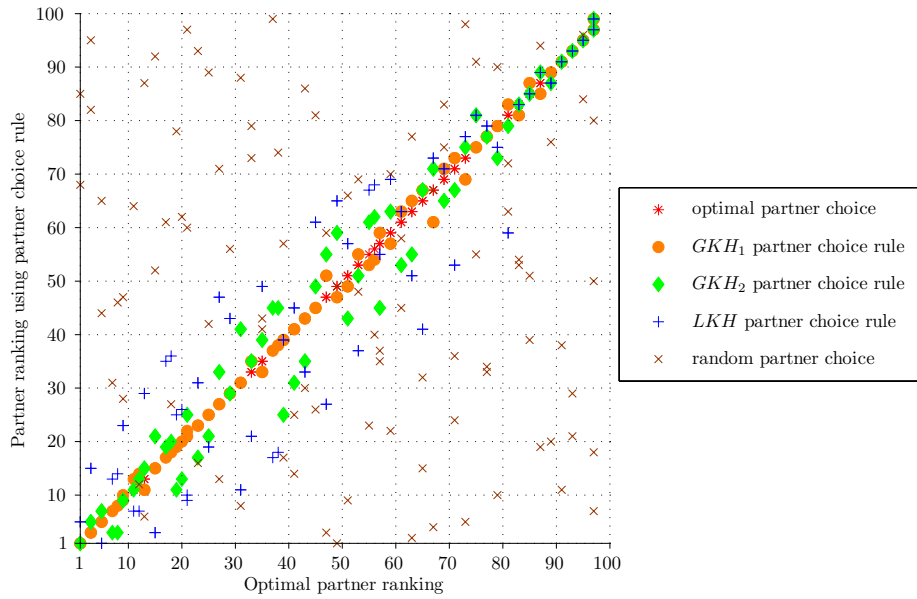


Figure 6.2: Partner node ranking using different partner choice rules vs. the optimal partner node ranking, for the reference system specified in Table 2.1 with $N=100$ candidate partner nodes regularly placed over a 100 m by 100 m network area.

measure of the degree of relationship present between two variables X and Y which are linearly related, and is given by

$$r = \frac{\sum_{i=1}^N x_i y_i - \frac{1}{N} \sum_{i=1}^N x_i \sum_{i=1}^N y_i}{\sqrt{\sum_{i=1}^N x_i^2 - \frac{1}{N} \left(\sum_{i=1}^N x_i \right)^2} \sqrt{\sum_{i=1}^N y_i^2 - \frac{1}{N} \left(\sum_{i=1}^N y_i \right)^2}} \quad (6.9)$$

where $\{x_1, x_2, \dots, x_N\}$ and $\{y_1, y_2, \dots, y_N\}$ are the N values of X and Y respectively [69]. The correlation coefficient is used throughout the remainder of this chapter to quantify the partner ranking performance of the proposed partner choice heuristics. A correlation coefficient of 1 corresponds to a perfect positive relationship between two variables, whereas a correlation coefficient of -1 represents a perfect negative relationship. It follows that if a partner choice rule specifies the identical partner node ranking as optimal partner choice, then the correlation coefficient between these two rankings is 1. Similarly, a near-optimal partner node ranking results in a positive coefficient close to 1. If there is no (linear) relationship between the ranking given by the rule and the optimal ranking, the correlation coefficient is 0. A completely random partner node ranking has no relationship with the optimal ranking and thus should result in a coefficient close to 0. Finally, in the worst case, a partner node ranking which is the reverse of the optimal ranking results in a correlation coefficient of -1.

Table 6.1 summarises the partner ranking performance of the different partner choice rules for the network shown in Fig. 6.1. These results confirm the observation from Fig. 6.2

Table 6.1: Performance of different partner choice rules compared to optimal partner selection, for the reference system specified in Table 2.1 with $N=100$ candidate partner nodes regularly placed over a 100 m by 100 m network area.

Partner choice rule	Energy saving achieved with 1 st ranked partner node (%)	Correlation coefficient with optimal partner node ranking
optimal partner choice	87.5210	1
GKH_1	87.5210	0.9982
GKH_2	87.5210	0.9822
LKH	84.1083	0.9230
random partner choice	53.5846	-0.1554

that GKH_1 and GKH_2 exhibit a very high positive correlation with optimal partner selection. Therefore, GKH_1 and GKH_2 achieve a near-optimal partner node ranking. By contrast, the correlation between LKH and optimal partner selection is only moderately high. Thus although LKH achieves a suboptimal partner node ranking, it is still closely related to the optimal partner ranking. As expected, random partner choice results in a correlation coefficient close to 0 and optimal partner choice has a correlation coefficient of 1 with itself. Table 6.1 also shows the $E_{saving_coop_total}$ achieved with the 1st ranked node for each partner choice rule. This metric is also used (together with the correlation coefficient) throughout the remainder of this chapter to quantify the performance of the proposed partner choice heuristics. Importantly, Table 6.1 shows that the energy saving achieved with the partner selected using the suboptimal partner choice heuristic LKH is still substantial, being only about 3.4% less than that achieved using optimal partner selection.

6.4.2 Random Candidate Partner Node Placement

Fig. 6.3 shows the ranking of $N=100$ candidate partner nodes randomly placed (with a uniform distribution) over the 100 m by 100 m network area using the proposed partner choice heuristics, alongside optimal and random partner selection. Fig. 6.1 exhibits very similar partner ranking results to those presented in Section 6.4.1 for a regular partner node placement: GKH_1 and GKH_2 rank most highly the nodes closest to the midway point between the source and the destination, whereas LKH ranks highest the nodes closest to the source. Specifically, for this particular random candidate partner placement, GKH_1 selects as the best partner the node that yields the highest energy saving (i.e. the same node as optimal partner selection) whereas GKH_2 and LKH select the nodes that yield the 2nd and 5th highest energy saving, respectively. Moreover, GKH_1 overall follows the optimal partner node ranking most closely, followed by GKH_2 and LKH , as for the regular partner node placement in Section 6.4.1. This is clearly illustrated by

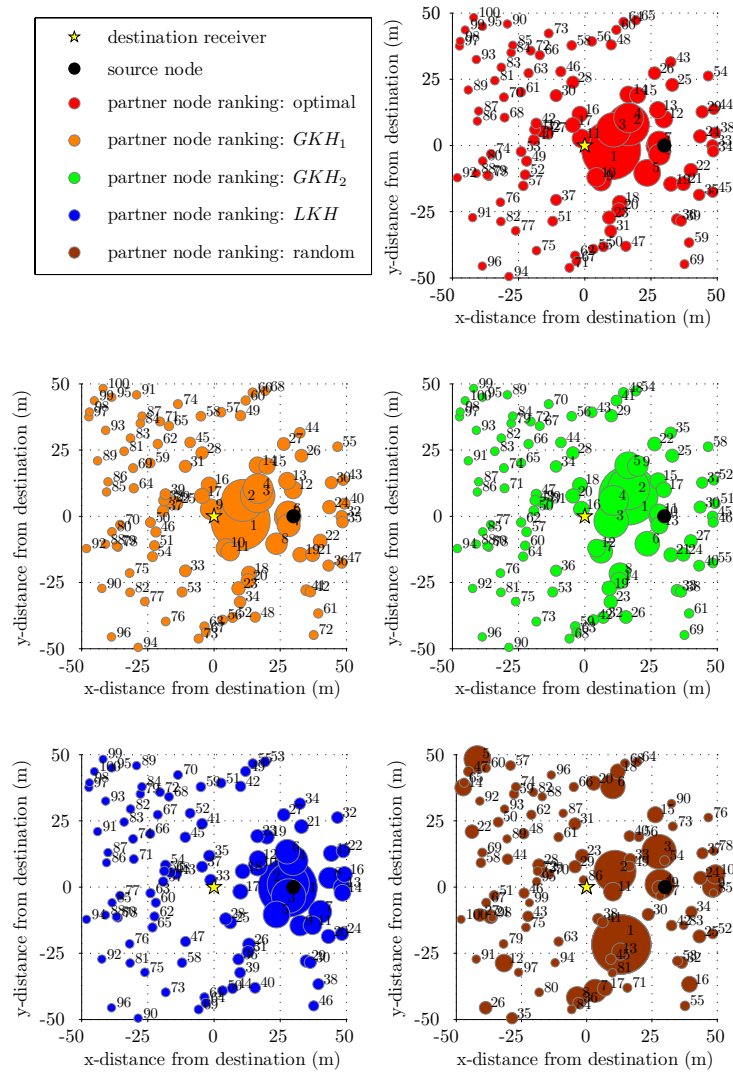


Figure 6.3: Ranking of $N=100$ candidate partner nodes randomly placed (with a uniform distribution) over a 100 m by 100 m network area, for different partner choice rules and the reference system specified in Table 2.1. The size of the partner node is inversely proportional to its ranking (each node is also marked with its partner ranking).

Fig. 6.4 where the candidate partner rankings given by the different partner choice rules (for the network in Fig. 6.3) are plotted against the optimal partner ranking. As shown in Table 6.2, GKH_1 and GKH_2 exhibit a very high positive correlation with optimal partner selection as they achieve a near-optimal partner node ranking. The correlation between LKH and optimal partner selection is only moderately high since LKH results in a suboptimal partner node ranking. Table 6.2 also shows that although the two lower complexity heuristics GKH_2 and LKH do not select the optimal partner node, the energy saving achieved with their selected partner is only about 0.5% and 2.8% less than that achieved using optimal partner selection, respectively.

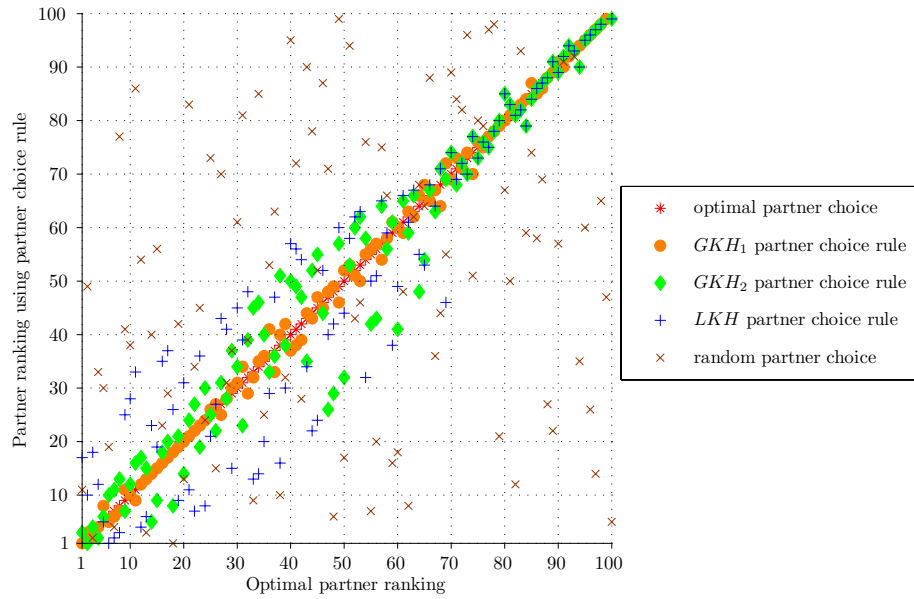


Figure 6.4: Partner node ranking using different partner choice rules vs. the optimal partner node ranking, for the reference system specified in Table 2.1 with $N=100$ candidate partner nodes randomly placed (with a uniform distribution) over a 100 m by 100 m network area.

Table 6.2: Performance of different partner choice rules compared to optimal partner selection, for the reference system specified in Table 2.1 with $N=100$ candidate partner nodes randomly placed (with a uniform distribution) over a 100 m by 100 m network area.

Partner choice rule	Energy saving achieved with 1 st ranked partner node (%)	Correlation coefficient with optimal partner node ranking
optimal partner choice	87.3794	1
GKH_1	87.3794	0.9984
GKH_2	86.8601	0.9741
LKH	84.5378	0.9341
random partner choice	72.8650	0.2681

6.5 Partner Ranking Performance of the Partner Choice Heuristics

In this section the performance of the proposed partner choice heuristics GKH_1 , GKH_2 , and LKH is evaluated across a wide range of communication system configurations, in order to demonstrate their validity in general. This analysis also enables a thorough comparison of the proposed heuristics, further demonstrating the trade-off between heuristic complexity and partner ranking performance. The partner ranking performance is quantified in terms of the two metrics introduced in Section 6.4: the correlation coefficient with the optimal partner ranking and the energy saving achieved with the selected (1st ranked) partner node.

The analysis presented in this section is based on the reference cooperative system parameters specified in Table 2.1. In Section 6.5.1 the effect of varying the size of the candidate partner set N is investigated. In Sections 6.5.2-6.5.5 the number of candidate partner nodes is set to $N=1000$ and the effect of varying several other system parameters is investigated. The results presented throughout this section are the averages of partner ranking performance results obtained from simulating $Q = \left(\frac{10^5}{N}\right)$ random network realisations of N candidate partner nodes placed over the reference 100 m by 100 m network area. The results presented for random partner selection are the average of $Q = 10^5$ runs, regardless of the candidate node density (since random partner selection is inherently highly variable regardless of N , as demonstrated in Section 6.5.1).

It is assumed that, following partner selection, the source node would check whether it is worthwhile to cooperate at all by calculating the expected $E_{\text{saving-coop-total}}$ with the 1st ranked partner node (regardless of which partner selection method had been employed). Namely, if the selected partner node would yield $E_{\text{saving-coop-total}} \leq 0\%$, the source node will opt for a non-cooperative transmission to the destination receiver. In this case, the energy saving achieved with the 1st ranked partner is recorded as zero (for that network realisation) in the presented simulation results.

6.5.1 Performance of the Partner Choice Heuristics as the Number of Candidate Partner Nodes is Varied

Fig. 6.5 shows the energy saving achieved with the 1st ranked partner node as the number of candidate partner nodes is varied ($N=\{1, 2, 3, 4, 5, 10, 30, 100, 300, 1000\}$), for the reference cooperative system using different partner selection rules. The energy saving achieved using optimal partner choice increases with increasing candidate partner node density. The energy saving achieved using the best available partner approaches the asymptote given by the cooperative energy saving achievable if the partner could be placed at the predetermined optimal location. This is given by the maximum energy saving achievable over all partner node locations presented⁵ in Chapter 5, where the partner node locations considered are on a uniform 1 m×1 m grid covering the network area (such that 10201 candidate partner nodes are considered over the 100 m by 100 m network area). Similarly, the energy saving achieved using random partner choice is given by the mean energy saving achieved over the 100 m by 100 m network area (obtained by averaging the energy saving results for the 10201 regularly placed candidate partner nodes). As shown by Fig. 6.5, the energy savings achieved by the different partner choice rules all converge to this value as the candidate partner node density $N \rightarrow 1$. The

⁵As heuristic power allocation yields virtually the same maximum energy efficiency of cooperation as optimal power allocation, only the discrepancy between the two power allocation methods is reported in Chapter 5, whilst referring to the maximum energy efficiency results shown in Chapter 4.

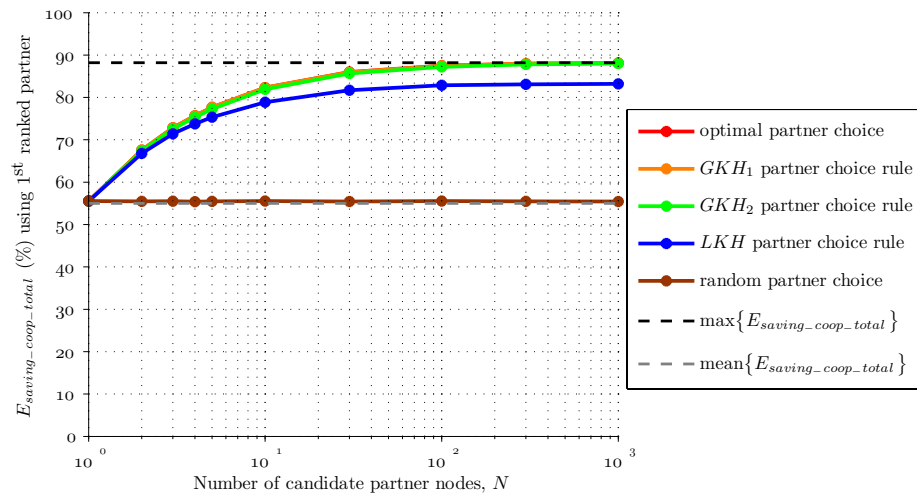


Figure 6.5: Energy saving achieved using the 1st ranked partner vs. number of candidate partner nodes, for different partner choice rules and the reference system specified in Table 2.1 (average of Q random network realisations of N candidate partner nodes placed over the 100 m by 100 m network area).

maximum and mean energy saving over the 100 m by 100 m network area are designated as $\max\{E_{saving_coop_total}\}$ and $\text{mean}\{E_{saving_coop_total}\}$ respectively in Fig. 6.5.

Importantly, Fig. 6.5 demonstrates that the heuristics GKH_1 and GKH_2 result in near-optimal partner selection regardless of candidate partner node density, achieving an energy saving within 0.025% and 0.4% of that given by optimal partner choice, respectively. By contrast, the energy saving obtained by selecting the best partner using the heuristic LKH is up to 4.9% less than that given by optimal partner choice. As the size of the candidate partner set increases, the likelihood of the source's nearest neighbour being a good cooperation partner increases; this is reflected in Fig. 6.5 by the increase in the LKH energy savings as N increases. However, the likelihood of a node existing at the near-optimal midway point between the source and destination is also higher for a larger candidate partner set. Consequently, a greater discrepancy between the energy savings achieved using LKH and optimal partner selection is observed in Fig. 6.5 for higher candidate partner densities.

Nevertheless, Fig. 6.5 shows that even the suboptimal LKH partner choice heuristic based solely on local knowledge achieves a significantly higher (up to 28%) energy saving than random partner selection. Moreover, the variability of the energy saving obtained using the proposed partner choice heuristics GKH_1 , GKH_2 , and LKH is significantly lower than when the partner is randomly selected (provided N is not too small). This is clearly illustrated by Fig. 6.6, which shows for each partner choice rule the interquartile range (IQR) of the energy savings achieved by the 1st ranked partner over the Q network realisations simulated for each value of the each candidate partner set size. Fig. 6.6 demonstrates that the IQR for random partner choice is about 30% regardless of N . By

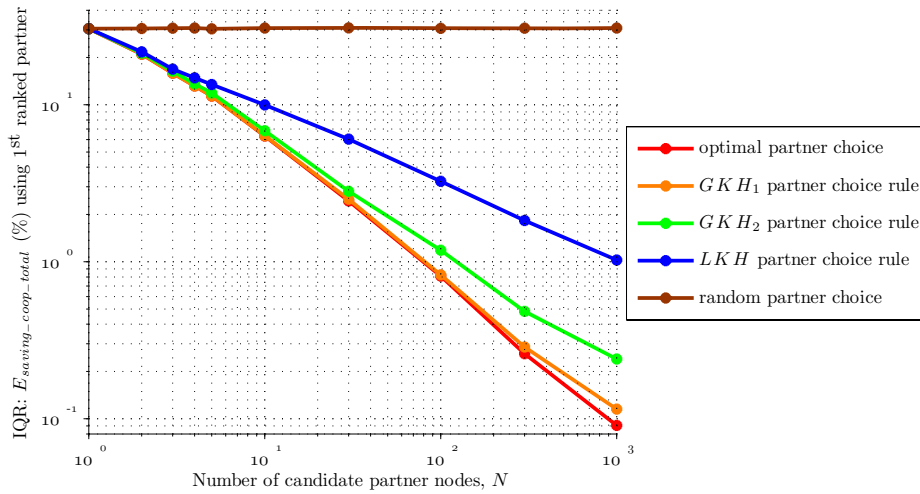


Figure 6.6: Variability of the energy saving achieved using the 1st ranked partner vs. number of candidate partner nodes, for different partner choice rules and the reference system specified in Table 2.1 (interquartile range (IQR) of Q random network realisations of N candidate partner nodes placed over the 100 m by 100 m network area).

contrast, the IQR for GKH_1 , GKH_2 , and LKH decreases as N is increased (since the existence of good partners becomes increasingly likely in a larger candidate partner set); for example, at $N = 1000$ the IQR is around 0.1%, 0.2%, and 1% for GKH_1 , GKH_2 , and LKH , respectively. This is important from the point of view of practical implementation, as it demonstrates that the proposed partner choice heuristics consistently yield substantial energy savings.

The partner ranking performance of the proposed partner choice heuristics vs. N is further quantified in Fig. 6.7 in terms of the correlation coefficient with the optimal partner ranking. As expected, the correlation coefficient for optimal and random partner choice is equal to 1 and around 0 respectively, regardless of N . The correlation coefficients for GKH_1 , GKH_2 , and LKH are somewhat lower for very small values of N , due to the inherent variability in low density partner networks illustrated in Fig. 6.6. Specifically, the correlation coefficient for GKH_1 , GKH_2 , and LKH ranges between 0.98 and 0.999, 0.89 and 0.98, and 0.78 and 0.92, respectively. Therefore Fig. 6.7 demonstrates that GKH_1 and GKH_2 consistently exhibit a very high positive correlation with optimal partner selection, whereas LKH consistently exhibits a moderately high correlation. Namely, the partner rankings given by the proposed heuristics are closely related to the optimal partner ranking for both sparse and dense candidate partner node deployments.

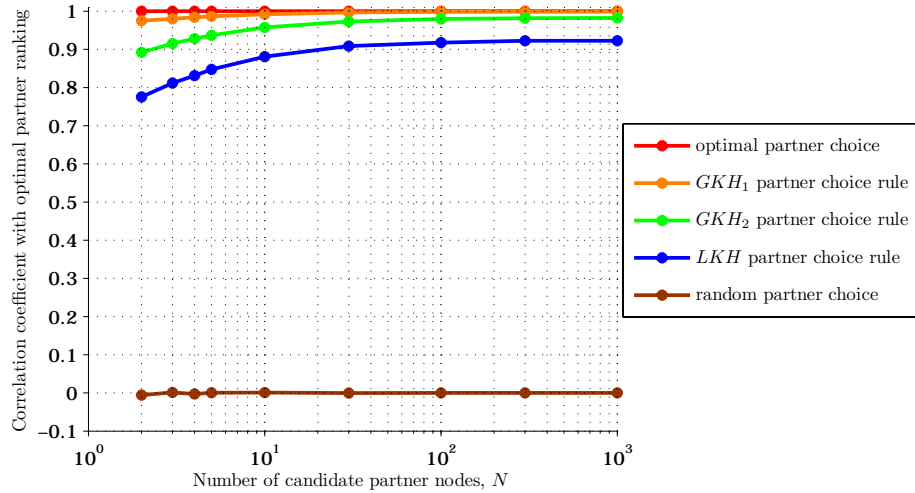


Figure 6.7: Correlation coefficient with the optimal partner ranking vs. number of candidate partner nodes, for different partner choice rules and the reference system specified in Table 2.1 (average of Q random network realisations of N candidate partner nodes placed over the 100 m by 100 m network area).

6.5.2 Effect of Varying the Transceiver Circuit Power

The energy conservation performance of the proposed partner choice heuristics for different values of the transceiver circuit power consumption ($P_{CCT-tx} = P_{CCT-rx} = \{0 \text{ W}, 10 \text{ mW}, 100 \text{ mW}, 500 \text{ mW}, 1 \text{ W}\}$) is quantified in Fig. 6.8 in terms of the energy saving achieved with the 1st ranked partner node. Fig. 6.8 confirms that the energy savings achieved using optimal and random partner selection match the maximum and mean energy saving over the 100 m by 100 m network area, respectively (obtained by considering partner nodes located on a uniform 1 m \times 1 m grid covering the network area). Importantly, Fig. 6.8 demonstrates that the heuristics GKH_1 and GKH_2 result in near-optimal partner selection for all considered values of the transceiver circuit power consumption, achieving an energy saving within 0.035% and 0.15% of that given by optimal partner choice, respectively. Fig. 6.8 also shows that the energy saving obtained using the heuristic LKH is up to 5% less than that given by optimal partner choice. Nonetheless, the suboptimal LKH partner choice heuristic achieves a substantially higher (up to 28%) energy saving than random partner selection.

The overall partner ranking performance of the proposed partner choice heuristics for different values of the transceiver circuit power consumption is quantified in Fig. 6.9 in terms of the correlation coefficient with the optimal partner ranking. Importantly, Fig. 6.9 demonstrates that the partner rankings given by all three proposed heuristics are closely related to the optimal partner ranking for all considered values of the transceiver circuit power consumption. Specifically, GKH_1 , GKH_2 , and LKH exhibit a correlation coefficient with optimal partner selection of at least 0.999, 0.97, and 0.88, respectively.

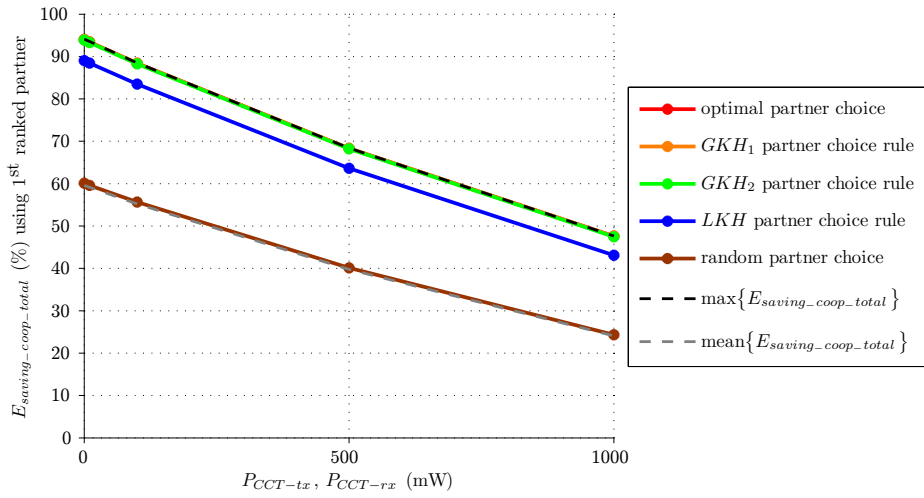


Figure 6.8: Energy saving achieved using the 1st ranked partner vs. the transceiver circuit power consumption, for different partner choice rules (average of Q random network realisations of $N = 1000$ candidate partner nodes placed over the 100 m by 100 m network area).

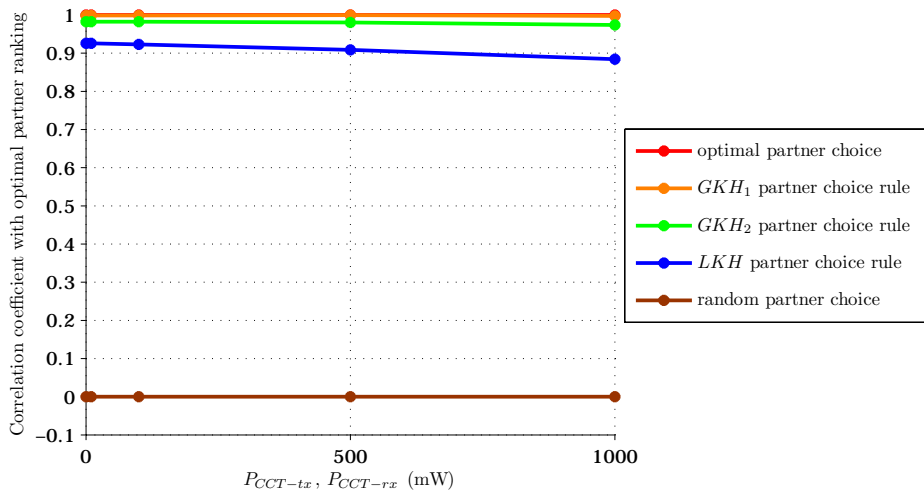


Figure 6.9: Correlation coefficient with the optimal partner ranking vs. the transceiver circuit power consumption, for different partner choice rules (average of Q random network realisations of $N = 1000$ candidate partner nodes placed over the 100 m by 100 m network area).

Fig. 6.9 also shows that the correlation exhibited by the proposed heuristics decreases somewhat as the transceiver circuit power consumption is increased. As the transceiver circuit power consumption is increased the size of the partner choice region for energy efficient cooperation decreases, as shown in Fig. 5.7 of Chapter 5 (and discussed for aDF cooperation in general in Chapter 4). It follows that a larger proportion of the candidate partner nodes randomly placed over the 100 m by 100 m network area are located outside the energy efficient partner choice region boundary. As discussed in Section 6.4, whereas all such partner nodes are ranked last-equal using optimal partner selection, the heuristics wrongly differentiate between these equally unsuitable partner nodes (being ignorant

of the actual $E_{saving_coop_total}$ associated with each node). Consequently, the proposed heuristics achieve a slightly lower correlation with the optimal partner ranking as the transceiver circuit power consumption is increased. However, it should be noted that this is to an extent an artificial effect, since the size of the reference candidate partner network area is arbitrarily chosen in this analysis. Namely, this effect would not be observed if a smaller partner network area was instead considered (and conversely, this effect would be more pronounced if a larger partner network area was considered).

6.5.3 Effect of Varying the Source-Destination Separation

The energy conservation performance of the proposed partner choice heuristics for different values of the source-destination separation ($d_{s-d} = \{15 \text{ m}, 20 \text{ m}, 30 \text{ m}, 40 \text{ m}, 50 \text{ m}, 60 \text{ m}, 70 \text{ m}, 80 \text{ m}, 90 \text{ m}, 100 \text{ m}\}$) is quantified in Fig. 6.10 in terms of the energy saving achieved with the 1st ranked partner node. Fig. 6.10 confirms that the energy saving achieved using optimal and random partner selection corresponds to the maximum and mean energy saving over the 100 m by 100 m network area, respectively. Importantly, Fig. 6.10 demonstrates that the heuristics GKH_1 and GKH_2 result in near-optimal partner selection for all considered values of the transceiver circuit power consumption, achieving an energy saving within 0.05% and 0.18% of that given by optimal partner choice, respectively. Fig. 6.10 also shows that the energy saving obtained using the heuristic LKH is up to 5% less than that given by optimal partner choice, but up to 43% higher than that given by random partner selection.

It should be noted that for $d_{s-d} > 50 \text{ m}$ the source node is located outside the reference 100 m by 100 m candidate partner network area. As d_{s-d} is increased past 50m the optimal partner location (around midway between the destination and the source) moves increasingly closer to the edge of the network area, such that LKH partner choice becomes increasingly optimal. For example, for $d_{s-d} = 100 \text{ m}$ the optimal partner node location is roughly on the edge of the network boundary (50m away from the destination), which coincides with the partner node location closest to the source chosen by LKH . As a consequence, the discrepancy between LKH and optimal partner selection for $d_{s-d} > 50 \text{ m}$ observed in Fig. 6.10 decreases with increasing d_{s-d} .

The overall partner ranking performance of the proposed partner choice heuristics for different values of the source-destination separation is quantified in Fig. 6.11 in terms of the correlation coefficient with the optimal partner ranking. Importantly, Fig. 6.11 demonstrates that the partner rankings given by all three proposed heuristics are closely related to the optimal partner ranking for all considered values of the source-destination separation. Specifically, GKH_1 , GKH_2 , and LKH exhibit a correlation coefficient with optimal partner selection ranging from 0.72 to 0.999, 0.72 to 0.98, and 0.68 to 0.98,

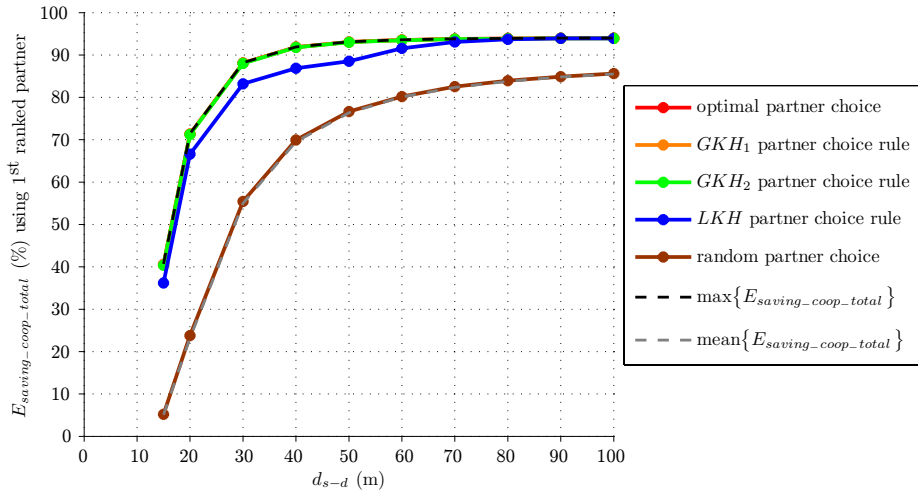


Figure 6.10: Energy saving achieved using the 1st ranked partner vs. the source-destination separation, for different partner choice rules (average of Q random network realisations of $N = 1000$ candidate partner nodes placed over the 100 m by 100 m network area).

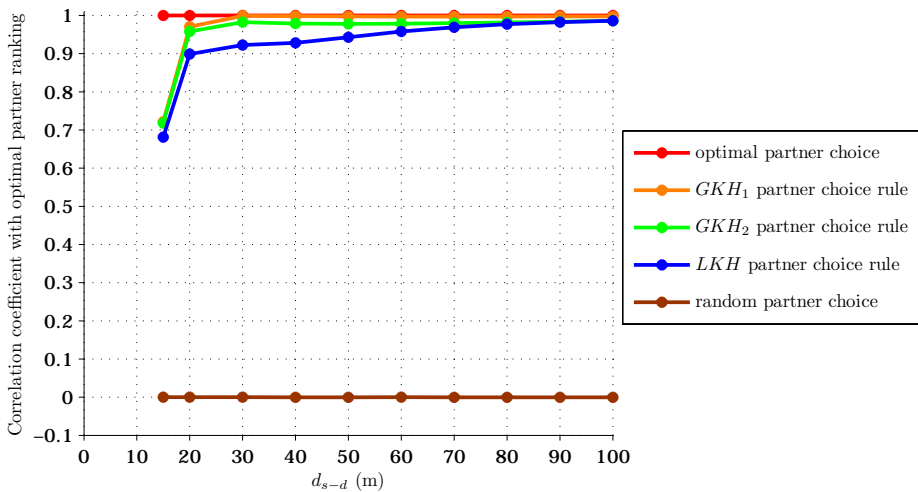


Figure 6.11: Correlation coefficient with the optimal partner ranking vs. the source-destination separation, for different partner choice rules (average of Q random network realisations of $N = 1000$ candidate partner nodes placed over the 100 m by 100 m network area).

respectively. It should be noted that the relatively low correlation exhibited by the proposed heuristics for low values of d_{s-d} in Fig. 6.11 is due to a smaller associated partner choice region boundary (as shown in Fig. 5.8 of Chapter 5 and discussed in Chapter 4). As discussed in Section 6.5.2, the proposed heuristics wrongly differentiate between equally unsuitable partner nodes which exist outside of the partner choice region boundary. Since the energy efficient partner choice region is a smaller proportion of the overall partner network area for low values of d_{s-d} , such unsuitable partner nodes are more numerous, resulting in lower correlation with the optimal partner ranking. It should also be noted that the high LKH correlation observed in Fig. (6.11) for $d_{s-d} > 50$ m is due to the

source node being located outside the 100 m by 100 m candidate partner network area, as discussed above.

6.5.4 Effect of Varying the Channel Path Loss Exponent

The energy conservation performance of the proposed partner choice heuristics for different values of the channel path loss exponent ($k = \{3, 3.5, 4, 5, 6, 7, 8, 9, 10\}$) is quantified in Fig. 6.12 in terms of the energy saving achieved with the 1st ranked partner node. Fig. 6.12 confirms that the average energy saving achieved using optimal and random partner selection matches the maximum and mean energy saving over the 100 m by 100 m network area, respectively. Importantly, Fig. 6.12 demonstrates that the heuristics GKH_1 and GKH_2 result in near-optimal partner selection for all considered values of the channel path loss exponent, achieving an energy saving within 0.03% and 0.13% of that given by optimal partner choice, respectively. Fig. 6.12 also shows that the energy saving obtained using the heuristic LKH is up to 10.4% less than that given by optimal partner choice, but up to 64% higher than that given by random partner selection. It is interesting to note that although LKH is increasingly suboptimal as k is increased, it increasingly outperforms random partner selection. The latter is due to the decrease in the mean energy saving achieved over the partner network area resulting from the smaller energy efficient partner choice region as k is increased, whereas the former is due to the increase in the maximum achievable energy savings as k is increased (as discussed in Chapter 4).

The overall partner ranking performance of the proposed partner choice heuristics for different values of the channel path loss exponent is quantified in Fig. 6.13 in terms of the correlation coefficient with the optimal partner ranking. Importantly, Fig. 6.13 demonstrates that the partner rankings given by all three proposed heuristics are closely related to the optimal partner ranking for all considered values of the channel path loss exponent. Specifically, GKH_1 , GKH_2 , and LKH exhibit a correlation coefficient with optimal partner selection ranging from 0.82 to 0.9999, 0.82 to 0.98, and 0.71 to 0.91, respectively. It should be noted that the relatively low correlation exhibited by the proposed heuristics for high values of k in Fig. 6.13 is due to a smaller associated partner choice region boundary (as shown in Fig. 5.9 of Chapter 5 and discussed in Chapter 4). The energy efficient partner choice region is thus a smaller proportion of the overall partner network area for high values of k , such that unsuitable partner nodes outside of the partner choice region boundary are more numerous. As discussed in Section 6.5.2, the proposed heuristics wrongly differentiate between these equally unsuitable partner nodes, resulting in a lower correlation with the optimal partner ranking.

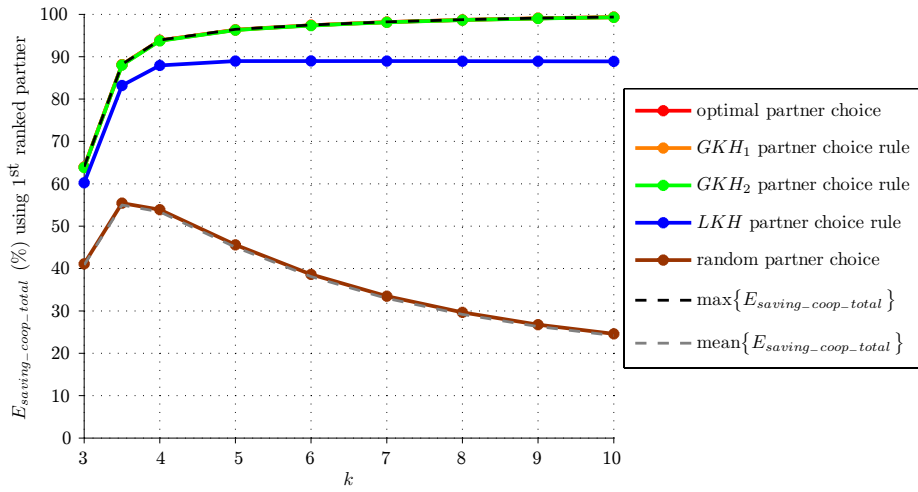


Figure 6.12: Energy saving achieved using the 1st ranked partner vs. the channel path loss exponent, for different partner choice rules (average of Q random network realisations of $N = 1000$ candidate partner nodes placed over the 100 m by 100 m network area).

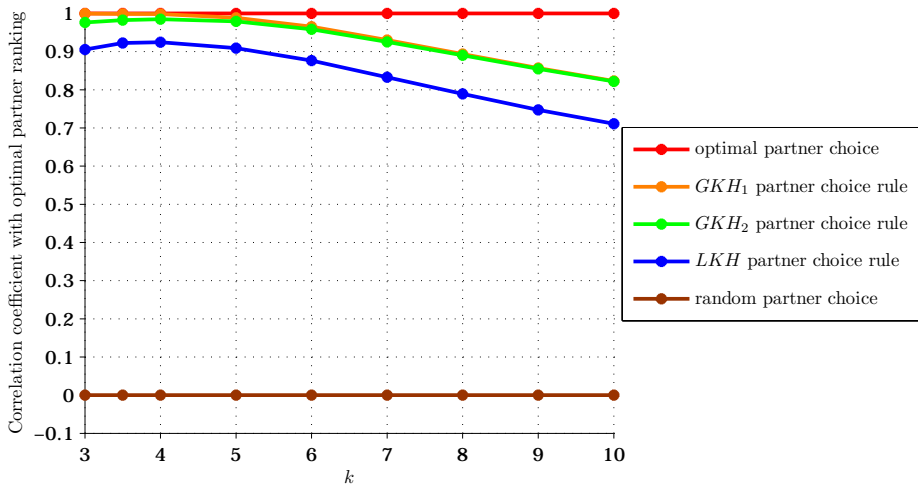


Figure 6.13: Correlation coefficient with the optimal partner ranking vs. the channel path loss exponent, for different partner choice rules (average of Q random network realisations of $N = 1000$ candidate partner nodes placed over the 100 m by 100 m network area).

6.5.5 Effect of Varying the Target Bit Error Rate

The energy conservation performance of the proposed partner choice heuristics for different values of the target BER ($p_b = \{10^{-2}, 10^{-3}, 10^{-4}, 10^{-5}, 10^{-6}\}$) is quantified in Fig. 6.14 in terms of the energy saving achieved with the 1st ranked partner node. Fig. 6.14 confirms that the average energy saving achieved using optimal and random partner selection matches the maximum and mean energy saving over the 100 m by 100 m network area, respectively. Importantly, Fig. 6.14 demonstrates that the heuristics GKH_1 and GKH_2 result in near-optimal partner selection for all considered values of the target BER, achiev-

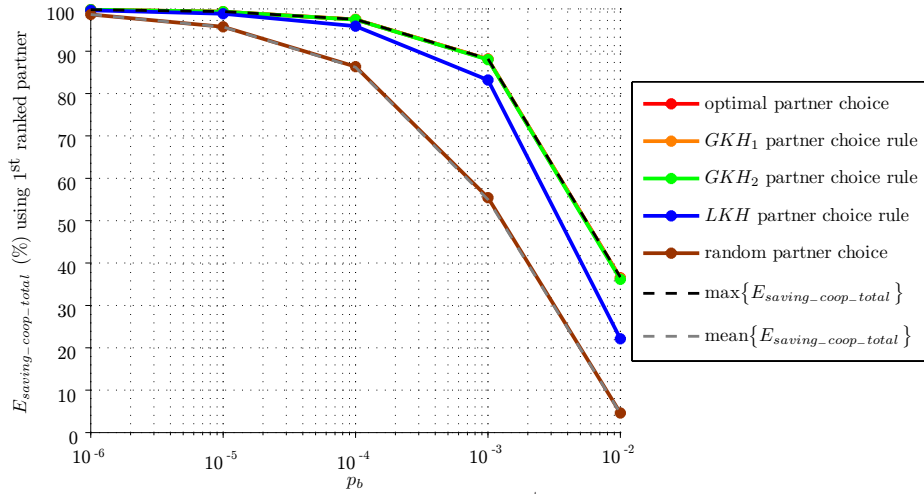


Figure 6.14: Energy saving achieved using the 1st ranked partner vs. the target BER, for different partner choice rules (average of Q random network realisations of $N = 1000$ candidate partner nodes placed over the 100 m by 100 m network area).

ing an energy saving within 0.13% and 0.39% of that given by optimal partner choice, respectively. Fig. 6.14 also shows that the energy saving obtained using the heuristic LKH is up to 14.4% less than that given by optimal partner choice, but up to 28% higher than that given by random partner selection.

The overall partner ranking performance of the proposed partner choice heuristics for different values of the target BER is quantified in Fig. 6.15 in terms of the correlation coefficient with the optimal partner ranking. Importantly, Fig. 6.15 demonstrates that the partner rankings given by all three proposed heuristics are closely related to the optimal partner ranking for all considered values of the target BER. Specifically, GKH_1 , GKH_2 , and LKH exhibit a correlation coefficient with optimal partner selection ranging from 0.71 to 0.999, 0.70 to 0.98, and 0.59 to 0.93, respectively. It should be noted that the relatively low correlation exhibited by the proposed heuristics for high p_b in Fig. 6.15 is due to the smaller associated partner choice region boundary (as shown in Fig. 5.10 of Chapter 5 and discussed in Chapter 4). The energy efficient partner choice region is thus a smaller proportion of the overall partner network area for high p_b , such that a larger proportion of the candidate partner nodes are outside of the partner choice region boundary. As discussed in Section 6.5.2, the proposed heuristics wrongly differentiate between these equally unsuitable partner nodes, giving a lower correlation with the optimal partner ranking.

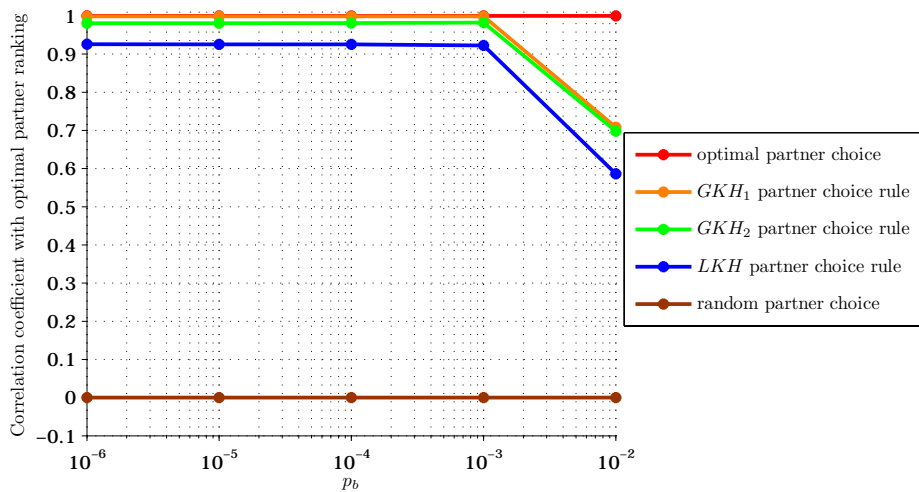


Figure 6.15: Correlation coefficient with the optimal partner ranking vs. the target BER, for different partner choice rules (average of Q random network realisations of $N = 1000$ candidate partner nodes placed over the 100 m by 100 m network area).

6.6 Discussion of the Practical Significance of the Partner Choice Heuristics

The analysis presented in the preceding sections has demonstrated that the proposed GKH_1 and GKH_2 partner choice heuristics achieve near-optimally energy efficient partner selection across a wide range of communication system configurations. The analysis has also consistently shown that, although the proposed LKH partner choice heuristic is suboptimal, partner selection using LKH still achieves very substantial energy savings. Importantly, the proposed heuristics are practical partner selection strategies which simple sensor nodes can implement.

Firstly, the computational burden of partner choice is minimal using the proposed heuristics, making feasible the autonomous selection of cooperation partners by resource-constrained sensor nodes. Specifically, GKH_1 requires a simple calculation to produce the partner rating metric, GKH_2 requires only a comparison of two measurements, and LKH directly uses a single measurement. By contrast, it would be prohibitively computationally expensive for a sensor node to explicitly calculate the actual energy saving expected from each candidate partner node.

Secondly, the proposed partner choice heuristics are based solely on knowledge of average path loss values in the network. This is a distinct practical advantage for resource-constrained distributed wireless networks, where nodes can measure average received signal strength but would have to infer (or obtain from an external entity) network distances.

Finally, the most computationally efficient of the proposed heuristics, LKH , only requires knowledge of local network path losses, which the source node can obtain au-

tonomously via direct measurement. Thus using *LKH* resource-constrained sensor nodes can cooperate autonomously in a fully distributed and scalable manner to substantially reduce their energy consumption.

6.7 Summary

In this chapter three partner choice heuristics for practical energy efficient aDF cooperation have been proposed. The heuristics are computationally efficient and based solely on knowledge of average path loss values in the network. This is practically very significant for a wireless sensor network, where nodes can measure average received signal strength but would have to infer the location of other nodes in the network.

Two heuristics have been developed which require full information about each candidate partner node (the source-partner and partner-destination channel quality). The first, GKH_1 , involves a simple calculation to produce the partner rating metric whereas the second, GKH_2 , requires only a comparison of two measurements. These computationally efficient heuristics are designed to closely estimate the actual usefulness of a potential partner node (i.e. the associated cooperative energy saving), however the source node must acquire global knowledge of network path losses to employ them. This entails a signalling overhead as this information must be exchanged among nodes in the network. The third proposed heuristic, *LKH*, only requires local knowledge of network path losses (the source-partner channel quality), which the source can obtain autonomously. Moreover, this is the lowest complexity heuristic, as it directly uses a single measurement as the partner rating metric.

The performance of the proposed partner choice heuristics has been analysed by comparing their partner ranking performance against that of optimal partner selection. The validity of the heuristics has thereby been thoroughly evaluated across a wide range of communication system configurations. Moreover, the trade-off between heuristic complexity and performance has been examined through this investigation. The results of this analysis have consistently shown that the GKH_1 and GKH_2 partner choice heuristics achieve near-optimally energy efficient partner selection. This suggests that GKH_2 is the preferable of the two global knowledge heuristics, since it achieves a very similar energy efficiency as GKH_1 at a lower computational cost. Importantly, the analysis has also demonstrated that the *LKH* partner choice heuristic is suboptimal but nevertheless consistently achieves highly energy efficient partner selection. This result is of great practical significance, as it indicates that a simple sensor node can completely independently make cooperation decisions to achieve very substantial energy savings.

Therefore, the partner choice heuristics proposed in this chapter are practical and robust partner selection strategies which can be autonomously implemented by resource-

constrained sensor nodes to obtain significant cooperative energy savings. Together with the aDF power allocation heuristic developed in Chapter 5, these partner choice heuristics form the core of the distributed cooperation strategy for energy-constrained wireless networks presented and analysed in Chapters 7-11.

Chapter 7

ECO-OP: A Distributed Cooperation Strategy for Energy-Constrained Wireless Sensor Networks

7.1 Introduction

In Chapters 5 and 6 simple yet near-optimal power allocation and partner choice heuristics were proposed for practical energy efficient aDF cooperation. Importantly, these computationally efficient heuristics enable a resource-constrained sensor node to autonomously make energy efficient cooperation decisions. In this chapter a novel low-complexity distributed cooperation strategy for energy-constrained wireless sensor networks is presented. The proposed cooperation strategy is named ECO-OP in reference to the energy-conserving cooperation it facilitates, and is based on the power allocation and partner choice heuristics presented in Chapters 5 and 6. The ultimate aim of ECO-OP is to extend the operational lifetime of a wireless sensor network by coordinating network-wide cooperation among its sensor nodes.

The ECO-OP cooperation strategy is described in detail in Section 7.2. The behaviour and performance of ECO-OP is thoroughly analysed in Chapters 8-11; an overview of these investigations is presented in Section 7.3. Specifically, the investigation of the energy conservation performance of network-wide cooperation using ECO-OP in Chapters 8 and 9 is outlined in Section 7.3.1, whereas the investigation of the network lifetime extension performance of ECO-OP in Chapters 10 and 11 is outlined in Section 7.3.1. The wireless sensor network model and simulation parameters employed in generating the simulation results of network-wide cooperative communication in Chapters 8-11 are presented in Section 7.4. Finally, the node energy consumption definitions and metrics which are employed in the analysis in Chapters 8 and 9 are presented in Section 7.5, whereas the

node and network lifetime definitions and metrics which are employed in the analysis in Chapters 10 and 11 are presented in Section 7.6.

7.2 The ECO-OP Cooperation Strategy

This section presents ECO-OP, a novel low-complexity distributed cooperation strategy for energy-constrained wireless sensor networks. The ultimate aim of ECO-OP is to extend the lifetime of a wireless sensor network by facilitating energy-conserving network-wide cooperation among its sensor nodes. ECO-OP is based on the power allocation and partner choice heuristics for practical energy efficient aDF cooperation presented in Chapters 5 and 6. Using ECO-OP individual source nodes independently make cooperation decisions to minimise the total energy consumed per bit over their own cooperative link, ignorant of the cooperation decisions of the other source nodes in the network. Moreover, each source node makes its cooperation decisions based solely on measurements of average path loss. Finally, all nodes in the network are altruistic in the sense that a node will unconditionally accept any requests to serve as cooperation partner for other source nodes in the network.

Importantly, ECO-OP has been specifically designed to be suitable for practical implementation on resource-constrained sensor nodes; ECO-OP is a distributed and computationally efficient cooperation strategy with low signalling overhead. At the time of writing this thesis, no other distributed cooperation strategy¹ for extending the lifetime of a wireless sensor network has been proposed in the literature. A centralised greedy algorithm was proposed in [18] for maximising the minimum node lifetime in an energy-constrained wireless network using cooperative communication, whereby a central controller performs a computationally intensive offline greedy search to allocate cooperation partners and transmit power for each node in the network. Whereas in ECO-OP each node independently makes cooperation decisions using only knowledge of average channel quality, the centralised greedy cooperation algorithm in [18] additionally uses information about the residual energy of all sensor nodes. The network lifetime extension performance of ECO-OP will be extensively compared against that of the centralised greedy cooperation algorithm [18] in the investigation presented in Chapters 10 and 11, an overview of which is presented in Section 7.3.2. Importantly, the analysis in Chapters 10 and 11 will show that the low-complexity distributed ECO-OP cooperation strategy overall achieves

¹In another line of research, an energy efficient selective relay cooperative diversity scheme was proposed in [66], whereby for each message transmitted by the source, candidate partner nodes compete in a distributed contention process based on instantaneous channel quality and an explicit calculation of the energy consumption associated with each potential cooperation partner. However, as discussed in Section 2.4.3, the significant signalling and computational overhead involved with reselecting a partner on a per-message basis is highly undesirable in resource-constrained wireless sensor networks.

a comparable network lifetime improvement to the centralised computationally intensive cooperation algorithm proposed in [18].

The core of the ECO-OP distributed cooperation strategy is described in Fig. 7.1, which presents the partner choice and power allocation method employed by each source node in the network. Fig. 7.1 shows that a given source node j selects its preferred cooperation partner from its set of candidate partner nodes φ_j using one of the partner choice heuristics² GKH_1 , GKH_2 , or LKH as defined by (6.6)-(6.8). Having chosen node \hat{i} as its best cooperation partner³, source node j calculates the most energy efficient power allocation for the cooperative transmission using the heuristic in (5.13), (5.14). Finally, source node j checks whether cooperative communication with its chosen partner node \hat{i} will be worthwhile by substituting $E_{tx-s(j,\hat{i})}$, $E_{tx-p(\hat{i},j)}$ into (2.17). If the expected energy efficiency of its cooperative link is negative, source node j will henceforth opt to transmit its own messages to the destination receiver non-cooperatively. Otherwise, source node j sends its chosen partner node \hat{i} a message informing it of its allocated transmit power, $E_{tx-p(\hat{i},j)}$.

Fig. 7.2 describes the overall ECO-OP cooperation strategy followed by any given node j in the network throughout its lifetime. It is assumed that the wireless sensor network consists of M nodes and that each node acts as a source and is eligible to serve as a cooperation partner. Fig. 7.2 shows that, following network activation, each source node in the wireless sensor network selects another node in the network as its partner using the process specified in Fig. 7.1. Namely, source node j initialises its candidate partner set φ_j as consisting of all the other nodes in the network (i.e. the set \mathbf{M} of all M nodes⁴ in the network, excluding node j itself). After this initial partner selection round, source node j sends its messages to the destination receiver as per the network's multiple access scheme (e.g. TDMA schedule), addressing the message to both the destination receiver and its chosen partner node \hat{i} . If node j has been selected to serve as cooperation partner to some source node h , it forwards messages received from source node h to the destination receiver as per the aDF cooperative diversity scheme described in Section 2.2.4. After node j transmits a message (acting as either source or partner) it checks its battery

²Prior to network activation, the network designer would specify one of these partner choice rules to be employed by all nodes in the network.

³If several candidate partner nodes are ranked 1st-equal after applying a given partner choice rule, the source node would simply select one of the partner nodes at random. This case of several nodes being tied as the best partner is very unlikely to occur in a network of randomly deployed nodes, but occurs often when nodes are placed on a regular grid (as for the sake of illustration in Chapters 8 and 10).

⁴It should be noted that the following notation is adopted throughout this thesis: the number of elements in set \mathbf{A} (i.e. the size of set \mathbf{A}) is signified by A .

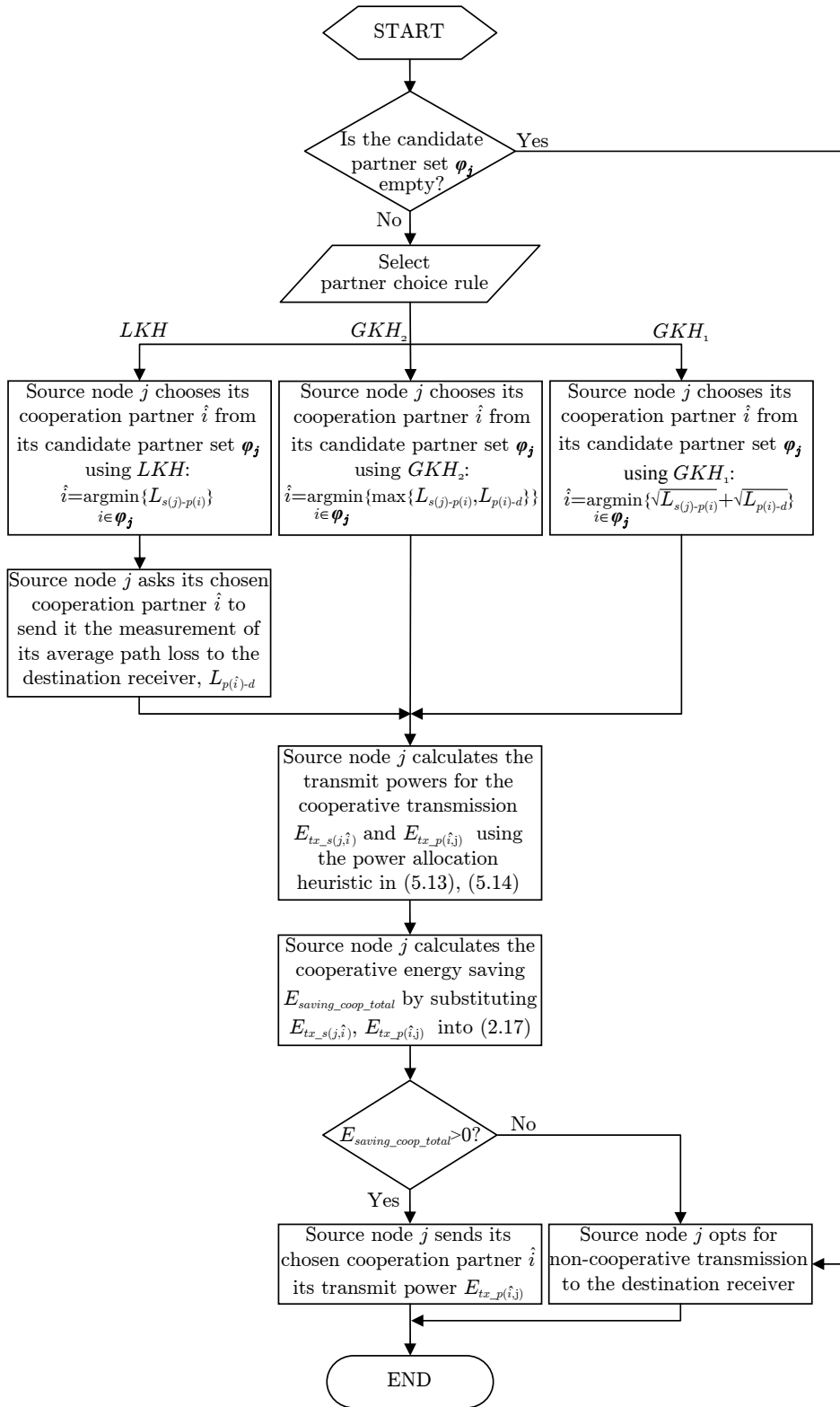


Figure 7.1: Flowchart describing the partner choice and power allocation method employed by any given source node j in the network using the distributed ECO-OP cooperation strategy.

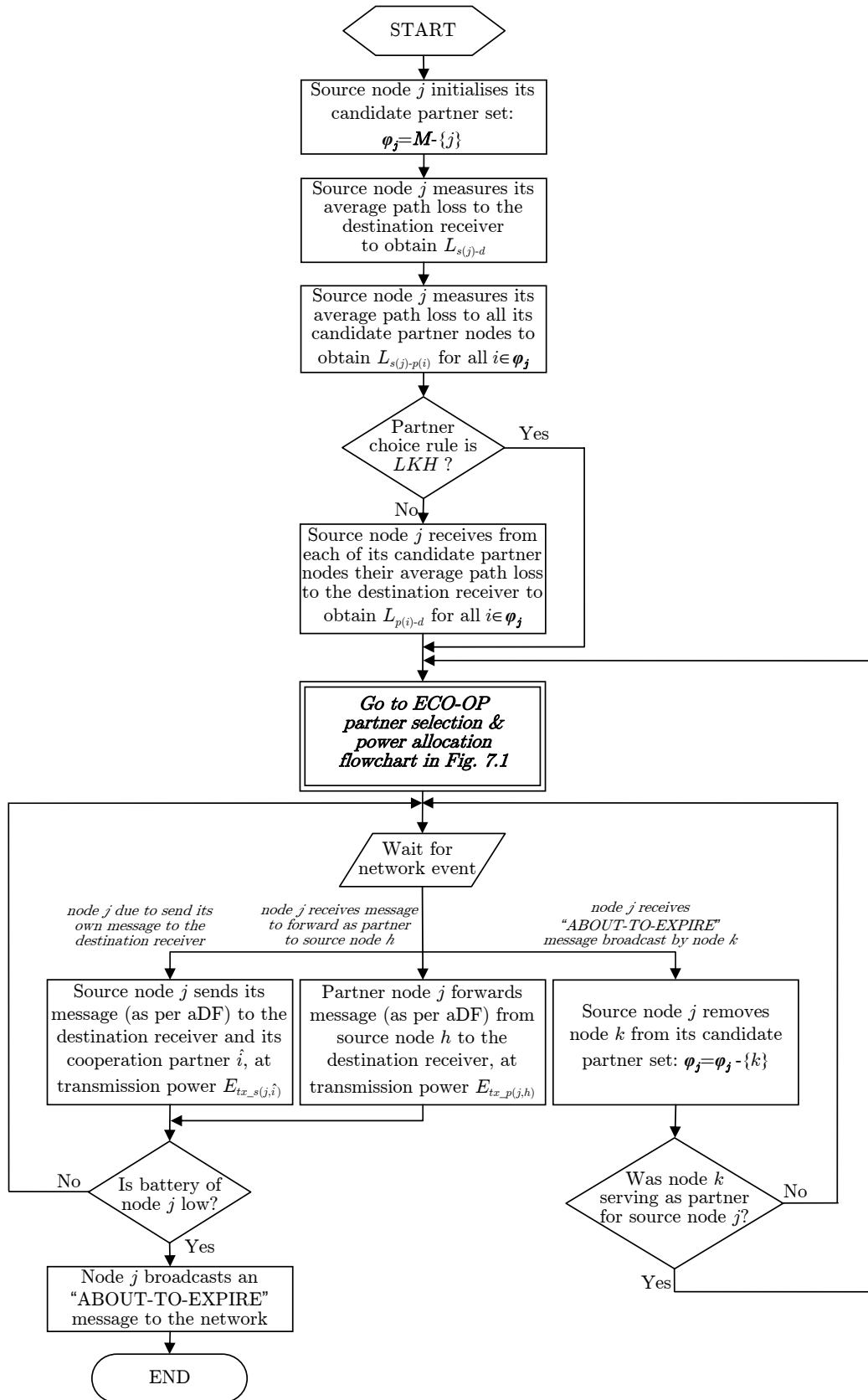


Figure 7.2: Flowchart describing the overall distributed ECO-OP cooperation strategy employed by any given node j in the cooperative network throughout its lifetime. It is assumed that the wireless sensor network consists of the set M of M sensor nodes, whereby each node acts as a source and is eligible to serve as a cooperation partner.

levels⁵. Once node j detects that its battery energy is about to be depleted, it broadcasts an “ABOUT-TO-EXPIRE” message and thenceforth ceases to operate. When node j receives an “ABOUT-TO-EXPIRE” message from some other node k in the network, node j updates its candidate partner set φ_j by removing the expired node k . Additionally, if source node j had hitherto been served by the expired partner node k , source node j must reselect a cooperation partner from one of the other surviving nodes, as per the process specified in Fig. 7.1. Therefore, using ECO-OP a source node only reselects its cooperation partner if its current partner node is about to deplete its batteries. This means that ECO-OP entails a relatively low signalling overhead.

Moreover, Fig. 7.1 shows that using ECO-OP a given source node j makes its cooperation decisions based on measurements of the average path loss on the source-destination channel ($L_{s(j)-d}$) and the average path loss on the source-partner and partner-destination channels of all of its candidate partner nodes ($L_{s(j)-p(i)}$ and $L_{p(i)-d}$ for all $i \in \varphi_j$, respectively⁶). Assuming a static wireless sensor network, each sensor node in the network must only obtain knowledge of these measurements once, following network activation, as shown in Fig. 7.2. Assuming channel reciprocity, source node j can obtain knowledge of $L_{s(j)-d}$ and $L_{s(j)-p(i)}$ for all $i \in \varphi_j$ via direct measurement of average received signal strength, whereas it can obtain knowledge of $L_{p(i)-d}$ for all $i \in \varphi_j$ during its discovery of candidate partner nodes.

An example of how this would be achieved in practice is as follows. Let us assume a static network of M sensor nodes communicating with a common destination receiver, where \mathbf{M} denotes the set of all nodes in the network. The destination receiver would firstly broadcast a message to all sensor nodes at a predetermined transmission power. Each sensor node $j \in \mathbf{M}$ would estimate its average path loss to the destination by measuring the received signal strength of the broadcast message, thereby acquiring knowledge of $L_{s(j)-d}$. Then each sensor node $j \in \mathbf{M}$ would in turn broadcast its $L_{s(j)-d}$ measurement to all the other $M - 1$ sensor nodes in the network at a predetermined transmission power. Nodes would thereby exchange knowledge of their path loss to the destination, enabling each sensor node $j \in \mathbf{M}$ to acquire knowledge of $L_{p(i)-d}$ for all $i \in \varphi_j$. Additionally, by measuring the received signal strength of the broadcast message, each sensor node $j \in \mathbf{M}$ would be able to estimate the average path loss to its candidate partner nodes, thereby acquiring knowledge of $L_{s(j)-p(i)}$ for all $i \in \varphi_j$.

Finally, it should be noted that although a static network is assumed in this thesis, the proposed ECO-OP cooperation strategy is also valid for low-mobility networks, whereby

⁵It is important to note that this does not require the node to measure its precise residual battery energy level. Rather, only a battery alarm, which is triggered once the node’s energy level has fallen below a set threshold, is required.

⁶Knowledge of $L_{p(i)-d}$ for all $i \in \varphi_j$ is only required if nodes select partners using GKH_1 or GKH_2 , but not if LKH is employed.

network-wide channel measurement and partner selection would simply need to be repeated whenever the network layout is deemed to have changed considerably. Moreover, although ECO-OP has been proposed in this thesis as a cooperation strategy for wireless sensor networks, its applicability is in no way restricted to these networks. ECO-OP has simply been designed to satisfy the constraints inherent in a wireless sensor network (i.e. a distributed low-complexity strategy suitable for resource-constrained nodes), but it is generally applicable to any energy-constrained wireless network.

7.3 Overview of Investigations Analysing the Performance of ECO-OP

This section presents an overview of the investigations in Chapters 8-11 which constitute a thorough analysis of the behaviour and performance of the ECO-OP cooperation strategy presented in Section 7.2. ECO-OP is designed to simply maximise the energy efficiency of individual cooperative links in the network, without any regard to the resulting distribution of cooperation partner service, individual node energy consumption, or resulting node lifetimes over the network. This means that the low-complexity distributed ECO-OP cooperation strategy is intended to achieve its overall aim of network lifetime extension *indirectly*. Consequently, it is necessary to thoroughly analyse the behaviour of ECO-OP as a network-wide cooperation strategy in order to demonstrate its effectiveness as an energy saving technique for wireless sensor networks. Furthermore, it is important to explicitly investigate the long-term benefit of network-wide cooperation using ECO-OP in order to establish the validity of ECO-OP as an effective technique for extending the lifetime of a wireless sensor network.

Firstly, an investigation of the energy conservation performance of network-wide cooperation using ECO-OP will be presented in Chapters 8 and 9, an overview of which is presented in Section 7.3.1. The analysis in Chapters 8 and 9 will serve to demonstrate that the distributed cooperation decisions made by individual nodes using ECO-OP indeed constitute an effective network-wide cooperation strategy for reducing a wireless sensor network's energy consumption.

Secondly, an investigation of the lifetime extension performance of network-wide cooperation using ECO-OP will be presented in Chapters 10 and 11, an overview of which is presented in Section 7.3.2. The analysis in Chapters 10 and 11 will show that distributed cooperation among simple independently-acting sensor nodes using ECO-OP significantly extends the lifetime of the wireless sensor network as a whole.

Moreover, the network lifetime extension performance of ECO-OP will be extensively compared against that of the centralised greedy cooperation algorithm from the litera-

ture [18] in the simulation results presented in Chapters 10 and 11. An overview of this investigation is presented in Section 7.3.2, whereas a detailed description of the algorithm proposed in [18] is presented in Appendix A. Importantly, the analysis in Chapters 10 and 11 will serve to demonstrate that the low-complexity distributed ECO-OP cooperation strategy overall achieves a comparable network lifetime improvement to the centralised greedy cooperation algorithm proposed in [18].

7.3.1 Investigation of Energy Conservation via Network-wide Cooperation

In Chapters 5 and 6 it was demonstrated that the power allocation and partner choice heuristics proposed in this thesis for practical aDF cooperation are near-optimally energy efficient with respect to the individual cooperative link (i.e. the communication link consisting of the source node communicating its message to the destination receiver by cooperating with its chosen partner node). These partner choice and power allocation heuristics form the core of each individual node's cooperation strategy using ECO-OP; each source node in the network simply makes cooperation decisions to maximise the energy efficiency of its own cooperative link, as specified by Fig. 7.1. However, maximising the energy efficiency of individual cooperative links in the network does not automatically guarantee ECO-OP's effectiveness as a network-wide cooperation strategy. Namely, a cooperation strategy which overall conserves energy at the expense of overburdening individual partner nodes is unsustainable. Therefore, in order to properly evaluate the overall effectiveness of ECO-OP it is crucial to consider the resulting distribution of cooperation partner service and individual node energy consumption over the network, as well as the reduction in the total network energy expenditure achieved. To address this, an investigation of the energy conservation performance of network-wide cooperation using ECO-OP will be presented in Chapters 8 and 9. The analysis in Chapters 8 and 9 will thus serve to establish the general validity of network-wide cooperation using ECO-OP as an effective energy saving technique for wireless sensor networks.

In Chapter 8 the fundamental behaviour of network-wide cooperation using ECO-OP will be illustrated by considering cooperation among $M=100$ nodes regularly placed over a 100 m by 100 m network area. The basic operation of ECO-OP will be firstly demonstrated via the $E_{saving_coop_total}$ achieved by each source node in the network for its transmission to the destination receiver. The impact of network-wide cooperation will then be analysed by considering the distribution of cooperation partner service among the network's nodes, and the individual node energy consumption across the non-cooperative network versus the cooperative network. Finally, the overall energy conservation performance of network-

wide cooperation will be quantified in terms of the reduction in the total network energy consumption achieved.

In Chapter 9 the typical energy conservation performance of network-wide cooperation using ECO-OP will be evaluated for the general case of randomly deployed networks of various node density. Specifically, a range of node density values will be investigated by simulating cooperation among $M=\{2, 3, 4, 5, 6, 10, 30, 100, 300, 1000\}$ nodes randomly placed over a 100 m by 100 m network area. In order to represent the typical behaviour of ECO-OP, the results presented in Chapter 9 are given by the median of $Q = \left(\frac{10^5}{M}\right)$ simulation runs. Firstly, the basic operation of ECO-OP as M is varied will be presented in terms of the average $E_{saving_coop_total}$ achieved over the M -node network. Secondly, the overall energy conservation performance of ECO-OP as M is varied will be quantified in terms of the reduction in the total network energy consumption achieved via network-wide cooperation. Lastly, in order to gain some basic insight into the general long-term viability of ECO-OP, the distribution of node energy consumption across the cooperative versus the non-cooperative network will be examined as M is varied.

The performance of ECO-OP with different partner choice rules will be investigated in Chapters 8 and 9, with the proposed partner choice heuristics GKH_1 , GKH_2 , and LKH being analysed alongside random partner choice for comparison. It is important to note that the analysis presented in Chapters 8 and 9 is concerned solely with the network-wide energy impact of the initial partner selection round at the time of the network's deployment, as specified in Fig. 7.1 (i.e. a static distribution of cooperation partner service). The results presented in Chapters 8 and 9 are based on MATLAB simulations of network-wide cooperation in three representative network topologies, which are introduced in Section 7.4 along with other relevant simulation parameters and assumptions. The node energy consumption definitions and metrics which are employed in the analysis in Chapters 8 and 9 are presented in Section 7.5.

7.3.2 Investigation of Network Lifetime Extension via Network-wide Cooperation

The ultimate aim of ECO-OP is to extend the lifetime of a wireless sensor network by facilitating energy-conserving cooperation among its sensor nodes. However, the analysis of the energy conservation performance of ECO-OP in Chapters 8 and 9 only provides some tentative conclusions regarding the long-term viability of ECO-OP, being concerned solely with the network-wide energy impact of the initial ECO-OP partner selection round at the time of the network's deployment. Therefore in order to establish the validity of ECO-OP as an effective technique for extending the lifetime of a wireless sensor network, it is crucial to explicitly investigate the long-term benefit of network-wide cooperation using

ECO-OP⁷. To address this, an investigation of the network lifetime extension performance of ECO-OP will be presented in Chapters 10 and 11. The analysis in Chapters 10 and 11 will thus serve to establish the general validity of the proposed ECO-OP cooperation strategy as an effective technique for extending the lifetime of a wireless sensor network.

Moreover, the performance of the low-complexity distributed ECO-OP cooperation strategy will be compared throughout Chapters 10 and 11 against that of a computationally intensive centralised greedy cooperation algorithm from the literature [18]. The analysis in Chapters 10 and 11 will thus enable a thorough comparison of the long-term behaviour and performance of these two fundamentally distinct approaches to coordinating cooperative communication in an energy-constrained wireless network. Importantly, the network lifetime extension performance of the centralised greedy cooperation algorithm [18] will serve as a benchmark for evaluating the effectiveness of the distributed ECO-OP cooperation strategy proposed in this thesis as a technique for extending the lifetime of a wireless sensor network.

The algorithm proposed in [18] is designed to maximise the minimum node lifetime in an energy-constrained wireless network using cooperative communication, whereby a central controller performs a computationally intensive offline greedy search to allocate cooperation partners and transmit power for each node in the network. Whenever a node depletes its energy, the centralised greedy cooperation algorithm [18] must be repeated in order to reallocate a cooperation partner to each surviving source node in the network. Importantly, this affords the centralised greedy cooperation algorithm [18] the advantage of continually balancing the projected lifetimes of all remaining nodes based on the distribution of residual energy in the network. By contrast, using ECO-OP only the source nodes associated with the expired partner node reselect a partner, and nodes are ignorant of the residual energy of other nodes. However, the fact that the computationally intensive centralised greedy cooperation algorithm [18] must be repeated each time a node depletes its energy also effectively renders the cooperation strategy proposed in [18] prohibitively computationally expensive for practical long-term cooperation in dense wireless networks. Nonetheless, to enable a thorough comparison of these two distinct cooperation strategies, simulation results for the centralised greedy cooperation algorithm [18] will still be presented alongside ECO-OP in Chapters 10 and 11 for dense networks. For a detailed

⁷It should be noted that it is possible for a cooperation strategy to reduce the overall network energy expenditure yet also reduce the network lifetime. For this reason, it is necessary to explicitly analyse the long-term performance of ECO-OP in terms of the lifetime extension it achieves, in addition to the analysis of its energy conservation performance in Chapters 8 and 9. For example, consider a cooperation strategy which achieves a high overall network energy saving at the expense of overburdening several partner nodes to the extent that they deplete their energy before any node in a non-cooperative network. Such a cooperation strategy would be ineffective if the network lifetime was defined as the time until the first node death. However, if the network lifetime was instead defined as the time until a higher proportion of nodes dies (say 50%), a cooperation strategy which sacrifices a few partner nodes in order to extend the lifetimes of the rest of the network's nodes is nonetheless beneficial to the network overall.

description of the centralised greedy cooperation algorithm [18] and further details of its implementation in generating the simulation results presented in Chapters 10 and 11, please refer to Appendix A.

In Chapter 10 the fundamental long-term behaviour of network-wide cooperation will be illustrated throughout the lifetime of the wireless sensor network by simulating cooperation among 100 nodes regularly placed over a 100 m by 100 m network area. The long-term behaviour of each considered cooperation strategy will be demonstrated in terms of the distribution of the individual node lifetimes across the cooperative versus the non-cooperative network and the average distribution of cooperation partner service and selection among the network's nodes. Moreover, the network lifetime extension performance of each cooperation strategy will be analysed in terms of the cooperative lifetime improvement achieved from network activation through to the last node death, and summarised overall by the average network lifetime improvement achieved.

In Chapter 11 the typical network lifetime extension performance of network-wide cooperation will be evaluated for the general case of randomly deployed networks of various node density. Specifically, a range of node density values will be investigated by simulating cooperation among $M=\{2, 3, 4, 5, 6, 10, 30, 100, 300, 1000\}$ nodes randomly placed over a 100 m by 100 m network area. In order to represent the typical behaviour of ECO-OP, the results presented in Chapter 11 are given by the median of $Q = \left(\frac{10^5}{M}\right)$ simulation runs⁸. Firstly, the typical node lifetime curve (i.e. node lifetime versus the number of node deaths since network activation) will be presented for a network of $M=100$ randomly placed nodes, thereby examining the characteristic long-term behaviour of different cooperation strategies. Secondly, the overall network lifetime extension performance of each cooperation strategy as M is varied will be quantified in terms of the average network lifetime improvement achieved via network-wide cooperation.

As in Chapters 8 and 9, the performance of ECO-OP with different partner choice rules (GKH_1 , GKH_2 , LKH , and random partner choice) will be investigated in Chapters 10 and 11. The results presented in Chapters 10 and 11 are based on MATLAB simulations of network-wide cooperation throughout the lifetime of the wireless sensor network in three representative network topologies, which are introduced in Section 7.4 along with other relevant simulation parameters and assumptions. It is important to note that the ECO-OP simulation results presented in Chapters 10 and 11 are based on an implementation of the overall distributed ECO-OP cooperation strategy employed by each source node in the cooperative network throughout its lifetime, as specified in Fig. 7.2 (cf. the simulation results in Chapters 8 and 9 which are based on a static distribution of cooperation partner service from the initial ECO-OP partner selection round at the

⁸The results presented in Chapter 11 for the centralised greedy cooperation algorithm [18] for large values of M are based on a smaller number of network realisations, due to the extremely long simulation times (please refer to Appendix A for further details).

time of the network's deployment). The node and network lifetime definitions and metrics which are employed in the analysis in Chapters 10 and 11 are presented in Section 7.6.

7.4 Wireless Sensor Network Model and Simulation Parameters

In generating the simulation results presented in Chapters 8-11, a static wireless sensor network of M sensor nodes placed over a square network area of 100 m by 100 m is assumed. A regular node placement is assumed in Chapters 8 and 10 for the purpose of illustration, whereas the more general case of randomly placed nodes is thoroughly examined in Chapters 9 and 11. Three basic network configurations are considered in the analysis of network-wide cooperation presented in Chapters 8-11:

Topology A Network, Central Destination Receiver: In a Topology A network all M sensor nodes communicate with a single central destination receiver, located at [50 m, 50 m] from the bottom left-hand corner of the 100m by 100m network area, as illustrated in Fig. 7.3. This topology is representative of a wireless sensor network with a central data gathering node or gateway.

Topology B Network, Remote Destination Receiver: In a Topology B network all M sensor nodes communicate with a single remote destination receiver, located at [50 m, 200 m] from the bottom left-hand corner of the 100m by 100m network area, as illustrated in Fig. 7.4. This topology is representative of a wireless sensor network where nodes send information back to the end-user via a remote base station or Internet gateway. Thus Topology A and B networks are two distinct variations of the directed data flow network.

Topology C Network, Node-to-Node Communication: In a Topology C network each sensor node is randomly allocated one of the other nodes in the network as its destination receiver for the duration of the network's operation, as illustrated in Fig. 7.5. The non-directed data flow in this random node-to-node communication roughly models communication in a multi-hop or ad-hoc sensor network. This topology thus provides a basic *general* network model for evaluating the performance of network-wide cooperation. Moreover, this topology is similar to that adopted in [18]. It should be noted that a node r serving as the destination receiver for a given source node j in a Topology C network is not eligible to serve as a cooperation partner to node j ; thus in a Topology C network source node j initialises its candidate partner set as $\varphi_j = \mathbf{M} - \{j\} - \{r\}$ in Fig. 7.2. Similarly, in a Topology C network node r would also check its battery levels after serving as a destination receiver (i.e. in

addition to checking its energy levels after serving as source or partner, as shown in Fig. 7.2).

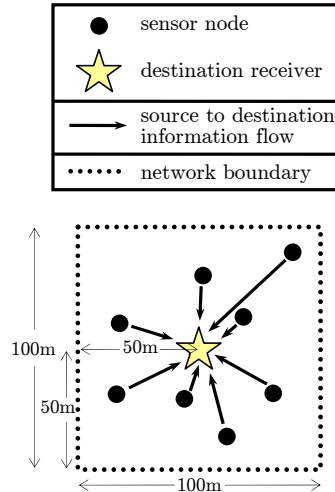


Figure 7.3: Illustration of the Topology A wireless sensor network configuration, showing the information flow from each source node to the central destination receiver.

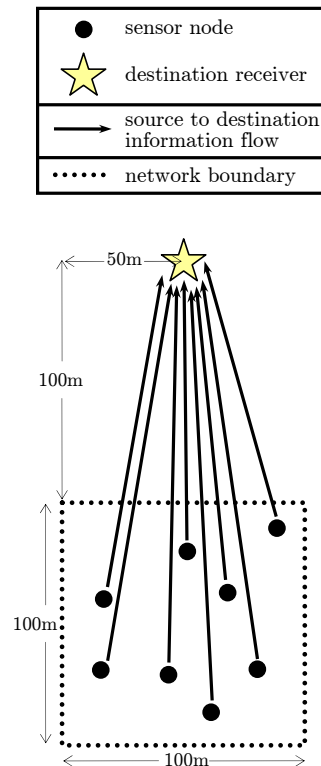


Figure 7.4: Illustration of the Topology B wireless sensor network configuration, showing the information flow from each source node to the remote destination receiver.

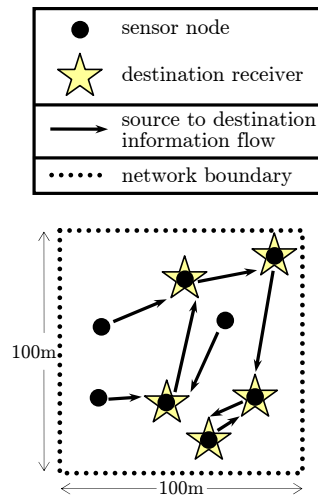


Figure 7.5: Illustration of the Topology C wireless sensor network configuration, showing the information flow from each source node to another randomly allocated destination receiver node.

Together these three network topologies are representative of a wide range of wireless sensor network configurations (i.e. two distinct variations of directed data flow and a random data flow topology). Therefore, analysing the behaviour and performance of network-wide cooperation within these three network topologies in Chapters 8-11 is intended to provide a sufficient context for a robust analytical evaluation of the effectiveness of the proposed ECO-OP cooperation strategy. It should also be noted that, for all three considered network topologies, the performance of cooperative communication is compared against non-cooperative source to destination communication over a single hop. Namely, the analysis in Chapters 8-11 has been deliberately restricted to the case of a network of single-hop links in order to discern the fundamental behaviour of network-wide cooperative communication.

The results presented in Chapters 8-11 are based on MATLAB simulations of network-wide cooperation in these three representative network topologies using the reference cooperative system parameters⁹ specified in Table 2.1. It should be noted that since the effect of varying several different system parameters on the energy efficiency of a cooperative link has already been thoroughly investigated in Chapters 4-6, only the reference cooperative system is considered in the analysis presented henceforth in this thesis. In the investigations of the lifetime extension performance of network-wide cooperation presented in Chapters 10 and 11, it is assumed that the wireless sensor network operates under a schedule-based channel access protocol¹⁰ with a uniform traffic scenario, where every source node in the network in turn sends a message block of $B=100$ bits to its desti-

⁹Obviously, d_{s-d} varies in the analysis of network-wide cooperation, depending on the location of each source node relative to the destination receiver.

¹⁰It should be noted that schedule-based channel access such as TDMA (time division multiple access), whereby nodes' transmissions do not interfere with each other (i.e. collisions are avoided), is assumed for the sake of simplicity.

nation receiver in each transmission round. Moreover, it is assumed that prior to network activation all sensor nodes have an initial battery energy of $E_{battery}$, where $E_{battery}=10$ J for Topology A and C networks and $E_{battery}=100$ J for Topology B networks¹¹. It should be noted that these battery energy values were chosen purely to allow reasonable simulation times, rather than to reflect the realistic battery capacity of a sensor node (which would be much higher). Importantly, it should be noted that the basic network model of uniform scheduled traffic within three elementary network topologies has been deliberately adopted in this thesis in order to derive general conclusions about the behaviour and performance of network-wide communication using the proposed ECO-OP cooperation strategy. Namely, analysing network-wide cooperation using this simple generic network model enables a clear evaluation of the fundamental behaviour of ECO-OP itself, by removing the idiosyncrasies of a specific existing network protocol¹².

Finally, it should be noted that partner selection based on explicitly maximising $E_{saving_coop_total}$ for each source node (referred to as “optimal” partner selection in Chapter 6) has been intentionally excluded from the analysis presented in Chapters 8-11; the analysis in Chapter 6 has already established that the proposed partner choice heuristics are near-optimally energy efficient with respect to an individual cooperative link and thus further comparison would be superfluous. Importantly, whereas it was possible to perform an exhaustive search to find the partner allocation which maximises the energy efficiency of an individual cooperative link in Chapter 6, it is not practically feasible to compare the results of network-wide cooperation using ECO-OP in Chapters 8-11 against that of an “optimal” partner service allocation which maximises some network performance metric¹³. However, the performance of ECO-OP with the proposed partner choice heuristics GKH_1 , GKH_2 , and LKH is still compared against that of random partner choice in Chapters 8-11, since this serves as a useful elementary benchmark for the performance of different partner choice rules. A given source node j using ECO-OP with random partner choice would choose its partner randomly from its candidate partner set as φ_j and acquire measurements of $L_{p(i)-d}$ and $L_{s(j)-p(i)}$, and then, as per the ECO-OP flowchart in

¹¹The $E_{battery}$ value assumed in generating simulation results for a Topology B network is higher than that for Topology A and C networks because node energy consumption in the remote destination receiver Topology B network is inherently much higher than in the other two network topologies.

¹²Of course, this is not to say that the analytical evaluation of ECO-OP presented in this thesis renders unnecessary any further performance analysis of ECO-OP prior to its deployment in a specific real-world network. Rather, the fundamental analysis in this thesis serves as an essential foundation towards fully evaluating the performance of ECO-OP in the context of various specific network protocols.

¹³It is easy to show that an exhaustive search to find a partner service allocation which optimises a given network performance metric in Chapters 8 and 9 would require a search over $(M-1)^M$ possible partner distribution permutations for a single M -node network realisation. Thus for example, even in a relatively sparse network of $M=10$ nodes there are over 3.5×10^9 possible partner allocation combinations, which obviously makes a simulation involving such an exhaustive search impractical. The total number of possible partner allocation permutations throughout the lifetime of the network in Chapters 10 and 11 is greatly larger still, since the partner service distribution over the network must change each time a node in the M -node network expires.

Fig. 7.1, perform cooperative transmit power allocation and check whether cooperative communication with its chosen partner node is beneficial.

7.5 Wireless Sensor Network Energy Consumption Definitions and Metrics

The analysis presented in Chapters 3-6 was concerned with investigating the energy efficiency of an individual cooperative link, which consists of one source node communicating its message to the destination receiver by cooperating with its chosen partner node. Consequently, the energy efficiency of cooperation was defined in Section 2.3 in terms of the total energy per bit consumed by a single communication link using non-cooperative and cooperative communication (i.e. a message-centric energy model). By contrast, the analysis presented in Chapters 8 and 9 will be concerned with investigating the effectiveness of network-wide cooperative communication, whereby multiple cooperative links co-exist in a single wireless sensor network of M nodes and individual sensor nodes may take on the role of both source and partner node¹⁴. As stated in Section 7.2, it is assumed that each node in the network acts as a source and selects one partner node from the other $(M - 1)$ nodes in the network. The average energy efficiency of the individual cooperative links in the wireless sensor network may then be quantified as

$$\text{Average } E_{\text{saving-coop-total}} \text{ achieved over the } M\text{-node network} = \frac{1}{M} \sum_{j=1}^M E_{\text{saving-coop-total}(j)}, \quad (7.1)$$

where $E_{\text{saving-coop-total}}$ is given by (2.17). However, the average $E_{\text{saving-coop-total}}$ achieved over the network is an insufficient measure of the benefit of network-wide cooperation, as it gives equal weighting to the relative energy saving achieved over each cooperative link in the network, regardless of the absolute energy conserved. Namely, in order to properly evaluate the impact of network-wide cooperation it is necessary to also consider the distribution of individual node energy consumption over the network.

To this end, a node-centric energy model is presented in this section, which defines the total energy per bit consumed by an individual node¹⁵ in a non-cooperative and cooperative wireless sensor network as $E_{\text{non-coop-node}}$ and $E_{\text{coop-node}}$ respectively. The total energy per bit consumed by a non-cooperative network of M nodes may then be expressed as

¹⁴A node always acts as a source but may serve as partner to none, one, or several other source nodes.

¹⁵It is important to note that the node energy consumption definitions presented in this section are still based on the communication energy model presented in Section 2.3, only expressed from the point of view of an individual node rather than that of an individual cooperative link.

$$E_{non-coop-NETWORK} = \sum_{j=1}^M E_{non-coop-node(j)}, \quad (7.2)$$

and the total energy per bit consumed by a cooperative network of M nodes may be expressed as

$$E_{coop-NETWORK} = \sum_{j=1}^M E_{coop-node(j)}. \quad (7.3)$$

It follows that the overall energy conservation performance of network-wide cooperation may be quantified in terms of the total reduction in network energy consumption achieved by cooperative communication,

$$\text{Network energy reduction factor} = \frac{E_{non-coop-NETWORK}}{E_{coop-NETWORK}}. \quad (7.4)$$

The node energy consumption metrics defined in this section are employed in the investigation of the energy conservation performance of network-wide cooperation using ECO-OP in Chapters 8 and 9, an overview of which was presented in Section 7.3.1. It is important to note that the definitions presented in this section are thus based on a static distribution of cooperation partner service (i.e. the initial partner selection round at the time of the network's deployment, as specified in Fig. 7.1). The case of a dynamic distribution of cooperation partner service is only relevant in considering network-wide cooperation throughout the lifetime of a wireless sensor network, and will be treated in Section 7.6 where node lifetime metrics are defined.

7.5.1 Node Energy Consumption in a Non-Cooperative Network

The total energy per bit consumed by node j in a non-cooperative network, $E_{non-coop-node(j)}$, is given by

$$E_{non-coop-node(j)} = E_{non-coop-source-node(j)} + E_{non-coop-destination-node(j)}. \quad (7.5)$$

The first term in (7.5) represents the total energy per bit consumed by node j acting as a source,

$$E_{non-coop-source-node(j)} = \frac{\xi}{\eta} E_{tx-s(j)-non-coop} + \frac{P_{CCT-tx}}{R_b}, \quad (7.6)$$

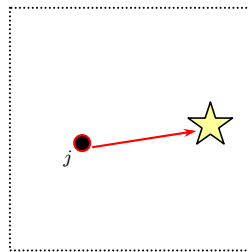
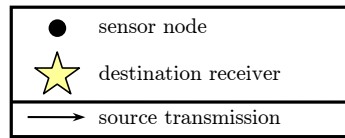
where $E_{tx-s(j)-non-coop}$ represents the transmit energy per bit of source node j , and is given by (3.6).

The second term in (7.5) represents the total energy per bit consumed by node j serving as the destination receiver for other source nodes in the network. This term is non-zero only for Topology C networks. Let \mathbf{G} be the set of source nodes using node j as their destination, such that node j serves as destination receiver to G other nodes in the network, giving

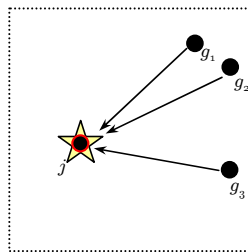
$$E_{non-coop_destination_node(j)} = G \left(\frac{P_{CCT_rx}}{R_b} \right), \quad (7.7)$$

where $0 \leq G \leq (M - 1)$ for a network of M nodes.

The individual node energy consumption in a non-cooperative network, as expressed by (7.5), is illustrated in Fig. 7.6 by way of an example network configuration. Node j and its transmissions are marked in red in Fig. 7.6 to represent the circuit and transmission energy consumption associated with node j in its role as a source and destination receiver node. Fig. 7.6a illustrates (7.6) by showing node j acting as a source, whereas Fig. 7.6b illustrates (7.7) by showing node j serving as a destination receiver in an example Topology C network configuration. It should be noted that the transmissions shown in Fig. 7.6 are not simultaneous.



(a) Illustration of (7.6): node j consumes energy in acting as a source.



(b) Example of a non-cooperative Topology C network configuration illustrating (7.7): node j consumes energy in acting as a destination receiver to a set of $G=3$ source nodes, $\mathbf{G}=\{g_1, g_2, g_3\}$.

Figure 7.6: Illustration of node energy consumption in a non-cooperative network as expressed by (7.5): node j may consume energy acting as (a) a source and (b) a destination receiver.

7.5.2 Node Energy Consumption in a Cooperative Network

The total energy per bit consumed by node j in a cooperative network, $E_{coop_node(j)}$, is given by

$$E_{coop_node(j)} = E_{coop_source_node(j)} + E_{coop_partner_node(j)} + E_{coop_destination_node(j)}. \quad (7.8)$$

The first term in (7.8) represents the total energy per bit consumed by node j acting as a source,

$$E_{coop_source_node(j)} = \frac{\xi}{\eta} E_{tx_s(j,\hat{i})} + \frac{P_{CCT_tx}}{R_b}, \quad (7.9)$$

where $E_{tx_s(j,\hat{i})}$ represents the transmit energy per bit of source node j when cooperating with partner node \hat{i} , and is given by (5.13). It should be noted that, should source node j opt for non-cooperative communication for its own transmission to the destination receiver (if $E_{saving_coop_total} \leq 0$, as specified in Section 7.2), the transmit energy is instead given by $E_{tx_s(j,\hat{i})} = E_{tx_s(j)}_{non-coop}$.

The second term in (7.8) represents the total energy per bit consumed by node j acting as a partner. Let \mathbf{H} be the set of source nodes using node j as their partner, such that node j serves as partner to H other nodes in the network, giving

$$E_{coop_partner_node(j)} = H \left(\frac{P_{CCT_rx}}{R_b} \right) + \sum_{h \in \mathbf{H}} (1 - BLER_{s(h)-p(j)}) \left(\frac{\xi}{\eta} E_{tx_p(j,h)} + \frac{P_{CCT_tx}}{R_b} \right), \quad (7.10)$$

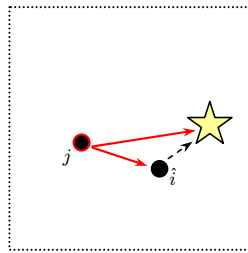
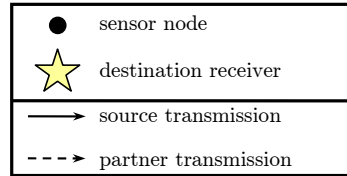
where $E_{tx_p(j,h)}$ represents the transmit energy per bit of node j acting as partner to source node h (given by (5.14)) and $BLER_{s(h)-p(j)}$ is the BLER of the transmission from source node h to the partner node j . As stated in Section 7.2, it is assumed that every node in the network is eligible to be selected as a cooperation partner by any other source node in the network. Thus for a network of M nodes, $0 \leq H \leq (M - 1)$, except for Topology C networks where $0 \leq H \leq (M - 2)$ since a source node's destination receiver cannot be part of its candidate partner set.

The third term in (7.8) represents the total energy per bit consumed by node j serving as the destination receiver for other nodes in the Topology C network. Let \mathbf{G} be the set of source nodes using node j as their destination, such that node j serves as destination receiver to G other nodes in the network, where each source node $g \in \mathbf{G}$ cooperates with some partner node f , giving

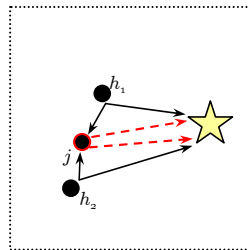
$$E_{coop_destination_node(j)} = \sum_{g \in \mathbf{G}} (2 - BLEER_{s(g)-p(f)}) \frac{P_{CCT-rx}}{R_b}, \quad (7.11)$$

where $BLEER_{s(g)-p(f)}$ is the BLER of the transmission from source node g to partner node f and $0 \leq G \leq (M - 1)$ for a network of M nodes. It should be noted that, should source node g opt for non-cooperative communication for its transmission to the destination receiver (if $E_{saving-coop-total} \leq 0$, as specified in Section 7.2), the energy per bit consumed by node j in serving as the destination receiver to node g is instead given by $\frac{P_{CCT-rx}}{R_b}$, which is equivalent to setting $BLEER_{s(g)-p(f)} = 1$ in (7.11).

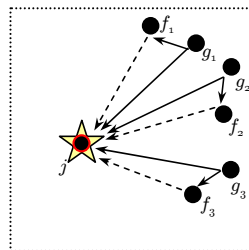
The individual node energy consumption in a cooperative network, as expressed by (7.8), is illustrated in Fig. 7.7 by way of an example network configuration. Node j and its transmissions are marked in red in Fig. 7.7 to represent the circuit and transmission energy consumption associated with node j in its various roles. Specifically, Figs. 7.7a, 7.7b, and 7.7c illustrate (7.9), (7.10), and (7.11) by showing node j acting as a source, partner, and destination receiver node, respectively.



(a) Illustration of (7.9): node j consumes energy in acting as a source, cooperating with partner node \hat{i} .



(b) Example of a cooperative network configuration illustrating (7.10): node j consumes energy in acting as a partner to a set of $H=2$ source nodes, $H=\{h_1, h_2\}$.



(c) Example of a cooperative Topology C network configuration illustrating (7.11): node j consumes energy in acting as a destination receiver to a set of $G=3$ source nodes, $G=\{g_1, g_2, g_3\}$, where each source node in set G cooperates with some partner node f .

Figure 7.7: Illustration of node energy consumption in a cooperative network as expressed by (7.8): node j may consume energy acting as (a) a source, (b) a partner, and (c) a destination receiver.

7.6 Wireless Sensor Network Lifetime Definitions and Metrics

The operational lifetime of a wireless sensor network can be generally defined as the time from network activation until the network is no longer considered to be functional [5]. However, what constitutes a functional network varies from application to application, and thus various definitions of wireless sensor network lifetime have been proposed in the literature. Commonly used definitions¹⁶ include the time until the first sensor node dies (first node death), the last sensor node dies (last node death), or a certain proportion of nodes die (e.g. death of the 60th percentile of nodes) [5]. These can be collectively defined as the time until the x^{th} node death, where $x = 1, 2, \dots, M$ is the order in which sensor nodes die in a wireless sensor network of M nodes.

The x^{th} node lifetime $T_{\text{node}(x)}$ is defined as the number of transmission rounds the x^{th} node survives from the time of the network's activation. The improvement in the x^{th} node lifetime using cooperative communication is then defined as

$$x^{\text{th}} \text{ node lifetime improvement factor} = \frac{T_{\text{coop_node}(x)}}{T_{\text{non-coop_node}(x)}}, \quad (7.12)$$

where $T_{\text{coop_node}(x)}$ and $T_{\text{non-coop_node}(x)}$ represent the x^{th} node lifetime in a cooperative and a non-cooperative wireless sensor network, respectively. It should be noted that the order in which individual nodes in the wireless sensor network deplete their energy will likely differ between a non-cooperative and a cooperative network. In general, per-node fairness is unimportant in wireless sensor networks compared to the network's overall survival. Accordingly, (7.12) quantifies the cooperative lifetime improvement for the $(\frac{x}{M})^{\text{th}}$ percentile of nodes, rather than the lifetime improvement per individual node.

Moreover, the value of x must be chosen appropriately in quantifying the lifetime of a wireless sensor network to accurately represent the proportion of nodes that must remain alive to maintain a functional network. The time to first node death ($x=1$) generally underestimates the useful network lifetime, whereas the time to last node death ($x=M$) overestimates it. Other values of x are largely arbitrary, unless the specific sensor network application is known. Thus it is desirable to define a single metric to simultaneously capture the cooperative lifetime improvement of the sensor network from its activation through to the last node death. Therefore, the primary performance metric employed in this thesis to quantify the overall network lifetime improvement achieved by cooperative

¹⁶Various other definitions of network lifetime have also been proposed in the literature, such as the time until loss of sensing coverage occurs or the network partitions [5, 70]. Such definitions are particularly application-specific and are thus not considered in this thesis. Instead, a more generic network lifetime definition is adopted in this thesis, which is intuitively meaningful regardless of application (i.e. the time until a certain number of node deaths occurs).

communication is defined as the average of the x^{th} node lifetime improvement factors achieved over the entire lifetime of the network,

$$\text{Average network lifetime improvement factor} = \frac{1}{M} \sum_{x=1}^M \frac{T_{coop_node(x)}}{T_{non-coop_node(x)}}. \quad (7.13)$$

The node and network lifetime metrics defined in this section are employed in the investigation of the lifetime extension performance of network-wide cooperation using ECO-OP in Chapters 10 and 11, an overview of which was presented in Section 7.3.2. It is important to note that the definitions presented in this section are based on a dynamic distribution of cooperation partner service. Namely, throughout the lifetime of a wireless sensor network, source node must reselect their cooperation partner once the previous partner node has depleted its batteries, as specified in Fig. 7.2. By contrast, the definitions of node energy consumption presented in Section 7.5 are based on a static distribution of cooperation partner service (i.e. the initial partner selection round at the time of the network's deployment, as specified in Fig. 7.1). Accordingly, the node lifetime definitions presented in this section employ the concept of *average* node energy consumption over the node's lifetime.

7.6.1 Node Lifetime in a Non-cooperative Network

The x^{th} node lifetime in a non-cooperative network may be expressed as

$$T_{non-coop_node(x)} = \frac{E_{battery}}{B \times \bar{E}_{non-coop_node(x)}}, \quad (7.14)$$

where $\bar{E}_{non-coop_node(x)}$ is the average total energy per bit (averaged of over the x^{th} node's lifetime) consumed by the x^{th} sensor node in a non-cooperative network,

$$\bar{E}_{non-coop_node(x)} = E_{non-coop_source_node(x)} + \bar{E}_{non-coop_destination_node(x)}. \quad (7.15)$$

It is important to note that (7.15) is analogous to the definition of $E_{non-coop_node(x)}$ given in (7.5)¹⁷.

The first term in (7.15) represents the total energy per bit consumed by the x^{th} node acting as a source and is given by (7.6). The energy consumed by the x^{th} node in serving as a source in a non-cooperative network has been previously illustrated in Fig. 7.6a.

¹⁷It should be noted that the node energy definitions in Section 7.5 consider an arbitrary node j ; in referring to the x^{th} node in this section, the node-identifying subscript is changed from j to x (e.g. $E_{non-coop_node(j)}$ becomes $E_{non-coop_node(x)}$).

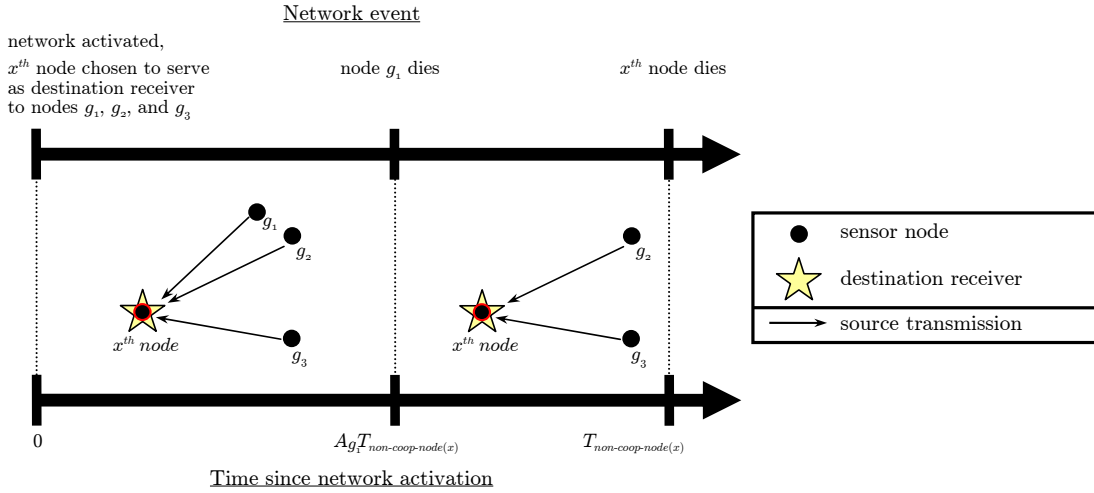


Figure 7.8: Example of a non-cooperative Topology C network event timeline illustrating (7.16): throughout its lifetime of $T_{non-coop-node(x)}$ transmission rounds, the x^{th} node consumes energy acting as a destination receiver for the source nodes g_1 , g_2 , and g_3 . The x^{th} node receives messages from nodes g_2 and g_3 for the duration of its lifetime, whereas it receives messages from node g_1 for the proportion A_{g_1} of its lifetime.

The second term in (7.15) represents the average total energy per bit consumed by the x^{th} node serving as the destination receiver for other source nodes in the Topology C network. As defined in Section 7.5.1, \mathbf{G} is the set of all source nodes using the x^{th} node as their destination receiver, such that the x^{th} node serves as destination receiver to G other nodes in the network, giving

$$\bar{E}_{non-coop-destination-node(x)} = \sum_{g \in \mathbf{G}} A_g \left(\frac{P_{CCT-rx}}{R_b} \right), \quad (7.16)$$

where $0 \leq G \leq (M - 1)$ for a network of M nodes and A_g is the proportion of the x^{th} node's lifetime it receives messages from source node $g \in \mathbf{G}$, where $0 < A_g \leq 1$. It is interesting to note that if the x^{th} node depletes its energy before any of the G source nodes that it serves as destination receiver, then $A_g = 1$ for all $g \in \mathbf{G}$ and $\bar{E}_{non-coop-destination-node(x)} = E_{non-coop-destination-node(x)}$ as given by (7.16). Fig. 7.8 presents an example network event timeline illustrating the energy consumed by the x^{th} node throughout its lifetime in serving as a destination receiver in a non-cooperative Topology C network, as expressed by (7.16). The x^{th} node is marked in red in Fig. 7.8 to represent the circuit energy consumption associated with the x^{th} node in its role as destination receiver node to the set of source nodes $\mathbf{G} = \{g_1, g_2, g_3\}$. It should be noted that the same example set of source nodes \mathbf{G} is shown in Figs. 7.8 and 7.6b for the sake of continuity.

Finally, it should be noted that once a destination receiver node depletes its energy in a Topology C network, any surviving associated source nodes in the set \mathbf{G} are no longer considered to be functional and thus their lifetimes are recorded as ending at

the time of their destination receiver node depleting its energy. However, these defunct source nodes do continue to serve as destination receivers to other source nodes in the non-cooperative network until they actually deplete their own batteries. For example, once the x^{th} node depletes its energy in Fig. 7.8, the lifetimes of source nodes g_2 and g_3 would be recorded as being equal to $T_{non-coop_node(x)}$. Nodes g_2 and g_3 would thus be considered the $(x+1)^{th}$ and $(x+2)^{th}$ nodes to die since the network's activation, such that $T_{non-coop_node(x)} = T_{non-coop_node(x+1)} = T_{non-coop_node(x+2)}$. The defunct source nodes g_2 and g_3 would nevertheless continue to serve as destination receiver to any of their own associated source nodes (not shown in Fig. 7.8) until the nodes g_2 and g_3 have actually depleted their own batteries.

7.6.2 Node Lifetime in a Cooperative Network

The x^{th} node lifetime in a cooperative network may be expressed as

$$T_{coop_node(x)} = \frac{E_{battery}}{B \times \bar{E}_{coop_node(x)}} \quad (7.17)$$

where $\bar{E}_{coop_node(x)}$ is the average total energy per bit (averaged over the x^{th} node's lifetime) consumed by the x^{th} sensor node in a cooperative network,

$$\bar{E}_{coop_node(x)} = \bar{E}_{coop_source_node(x)} + \bar{E}_{coop_partner_node(x)} + \bar{E}_{coop_destination_node(x)} \quad (7.18)$$

It is important to note that (7.18) is analogous to the definition of $E_{coop_node(x)}$ given in (7.8).

The first term in (7.18) represents the average total energy per bit consumed by the x^{th} node acting as a source. Let \mathbf{I} be the set of partner nodes that the x^{th} source node selects throughout its lifetime, such that the x^{th} source node cooperates with I different partner nodes throughout its lifetime and $C_{\hat{i}}$ is the proportion of the x^{th} source node's lifetime it is served by partner node $\hat{i} \in \mathbf{I}$, such that $\sum_{\hat{i} \in \mathbf{I}} C_{\hat{i}} = 1$. This gives

$$\bar{E}_{coop_source_node(x)} = \sum_{\hat{i} \in \mathbf{I}} C_{\hat{i}} \left(\frac{\xi}{\eta} E_{tx-s(x,\hat{i})} + \frac{P_{CCT-tx}}{R_b} \right), \quad (7.19)$$

where $E_{tx-s(x,\hat{i})}$ represents the transmit energy per bit of x^{th} source node when cooperating with partner node \hat{i} and is given by (5.13). It should be noted that, should the x^{th} source node opt for non-cooperative communication at the time of the network's deployment (i.e. if the expected $E_{saving_coop_total}$ with its best available cooperation partner is not positive, as specified in Fig. 7.1), the set of selected partner nodes \mathbf{I} is empty and $\bar{E}_{coop_source_node(x)}$ is instead given by (7.6). Similarly, if the x^{th} source node opts for non-cooperative trans-

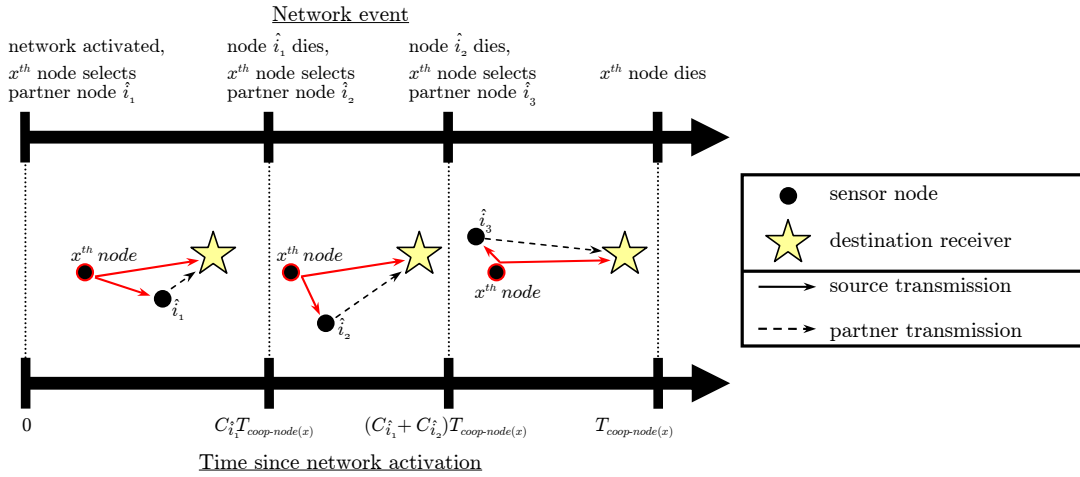


Figure 7.9: Example of a cooperative network event timeline illustrating (7.19): throughout its lifetime of $T_{coop_node(x)}$ transmission rounds, the x^{th} node consumes energy in acting as a source cooperating with partner nodes \hat{i}_1 , \hat{i}_2 , and \hat{i}_3 . The x^{th} node is served by partner nodes \hat{i}_1 and \hat{i}_2 for the proportion $C_{\hat{i}_1}^*$ and $C_{\hat{i}_2}^*$ of its lifetime, respectively, and by partner node \hat{i}_3 for the remainder of its lifetime.

mission after its previous cooperation partner has depleted its energy, the total energy per bit consumed by the x^{th} node as a source is given by (7.6) for the remainder of the x^{th} node's lifetime. It is also interesting to note that if the x^{th} node dies before its initially selected partner node, then $I = 1$ and $\bar{E}_{coop_source_node(x)} = E_{coop_source_node(x)}$ as given by (7.9). Fig. 7.9 presents an example network event timeline illustrating the energy consumed by the x^{th} node throughout its lifetime in serving as a source in a cooperative network, as expressed by (7.19). The x^{th} node and its transmissions are marked in red in Fig. 7.9 to represent the circuit and transmission energy consumption associated with the x^{th} node in its role as a source node cooperating throughout its lifetime with the set of source nodes $\mathbf{I} = \{\hat{i}_1, \hat{i}_2, \hat{i}_3\}$. It should be noted that the partner node \hat{i}_1 , which is initially chosen by the x^{th} node at the time of the network's deployment in the example in Fig. 7.9, is equivalent to partner node \hat{i} in Fig. 7.7a.

The second term in (7.18) represents the average total energy per bit consumed by the x^{th} node acting as a partner. Let \mathbf{H}' be the set of source nodes that select the x^{th} node as their partner throughout the x^{th} node's lifetime, such that the x^{th} node serves as partner to H' other nodes in the network throughout its lifetime and D_h is the proportion of the x^{th} node's lifetime that it serves as partner to node $h \in \mathbf{H}'$, where $0 < D_h \leq 1$. This gives:

$$\begin{aligned} \bar{E}_{coop_partner_node(x)} = & \sum_{h \in \mathbf{H}'} D_h \left(\frac{P_{CCT-rx}}{R_b} \right) + \\ & \sum_{h \in \mathbf{H}'} D_h (1 - BLE R_{s(h)-p(x)}) \left(\frac{\xi}{\eta} E_{tx-p(x,h)} + \frac{P_{CCT-tx}}{R_b} \right), \end{aligned} \quad (7.20)$$

where $E_{tx-p(x,h)}$ represents the transmit energy per bit of the x^{th} node acting as partner to source node h (given by (5.14)) and $BLE R_{s(h)-p(x)}$ is the BLER of the transmission from source node h to the x^{th} partner node. As stated in Section 7.2, it is assumed that any surviving node in the network is eligible to be selected as a cooperation partner by an other source node in the network. Thus for a network of M nodes, $0 \leq H' \leq (M - 1)$, except for Topology C networks where $0 \leq H' \leq (M - 2)$ since a source node's destination receiver cannot be part of its candidate partner set. It is important to note that in general $\mathbf{H} \subseteq \mathbf{H}'$ and $H \leq H'$. Namely, after the initial partner selection round at the time of the network's deployment¹⁸ further source nodes (whose previously selected partner nodes had subsequently died) may select the x^{th} node as their partner. Fig. 7.10 presents an example network event timeline illustrating the energy consumed by the x^{th} node throughout its lifetime in serving as a partner in a cooperative network, as expressed by (7.20). The x^{th} node and its transmissions are marked in red in Fig. 7.10 to represent the circuit and transmission energy consumption associated with the x^{th} node in its role as a partner node to the set of source nodes $\mathbf{H}' = \{h_1, h_2, h_3\}$. It should be noted that the set $\mathbf{H} = \{h_1, h_2\}$ shown in Fig. 7.10 is the same as the set \mathbf{H} shown in Fig. 7.7b for the sake of continuity.

The third term in (7.18) represents the average total energy per bit consumed by the x^{th} node serving as the destination receiver for other nodes in the Topology C network. As defined in Section 7.5.2, \mathbf{G} is the set of all source nodes using the x^{th} node as their destination receiver, such that the x^{th} node serves as destination receiver to G other nodes in the network, where each source node $g \in \mathbf{G}$ cooperates with some partner node $f \in \mathbf{F}$. Let \mathbf{F} be the set of partner nodes that source node $g \in \mathbf{G}$ selects throughout its lifetime, such that source node g cooperates with F different partner nodes throughout its lifetime and E_f is the proportion of the lifetime of source node g that it is served by partner node $f \in \mathbf{F}$, such that $\sum_{f \in \mathbf{F}} E_f = 1$. This gives

$$\bar{E}_{coop_destination_node(x)} = \sum_{g \in \mathbf{G}} A_g \sum_{f \in \mathbf{F}} E_f (2 - BLE R_{s(g)-p(f)}) \frac{P_{CCT-rx}}{R_b}, \quad (7.21)$$

where $BLE R_{s(g)-p(f)}$ is the BLER of the transmission from source node g to partner node f and $0 \leq G \leq (M - 1)$ for a network of M nodes. As defined in Section 7.5.2, A_g is

¹⁸The set of source nodes that select the x^{th} node as their partner at the time of the network's deployment is denoted as \mathbf{H} in Section 7.5.2.

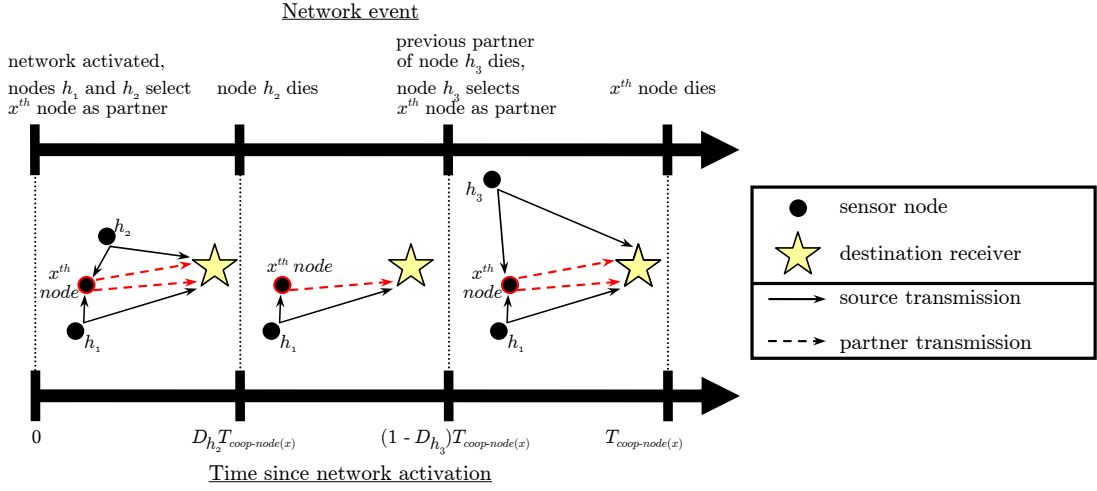


Figure 7.10: Example of a cooperative network event timeline illustrating (7.20): throughout its lifetime of $T_{coop_node(x)}$ transmission rounds, the x^{th} node consumes energy in acting as a cooperation partner for source nodes h_1 , h_2 , and h_3 . The x^{th} node serves as cooperation partner to node h_1 for the duration of its lifetime, whereas it serves as partner to nodes g_2 and g_3 for the proportion D_{h_2} and D_{h_3} of its lifetime, respectively.

the proportion of the x^{th} node's lifetime it receives messages from source node $g \in \mathbf{G}$, where $0 < A_g \leq 1$. It is interesting to note that if the x^{th} node depletes its energy before any of the G source nodes that it serves as destination receiver, then $A_g = 1$ for all $g \in \mathbf{G}$ and $\bar{E}_{coop_destination_node(x)} = E_{coop_destination_node(x)}$ as given by (7.11). It should also be noted that, should source node g opt for non-cooperative communication at the time of the network's deployment, its set of selected partner nodes \mathbf{F} is empty and the total energy per bit consumed by the x^{th} node in serving as the destination receiver to node g is instead given by $A_g \left(\frac{P_{CCT-rx}}{R_b} \right)$. Similarly, if source node g opts for non-cooperative transmission after its previous cooperation partner has depleted its energy, the energy per bit consumed by the x^{th} node in serving as the destination receiver to node g for the remainder of node g 's lifetime is given by $A_g \left(\frac{P_{CCT-rx}}{R_b} \right)$. Fig. 7.11 presents an example network event timeline illustrating the energy consumed by the x^{th} node throughout its lifetime in serving as a destination receiver in a cooperative Topology C network, as expressed by (7.21). The x^{th} node and its transmissions are marked in red in Fig. 7.11 to represent the circuit and transmission energy consumption associated with the x^{th} node in its role as a destination receiver node to the set of source nodes $\mathbf{G} = \{g_1, g_2, g_3\}$. It should be noted that, for the sake of continuity, the same example set of source nodes \mathbf{G} is shown in Figs. 7.11 and 7.7c and the partner nodes f_1 , f_2 , and f_3 shown in Fig. 7.7c are the same as those which are initially chosen by the source nodes in set \mathbf{G} in Fig. 7.11.

Finally, it should be noted that once a destination receiver node depletes its energy in a Topology C network, any surviving associated source nodes in the set \mathbf{G} are no longer

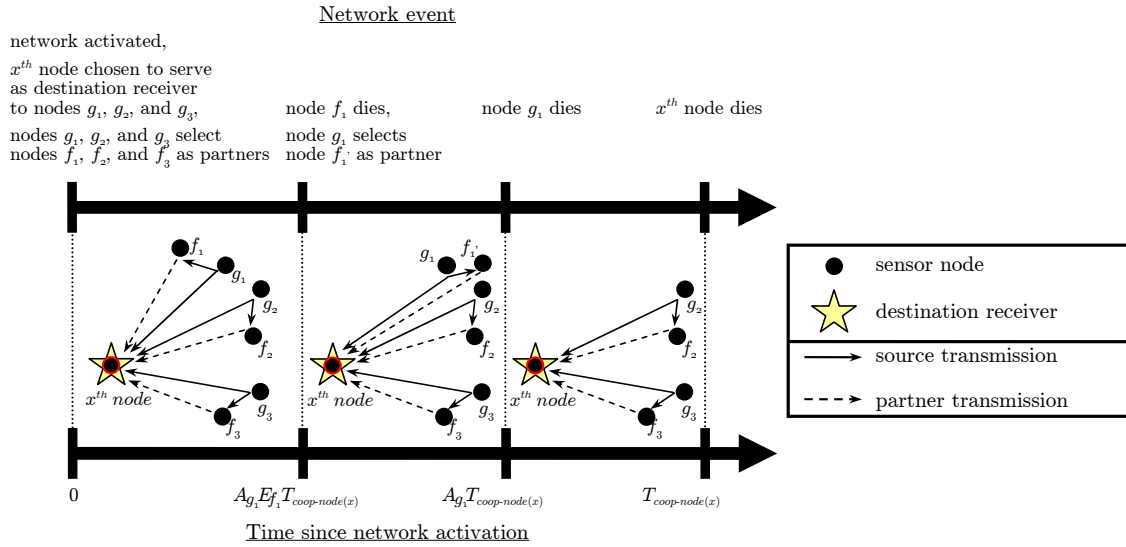


Figure 7.11: Example of a cooperative Topology C network event timeline illustrating (7.21): throughout its lifetime of $T_{coop_node(x)}$ transmission rounds, the x^{th} node consumes energy in acting as a destination receiver for the source nodes $g_1, g_2,$ and g_3 . The x^{th} node receives messages from nodes g_2 and g_3 for the duration of its lifetime, whereas it receives messages from node g_1 for the proportion A_{g_1} of its lifetime. The source nodes g_2 and g_3 cooperate throughout their lifetimes with partner nodes f_2 and f_3 respectively. The source node g_1 cooperates with partner node f_1 for the proportion E_{f_1} of its lifetime and with partner node f_1' for the remainder of its lifetime.

considered to be functional and thus their lifetimes are recorded as ending at the time of their destination receiver node depleting its energy¹⁹. However, these defunct source nodes do continue to serve as partners and destination receivers to other source nodes in the cooperative network until they actually deplete their own batteries. For example, once the x^{th} node depletes its energy in Fig. 7.11, the lifetimes of source nodes g_2 and g_3 would be recorded as being equal to $T_{coop_node(x)}$ and the associated partner nodes f_2 and f_3 would no longer serve the defunct source nodes g_2 and g_3 . Nodes g_2 and g_3 would thus be considered the $(x + 1)^{th}$ and $(x + 2)^{th}$ nodes to die since the network's activation, such that $T_{coop_node(x)} = T_{coop_node(x+1)} = T_{coop_node(x+2)}$. The nodes g_2 and g_3 would nevertheless continue to serve as partner and destination receiver to any of their own associated source nodes (not shown in Fig. 7.11) until the nodes g_2 and g_3 have actually depleted their own batteries.

¹⁹This assumption is implicit in the definition of E_f as the proportion of the lifetime of source node g that it is served by partner node $f \in \mathbf{F}$, such that $\sum_{f \in \mathbf{F}} E_f = 1$.

7.7 Summary

In this chapter the low-complexity distributed ECO-OP cooperation strategy for energy-constrained wireless sensor networks has been proposed, based on the simple yet near-optimal power allocation and partner choice heuristics for practical energy efficient aDF cooperation presented in Chapters 5 and 6. The ultimate aim of ECO-OP is to extend the operational lifetime of a wireless sensor network by coordinating network-wide cooperation among its sensor nodes. Importantly, ECO-OP has been specifically designed to be suitable for practical implementation on resource-constrained sensor nodes. Using ECO-OP individual source nodes independently make cooperation decisions to minimise the total energy consumed per bit over their own cooperative link, ignorant of the cooperation decisions of the other source nodes in the network. Moreover, each sensor node makes its cooperation decisions based solely on measurements of average path loss and is altruistic in the sense that it will unconditionally accept any requests to serve as cooperation partner for other source nodes in the network. Therefore, ECO-OP is a distributed and computationally efficient cooperation strategy with low signalling overhead.

However, the fact that ECO-OP is designed to simply maximise the energy efficiency of individual cooperative links in the network, without any regard to the resulting distribution of cooperation partner service, individual node energy consumption, or resulting node lifetimes over the network, means that ECO-OP is intended to achieve its overall aim of network lifetime extension *indirectly*. Consequently, the behaviour and performance of the proposed ECO-OP cooperation strategy will be thoroughly analysed in the investigations presented in Chapters 8-11, which have been outlined in this chapter. The node energy consumption and network lifetime definitions, wireless sensor network model, and simulation parameters employed in generating and analysing the simulation results of network-wide cooperative communication in Chapters 8-11 have also been presented in this chapter.

An investigation of the energy conservation performance of network-wide cooperation using ECO-OP will be presented in Chapters 8 and 9, serving to demonstrate that the distributed cooperation decisions made by individual nodes using ECO-OP constitute an effective energy saving technique for wireless sensor networks. An investigation of the lifetime extension performance of network-wide cooperation using ECO-OP will be presented in Chapters 10 and 11, whereby the proposed low-complexity distributed ECO-OP cooperation strategy will be extensively compared against a computationally intensive centralised greedy cooperation algorithm from the literature [18]. Importantly, the analysis in Chapters 10 and 11 will serve to demonstrate that altruistic distributed cooperation among autonomous resource-constrained sensor nodes using ECO-OP significantly extends the lifetime of the wireless sensor network as a whole.

Chapter 8

Illustration of Energy Conservation via Network-wide Cooperation

8.1 Introduction

In Chapter 7 a low-complexity distributed cooperation strategy for energy-constrained wireless sensor networks was presented. This strategy has been named ECO-OP and is based on the power allocation and partner choice heuristics for practical energy efficient aDF cooperation presented in Chapters 5 and 6. Individual source nodes independently make cooperation decisions to minimise the total energy consumed per message bit over their own cooperative link¹, ignorant of the cooperation decisions of the other source nodes in the network. Moreover, all nodes in the network are altruistic in the sense that a node will unconditionally accept any requests to serve as cooperation partner for other source nodes in the network. ECO-OP has thus been designed to maximise the energy efficiency of individual cooperative links, which does not automatically guarantee its effectiveness as a *network-wide* cooperation strategy. Namely, a cooperation strategy which overall conserves energy at the expense of overburdening individual partner nodes is unsustainable. Thus in order to properly evaluate the overall effectiveness of ECO-OP it is crucial to consider the resulting distribution of cooperation partner service over the network and the distribution of individual node energy consumption, as well as the reduction in the total network energy expenditure achieved.

In this chapter network-wide cooperation using ECO-OP is illustrated in the three representative network topologies (A, B, C) introduced in Section 7.4, by considering cooperation among $M=100$ nodes regularly placed over a 100 m by 100 m network area. The performance of ECO-OP with different partner choice rules is investigated, with the proposed partner choice heuristics GKH_1 , GKH_2 , and LKH being presented along-

¹An individual cooperative link consists of one source node communicating its message to the destination receiver by cooperating with its partner node.

side random partner choice for comparison. Firstly, the basic operation of ECO-OP is demonstrated via the $E_{saving_coop_total}$ achieved by each source node in the network for its transmission to the destination receiver. The average energy efficiency of individual cooperative links in the network is quantified by the average $E_{saving_coop_total}$ achieved over the M -node network, as given by (7.1). Secondly, the impact of network-wide cooperation is analysed by considering the distribution of cooperation partner service among the network's nodes, and the individual node energy consumption across the non-cooperative network versus the cooperative network ($E_{non-coop_node}$ vs. E_{coop_node} as given by (7.5) and (7.8) and respectively). Finally, the overall energy conservation performance of network-wide cooperation is quantified in terms of the total network energy reduction factor, as given by (7.4).

Network-wide cooperation using ECO-OP is thus illustrated for the Topology A (central destination receiver) network in Section 8.2, the Topology B (remote destination receiver) network in Section 8.3, and the Topology C (node-to-node communication) network in Section 8.4. The reference cooperative system parameters specified in Table 2.1 are employed throughout the analysis presented in this chapter. It is important to note that the analysis of ECO-OP presented in this chapter is concerned solely with the network-wide energy impact of the initial partner selection round at the time of the network's deployment, as specified in Fig. 7.1 (i.e. a static distribution of cooperation partner service). As specified in Chapter 7, it is assumed that each node in the network acts as a source and is eligible to be selected as a cooperation partner by any other source node in the network. For further details of the ECO-OP cooperation strategy, the simulation parameters and assumptions related to this investigation, and the node and network energy metrics employed in this chapter, please refer to Sections 7.2, 7.4, and 7.5 respectively. Finally, it should be noted that a regular node placement is considered in this chapter for ease of demonstration; the more general case of network-wide cooperation among randomly placed nodes will be thoroughly examined in Chapter 9.

8.2 Topology A Network: Central Destination Receiver

Fig. 8.1 presents the $E_{saving_coop_total}$ achieved by each source node in the Topology A network using ECO-OP cooperation with different partner choice rules. Fig. 8.1 shows that the majority of the $M=100$ source nodes in the network obtain a significant cooperative energy saving. Specifically, the average $E_{saving_coop_total}$ achieved over the M -node Topology A network is 85.1%, 85.0%, 80.2%, and 59.5% using GKH_1 , GKH_2 , LKH , and random partner choice, respectively, as shown by Table 8.1. Furthermore, Fig. 8.1 demonstrates that the further away the source node is from the central destination receiver, the higher the $E_{saving_coop_total}$ obtained; this is consistent with the results presented in Fig. 6.10

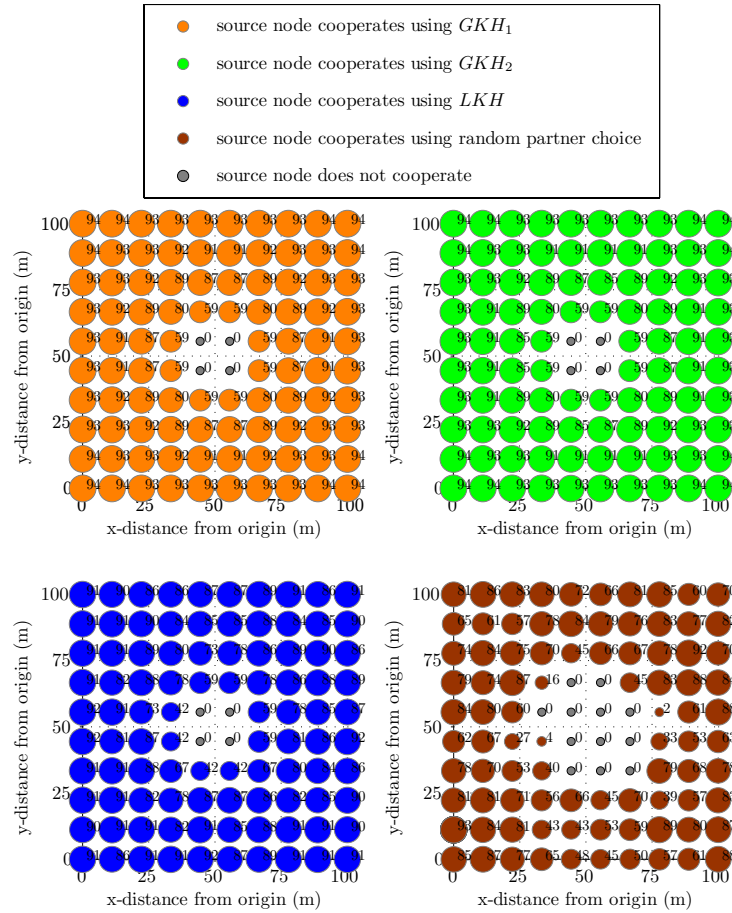


Figure 8.1: Total cooperative energy saving, $E_{saving_coop_total}$ (%), achieved by each source node in a Topology A network (central destination receiver) of $M=100$ nodes regularly placed over a 100 m by 100 m network area, using different partner choice rules. The size of each source node is proportional to its $E_{saving_coop_total}$ (each node is also marked with its $E_{saving_coop_total}$).

in Chapter 6 and the discussion in Section 4.4. Fig. 8.1 also shows that the four source nodes closest to the centre of the network opt for non-cooperative communication, regardless of partner choice rule. This is due to these four source nodes being too close to the destination receiver to benefit from cooperation (as discussed in Section 2.3.5, d_{s-d} must be above a break-even threshold transmission distance for energy efficient cooperation). In the case of random partner choice, eight other source nodes close to the centre of the network also do not cooperate, having randomly selected cooperation partners outside of their energy efficient partner choice region.

Fig. 8.2 presents the distribution of cooperation partner service in the Topology A network using different partner choice rules, in terms of the number of source nodes that each node in the network serves as cooperation partner to². Using GKH_1 and GKH_2 each source node selects the partner node closest to the midway point between itself and

²The number of source nodes that are served by some partner node j is denoted as H in Section 7.5.2, where \mathbf{H} is the set of source nodes using node j as their partner.

Table 8.1: Performance of network-wide cooperation in a Topology A network (central destination receiver) of $M=100$ nodes regularly placed over a 100 m by 100 m network area, using different partner choice rules.

Partner choice rule	Average $E_{saving_coop_total}$ (%) over M -node network	Network energy reduction factor
GKH_1	85.1	15.0
GKH_2	85.0	14.7
LKH	80.2	9.3
random partner choice	59.5	3.9

the destination receiver; thus only the nodes near the central destination receiver serve as cooperation partners for GKH_1 and GKH_2 , with up to 6 source nodes being served by a single partner node. Using LKH each source node selects its nearest neighbour as its cooperation partner; thus, unlike for GKH_1 and GKH_2 where the partner service burden is always concentrated in the centre of the Topology A network, for LKH the partner service is quite evenly distributed over the network, with the number of source nodes per partner ranging from 0 to 3 nodes³. Lastly, using random partner choice the partner service is also distributed over the network, with the number of nodes per partner ranging from 0 to 6.

Importantly, a comparison of Figs. 8.1 and 8.2 reveals that some nodes in the Topology A network in fact consume more energy in the cooperative network than they do in the non-cooperative network, because of the energy spent in serving as cooperation partners. Namely, Fig. 8.2 shows that the four nodes nearest the destination which do not use cooperation for their own transmissions to the destination (as shown by Fig. 8.1) nevertheless serve as cooperation partner to 3 to 5 other source nodes in the GKH_1 and GKH_2 cooperative networks. Similarly, several non-cooperating nodes in the LKH and random partner choice cooperative networks also serve as cooperation partners. It is important to consider whether these partner nodes consume significantly more energy in the cooperative network, since a cooperation strategy that overall conserves energy at the expense of overburdening individual partner nodes is unsustainable.

Therefore, in order to properly evaluate the true impact of network-wide cooperation it is necessary to consider the distribution of node energy consumption over the network. This is illustrated in Fig. 8.3, which shows the relative energy consumption of each individual node in the Topology A non-cooperative network and the cooperative networks

³In the case of a network with regular node placement (as considered in this chapter for ease of illustration), several candidate partner nodes will often be ranked 1st-equal after applying a given partner choice rule. For example, using LKH each source node must randomly select one of its (two to four) equidistant nearest neighbours as its cooperation partner. Therefore, the LKH partner service distribution results presented in Fig. 8.2 would exhibit more obvious symmetry (with roughly 1 source node for each partner node in the network) if they represented the average of several simulation runs of cooperation in the regularly deployed network, rather than a single simulation run as presented here.

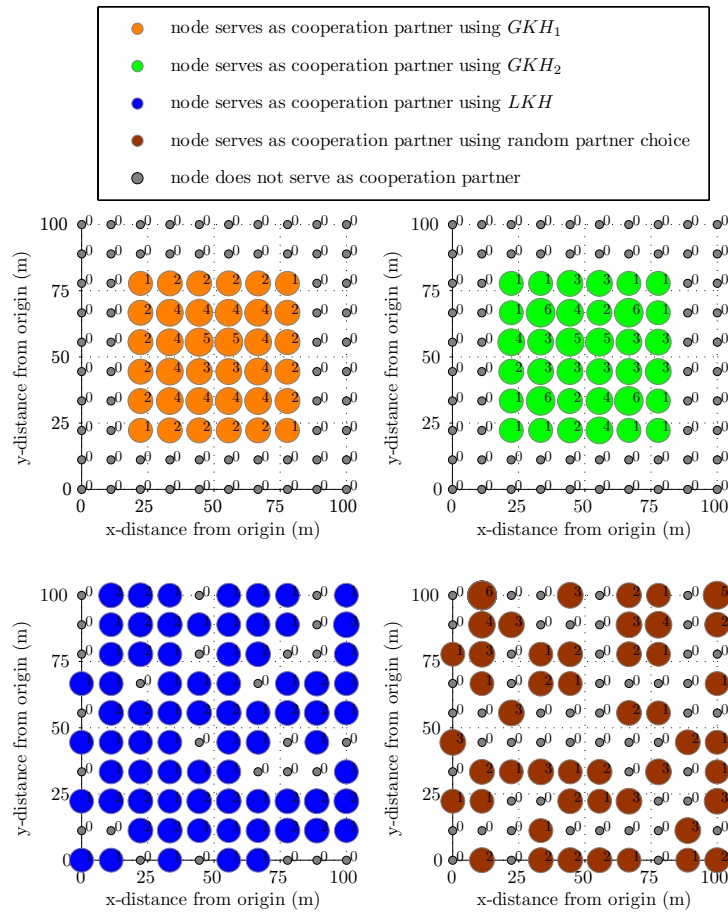


Figure 8.2: Distribution of cooperation partner service in a Topology A network (central destination receiver) of $M=100$ nodes regularly placed over a 100 m by 100 m network area, using different partner choice rules. The size of each node is proportional to the number of other source nodes it serves as cooperation partner to (each node is also marked with this number).

with different partner choice rules, $E_{non-coop_node}$ and E_{coop_node} respectively. The distribution of node energy consumption over each Topology A network is explicitly presented in the boxplot of Fig. 8.4, where the minimum, lower-quartile, median, upper-quartile, and maximum node energy consumption over the network are shown. Moreover, solely considering the average $E_{saving_coop_total}$ achieved over the network is an insufficient measure of the benefit of network-wide cooperation. Although this metric is very important for discerning the average quality of cooperation partner selected by the network's source nodes, it is only a relative measure of network-wide energy conservation as it gives equal weighting to the energy saving obtained by source nodes with low and high inherent communication energy requirements⁴. The actual overall energy conservation achieved by network-wide cooperation is quantified by the network energy reduction factor, given by (7.4), which is shown in Table 8.1 for the cooperative Topology A network.

Table 8.1 shows that cooperation using GKH_1 and GKH_2 in the Topology A network of Fig. 8.3 achieves a total network energy reduction factor of 15.0 and 14.7 respectively. Moreover, Fig. 8.4 shows that the maximum node energy consumption of the cooperative GKH_1 and GKH_2 Topology A network is less than the lower-quartile node energy consumption of the corresponding non-cooperative network. In other words, all of the nodes in the cooperative GKH_1 and GKH_2 Topology A network consume less energy than at least 75% of the nodes in the non-cooperative network. The energy conservation performance of GKH_1 and GKH_2 is thus very similar, with GKH_1 resulting in a slightly higher network energy reduction factor and a somewhat lower upper-quartile node energy consumption. This means that GKH_2 is the preferable cooperation strategy of the two for practical deployment in the Topology A network, since it achieves very similar energy conservation results as GKH_1 but entails a lower computational complexity.

Furthermore, Fig. 8.3 confirms that the four nodes nearest the centre of the network consume more energy in the cooperative GKH_1 and GKH_2 networks than the non-cooperative network (as reflected in the increased minimum node energy value for GKH_1 and GKH_2 compared to the non-cooperative network in Fig. 8.4). However, it is important to observe from Fig. 8.3 that in the cooperative GKH_1 and GKH_2 networks these four nodes nevertheless consume significantly less energy than the typical (median) node in the non-cooperative network. In fact, Fig. 8.4 shows that the minimum node energy expenditure in the cooperative GKH_1 and GKH_2 networks, although higher than the minimum $E_{non-coop_node}$, is significantly lower than the lower-quartile node energy expenditure in the non-cooperative network. Similarly, Fig. 8.3 shows that all of the partner nodes in the GKH_1 and GKH_2 cooperative networks consume significantly less energy than the typical node in the non-cooperative network, despite serving as partner

⁴The node with the highest "inherent" communication energy requirements is the node which consumes the most energy in the non-cooperative network, being located furthest from the destination receiver.

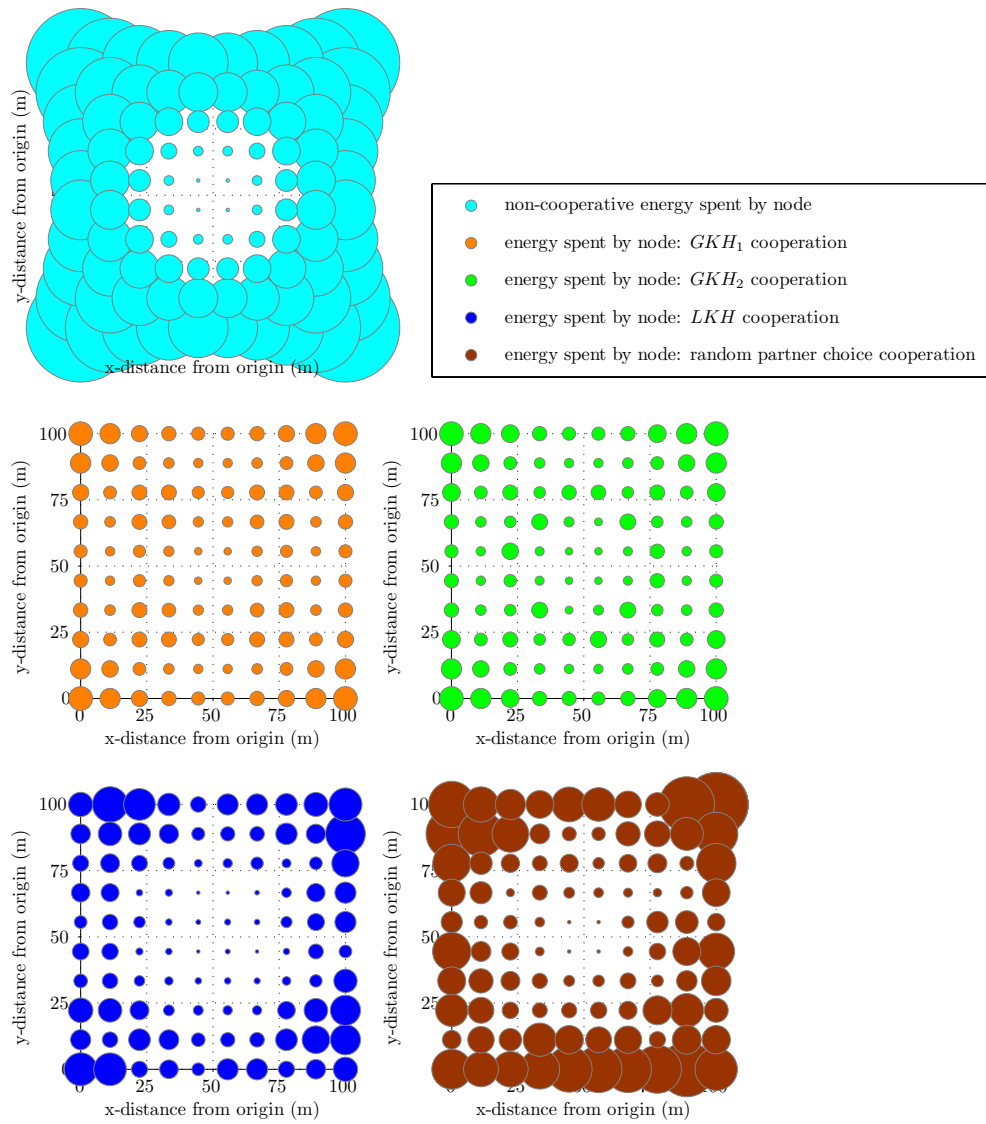


Figure 8.3: Node energy consumption in a Topology A network (central destination receiver) of $M=100$ nodes regularly placed over a 100 m by 100 m network area, for non-cooperative communication and cooperative communication with different partner choice rules. The size of each node is proportional to its energy consumption.

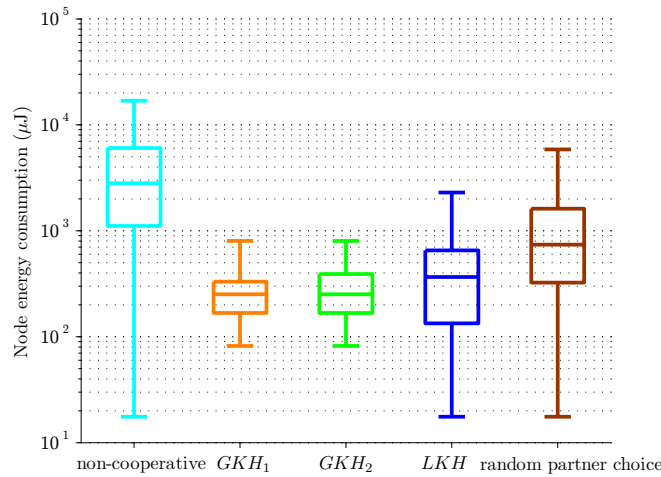


Figure 8.4: Boxplot showing the maximum, upper-quartile, median, lower-quartile, and minimum node energy consumption in a Topology A network (central destination receiver) of $M=100$ nodes regularly placed over a 100 m by 100 m network area, for non-cooperative communication and cooperative communication with different partner choice rules.

to up to 6 other nodes. Importantly, this indicates that the minority of nodes near the destination which serve as cooperation partners for the entire Topology A network are *not* overburdened by helping other nodes. As shown by Fig. 8.3, nodes closest to the central destination receiver consume the least energy in the non-cooperative Topology A network. Thus in the Topology A network the nodes chosen to serve as cooperation partners using GKH_1 and GKH_2 have relatively low inherent communication energy requirements and consequently can each afford to serve as cooperation partner to several other source nodes.

Thus by selecting these partner nodes to help source nodes with relatively high inherent energy requirements, cooperation using GKH_1 and GKH_2 leads to a more uniform distribution of energy consumption over the Topology A network, as can be observed from Fig. 8.3. This is confirmed by Fig. 8.4, which shows that the node energy distribution for the cooperative GKH_1 and GKH_2 networks has a significantly lower range than that of the non-cooperative network. Therefore, cooperation with GKH_1 and GKH_2 in the Topology A network not only reduces the overall network energy expenditure but also reallocates the total battery energy resource among nodes to produce a more even distribution of energy consumption over the network. Practically, this translates into both longer and more uniform predicted node lifetimes, such that the network will remain highly functional (with the majority of its nodes remaining operational) for a longer time.

Table 8.1 shows that cooperation using LKH in the Topology A network in Fig. 8.3 achieves a total network energy reduction factor of 9.3, which is 1.6 times less than that achieved by GKH_1 . Nonetheless, LKH achieves a very substantial network energy reduction which is 2.4 times higher than that obtained using random partner selection. Fig. 8.4 shows that the maximum node energy consumption of the cooperative LKH

Topology A network is slightly less than the median node energy consumption of the corresponding non-cooperative network. This can also be observed from Fig. 8.3 which shows that the highest node energy expenditure in the cooperative *LKH* Topology A network is roughly equal to the typical node energy consumption in the non-cooperative network. It is also interesting to note from Fig. 8.4 that the minimum node energy expenditure in the cooperative *LKH* network is equal to that of the non-cooperative network (unlike for *GKH₁* and *GKH₂*). However, Fig. 8.4 shows that the node energy distribution for the cooperative *LKH* network has a much higher range than that of the cooperative *GKH₁* and *GKH₂* networks. Thus, whereas cooperation using *GKH₁* and *GKH₂* significantly evens out the node energy consumption over the Topology A network, Fig. 8.3 reveals that *LKH* exhibits a similar distribution of node energy as the non-cooperative network. This is a consequence of neighbouring nodes with similar inherent communication energy requirements acting as each other's cooperation partners using *LKH*, maintaining the relative node energy consumption of the non-cooperative network.

Finally, Table 8.1 shows that cooperation using random partner choice in the Topology A network in Fig. 8.3 achieves a total network energy reduction factor of 3.9. Random partner choice results in the highest individual node energy consumption of the four cooperative networks, as shown by Figs. 8.3 and 8.4. Moreover, Fig. 8.4 shows that the median node energy consumption of the random partner choice cooperative Topology A network is only slightly lower than the maximum node energy consumption of the corresponding *GKH₁* and *GKH₂* cooperative network. Furthermore, Fig. 8.4 shows that the node energy distribution for the random partner choice cooperative network has the highest range of the four cooperative networks. This can also be observed from Fig. 8.3 which shows that random partner choice cooperation, like *LKH* and non-cooperative communication, exhibits an uneven distribution of node energy over the network.

8.3 Topology B Network: Remote Destination Receiver

Fig. 8.5 presents the $E_{saving_coop_total}$ achieved by each source node in the Topology B network using ECO-OP cooperation with different partner choice rules. Fig. 8.5 shows that all of the $M=100$ source nodes in the network obtain a significant cooperative energy saving. Specifically, the average $E_{saving_coop_total}$ achieved over the M -node Topology B network is 92.9%, 92.8%, 89.1%, and 86.0% using *GKH₁*, *GKH₂*, *LKH*, and random partner choice, respectively, as shown by Table 8.2. Every source node in the Topology B network has a large d_{s-d} , being located at least 100 m away from the remote destination receiver, which is located at (50 m, 200 m) with respect to the origin. This means that all nodes in the Topology B network are within each other's energy efficient partner

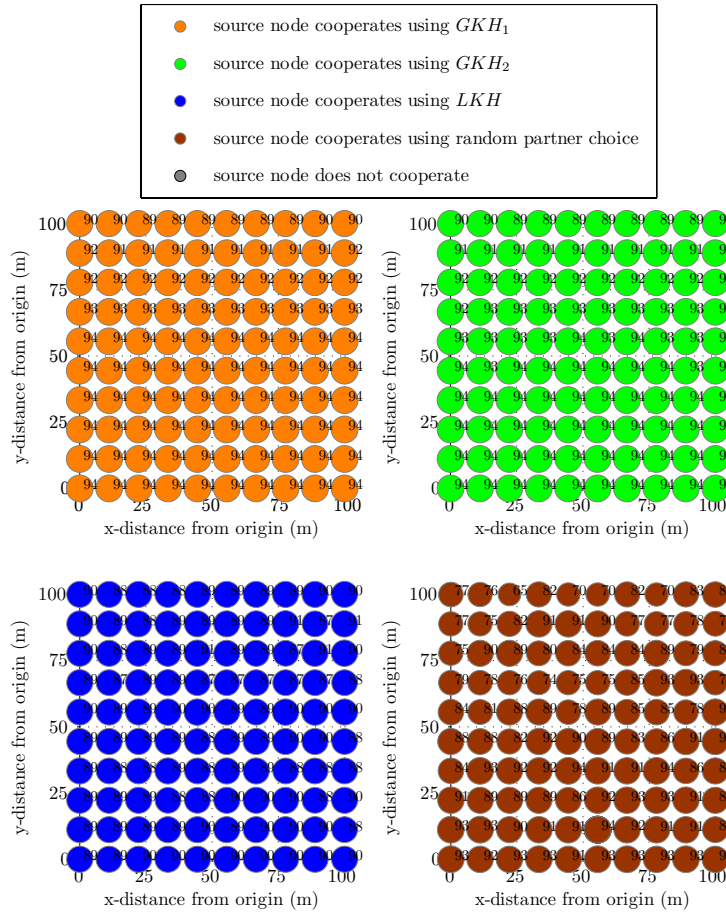


Figure 8.5: Total cooperative energy saving, $E_{saving_coop_total}$ (%), achieved by each source node in a Topology B network (remote destination receiver) of $M=100$ nodes regularly placed over a 100 m by 100 m network area, using different partner choice rules. The size of each source node is proportional to its $E_{saving_coop_total}$ (each node is also marked with its $E_{saving_coop_total}$).

choice region; this is clearly illustrated by considering the partner choice region for energy efficient aDF cooperation for $d_{s-d} = 100$ m in Fig. 4.12 with respect to the Topology B network boundary. Consequently, all source nodes in the Topology B network choose to cooperate and achieve large energy savings, regardless of partner choice rule. As for the Topology A network, the further away the source node is from the destination receiver the higher the $E_{saving_coop_total}$ achieved.

Fig. 8.6 presents the distribution of cooperation partner service in the Topology B network using different partner choice rules, in terms of the number of source nodes that each node in the network serves as cooperation partner to. Using GKH_1 and GKH_2 each source node selects the partner node closest to the midway point between itself and the destination receiver. The destination receiver is located 100 m away from the top boundary of the 100 m by 100 m Topology B network. Consequently, only the five nodes nearest the remote destination receiver serve as cooperation partners in the GKH_1 and GKH_2 Topology B network. The partner service burden for the entire network is thus

Table 8.2: Performance of network-wide cooperation in a Topology B network (remote destination receiver) of $M=100$ nodes regularly placed over a 100 m by 100 m network area, using different partner choice rules.

Partner choice rule	Average $E_{saving_coop_total}$ (%) over M -node network	Network energy reduction factor
GKH_1	92.9	15.8
GKH_2	92.8	15.5
LKH	89.1	9.3
random partner choice	86.0	9.1

heavily concentrated on only a handful of partner nodes, with up to 20 and 52 source nodes being served by a single partner node using GKH_1 and GKH_2 respectively. Moreover, the two nodes nearest the centre of the top boundary of the Topology B network together serve as partner to 40 and 94 source nodes using GKH_1 and GKH_2 respectively. This heavy bias towards a handful of partner nodes nearest the destination may be detrimental to the network's long-term wellbeing if any partner nodes are overburdened. Using LKH each source node selects its nearest neighbour as its cooperation partner; thus unlike for GKH_1 and GKH_2 , where the partner service burden is always concentrated in the very top of the Topology B network, for LKH the partner service is quite evenly distributed over the network, with the number of source nodes per partner ranging from 0 to 3. Finally, using random partner choice the partner service is also distributed over the network, with the number of nodes per partner ranging from 0 to 5.

The distribution of node energy consumption over the Topology B network is illustrated in Fig. 8.7, which shows the relative energy consumption of each individual node in the non-cooperative network and the cooperative networks with different partner choice rules, $E_{non-coop_node}$ and E_{coop_node} respectively⁵. The distribution of node energy consumption over each Topology B network is explicitly presented in the boxplot of Fig. 8.8, where the minimum, lower-quartile, median, upper-quartile, and maximum node energy consumption over the network are shown.

Table 8.2 shows that cooperation using GKH_1 and GKH_2 in the Topology B network in Fig. 8.7 achieves a total network energy reduction factor of 15.8 and 15.5 respectively. Moreover, Fig. 8.8 shows that the upper-quartile node energy consumption of the cooperative GKH_1 and GKH_2 Topology B network is less than the minimum node energy consumption of the corresponding non-cooperative network. In other words, at least 75% of the nodes in the cooperative GKH_1 and GKH_2 Topology B network consume less energy than the lowest energy consumed by any individual node in the non-cooperative

⁵It should be noted that different scaling factors are employed in Figs. 8.3, 8.7, and 8.11 to represent the relative node energy consumption over the Topology A, B, and C networks. Each network topology is associated with a different absolute node energy consumption range, and thus the relative node energy values illustrated in these three figures cannot be explicitly compared.

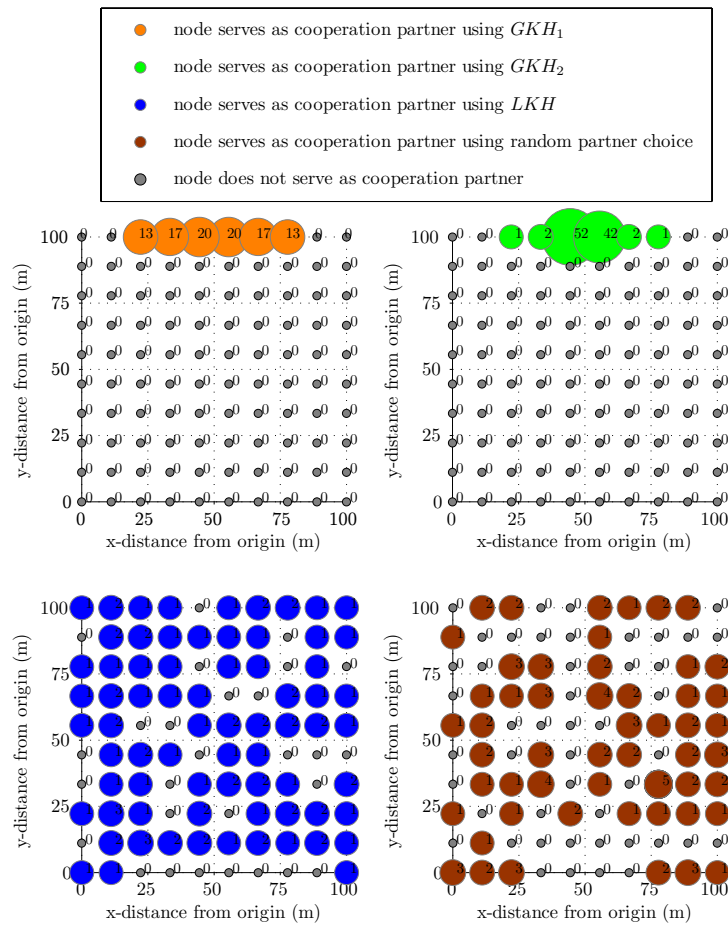


Figure 8.6: Distribution of cooperation partner service in a Topology B network (remote destination receiver) of $M=100$ nodes regularly placed over a 100 m by 100 m network area, using different partner choice rules. The size of each node is proportional to the number of other source nodes it serves as cooperation partner to (each node is also marked with this number).

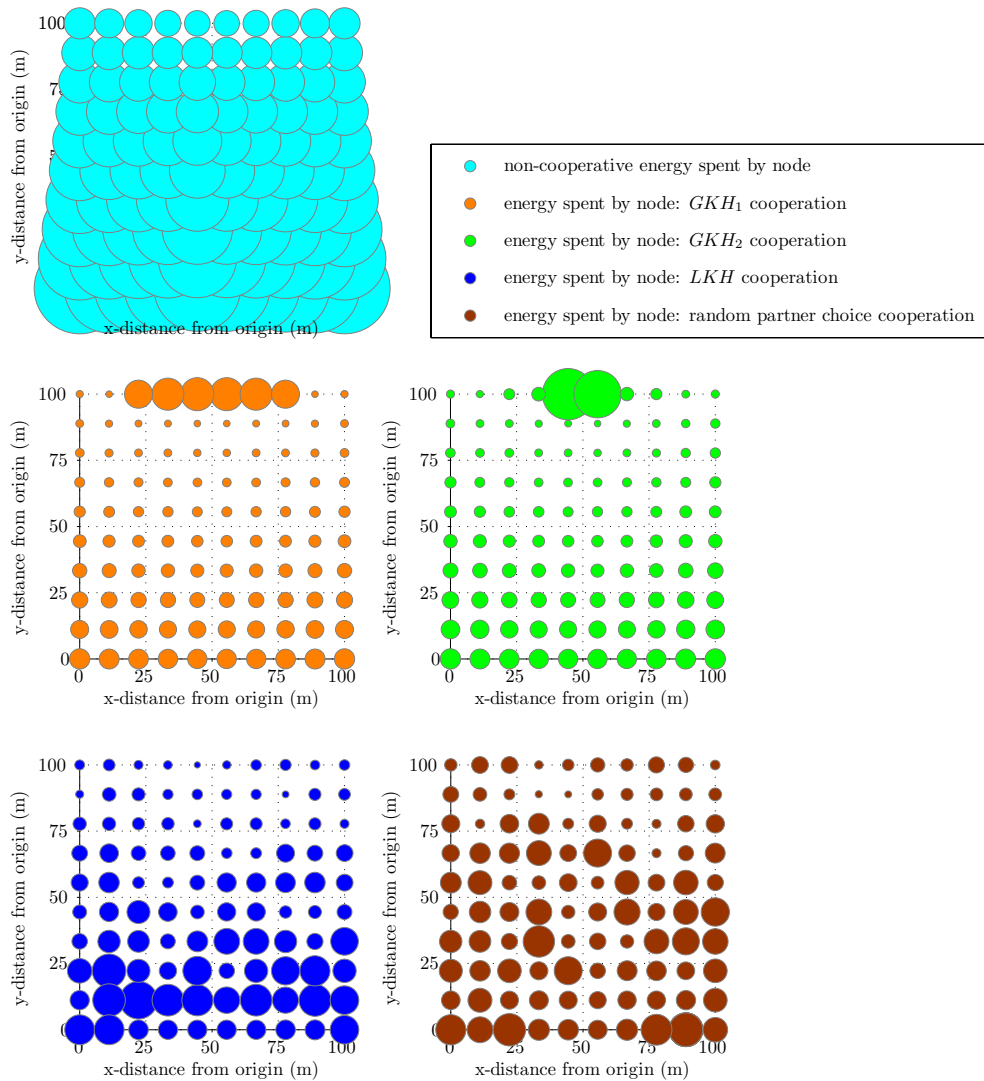


Figure 8.7: Node energy consumption in a Topology B network (remote destination receiver) of $M=100$ nodes regularly placed over a 100 m by 100 m network area, for non-cooperative communication and cooperative communication with different partner choice rules. The size of each node is proportional to its energy consumption.

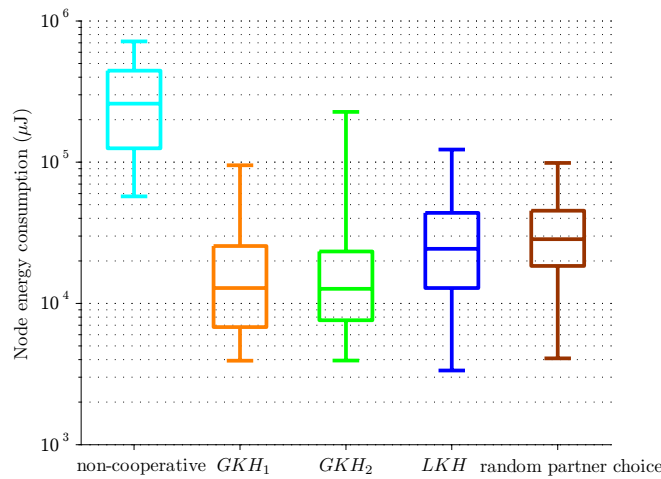


Figure 8.8: Boxplot showing the maximum, upper-quartile, median, lower-quartile, and minimum node energy consumption in a Topology B network (remote destination receiver) of $M=100$ nodes regularly placed over a 100 m by 100 m network area, for non-cooperative communication and cooperative communication with different partner choice rules.

network. The maximum node energy consumption of the cooperative GKH_1 and GKH_2 Topology B network is less than the lower-quartile and median node energy consumption of the corresponding non-cooperative network, respectively.

However, Fig. 8.8 also shows that in the GKH_1 and GKH_2 networks the maximum node energy consumption is significantly higher than the upper-quartile node energy consumption. This skewed node energy distribution is clearly illustrated in Fig. 8.7: the nodes with the highest energy consumption in the GKH_1 network are the five nodes shown to be serving as cooperation partners in Fig. 8.6, whereas the highest energy nodes by far in the GKH_2 network are the two partner nodes shown to be serving 42 and 52 source nodes each in Fig. 8.6. Importantly, this indicates that the several nodes which serve as cooperation partners for the entire Topology B network are *in a sense* overburdened by helping other nodes; even though the maximum node energy expenditure of the GKH_1 and GKH_2 network is less than the typical non-cooperative node energy consumption, popular partner nodes in the GKH_1 and GKH_2 Topology B network consume significantly more energy than the rest of the network's nodes. This indicates that GKH_1 and GKH_2 may be unsustainable partner choice strategies for the cooperative Topology B network, with popular partner nodes prematurely depleting their own energy supply in helping other nodes. Lastly, Fig. 8.8 demonstrates that the maximum GKH_2 node energy consumption is more than double the maximum GKH_1 node energy consumption, which suggests that GKH_2 may be a particularly unsustainable long-term cooperation strategy for the Topology B network. The energy conservation performance of GKH_2 in the Topology B network is thus overall inferior to that of GKH_1 , resulting in a substantially

more uneven node energy distribution as well as a slightly lower network energy reduction factor.

Table 8.2 shows that cooperation using *LKH* in the Topology B network of Fig. 8.7 achieves a total network energy reduction factor of 9.3. Although this is a substantial network energy reduction, it is 1.7 times less than that achieved by *GKH₁* and only 1.02 times higher than that obtained using random partner selection. Fig. 8.8 shows that the maximum node energy consumption of the cooperative *LKH* Topology B network is slightly less than the lower-quartile node energy consumption of the corresponding non-cooperative network. This can also be observed from Fig. 8.7 which shows that the highest node energy expenditure in the cooperative *LKH* Topology B network is less than the typical node energy consumption in the non-cooperative network. Furthermore, Fig. 8.8 shows that the range of the node energy distribution for the *LKH* network is smaller than that of the *GKH₂* network but higher than that of the *GKH₁* network. Fig. 8.8 also shows that the majority of nodes in the *LKH* network consume more energy than those in the *GKH₁* and *GKH₂* network. It is interesting to note that this is chiefly due to the energy consumed by nodes serving as partners to neighbouring nodes in the *LKH* network and *not* due to source nodes selecting significantly suboptimal cooperation partners using *LKH*, as evidenced by a comparison of Fig. 8.7 with Figs. 8.5 and 8.6.

Lastly, Table 8.2 shows that cooperation using random partner choice in the Topology B network in Fig. 8.7 achieves a total network energy reduction factor of 9.1. Random partner choice results in a lower maximum node energy consumption than *LKH* and *GKH₂* as shown by Fig. 8.8. Moreover, Fig. 8.8 shows that the median node energy consumption of the random partner choice cooperative Topology B network is only slightly higher than the median node energy consumption of the corresponding *LKH* cooperative network. Fig. 8.8 also shows that the range of the node energy distribution for the random partner choice cooperative network is smaller than that of the *LKH* network. It is interesting to note from Fig. 8.7 that for nodes near the bottom of the Topology B network with inherently high communication energy requirements, random partner choice results in lower node energy consumption than *LKH*. As shown in Fig. 8.6, these nodes are not randomly selected as cooperation partners and thus do not consume energy in serving as partners to neighbouring nodes with similarly high inherent energy requirements as in the *LKH* network. Additionally, whereas these nodes themselves necessarily select neighbouring partner nodes using *LKH*, they randomly select better partner nodes closer to the optimal partner location (midway between the source and the destination receiver). As a result, these nodes also consume less energy as the source in the random partner choice network than in the *LKH* network.

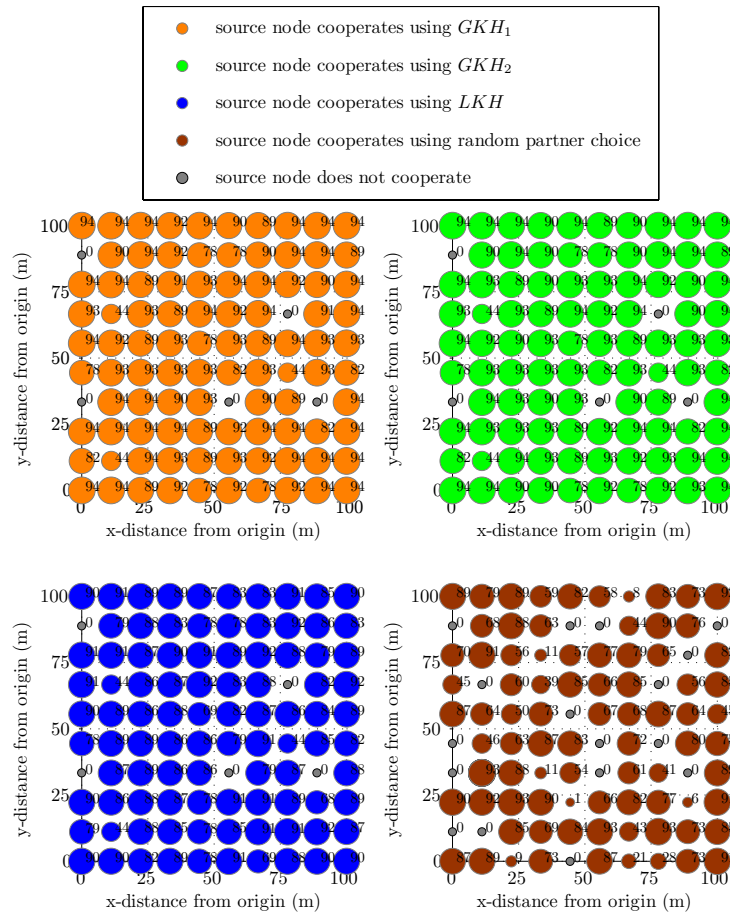


Figure 8.9: Total cooperative energy saving, $E_{saving_coop_total}$ (%), achieved by each source node in a Topology C network (node-to-node communication) of $M=100$ nodes regularly placed over a 100 m by 100 m network area, using different partner choice rules. The size of each source node is proportional to its $E_{saving_coop_total}$ (each node is also marked with its $E_{saving_coop_total}$).

8.4 Topology C Network: Node-to-Node Communication

Fig. 8.9 presents the $E_{saving_coop_total}$ achieved by each source node in the Topology C network using ECO-OP cooperation with different partner choice rules. Fig. 8.9 shows that the majority of the $M=100$ source nodes in the network obtain a significant cooperative energy saving. Specifically, the average $E_{saving_coop_total}$ achieved over the M -node Topology C network is 85.1%, 85.0%, 80.5%, and 56.7% using GKH_1 , GKH_2 , LKH , and random partner choice, respectively, as shown by Table 8.3. Fig. 8.9 also shows that five source nodes in the Topology C network opt for non-cooperative communication regardless of partner choice rule, being too close to their destination receiver node to benefit from cooperation. In the case of random partner choice, twelve other source nodes also do not cooperate, having randomly selected cooperation partners outside of their energy efficient partner choice region.

Table 8.3: Performance of network-wide cooperation in a Topology C network (node-to-node communication) of $M=100$ nodes regularly placed over a 100 m by 100 m network area, using different partner choice rules.

Partner choice rule	Average $E_{saving_coop_total}$ (%) over M -node network	Network energy reduction factor
GKH_1	85.1	15.7
GKH_2	85.0	15.5
LKH	80.5	9.1
random partner choice	56.7	6.3

Fig. 8.10 presents the distribution of cooperation partner service in the Topology C network using different partner choice rules, in terms of the number of source nodes that each node in the network serves as cooperation partner to. Using GKH_1 and GKH_2 each source node selects the partner node closest to the midway point between itself and the destination receiver; thus the nodes located around the perimeter of the Topology C network are unlikely to serve as cooperation partners. Over half of the nodes in the network serve as cooperation partners, with up to 5 and 4 source nodes being served by a single partner node using GKH_1 and GKH_2 respectively. Therefore, the GKH_1 and GKH_2 partner service is more evenly distributed in the random data flow Topology C network compared with that of the directed data flow Topology A and B networks. Using LKH each source node selects its nearest neighbour as its cooperation partner; thus the LKH partner service is still more evenly distributed over the network than GKH_1 and GKH_2 , with the number of source nodes per partner ranging from 0 to 3. Lastly, using random partner choice the partner service is also distributed over the network, with the number of nodes per partner ranging from 0 to 3.

The distribution of node energy consumption over the Topology C network is illustrated in Fig. 8.11, which shows the relative energy consumption of each individual node in the non-cooperative network and the cooperative networks with different partner choice rules, $E_{non-coop_node}$ and E_{coop_node} respectively. The distribution of node energy consumption over each Topology C network is explicitly presented in the boxplot of Fig. 8.12, where the minimum, lower-quartile, median, upper-quartile, and maximum node energy consumption over the network are shown.

Fig. 8.11 shows that in the non-cooperative Topology C network nodes at the corners of the network generally consume more energy than nodes near the centre of the network. This means that a weak positive correlation exists between a given node's distance from the centre of the network and its inherent communication energy requirements, despite the fact that destination receiver nodes are allocated randomly to each source node. This seeming contradiction may be explained by considering that the maximum possible source-destination separation in the Topology C network is the distance between two nodes

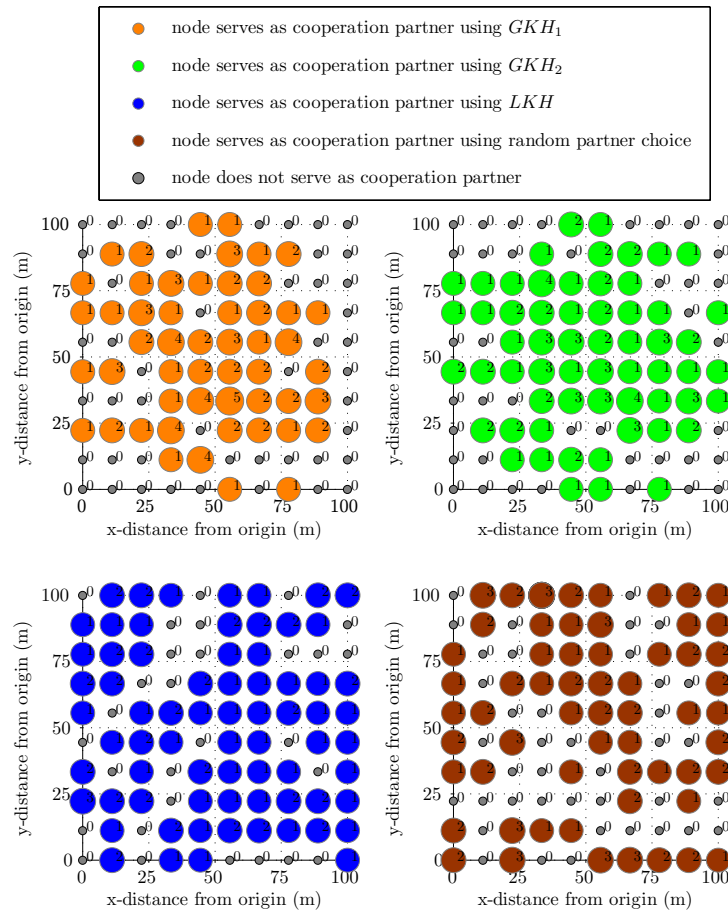


Figure 8.10: Distribution of cooperation partner service in a Topology C network (node-to-node communication) of $M=100$ nodes regularly placed over a 100 m by 100 m network area, using different partner choice rules. The size of each node is proportional to the number of other source nodes it serves as cooperation partner to (each node is also marked with this number).

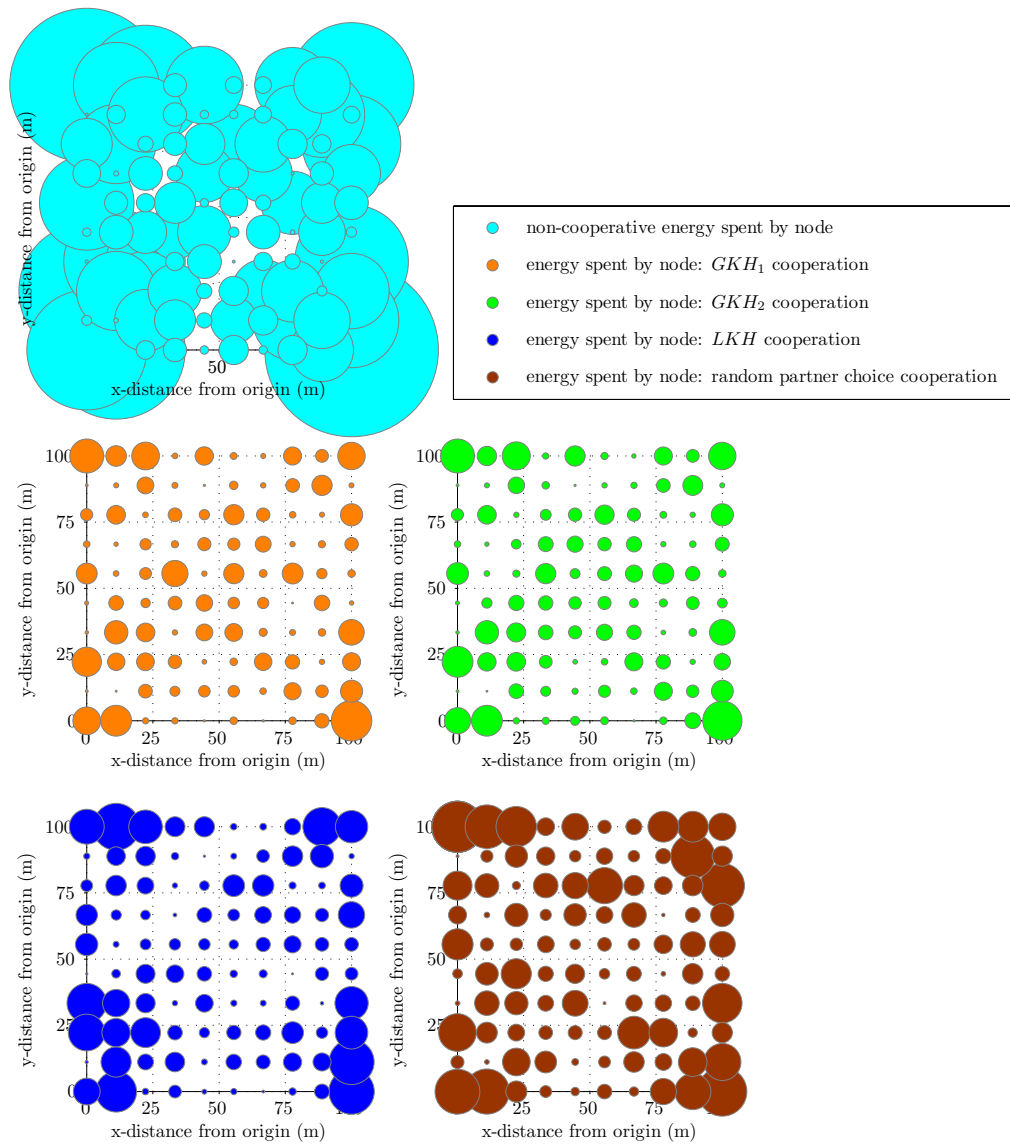


Figure 8.11: Node energy consumption in a Topology C network (node-to-node communication) of $M=100$ nodes regularly placed over a 100 m by 100 m network area, for non-cooperative communication and cooperative communication with different partner choice rules. The size of each node is proportional to its energy consumption.

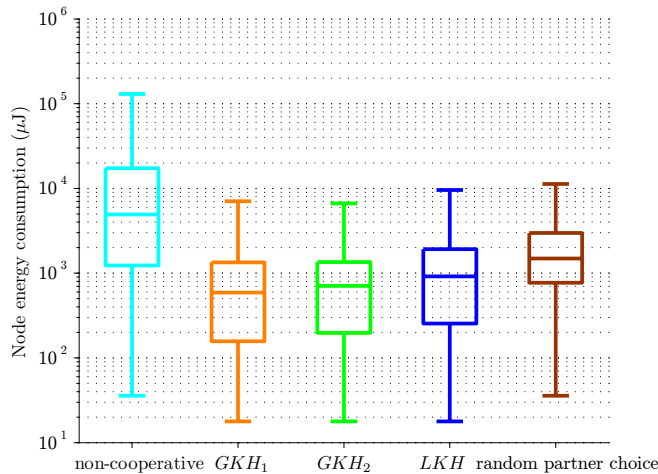


Figure 8.12: Boxplot showing the maximum, upper-quartile, median, lower-quartile, and minimum node energy consumption in a Topology C network (node-to-node communication) of $M=100$ nodes regularly placed over a 100 m by 100 m network area, for non-cooperative communication and cooperative communication with different partner choice rules.

located at opposite corners of the network. It follows that the distance from a randomly selected destination receiver node to a source node located at a corner of the network will be on average greater than the distance to a source node located in the centre of the network. Furthermore, it is interesting to note by comparing Figs. 8.10 and 8.11 that the nodes with the highest inherent communication energy requirements at the corners of the Topology C network are generally not selected to serve as cooperation partners using GKH_1 and GKH_2 , as in the Topology A network. Therefore, a negative correlation also exists between a node's inherent communication energy requirements and its popularity as a cooperation partner using GKH_1 and GKH_2 in the Topology C network, albeit a much weaker one than that exhibited in the Topology A network. Similarly, this means that nodes in the LKH network are likely to serve as partner to neighbouring nodes with roughly similar inherent communication requirements, despite not having a common destination receiver.

Table 8.3 shows that cooperation using GKH_1 and GKH_2 in the Topology C network in Fig. 8.11 achieves a total network energy reduction factor of 15.7 and 15.5 respectively. Cooperation using LKH in the Topology C network in Fig. 8.11 achieves a total network energy reduction factor of 9.1, which is 1.7 times less than that achieved by GKH_1 . Nonetheless, LKH achieves a very substantial network energy reduction which is 1.4 times higher than the factor 6.3 reduction obtained using random partner selection. Moreover, Fig. 8.12 shows that the maximum node energy consumption of the cooperative Topology C network is less than the upper-quartile node energy consumption of the corresponding non-cooperative network, regardless of partner choice rule. In other words, all of the nodes in the cooperative Topology C network consume less energy than at least 25% of

the nodes in the corresponding non-cooperative network. Importantly, Fig. 8.12 shows that the minimum, lower-quartile, median, upper-quartile, and maximum node energy consumption are all significantly reduced by cooperation, regardless of partner choice rule. This demonstrates that network-wide cooperation using ECO-OP consistently benefits the Topology C network as a whole.

This also indicates that partner nodes in the GKH_1 and GKH_2 Topology C network are not overburdened by helping several other nodes. This is because the nodes that are selected as cooperation partners are typically those which can most afford to serve as cooperation partners, having low inherent communication energy requirements, as discussed above. For example, Fig. 8.10 shows that the node located at (55.6m, 33.3m) from the origin, which does not use cooperation for its own transmissions to the destination as shown by Fig. 8.9, serves as cooperation partner to 5 other source nodes in the GKH_1 cooperative network. This node thus consumes more energy in the cooperative Topology C network than it does in the non-cooperative network. Nonetheless, Fig. 8.11 shows that this popular partner node in the GKH_1 cooperative network still consumes significantly less energy than the typical node in the non-cooperative network. Overall, the energy conservation performance of GKH_1 and GKH_2 is very similar, with GKH_1 resulting in a marginally lower median and lower-quartile node energy consumption and a slightly higher network energy reduction factor. Therefore, GKH_2 is the preferable practical cooperation strategy for the Topology C network, yielding very similar energy conservation results to GKH_1 at a lower computational cost.

Moreover, Fig. 8.12 shows that the node energy distributions of the four cooperative Topology C networks each have a significantly lower range than that of the non-cooperative network. This is also readily observed from Fig. 8.11 which demonstrates there is a much smaller variation in node energy consumption over the cooperative networks compared with the non-cooperative network. Therefore, energy-conserving cooperation in the Topology C network also reallocates the total battery energy resource among nodes to produce a more uniform distribution of energy consumption over the network. It is also interesting to note from Fig. 8.12 that the four cooperative Topology C networks exhibit similar node energy distributions, with those of random partner choice and LKH having an only slightly higher range than those of GKH_1 and GKH_2 . By contrast, in the Topology A network GKH_1 and GKH_2 result in a significantly more even node energy distribution than LKH and random partner choice, as discussed in Section 8.2. This is because there is a much stronger correlation between a node's inherent communication energy requirements and how likely it is to be selected as cooperation partner in the Topology A network than in the Topology C network, as discussed above.

8.5 Summary

In this chapter network-wide cooperation using the ECO-OP cooperation strategy proposed in Chapter 7 has been illustrated in three representative network topologies (A, B, C) by considering cooperation among 100 nodes regularly placed over a 100 m by 100 m network area. The performance and impact of network-wide cooperation has been investigated in terms of the reduction in the total network energy expenditure, the distribution of cooperation partner service among the network's nodes, and the distribution of the individual node energy consumption across the cooperative versus the non-cooperative network. The analysis in this chapter has thus afforded an opportunity to examine and compare the fundamental behaviour of ECO-OP with different partner choice rules (GKH_1 , GKH_2 , LKH , and random partner choice) in different basic network topologies.

The results presented in this chapter have demonstrated that network-wide cooperation using ECO-OP always significantly reduces the overall energy consumption of the regular network under consideration for all three network topologies. Regardless of network topology, GKH_1 and GKH_2 achieve the highest cooperative network energy reduction, of factor 15.5 and 15.2 on average, respectively. Cooperation using the suboptimal local knowledge heuristic LKH still results in a substantial network energy reduction factor of 9.2 on average. For comparison, the network energy reduction factor obtained using random partner choice ranges from 3.9 to 9.1.

It has been illustrated that partner service is inherently evenly distributed over the cooperative LKH network, regardless of network topology. By contrast, using GKH_1 and GKH_2 partner service is significantly less evenly distributed over the network, with the entire burden of partner service falling on an increasingly smaller number of popular partner nodes the more directed the network's data flow is. Namely, data flow in the remote destination receiver Topology B network is highly directed and consequently the partner service is heavily concentrated on a handful of nodes at the very top of the network. Specifically, in the 100 node Topology B network a single partner node serves up to 20 and 52 source nodes using GKH_1 and GKH_2 respectively. In the central destination receiver Topology A network with moderately directed data flow, the partner service burden using GKH_1 and GKH_2 is carried by a minority of nodes near the centre of the network, whereas it is carried by over half of the network's nodes in the node-to-node communication Topology C network with random data flow.

Importantly, it has been demonstrated that popular partner nodes in the GKH_1 and GKH_2 Topology A and C networks are not overburdened despite helping several other nodes. This is because the nodes which are selected to serve as cooperation partners are typically those which can most afford to, having low inherent communication energy requirements. Moreover, it has been shown that cooperation using GKH_1 and GKH_2

also reallocates the total battery energy resource among nodes to produce a more even distribution of energy consumption over the Topology A and C network. This is a result of selecting partner nodes with relatively low inherent communication energy requirements to help source nodes with relatively high inherent energy requirements. This is practically advantageous, as it translates into both longer and more uniform predicted node lifetimes.

However, it has also been shown that the most popular partner nodes in the GKH_1 and GKH_2 Topology B networks are in a sense overburdened; although their energy expenditure is less than the typical non-cooperative node energy consumption, it is considerably higher than that of the other nodes in the cooperative network. This suggests that GKH_1 and GKH_2 may be unsustainable partner choice strategies for the cooperative Topology B network, with popular partner nodes prematurely depleting their own energy supply in helping other nodes. By contrast, partner nodes are never overburdened in the LKH cooperative network, regardless of network topology, due to an inherently distributed partner service burden. Moreover, neighbouring nodes with similar inherent communication energy requirements act as each other's cooperation partners using LKH , thus essentially maintaining the relative node energy consumption of the non-cooperative network.

Having examined and illustrated the fundamental behaviour of ECO-OP in this chapter, the typical energy conservation performance of ECO-OP is evaluated in Chapter 9. Specifically, by considering the general case of randomly deployed networks of various node density, the analysis in Chapter 9 serves to establish the general validity of network-wide cooperation using ECO-OP as an effective energy saving technique for wireless sensor networks.

Chapter 9

Energy Conservation Performance of Network-wide Cooperation

9.1 Introduction

In Chapter 8 the fundamental behaviour of ECO-OP, the low-complexity distributed cooperation strategy presented in Chapter 7, was illustrated by considering cooperation among $M=100$ regularly placed nodes. In this chapter the typical energy conservation performance of network-wide cooperation using ECO-OP is evaluated for the general case of randomly deployed networks of various node density. Specifically, a range of node density values is investigated by simulating cooperation among $M=\{2, 3, 4, 5, 6, 10, 30, 100, 300, 1000\}$ nodes¹ randomly placed with a uniform distribution over a 100 m by 100 m network area. As in Chapter 8, the performance of ECO-OP with different partner choice rules (GKH_1 , GKH_2 , LKH , and random partner choice) is investigated for the three representative network topologies (A, B, and C) introduced in Section 7.4. The performance of ECO-OP is thus thoroughly examined for both sparse and dense networks with both directed and random data flow, serving to establish the general validity of network-wide cooperation using ECO-OP as an effective energy saving technique for wireless sensor networks.

Firstly, the basic operation of ECO-OP as M is varied is presented in terms of the average $E_{saving_coop_total}$ achieved over the M -node network, as given by (7.1). Secondly, the energy conservation performance of network-wide cooperation using ECO-OP is quantified in terms of the total network energy reduction factor, as given by (7.4). Finally, in order to gain some basic insight into the general long-term viability of ECO-OP, the distribution of node energy consumption across the cooperative versus the non-cooperative network is examined as M is varied, which is analogous to the boxplots presented in Chapter 8.

¹The minimum number of nodes considered for a Topology C network is $M=3$, since a node cannot simultaneously serve as another node's destination receiver and cooperation partner.

In order to represent the typical behaviour of ECO-OP, the results presented throughout this chapter are given by the median of $Q = \left(\frac{10^5}{M}\right)$ simulation runs. The results for the central destination receiver Topology A network are presented in Section 9.2, the remote destination receiver Topology B network in Section 9.3, and the node-to-node communication Topology C network in Section 9.4. In Section 9.5 the overall energy conservation performance of ECO-OP with different partner choice rules is compared, based on the results presented in the preceding sections. This leads to a recommendation of the best cooperation strategy to employ for a given set of network conditions, as well as the best overall cooperation strategy for a general energy-constrained wireless sensor network.

The reference cooperative system parameters specified in Table 2.1 are assumed throughout the analysis presented in this chapter. It is important to note that, as in Chapter 8, the analysis presented in this chapter is concerned solely with the network-wide energy impact of the initial partner selection round of ECO-OP at the time of the network's deployment, as specified in Fig. 7.1. As specified in Chapter 7, it is assumed that each node in the network acts as a source and is eligible to be selected as a cooperation partner by any other source node in the network. For further details of the ECO-OP cooperation strategy, the simulation parameters and assumptions related to this investigation, and the node and network energy metrics employed in this chapter, please refer to Sections 7.2, 7.4, and 7.5 respectively.

9.2 Topology A Network: Central Destination Receiver

Fig. 9.1 shows the average $E_{saving_coop_total}$ achieved over the Topology A network as the number of nodes in the network M is varied, using ECO-OP cooperation with different partner choice rules. The average $E_{saving_coop_total}$ achieved over the network ranges from 57.3% for a very sparse network to 83.0%, 82.9%, and 78.3% for a dense network using GKH_1 , GKH_2 , and LKH , respectively. The average $E_{saving_coop_total}$ achieved over the network using GKH_1 , GKH_2 , and LKH increases with increasing node density. This is due to the larger candidate partner set associated with a more dense network, which means that good cooperation partners are more likely to exist in the network. This trend is consistent with that previously illustrated in Fig. 6.5 for the case of a single source node selecting its cooperation partner from an increasingly large candidate partner set. For very sparse networks ($M < 6$) the average $E_{saving_coop_total}$ achieved over the network using random partner choice cooperation increases (from 57.3% to 60.2%) with increasing node density. This is because the likelihood of the majority of the network's nodes randomly selecting unsatisfactory cooperation partners (thus opting for non-cooperative communication, with $E_{saving_coop_total}=0\%$) is higher the fewer nodes there are in the network. However, for increasingly dense networks ($M > 6$) the average $E_{saving_coop_total}$

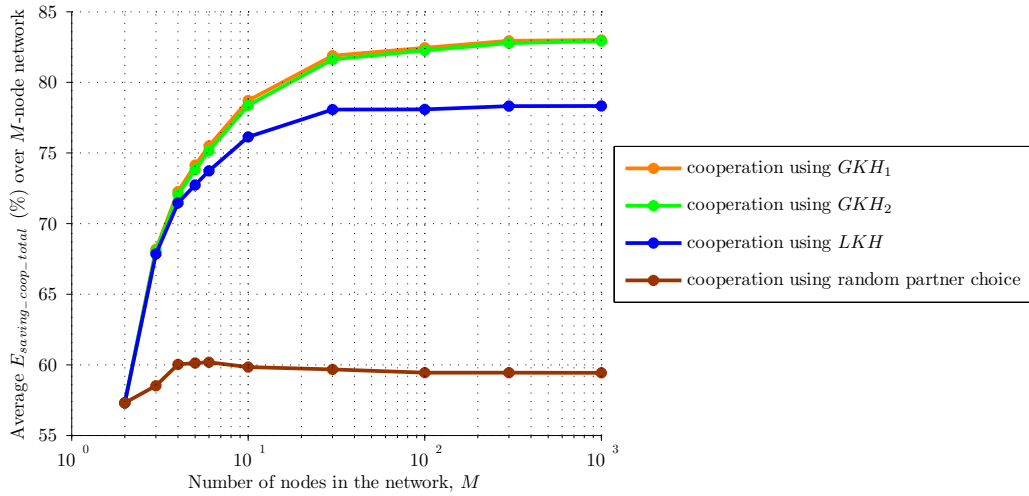


Figure 9.1: Average $E_{saving_coop_total}$ achieved over a Topology A network (central destination receiver) using different partner choice rules vs. number of nodes in the network (median of Q network realisations of M nodes randomly placed over a 100 m by 100 m network area).

achieved over the network using random partner choice decreases slightly (from 60.2% to 59.4%) because a larger candidate partner set reduces the probability of a given source node randomly selecting its best available cooperation partner.

Fig. 9.2 shows the network energy reduction factor achieved for a Topology A network as the number of nodes in the network M is varied, using ECO-OP cooperation with different partner choice rules. Importantly, Fig. 9.2 demonstrates that cooperation always significantly reduces the overall energy expenditure of a Topology A network for both sparse and dense networks, by a factor ranging from 4.1 to 14.5. The network energy reduction factor using GKH_1 and GKH_2 cooperation increases with increasing node density, ranging from 5.0 to 14.5 and 14.4 respectively. This trend is due to the increased energy efficiency of partner choice in a larger candidate partner set and is thus consistent with that exhibited by GKH_1 and GKH_2 in Fig. 9.1. By contrast, the trend exhibited by LKH in Fig. 9.2 differs somewhat from that observed in Fig. 9.1. Namely, the cooperative network energy reduction factor obtained using LKH increases with increasing node density for sparse networks (i.e. ranging from 5.0 to 8.9 for $M \leq 30$), but then decreases slightly (to 8.4) for increasingly dense networks. This trend may be explained by considering that a source node selects its closest neighbour as its partner using LKH . Thus on average the likelihood of a node's closest neighbour being a good cooperation partner increases with increasing node density due to a larger candidate partner set, as evidenced by the results in Fig. 9.1. However, for increasingly dense networks, the neighbouring partner node chosen by LKH will be increasingly close to the source node. For the nodes with the highest inherent energy requirements (i.e. those furthest from the central destination receiver) this leads to selecting partners which are increasingly far away

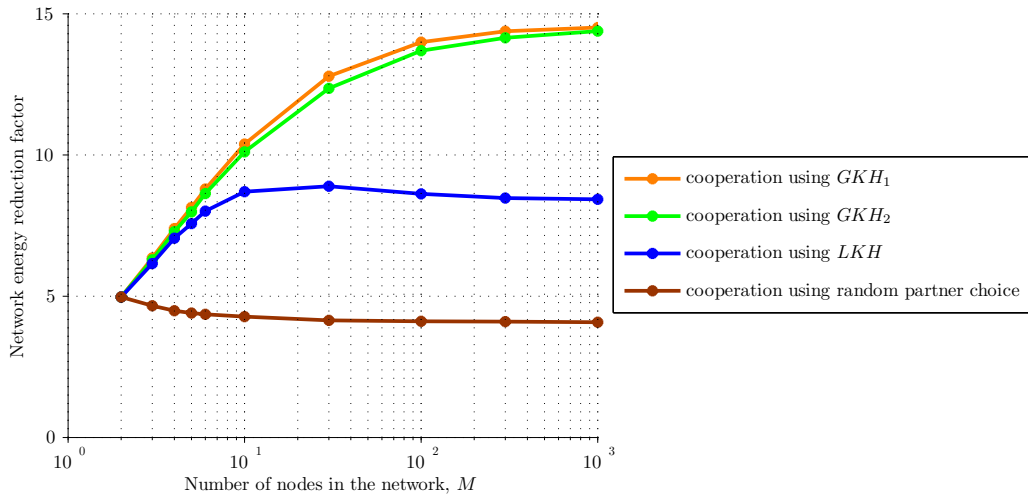


Figure 9.2: Reduction in total network energy consumption achieved by cooperation using different partner choice rules in a Topology A network (central destination receiver) vs. number of nodes in the network (median of Q network realisations of M nodes randomly placed over a 100 m by 100 m network area).

from the optimal partner location midway between the source and destination receiver. In a very dense network these nodes thus consume more energy as the source, due to selecting an increasingly sub-optimal cooperation partner, and typically spend more energy serving as partner, due to being selected by a source node with similarly high inherent energy requirements. This in turn leads to a reduced overall energy reduction factor, since the energy consumption of these nodes (with the highest inherent energy requirements) impacts most on this metric. Finally, Fig. 9.2 shows that the network energy reduction factor obtained via cooperation with random partner choice decreases slightly with increasing node density, ranging from 5.0 to 4.1. This is because in a dense network it is less likely that all nodes will randomly select a good cooperation partner, resulting in a higher overall network energy consumption.

Figs. 9.3, 9.4, and 9.5 present the typical distribution of node energy consumption over a Topology A network as the number of nodes in the network M is varied, for a non-cooperative network and cooperative networks with GKH_1 and GKH_2 , LKH , and random partner choice, respectively². Specifically, the minimum, lower-quartile, median, upper-quartile, and maximum node energy consumption ($E_{non-coop_node}$, E_{coop_node}) over the network are presented, making these plots analogous to the boxplot presented in Fig. 8.4 for the Topology A network of $M = 100$ regularly placed nodes. The maximum node energy consumption in the non-cooperative network increases with increasing node density since it is more likely in a dense network that a node exists located very far from

²Ideally, the results of all four cooperative networks would be presented together in a single plot, in order to explicitly compare their respective node energy distributions. However, for the sake of clarity the three major cooperative partner choice strategies are instead each shown separately alongside the non-cooperative network (the two variants of the global knowledge partner choice rule, GKH_1 and GKH_2 , are presented together as they yield similar results).

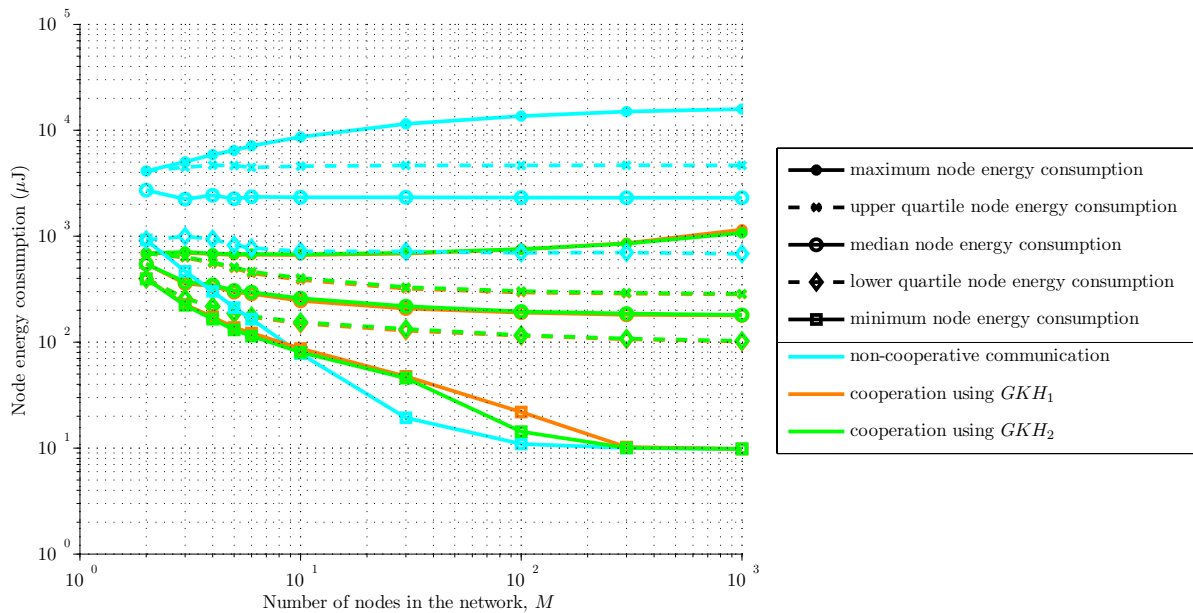


Figure 9.3: Distribution of node energy consumption over a Topology A network (central destination receiver) vs. number of nodes in the network, for non-cooperative communication and cooperative communication with GKH_1 and GKH_2 (median of Q network realisations of M nodes randomly placed over a 100 m by 100 m network area).

the central destination receiver. Conversely, the minimum node energy consumption in the non-cooperative network decreases with increasing node density since it is more likely in a dense network that a node exists located very close to the central destination receiver. The upper-quartile and lower-quartile node energy consumption exhibit a similar trend as the minimum and maximum node energy consumption, respectively, whereas the median node energy consumption in the non-cooperative network is roughly constant regardless of the node density.

Fig. 9.3 shows that the maximum node energy consumption of a cooperative GKH_1 and GKH_2 Topology A network is always less than the median node energy consumption of the corresponding non-cooperative network. More specifically, the maximum GKH_1 and GKH_2 node energy consumption is less than or comparable to the lower-quartile non-cooperative network node energy consumption for all but very high node densities (i.e. $M < 1000$). Furthermore, Fig. 9.3 shows that although the minimum node expenditure in the cooperative GKH_1 and GKH_2 networks is slightly higher than the minimum node energy consumption of the corresponding non-cooperative network for medium node density ($10 < M < 100$) networks³, it is always significantly lower than the lower-quartile

³This increase in the minimum node energy expenditure for medium density cooperative GKH_1 and GKH_2 networks results from the node nearest the centre of the network being too close to the destination to benefit from cooperation, but nevertheless consuming energy in serving as cooperation partner to other nodes in the Topology A network, as discussed in Section 8.2. For sufficiently sparse networks, the typical minimum node distance from the destination is large enough so as to ensure the minimum energy source node cooperates. This is consistent with the lower minimum node energy for

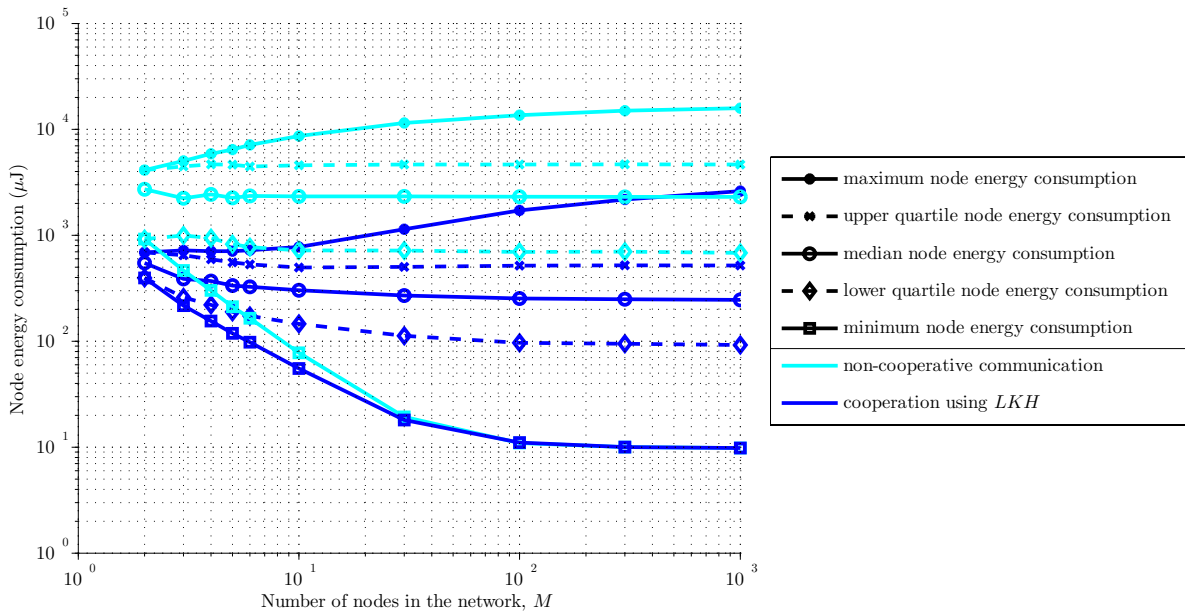


Figure 9.4: Distribution of node energy consumption over a Topology A network (central destination receiver) vs. number of nodes in the network, for non-cooperative communication and cooperative communication with *LKH* (median of Q network realisations of M nodes randomly placed over a 100 m by 100 m network area).

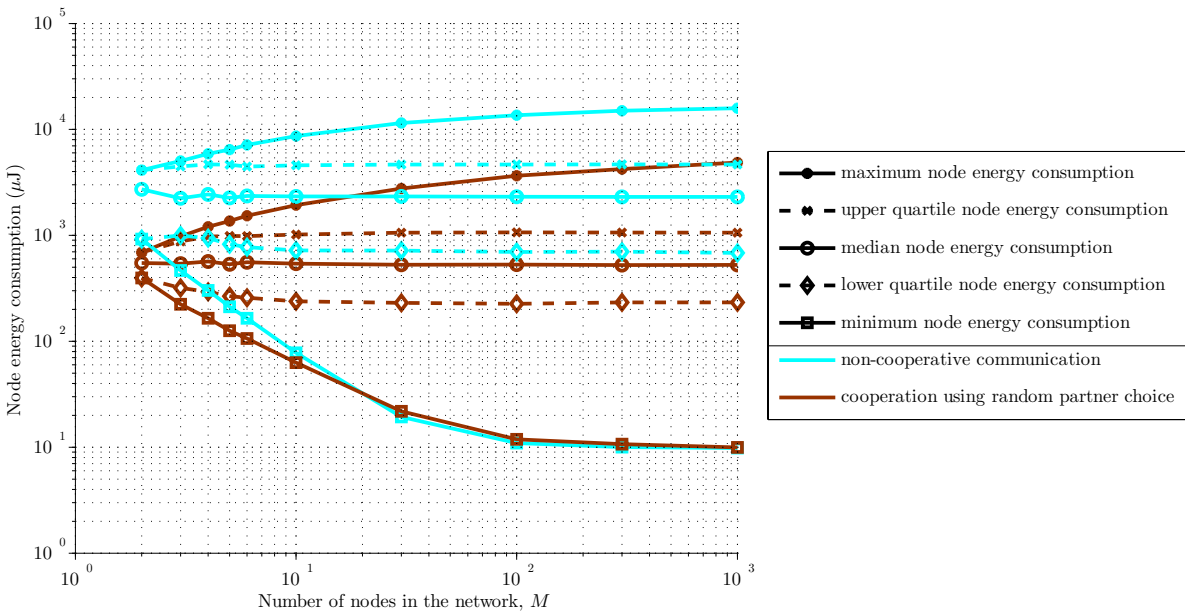


Figure 9.5: Distribution of node energy consumption over a Topology A network (central destination receiver) vs. number of nodes in the network, for non-cooperative communication and cooperative communication with random partner choice (median of Q network realisations of M nodes randomly placed over a 100 m by 100 m network area).

non-cooperative node energy expenditure. Importantly, Fig. 9.3 thus demonstrates that the popular partner nodes at the centre of the Topology A network are never overburdened by helping other nodes, regardless of node density. This confirms the result illustrated in Section 8.2 for the Topology A network of $M = 100$ regularly placed nodes. Therefore, ECO-OP with GKH_1 and GKH_2 is an effective and sustainable cooperation strategy for Topology A networks, achieving a significant reduction in overall network energy expenditure without overburdening individual partner nodes. Finally, Fig. 9.3 shows that the node energy distribution for a cooperative GKH_1 and GKH_2 Topology A network has a significantly lower range than that of the non-cooperative network, regardless of node density. Thus cooperation with GKH_1 and GKH_2 in a Topology A network always reallocates the network's combined energy resource among nodes so as to achieve a more even distribution of energy consumption over the network. Moreover, Figs. 9.2 and 9.3 show that the behaviour of GKH_1 and GKH_2 in a Topology A network is very similar regardless of node density; GKH_1 results in a slightly higher network energy reduction factor and a marginally lower upper-quartile, median, and lower-quartile node energy consumption, whereas GKH_2 results in a slightly lower minimum node energy consumption. Therefore GKH_2 is always the preferable cooperation strategy of the two for practical deployment in a Topology A network, since it achieves virtually identical energy conservation results as GKH_1 at a lower computational cost.

Fig. 9.4 shows that the maximum node energy consumption of a cooperative LKH Topology A network is less than the median node energy consumption of the corresponding non-cooperative network for all but very high node densities (for $M > 300$ the maximum LKH node energy consumption is comparable to the median non-cooperative node energy consumption). It is interesting to note that the maximum node energy consumption in the cooperative LKH network increases with increasing node density, as nodes near the boundary of the network select increasingly closer (and thus increasingly sub-optimal) neighbouring partner nodes, as discussed in above. It is also interesting to note from Fig. 9.4 that the minimum node energy expenditure in a cooperative LKH network never exceeds that of the non-cooperative network (unlike GKH_1 and GKH_2). Comparing Figs. 9.3 and 9.4 reveals that LKH results in a higher range and interquartile range of the node energy distribution over the network than GKH_1 and GKH_2 for all but very sparse Topology A networks. Cooperation with LKH thus generally maintains the uneven distribution of non-cooperative node energy consumption over the Topology A network.

the cooperative GKH_1 and GKH_2 networks (vs. the non-cooperative network) observed in Fig. 9.3 for $M < 10$. For sufficiently dense networks, the typical minimum node distance from the destination is less than half the break-even distance, so that the source nodes that would have selected this node as partner (at roughly twice this distance from the destination) also opt for non-cooperative communication. This is consistent with the non-cooperative network and the cooperative GKH_1 and GKH_2 networks having the same minimum node energy for $M > 300$ in Fig. 9.3.

Finally, Fig. 9.5 shows that the maximum node energy consumption of a random partner choice cooperative Topology A network is less than the upper-quartile node energy consumption of the corresponding non-cooperative network for all but very high node densities (for $M > 300$ the maximum random partner choice node energy consumption is comparable to the upper-quartile non-cooperative node energy consumption). Therefore, cooperation using random partner choice results in the highest individual node energy consumption of the four cooperative networks regardless of node density. Comparing Figs. 9.3, 9.4, and 9.5 shows that random partner choice results in a median node energy consumption which is only slightly lower than the maximum node energy consumption of the corresponding GKH_1 and GKH_2 cooperative networks and roughly equal to the upper-quartile node energy consumption of the corresponding LKH cooperative network.

9.3 Topology B Network: Remote Destination Receiver

Fig. 9.6 shows the average $E_{saving_coop_total}$ achieved over the Topology B network as the number of nodes in the network M is varied, using ECO-OP cooperation with different partner choice rules. The average $E_{saving_coop_total}$ achieved over the network ranges from 87.6% for a very sparse network to 93.0%, 92.9%, and 89.0% for dense networks using GKH_1 , GKH_2 , and LKH , respectively. The average $E_{saving_coop_total}$ achieved over the network using GKH_1 , GKH_2 , and LKH increases with increasing node density. This is due to the larger candidate partner set associated with more dense networks, which means that good cooperation partners are more likely to be found in the network. The average $E_{saving_coop_total}$ achieved over the network using random partner choice decreases slightly with increasing node density (from 87.6% to 86.7%) because a larger candidate partner set reduces the probability of a given source node randomly selecting its best available cooperation partner. It is interesting to note that random partner choice in a Topology B network exhibits a different trend for very sparse networks than that in Fig. 9.1 for a Topology A network. This is because, unlike in a Topology A network, a source node in a Topology B network never opts for non-cooperative communication, as discussed in Section 8.3.

Fig. 9.7 shows the network energy reduction factor achieved for a Topology B network as the number of nodes in the network M is varied, using ECO-OP cooperation with different partner choice rules. Importantly, Fig. 9.7 demonstrates that cooperation always significantly reduces the overall energy expenditure of a Topology B network for both sparse and dense networks, by a factor ranging from 9.1 to 15.8. The network energy reduction factor using GKH_1 and GKH_2 cooperation increases with increasing node density, ranging from 9.4 to 15.8 and 15.4 respectively. The cooperative network energy reduction factor obtained using LKH increases with increasing node density for

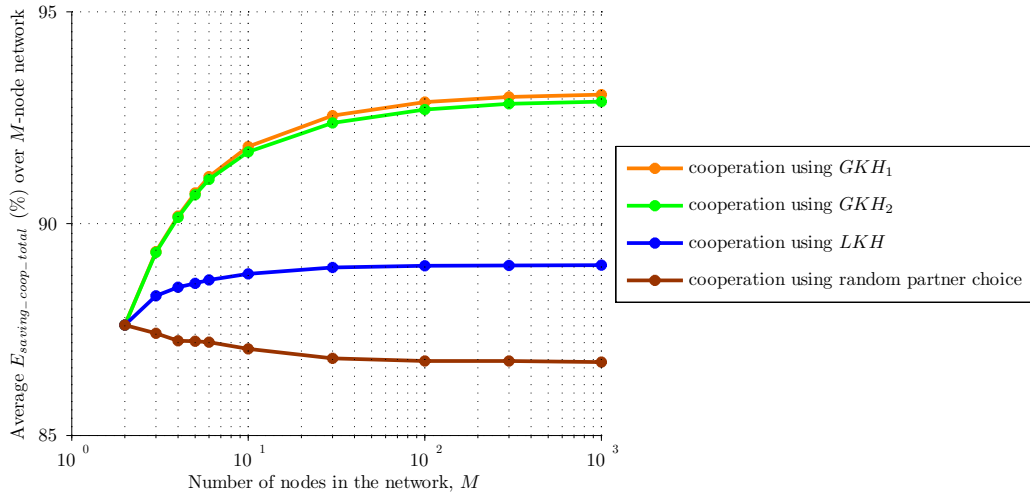


Figure 9.6: Average $E_{saving_coop_total}$ achieved over a Topology B network (remote destination receiver) using different partner choice rules vs. number of nodes in the network (median of Q network realisations of M nodes randomly placed over a 100 m by 100 m network area).

very sparse networks (i.e. increases from 9.3 for $M = 2$ to 9.7 for $M = 3$), but then decreases slightly (to 9.1) for increasingly dense networks. Lastly, the network energy reduction factor obtained via cooperation with random partner choice decreases slightly with increasing node density, ranging from 9.4 to 9.2. These trends are consistent with those observed for a Topology A network, and are due to the same reasons discussed in Section 9.2. However, unlike for a Topology A network, Fig. 9.7 reveals that the cooperative network energy reduction obtained using LKH in a Topology B network is slightly less than that obtained using random partner choice for all but very sparse networks. This is because random partner choice results in lower energy consumption than LKH for the nodes located furthest from the remote destination receiver. Namely, for these source nodes random partner choice generally selects a partner located closer to the optimal location midway between the source and destination than the neighbouring partner node chosen by LKH . Consequently, the nodes near the bottom of the Topology B network consume less energy as both source and partner in the random partner choice network, as evidenced by Fig. 8.7 and discussed in Section 8.3. And, since these nodes have the highest inherent communication energy requirements, a reduction in their energy consumption has the most significant impact on the overall network energy reduction factor metric.

Figs. 9.8, 9.9, and 9.10 present the typical distribution of node energy consumption over a Topology B network as the number of nodes in the network M is varied, for a non-cooperative network and cooperative networks with GKH_1 and GKH_2 , LKH , and random partner choice, respectively. Specifically, the minimum, lower-quartile, median, upper-quartile, and maximum node energy consumption ($E_{non-coop_node}$, E_{coop_node}) over the network are presented, making these plots analogous to the boxplot presented in

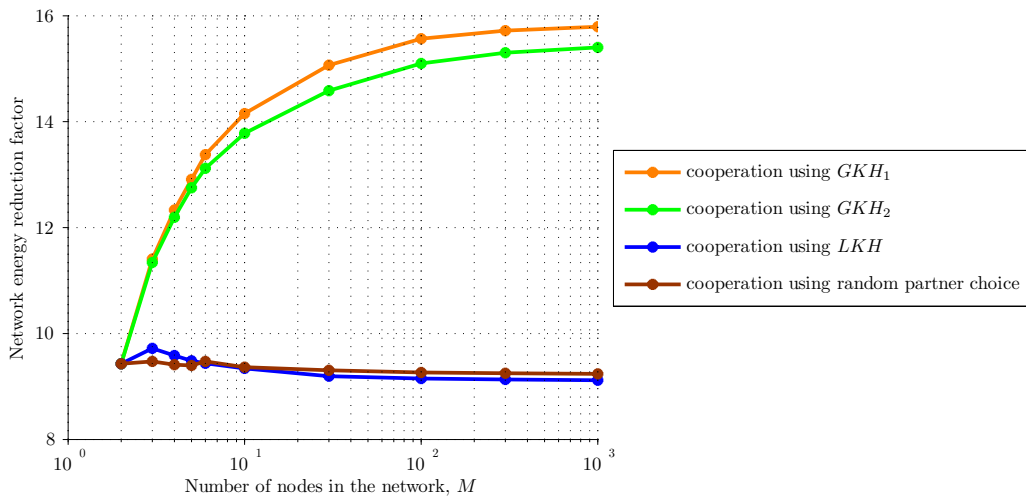


Figure 9.7: Reduction in total network energy consumption achieved by cooperation using different partner choice rules in a Topology B network (remote destination receiver) vs. number of nodes in the network (median of Q network realisations of M nodes randomly placed over a 100 m by 100 m network area).

Fig. 8.8 for the Topology B network of $M = 100$ regularly placed nodes. As the node density is increased the minimum, lower-quartile, median, upper-quartile, and maximum node energy consumption in the non-cooperative network exhibit the same trends as for a Topology A network, which are discussed in Section 9.2.

Fig. 9.8 shows that the upper-quartile node energy consumption of a cooperative GKH_1 and GKH_2 Topology B network is always substantially lower than the minimum node energy consumption of the corresponding non-cooperative network. However, Fig. 9.8 also shows that the maximum node energy consumption of the cooperative GKH_1 and GKH_2 Topology B network increases significantly with increasing node density. Importantly, the maximum GKH_1 and GKH_2 node energy consumption is higher than the maximum non-cooperative node energy consumption for a dense Topology B network (i.e. $M > 300$ for GKH_1 and $M > 100$ for GKH_2). This is because only a handful of nodes serve as cooperation partner to the entire Topology B network (as illustrated in Fig. 8.6) and as M increases these partner nodes serve an increasing number of source nodes each. Therefore, GKH_1 and GKH_2 achieve the highest overall network energy reduction at the cost of overburdening several partner nodes, to the extent that their energy consumption actually exceeds the maximum non-cooperative individual node energy consumption in a sufficiently dense network. This suggests that GKH_1 and GKH_2 may be unsustainable cooperation strategies for a dense Topology B network, as the heavy bias towards a handful of partner nodes causes these nodes to prematurely deplete their batteries in helping the rest of the network's nodes. A modified global knowledge partner choice strategy may be required to mitigate this effect, whereby a limit is placed on the number of source nodes a single partner node can serve, as will be discussed in Section 9.5. The long-term effect

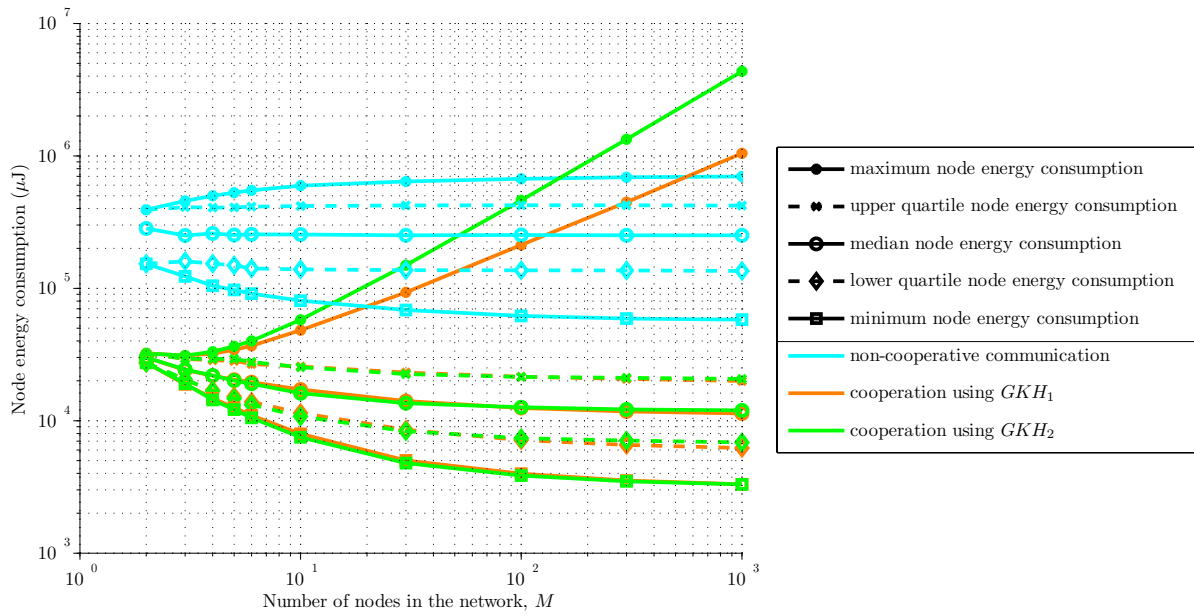


Figure 9.8: Distribution of node energy consumption over a Topology B network(remote destination receiver) vs. number of nodes in the network, for non-cooperative communication and cooperative communication with GKH_1 and GKH_2 (median of Q network realisations of M nodes randomly placed over a 100 m by 100 m network area).

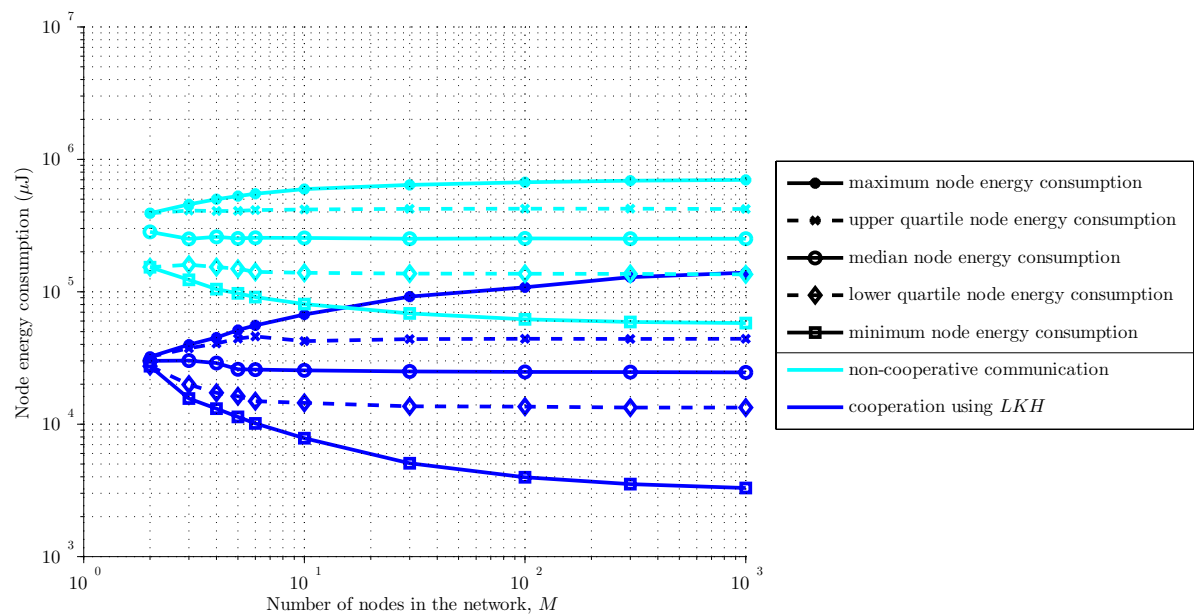


Figure 9.9: Distribution of node energy consumption over a Topology B network(remote destination receiver) vs. number of nodes in the network, for non-cooperative communication and cooperative communication with LKH (median of Q network realisations of M nodes randomly placed over a 100 m by 100 m network area).

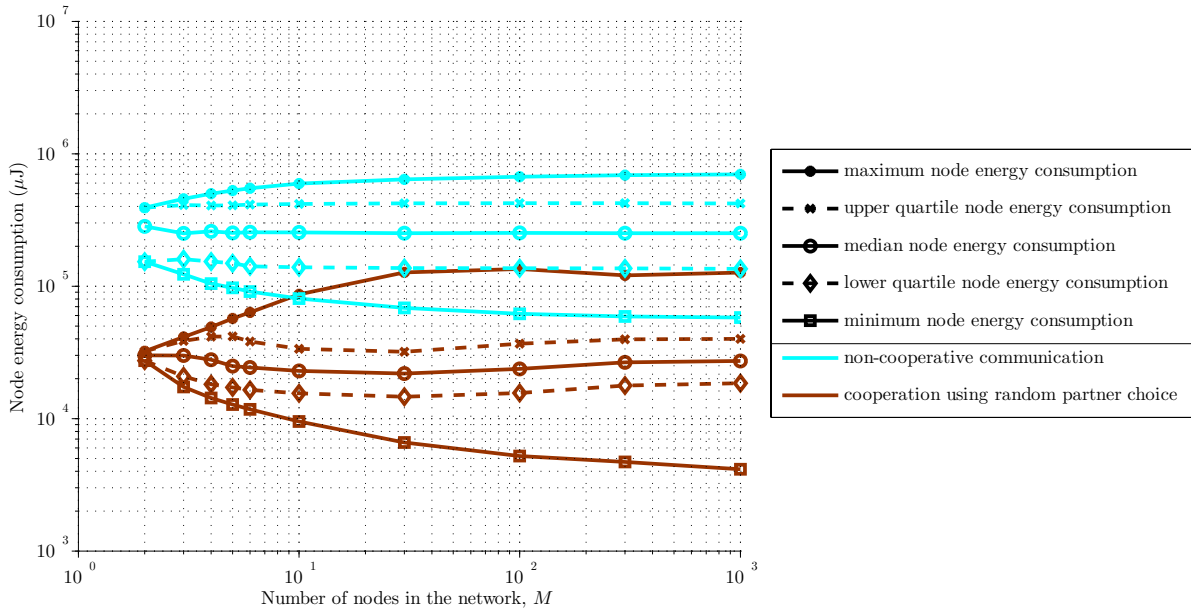


Figure 9.10: Distribution of node energy consumption over a Topology B network (remote destination receiver) vs. number of nodes in the network, for non-cooperative communication and cooperative communication with random partner choice (median of Q network realisations of M nodes randomly placed over a 100 m by 100 m network area).

of network-wide cooperation using ECO-OP with GKH_1 and GKH_2 in a Topology B network will be explicitly investigated in Chapters 10 and 11. Finally, Fig. 9.8 shows that GKH_1 results in a substantially lower maximum node energy consumption than GKH_2 , due to having a less heavily concentrated partner service distribution (as illustrated in Fig. 8.6). Thus GKH_1 is clearly the preferable of the two global knowledge partner choice heuristics for a cooperative Topology B network.

Fig. 9.9 shows that the maximum node energy consumption of a cooperative LKH Topology B network is less than the lower-quartile node energy consumption of the corresponding non-cooperative network for all but very high node densities (for $M > 300$ the maximum LKH node energy consumption is comparable to the lower-quartile non-cooperative node energy consumption). Therefore, for a dense Topology B network, LKH has the important advantage over GKH_1 and GKH_2 of a much lower maximum node energy consumption. Otherwise, LKH is inferior to GKH_1 and GKH_2 , resulting in a significantly higher upper-quartile, median, and lower-quartile node energy consumption as well as achieving a substantially lower network energy reduction factor.

Lastly, Fig. 9.10 shows that the maximum node energy consumption of a random partner choice cooperative Topology B network is less than the lower-quartile node energy consumption of the corresponding non-cooperative network for all node densities. Importantly, comparing Figs. 9.10 and 9.9 shows that the performance of random partner choice is overall comparable to that of LKH , with random partner choice achieving

a lower upper-quartile node energy consumption and for dense Topology B networks a somewhat lower maximum node energy consumption. These observations are consistent with the slightly higher network energy reduction factor obtained by random partner choice compared to *LKH* for dense Topology B networks, as discussed above.

9.4 Topology C Network: Node-to-Node Communication

Fig. 9.11 shows the average $E_{saving_coop_total}$ achieved over the Topology C network as the number of nodes in the network M is varied, using ECO-OP cooperation with different partner choice rules. The average $E_{saving_coop_total}$ achieved over the network ranges from 67.3% for a very sparse network to 85.2%, 85.1%, and 80.4% for dense networks using *GKH₁*, *GKH₂*, and *LKH*, respectively. The average $E_{saving_coop_total}$ achieved over the network using *GKH₁*, *GKH₂*, and *LKH* increases with increasing node density, due to the larger candidate partner set which means that good cooperation partners are more likely to exist in the network. The average $E_{saving_coop_total}$ achieved over the Topology C network using random partner choice generally decreases slightly with increasing node density (from 67.3% to 65.1%) because a larger candidate partner set reduces the probability of a given source node randomly selecting its best available cooperation partner.

Fig. 9.12 shows the network energy reduction factor achieved for a Topology C network as the number of nodes in the network M is varied, using ECO-OP cooperation with different partner choice rules. Importantly, Fig. 9.12 demonstrates that cooperation always significantly reduces the overall energy expenditure of a Topology C network for both sparse and dense networks, by a factor ranging from 6.7 to 15.8. The network energy reduction factor using *GKH₁* and *GKH₂* cooperation increases with increasing node density, ranging from 6.7 to 15.8 and 15.7 respectively. By contrast, the cooperative network energy reduction factor obtained using *LKH* increases with increasing node density for very sparse networks (i.e. ranges from 6.7 to 9.3 for $M \leq 10$), but then decreases slightly (to 8.8) for increasingly dense networks. These trends are consistent with those observed for Topology A and B networks, and are due to the same reasons discussed in Section 9.2. Unlike for Topology A and B networks, the network energy reduction factor obtained in a Topology C network via cooperation with random partner choice increases slightly with increasing node density, ranging from 6.7 to 7.0. For most of the nodes in a Topology C network (as in Topology A and B networks), a larger candidate partner set reduces the probability of a given source node randomly selecting its best available cooperation partner. However, the nodes with the highest inherent communication energy

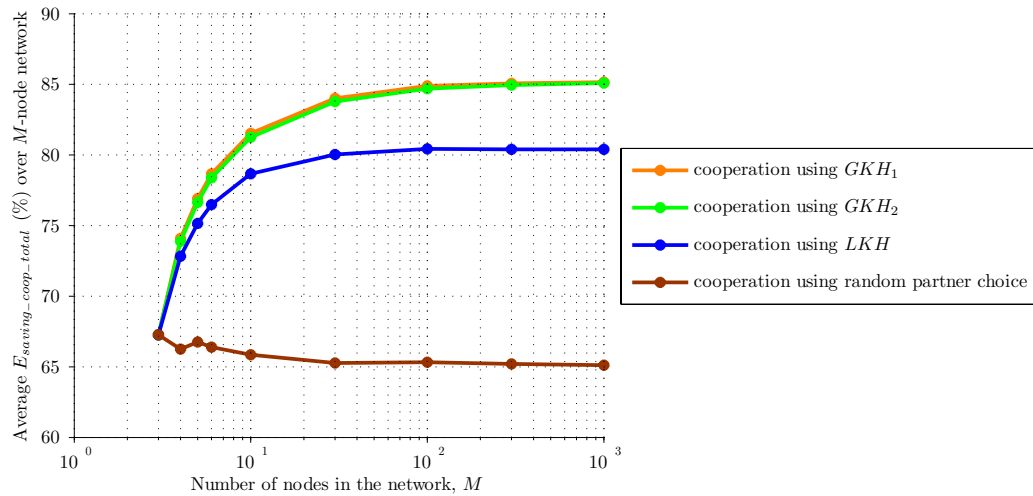


Figure 9.11: Average $E_{saving_coop_total}$ achieved in a Topology C network (node-to-node communication) using different partner choice rules vs. number of nodes in the network (median of Q network realisations of M nodes randomly placed over a 100 m by 100 m network area).

requirements typically find a better cooperation partner in a dense network Topology C network, resulting in a slightly higher overall network energy reduction factor⁴.

Figs. 9.13, 9.14, and 9.15 present the typical distribution of node energy consumption over a Topology C network as the number of nodes in the network M is varied, for a non-cooperative network and cooperative network with GKH_1 and GKH_2 , LKH , and random partner choice, respectively. Specifically, the minimum, lower-quartile, median, upper-quartile, and maximum node energy consumption ($E_{non-coop_node}$, E_{coop_node}) over the network are presented, making these plots analogous to the boxplot presented in Fig. 8.12 for the Topology C network of $M = 100$ regularly placed nodes. As the node density is increased the minimum, lower-quartile, median, upper-quartile, and maximum node energy consumption in the non-cooperative network exhibit the same trends as for Topology A and B networks, which are discussed in Section 9.2.

Fig. 9.13 shows that the maximum node energy consumption of a cooperative GKH_1 and GKH_2 Topology C network is less than the median node energy consumption of the corresponding non-cooperative network for all but very high node densities (for $M > 300$ the maximum GKH_1 and GKH_2 node energy is roughly equal to the median non-cooperative node energy consumption). Furthermore, Figs. 9.12 and 9.13 show that, as

⁴This is evidenced by the increasing reduction in the maximum node energy consumption achieved by random partner choice cooperation for increasing M in Fig. 9.15, and may be explained as follows. For a very dense Topology C network, the node with the maximum energy consumption and its destination receiver node will be located at opposite corners of the network, as discussed in Section 8.4. Thus most of the other nodes in the network will be located within the highly energy efficient partner choice region of this source-destination pair. The more dense the Topology C network is, the larger the maximum source-destination separation and the larger the proportion of the network's nodes that are located within this source node's highly energy efficient partner choice region. It follows that a randomly selected node is a better cooperation partner for the maximum energy source node in a dense Topology C network.

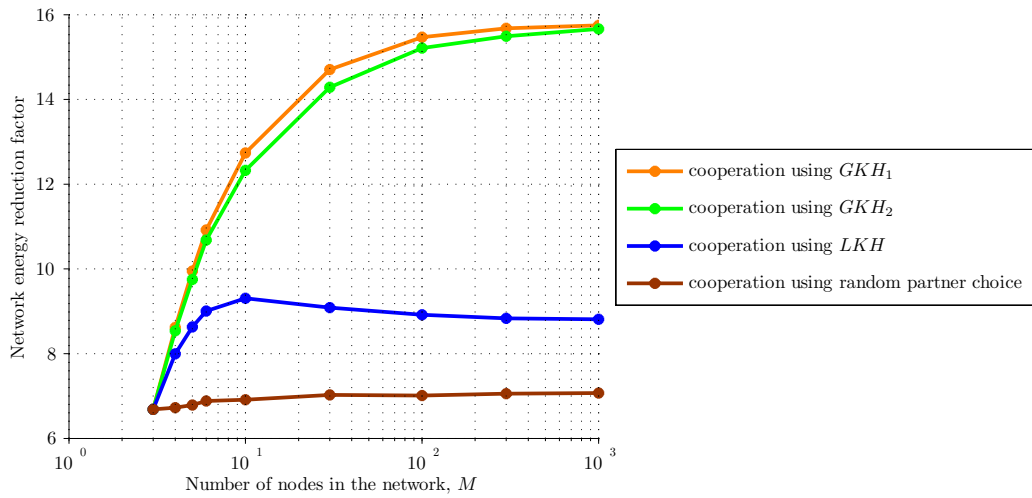


Figure 9.12: Reduction in total network energy consumption achieved by cooperation using different partner choice rules in a Topology C network (node-to-node communication) vs. number of nodes in the network (median of Q network realisations of M nodes randomly placed over a 100 m by 100 m network area).

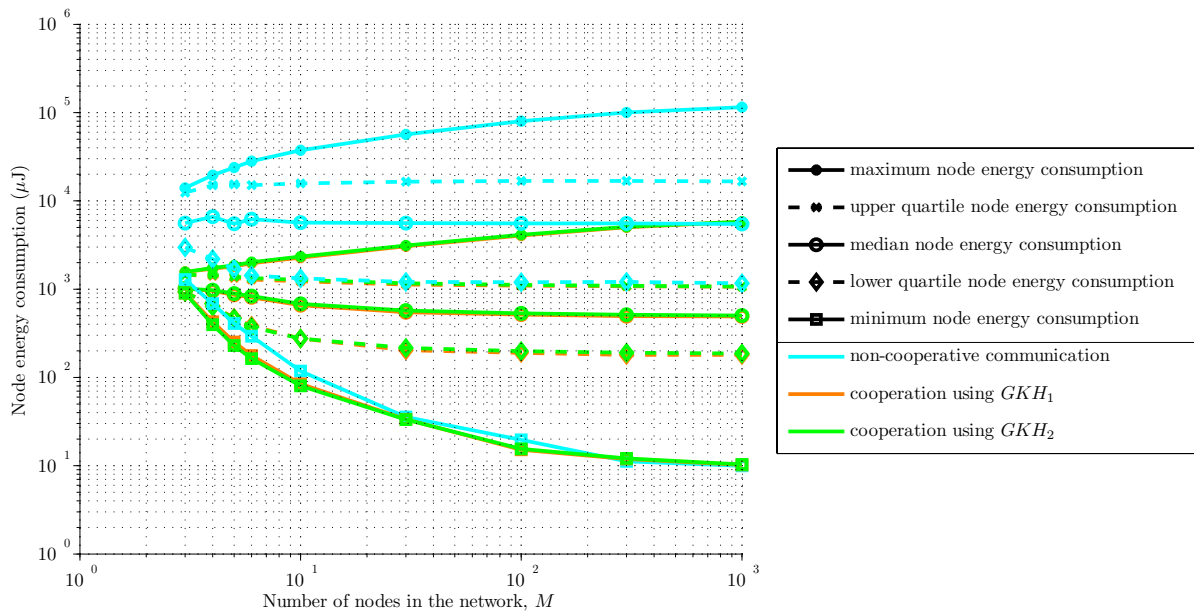


Figure 9.13: Distribution of node energy consumption over a Topology C network (node-to-node communication) vs. number of nodes in the network, for non-cooperative communication and cooperative communication with GKH_1 and GKH_2 (median of Q network realisations of M nodes randomly placed over a 100 m by 100 m network area).

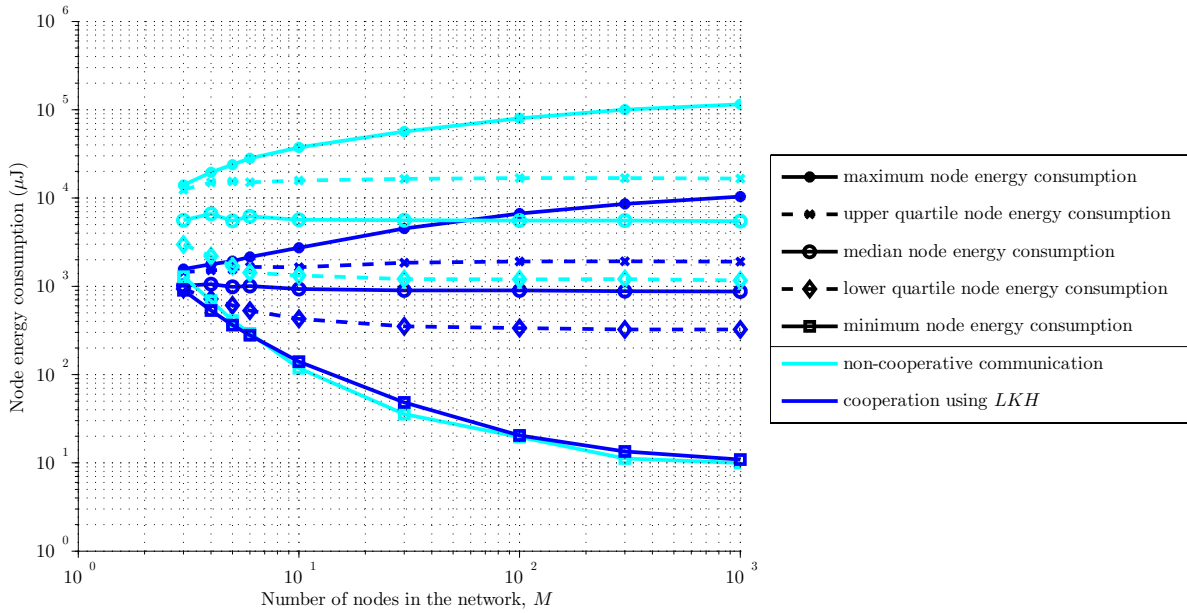


Figure 9.14: Distribution of node energy consumption over a Topology C network (node-to-node communication) vs. number of nodes in the network, for non-cooperative communication and cooperative communication with *LKH* (median of Q network realisations of M nodes randomly placed over a 100 m by 100 m network area).

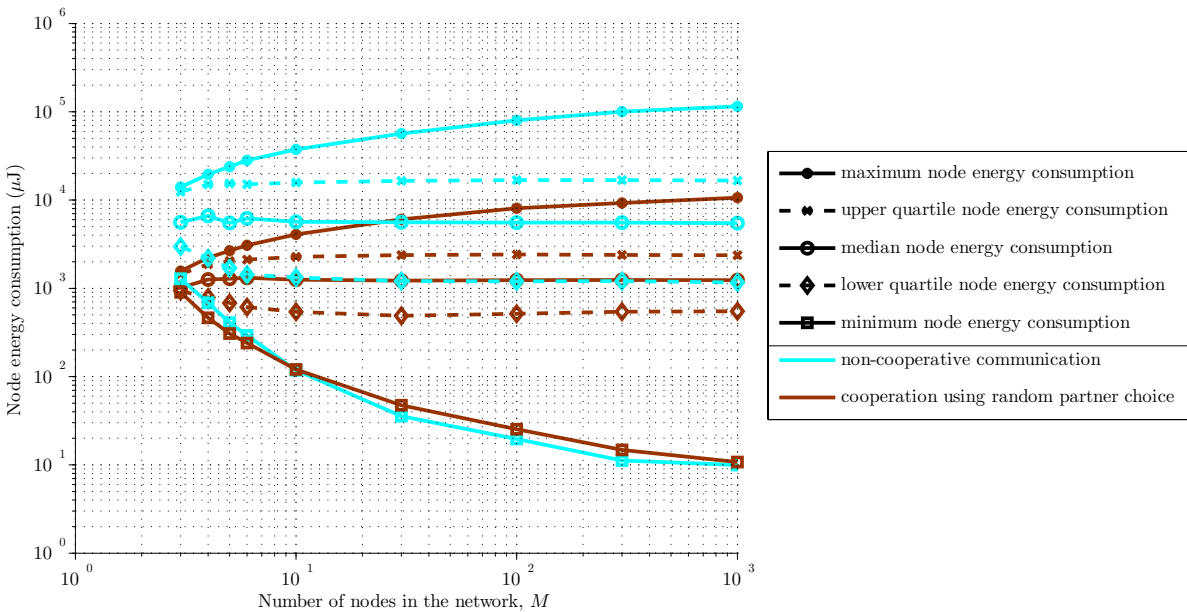


Figure 9.15: Distribution of node energy consumption over a Topology C network (node-to-node communication) vs. number of nodes in the network, for non-cooperative communication and cooperative communication with random partner choice (median of Q network realisations of M nodes randomly placed over a 100 m by 100 m network area).

in a Topology A network, the behaviour of GKH_1 and GKH_2 in a Topology C network is very similar regardless of node density; GKH_1 results in a slightly higher network energy reduction factor and a marginally lower maximum, upper-quartile, median, and lower-quartile node energy consumption than GKH_2 . Therefore GKH_2 is always the preferable cooperation strategy of the two for practical deployment in a Topology C network, as it yields virtually identical energy conservation results as GKH_1 but entails a lower computational complexity.

Figs. 9.14 and 9.15 show that the maximum node energy consumption of a cooperative LKH and random partner choice Topology C network is always less than the upper-quartile node energy consumption of the corresponding non-cooperative network. Comparing Figs. 9.13, 9.14, and 9.15 shows that the median node energy consumption of a cooperative random partner choice Topology C network is slightly higher than the upper-quartile GKH_1 and GKH_2 node energy consumption, whereas the median LKH node energy consumption is only slightly lower than the upper-quartile GKH_1 and GKH_2 node energy consumption.

Importantly, Figs. 9.13, 9.14, and 9.15 demonstrate that the lower-quartile, median, upper-quartile, and maximum node energy consumption are always significantly reduced by cooperation, regardless of partner choice rule. The minimum node energy consumption is also always reduced using GKH_1 and GKH_2 and only slightly increased using LKH and random partner choice cooperation. Therefore, network-wide cooperation using ECO-OP consistently benefits the Topology C network as a whole. This also indicates that the popular partner nodes selected using GKH_1 and GKH_2 near the middle of the Topology C network (as illustrated by Fig. 8.10) are never overburdened by helping other nodes, regardless of node density. This confirms the results presented in Section 8.4 for the Topology C network of $M = 100$ regularly placed nodes. Therefore, ECO-OP with GKH_1 and GKH_2 is an effective and sustainable cooperation strategy for Topology C networks, achieving a significant reduction in overall network energy expenditure without overburdening individual partner nodes.

Finally, Figs. 9.13, 9.14, and 9.15 show that the node energy distribution of a cooperative Topology C network has a significantly lower range than that of a non-cooperative network, regardless of partner choice rule or node density. Therefore, cooperation in a Topology C network always both reduces the overall network energy consumption and reallocates the network's combined energy resource among nodes to produce a more even distribution of energy expenditure over the network.

9.5 Discussion

In this section the overall energy conservation performance of ECO-OP with different partner choice rules is compared based on the results presented in the preceding sections. This analysis serves to determine the recommended cooperation strategy for a given set of network conditions. The practical advantages of employing some partner choice rules are also discussed, along with the shortcomings of other partner choice heuristics and some potential refinements that could be made to the ECO-OP strategy to mitigate these.

The results presented in this chapter show that GKH_1 and GKH_2 always achieve the best overall energy conservation results in a Topology A and C network. Aside from consistently yielding the highest total network energy reduction of the four partner choice rules considered, GKH_1 and GKH_2 result in the lowest median, upper-quartile, and maximum node energy consumption for a Topology A network and the lowest minimum, lower-quartile, median, upper-quartile, and maximum node energy consumption for a Topology C network. Moreover, of the two global knowledge heuristics, GKH_1 performs only marginally better than the lower computational complexity heuristic GKH_2 . Therefore, GKH_2 is the best cooperation strategy for practical network-wide cooperation among energy-constrained nodes in a Topology A and C network.

As for a Topology A and C network, GKH_1 and GKH_2 always achieve the highest total network energy reduction in a Topology B network, in addition to consistently yielding the lowest minimum, lower-quartile, median, and upper-quartile node energy consumption of the four partner choice rules considered. However, for dense Topology B networks ($M \geq 30$) GKH_1 and GKH_2 also result in the highest maximum node energy consumption, due to only a handful of nodes each serving as cooperation partner to an increasing number of source nodes as the network density increases. Of the two global knowledge heuristics, GKH_1 is clearly the preferable in a Topology B network as it results in a substantially lower maximum node energy consumption than GKH_2 . Nonetheless, GKH_1 achieves the highest network energy reduction at the cost of overburdening several partner nodes in a dense Topology B network; the maximum GKH_1 node energy consumption is substantially higher than the maximum LKH node energy consumption for $M \geq 100$ and actually exceeds the maximum non-cooperative node energy consumption for $M \geq 1000$. By contrast, LKH and random partner choice achieve a substantial network energy reduction (with random partner choice performing slightly better than LKH) without overexploiting individual partner nodes, making them better candidates than GKH_1 for sustainable long-term energy-conserving cooperation. Therefore, random partner choice and LKH are the best cooperation strategies for a dense Topology B network, whereas GKH_1 is the best cooperation strategy for a sparse Topology B network.

Table 9.1: Summary of the best partner choice rule to employ with ECO-OP for energy-conserving cooperation in sparse and dense wireless sensor networks of various topology.

Network topology	Network node density	Best partner choice rule
A	sparse	GKH_2
	dense	GKH_2
B	sparse	GKH_1
	dense	random partner choice, LKH
C	sparse	GKH_2
	dense	GKH_2

The recommendations given above for the best partner choice rule to employ with ECO-OP under different network conditions are summarised in Table 9.1. The results in Table 9.1 are thus a guide to selecting the best energy-conserving cooperation strategy given a particular network topology and node density. However, if these network conditions are not known in advance, it is important to be able to deploy a cooperation strategy which works well in general. Unfortunately, the results in Table 9.1 indicate that there is no single cooperation strategy which is superior under all network conditions. Moreover, the best cooperation strategy under certain conditions may perform the worst under different conditions; for example, GKH_2 is the best in a Topology A or C network but the worst in a Topology B network and vice versa for random partner choice.

The results presented in this chapter have demonstrated that cooperation using the LKH partner choice heuristic always yields a very substantial network energy reduction, albeit inferior to GKH_1 and GKH_2 . For comparison, random partner choice achieves a considerably lower network energy reduction than LKH in a Topology A or C network and a comparable network energy reduction in a Topology B network. Importantly, unlike for GKH_1 and GKH_2 , partner nodes are never overburdened in the LKH cooperative network, regardless of network topology or node density. This versatility and scalability of the LKH cooperation strategy is due to an inherently distributed partner service burden, whereby neighbouring nodes with similar inherent communication energy requirements help each other⁵. Therefore, LKH is overall the best cooperation strategy for a general energy-constrained wireless sensor network of an unknown topology and node density. Furthermore, as discussed in Chapter 6, LKH has the important practical advantage over GKH_1 and GKH_2 of requiring solely local knowledge of network path losses and being the most computationally efficient cooperation strategy. The results presented in this chapter thus demonstrate that ECO-OP with LKH always enables resource-constrained

⁵As illustrated in Chapter 8, nodes in an LKH Topology C network are also likely to serve as partner to neighbouring nodes with roughly similar inherent communication requirements, despite not having a common destination receiver.

sensor nodes to substantially improve the energy efficiency of the network as a whole by making fully autonomous distributed cooperation decisions.

Finally, Table 9.1 shows that GKH_2 is the best practical cooperation strategy in Topology A and C networks but has the flaw of resulting in the most concentrated partner service burden which renders it unsuitable for Topology B networks. A minor modification of ECO-OP might be able to mitigate this effect, making GKH_2 an effective long-term cooperation strategy under all network conditions. An example of such a modification would be setting an upper limit on the number of source nodes a single partner node can serve. Practically, this could be implemented in a distributed way with minor additional overhead by having partner nodes accept cooperation requests as long as their total energy consumption remains below a threshold maximum node energy consumption (which is set to the same value for all nodes by the network designer, say equal to the upper quartile non-cooperative node energy). Once this threshold energy consumption has been exceeded for a popular partner node, the node broadcasts a message to inform all source nodes which have yet to select their cooperation partner that it has removed itself from the pool of available candidate partners.

In a Topology B network this modified ECO-OP strategy should be able to distribute the partner service burden using GKH_2 among a greater number of nodes which are nonetheless very good cooperation partners. Alternatively, the problem of overburdening popular partner nodes in the GKH_2 Topology B network could be addressed by simply placing several nodes with a higher battery capacity at the centre of the top boundary of the Topology B network, which is necessarily the location of the partner nodes selected using GKH_2 , as illustrated in Section 8.3. This heterogeneous network solution, whereby nodes with two different energy levels are deployed inside the network, is a feasible practical strategy precisely because there are only a handful of nodes in a predetermined location which serve as cooperation partners in the GKH_2 Topology B network; the additional expense of equipping two or three nodes with high capacity batteries should be a satisfactory engineering trade-off if it enables superior long-term energy conservation results over the whole network. An investigation of the effectiveness and viability of these two suggested modifications to the ECO-OP cooperation strategy is an interesting future research direction.

9.6 Summary

In this chapter the energy conservation performance of network-wide cooperation using the ECO-OP cooperation strategy proposed in Chapter 7 has been evaluated in three representative network topologies (A, B, C) for the general case of randomly deployed networks of various node density. The typical performance of ECO-OP with different

partner choice rules (GKH_1 , GKH_2 , LKH , and random partner choice) has thus been thoroughly analysed for both sparse and dense networks with both directed and random data flow.

Importantly, the results presented in this chapter have consistently demonstrated that cooperation using ECO-OP always significantly reduces the overall network energy expenditure, regardless of network topology or node density. Specifically, the total network energy consumption is reduced by a factor ranging from 4.1 to 14.5 for a Topology A (central destination receiver) network, from 9.1 to 15.8 for a Topology B (remote destination receiver) network, and from 6.7 to 15.8 for a Topology C (node-to-node communication) network. This demonstrates the general validity of network-wide cooperation using ECO-OP as an effective energy saving technique for wireless sensor networks. The analysis in this chapter has demonstrated that GKH_1 and GKH_2 always achieve the highest total network energy reduction of the four partner choice rules considered, regardless of network topology or node density. It has also been shown that LKH always yields a very substantial network energy reduction, albeit inferior to GKH_1 and GKH_2 . For comparison, random partner choice achieves a considerably lower network energy reduction than LKH in a Topology A or C network and a comparable network energy reduction in a Topology B network.

Moreover, a preliminary analysis of the general long-term viability of ECO-OP has been undertaken in this chapter by considering the typical distribution of node energy consumption over the cooperative network as the node density is increased. This analysis has revealed that ECO-OP with GKH_1 or GKH_2 is always an effective and sustainable cooperation strategy for Topology A and C networks, achieving a significant reduction in overall network energy expenditure without overburdening individual partner nodes. However, in a dense Topology B network ECO-OP with GKH_1 and GKH_2 achieves the highest overall network energy reduction at the cost of overburdening several partner nodes, to the extent that their energy consumption actually exceeds the maximum non-cooperative node energy consumption in a very dense network. This suggests that GKH_1 and GKH_2 may be unsustainable cooperation strategies for a dense Topology B network, as very popular partner nodes would prematurely deplete their own energy supply in helping other nodes. By contrast, partner nodes are never overburdened in the LKH cooperative network due to an inherently distributed partner service burden. Therefore, ECO-OP with LKH is a sustainable energy-conserving cooperation strategy regardless of network topology or node density.

Finally, the analysis presented in this chapter has served to ascertain the best partner choice rule to employ with ECO-OP under different network conditions. The recommended cooperation strategy for practical network-wide cooperation among energy-constrained nodes is GKH_2 for a Topology A and C network, GKH_1 for a sparse Topology

B network, and random partner choice or *LKH* for a dense Topology B network. Moreover, it has been shown that *LKH* is overall the best cooperation strategy for a general energy-constrained wireless sensor network of an unknown topology and node density. Importantly from the point of view of practical implementation, this demonstrates that resource-constrained sensor nodes can cooperate in a fully autonomous and distributed manner to substantially improve the energy efficiency of the wireless sensor network as a whole.

The analysis presented in Chapter 8 has illustrated the fundamental behaviour of ECO-OP, whereas the analysis presented in this chapter has established the general validity of network-wide cooperation using ECO-OP as an effective energy saving technique for wireless sensor networks. In Chapters 10 and 11 the long-term effectiveness of network-wide cooperation using ECO-OP is explicitly investigated in terms of the network lifetime extension achieved via cooperative communication. Moreover, in Chapters 10 and 11 the performance of the low-complexity distributed ECO-OP cooperation strategy proposed in this thesis is compared against that of a computationally intensive centralised cooperation algorithm from the literature [18].

Chapter 10

Illustration of Network Lifetime Extension via Network-wide Cooperation

10.1 Introduction

The low-complexity distributed ECO-OP cooperation strategy presented in Chapter 7 has been proposed in this thesis as a technique for extending the lifetime of a wireless sensor network by facilitating energy-conserving cooperation among its sensor nodes. However, ECO-OP is designed to simply maximise the energy efficiency of individual cooperative links in the network, without any regard to the resulting distribution of cooperation partner service or node lifetimes over the network. This means that ECO-OP is intended to achieve its overall aim of network lifetime extension *indirectly*. The energy conservation performance of network-wide cooperation using ECO-OP was examined in Chapters 8 and 9, serving to demonstrate that the distributed cooperation decisions made by individual nodes using ECO-OP indeed constitute an effective energy saving technique for wireless sensor networks. However, the analysis in Chapters 8 and 9 only provides some tentative conclusions regarding the long-term viability of ECO-OP, being concerned solely with the network-wide energy impact of the initial ECO-OP partner selection round at the time of the network's deployment. Thus in order to establish the validity of ECO-OP as an effective technique for extending the lifetime of a wireless sensor network, it is crucial to explicitly investigate the long-term benefit of network-wide cooperation using ECO-OP.

In this chapter network-wide cooperation using ECO-OP is illustrated throughout the lifetime of the wireless sensor network. The long-term impact of ECO-OP is thus explicitly examined in terms of the network lifetime extension achieved via cooperative communication. Moreover, the performance of the low-complexity distributed ECO-OP

cooperation strategy is compared throughout this chapter against that of a computationally intensive centralised greedy cooperation algorithm from the literature [18]. The algorithm proposed in [18] is designed to maximise the minimum node lifetime in an energy-constrained wireless network using cooperative communication, whereby a central controller performs a computationally intensive offline greedy search to allocate cooperation partners and transmit power for each node in the network. Whenever a node depletes its energy, the centralised greedy cooperation algorithm [18] must be repeated in order to reallocate a cooperation partner to each surviving source node in the network¹. Importantly, this affords the centralised greedy cooperation algorithm [18] the advantage of continually balancing the projected lifetimes of all remaining nodes based on the distribution of residual energy in the network. By contrast, using ECO-OP only the source nodes associated with the expired partner node reselect a partner, and nodes are ignorant of the residual energy of other nodes. The analysis in this chapter serves to illustrate the difference in the long-term behaviour and performance of these two fundamentally distinct approaches to coordinating cooperative communication in an energy-constrained wireless network. Importantly, the network lifetime extension performance of the centralised greedy cooperation algorithm [18] thus serves as a benchmark for evaluating the effectiveness of the distributed ECO-OP cooperation strategy proposed in this thesis as a technique for extending the lifetime of a wireless sensor network.

In this chapter network-wide cooperation is illustrated throughout the lifetime of the wireless sensor network in the three representative network topologies (A, B, C) introduced in Section 7.4, by simulating cooperation among $M=100$ nodes regularly placed over a 100 m by 100 m network area. The network lifetime extension performance of ECO-OP with different partner choice rules (GKH_1 , GKH_2 , and LKH , random partner) and the centralised greedy cooperation algorithm [18] is investigated. Firstly, the overall impact of network-wide cooperation over the lifetime of the wireless sensor network is demonstrated for each cooperation strategy by considering the resulting lifetime of each individual node in the cooperative network versus the non-cooperative network. Secondly, the lifetime extension performance of each cooperation strategy is presented in terms of the x^{th} node lifetime versus the number of node deaths since network activation x , where the x^{th} node lifetime in a non-cooperative and cooperative wireless sensor network are defined as $T_{non-coop_node(x)}$ and $T_{coop_node(x)}$ as given by (7.14) and (7.17) respectively. Moreover, an alternative representation of these lifetime extension results is presented in terms of the x^{th} node lifetime improvement factor, which is defined as the ratio of $T_{coop_node(x)}$ to

¹Whereas the analysis presented in [18] only considers network lifetime in terms of the time to first node death, the analysis presented in this chapter investigates network-wide cooperative communication from network activation through to the last node death. Therefore in generating the simulation results in this chapter, the centralised greedy algorithm [18] was first performed following network activation and then re-run each time a node depletes its battery energy.

$T_{non-coop_node(x)}$, as given by (7.12). The overall network lifetime extension performance of network-wide cooperation is then quantified in terms of the average network lifetime improvement factor achieved by each cooperation strategy, which is defined as the average of the x^{th} node lifetime improvement factors achieved over all values of x , as given by (7.13). Finally, the long-term behaviour of network-wide cooperation is illustrated by considering “who helps whom” using different cooperation strategies, in terms of the average distribution of cooperation partner service and selection throughout the lifetime of the wireless sensor network. Network lifetime extension via cooperative communication is thus investigated for the Topology A (central destination receiver) network in Section 10.2, the Topology B (remote destination receiver) network in Section 10.3, and the Topology C (node-to-node communication) network in Section 10.4.

The reference cooperative system parameters specified in Table 2.1 are employed throughout the analysis presented in this chapter. As stated in Chapter 7, a TDMA wireless sensor network with uniform traffic is assumed in generating the simulation results presented in this chapter, whereby every source node in the network in turn sends a message block of $B=100$ bits to its destination receiver in each transmission round. Moreover, it is assumed that prior to network activation all sensor nodes have an initial battery energy of $E_{battery}=10$ J for Topology A and C networks and $E_{battery}=100$ J for Topology B networks, and that each node in the network acts as a source and is eligible to be selected as a cooperation partner by any other source node. It is important to note that the ECO-OP simulation results presented in this chapter are based on an implementation of the overall distributed ECO-OP cooperation strategy employed by each source node in the cooperative network throughout its lifetime², as specified in Fig. 7.2. For further details of the ECO-OP cooperation strategy, the simulation parameters and assumptions related to this investigation, and the node and network lifetime metrics employed in this chapter, please refer to Sections 7.2, 7.4, and 7.6 respectively. For a detailed description of the centralised greedy cooperation algorithm [18] and further details of its implementation in generating the simulation results presented in this chapter, please refer to Appendix A.

²By contrast, the simulation results in Chapters 8 and 9 are based on a static distribution of cooperation partner service from the initial ECO-OP partner selection round at the time of the network’s deployment, as specified in Fig. 7.1.

10.2 Topology A Network: Central Destination Receiver

Fig. 10.1 shows the relative lifetime³ of each individual node in the Topology A network, using non-cooperative communication and cooperative communication with different cooperation strategies. Fig. 10.1 illustrates that network-wide cooperation significantly extends the lifetime of the majority of the $M = 100$ nodes in the Topology A network, for all considered cooperation strategies. In particular, Fig. 10.1 clearly demonstrates that cooperation significantly increases the minimum and median node lifetimes in the Topology A network. Fig. 10.1 also shows that the lifetimes of the four nodes closest to the central destination receiver are up to seven times shorter in the cooperative networks. As discussed in Section 8.2, this is due to these nodes being too close to the destination receiver to benefit from cooperation themselves but nevertheless serving as partners for other source nodes in the network.

Fig. 10.1 also illustrates that the order in which individual nodes in the network deplete their energy typically differs between the non-cooperative and cooperative networks; this is most evident in comparing the cooperative GKH_2 network to the non-cooperative network. As discussed in Section 7.6, per-node fairness is unimportant in a wireless sensor network compared to the overall well-being of the network. Consequently, the cooperative lifetime improvement for the $(\frac{x}{M})^{th}$ percentile of nodes is of interest in this thesis (rather than the cooperative lifetime improvement per individual node). The x^{th} node lifetime in a non-cooperative and cooperative wireless sensor network are defined as $T_{non-coop_node(x)}$ and $T_{coop_node(x)}$ and are given by (7.14) and (7.17) respectively. Fig. 10.2 shows the x^{th} node lifetime versus x , the number of node deaths since network activation, for the Topology A network of Fig. 10.1, using non-cooperative communication and cooperative communication with different cooperation strategies. An alternative representation of the results in Fig. 10.2 is presented in Fig. 10.3, which shows the x^{th} node lifetime improvement factor versus x for the Topology A network of Fig. 10.1 using different cooperation strategies. As discussed in Section 7.6, it is common to define the operational lifetime of a wireless sensor network as the time until the x^{th} node death [5], where x must be appropriately chosen to represent the proportion of nodes that must remain alive to maintain a functional network. Fig. 10.3 thus shows the cooperative network lifetime improvement as quantified by selecting different values of x to represent the lifetime of the network.

³Node lifetimes are only indicated graphically in Figs. 10.1, 10.6, and 10.11 without any numerical data, since the primary purpose of these plots is to illustrate the distribution of node lifetime over the cooperative Topology A, B, and C networks respectively.

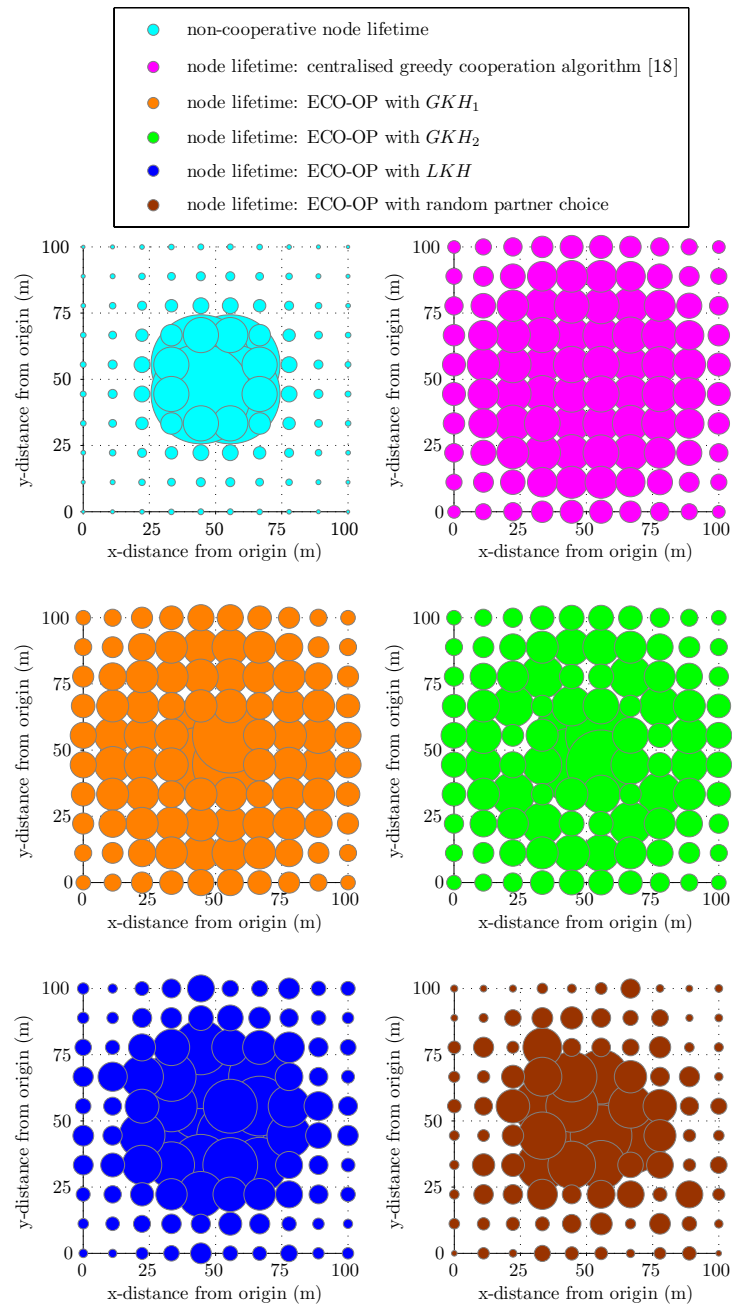


Figure 10.1: Node lifetime in a Topology A network (central destination receiver) of $M=100$ nodes regularly placed over a 100 m by 100 m network area, using non-cooperative communication and cooperative communication with different cooperation strategies. The size of each node is proportional to its lifetime.

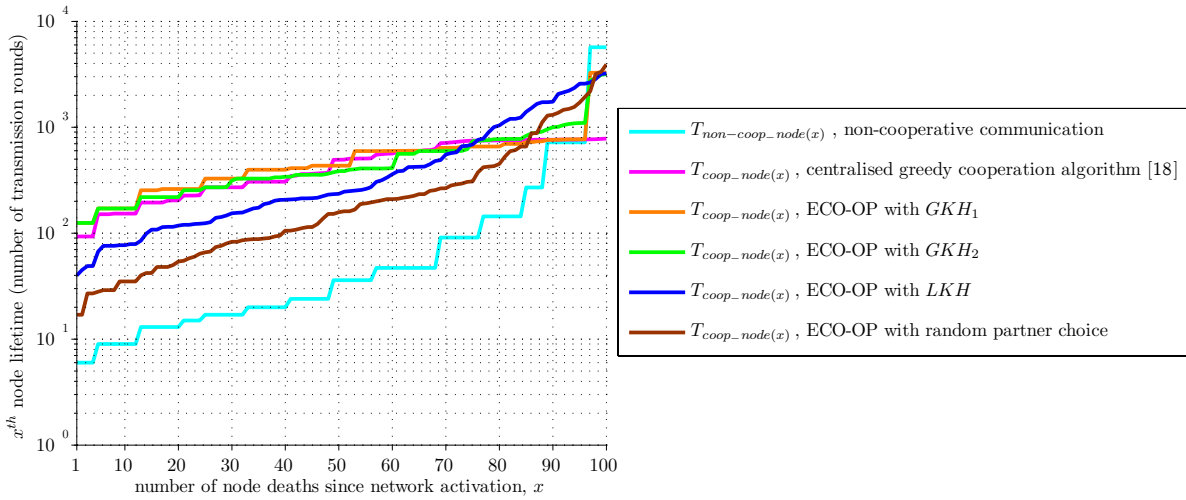


Figure 10.2: Node lifetime vs. number of node deaths since network activation for a Topology A network (central destination receiver) of $M=100$ nodes regularly placed over a 100 m by 100 m network area, using non-cooperative communication and cooperative communication with different cooperation strategies.

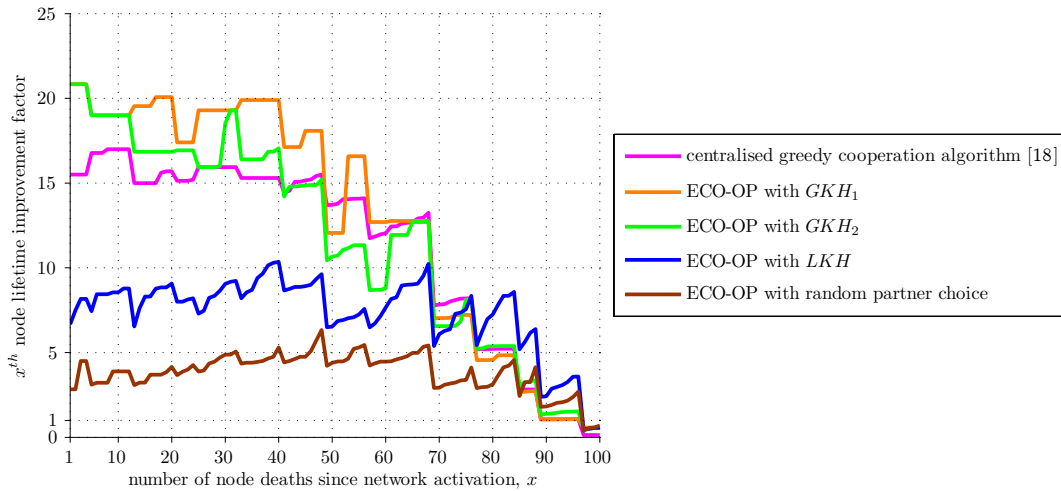


Figure 10.3: x^{th} node lifetime improvement factor vs. x for a Topology A network (central destination receiver) of $M=100$ nodes regularly placed over a 100 m by 100 m network area, using different cooperation strategies.

Lastly, in order to summarise the cooperative lifetime improvement achieved over the entire lifetime of the network, the average network lifetime improvement factor was defined in (7.13) as the average of the x^{th} node lifetime improvement factors achieved over all values of x . Table 10.1 summarises the x^{th} node lifetime improvement results presented in Fig. 10.3 in terms of the average network lifetime improvement factor achieved by each cooperation strategy.

Table 10.1: Cooperative network lifetime improvement in a Topology A network (central destination receiver) of $M=100$ nodes regularly placed over a 100 m by 100 m network area, using different cooperation strategies.

Cooperation strategy	Average network lifetime improvement factor
centralised greedy cooperation algorithm [18]	11.4
ECO-OP with GKH_1	13.0
ECO-OP with GKH_2	11.7
ECO-OP with LKH	7.3
ECO-OP with random partner choice	3.8

Fig. 10.2 confirms that the x^{th} node lifetime achieved by cooperative communication is substantially higher than that resulting from non-cooperative communication for the Topology A network of Fig. 10.1, for all but the last four node deaths. Specifically, network-wide cooperation in the Topology A network achieves an x^{th} node lifetime improvement factor ranging from 20.8 to 0.14, as shown by Fig. 10.3. Importantly, Figs. 10.2 and 10.3 reveal that the distributed ECO-OP cooperation strategy with GKH_1 or GKH_2 overall achieves a comparable x^{th} node lifetime improvement in the Topology A network to the centralised greedy cooperation algorithm proposed in [18]. This is reflected in Table 10.1, which reveals that ECO-OP with GKH_1 achieves the highest average network lifetime improvement factor of 13.0, followed by ECO-OP with GKH_2 which results in an average network lifetime improvement factor of 11.7. For comparison, the centralised greedy cooperation algorithm [18] yields an average network lifetime improvement factor of 11.4, which is slightly lower than that achieved by ECO-OP with GKH_1 and GKH_2 . Furthermore, Table 10.1 shows that ECO-OP with LKH achieves an average network lifetime improvement factor of 7.3, which is 1.8 times lower than that achieved by ECO-OP with GKH_1 . Nonetheless, ECO-OP with LKH yields a very substantial network lifetime improvement which is 1.9 times higher than that achieved by ECO-OP with random partner choice. This is also readily observed in Fig. 10.2, which shows that ECO-OP with LKH generally results in a substantially lower x^{th} node lifetime than ECO-OP with GKH_1 , but consistently achieves a higher x^{th} node lifetime than ECO-OP with random partner choice.

It is interesting to note from Fig. 10.2 that the centralised greedy cooperation algorithm [18] and ECO-OP with GKH_1 and GKH_2 exhibit a noticeably less steep lifetime curve than that of non-cooperative communication, whereas the lifetime curves of ECO-OP with LKH and random partner choice are nearly as steep as that of non-cooperative communication. A less steep lifetime curve is a reflection of a more uniform distribution of node lifetimes over the network; in general, the ideal x^{th} node lifetime

vs. x curve is a horizontal line (such that all nodes have equal lifetimes and the network remains fully functional throughout its operation) which crosses the y-axis at the highest value possible (corresponding to the longest possible network lifetime). Fig. 10.1 confirms that the former three cooperation strategies result in a significantly more uniform node lifetime distribution over the Topology A network than non-cooperative communication. This improved node lifetime fairness is achieved by extending the lifetimes of the nodes with the lowest non-cooperative lifetimes the most, as illustrated by the decreasing x^{th} node lifetime improvement factor as x is increased in Fig. 10.3. By contrast, Fig. 10.3 shows that ECO-OP with *LKH* and random partner choice result in a relatively constant x^{th} node lifetime improvement factor. This is consistent with the node lifetime distributions exhibited by these two cooperation strategies in Fig. 10.1 which are similar to that of non-cooperative communication.

These node lifetime fairness results may be explained by considering “who helps whom” using each cooperation strategy. Fig. 10.4 presents the average distribution of cooperation partner service throughout the lifetime of the Topology A network of Fig. 10.1 using different cooperation strategies, in terms of the number of source nodes that each node in the network serves as cooperation partner to per transmission round⁴. Fig. 10.4 shows that using ECO-OP with *LKH* all nodes serve as partner to around one other source node per transmission round. Neighbouring nodes with similar non-cooperative lifetimes act as each other’s cooperation partners; consequently ECO-OP with *LKH* maintains the relative node lifetime distribution of the non-cooperative network, as illustrated by Fig. 10.1. Similarly, Figs. 10.1 and 10.4 illustrate that ECO-OP with random partner choice results in an uneven distribution of node lifetime over the Topology A network due to nodes serving as cooperation partners regardless of their own non-cooperative lifetime. By contrast, comparing Figs. 10.1 and 10.4 reveals that the centralised greedy cooperation algorithm [18], ECO-OP with *GKH*₁, and ECO-OP with *GKH*₂ all select nodes with high non-cooperative lifetimes to serve as partners to nodes with low non-cooperative lifetimes. By doing so, these three cooperation strategies reallocate the network’s combined energy resource to achieve a substantially more uniform node lifetime distribution over the network.

It is interesting to note that the ECO-OP node lifetime results in Fig. 10.1 are thus consistent with those predicted by the node energy consumption over the Topology A network in Fig. 8.3 corresponding to the initial partner selection at the time of the network’s deployment. Similarly, the average distribution of cooperation partner service throughout

⁴The average number of source nodes per transmission round that are served by some partner node x is given by $\left(\sum_{h \in \mathbf{H}'} D_h \right)$ in terms of the notation presented in Section 7.6.2, where D_h is the proportion of the x^{th} node’s lifetime that it serves as partner to node $h \in \mathbf{H}'$ and \mathbf{H}' is the set of source nodes that select the x^{th} node as their partner throughout its lifetime.

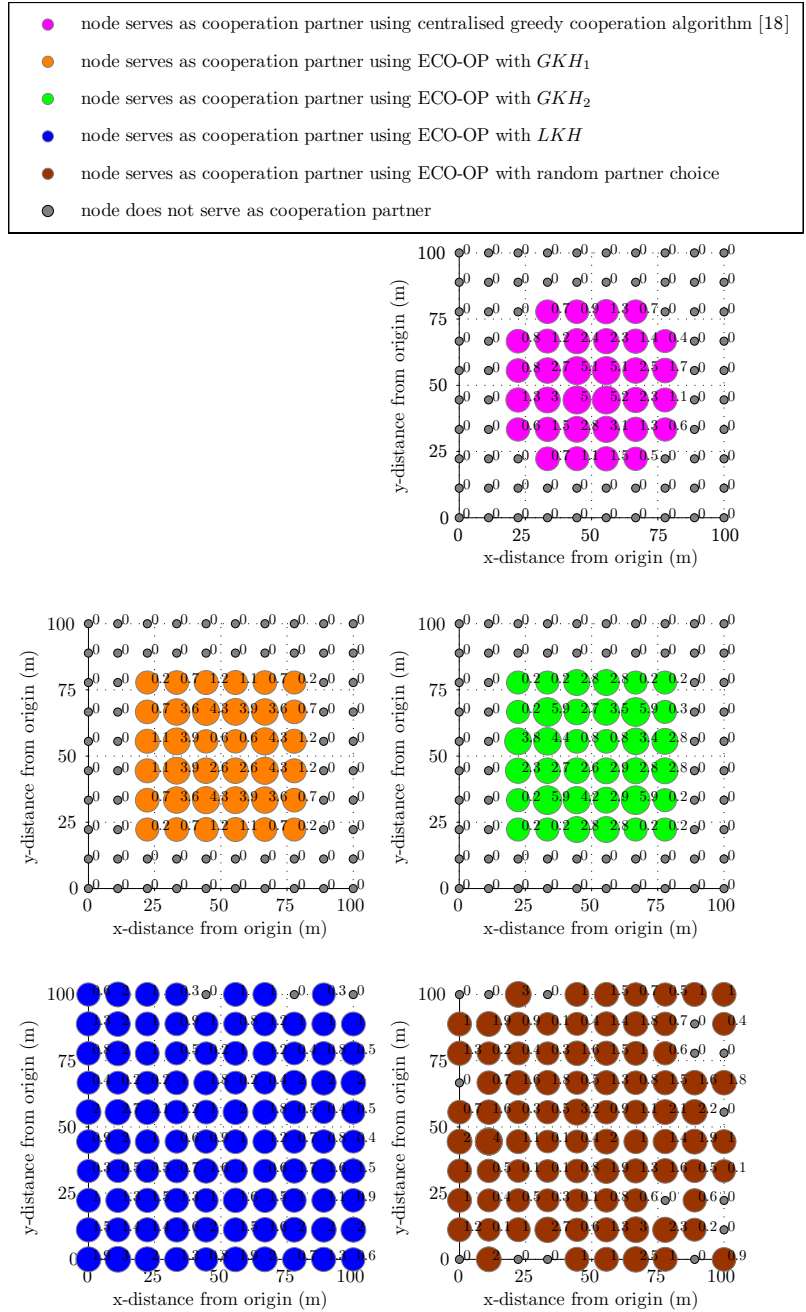


Figure 10.4: Average distribution of cooperation partner service throughout the lifetime of a Topology A network (central destination receiver) of $M=100$ nodes regularly placed over a 100 m by 100 m network area, using different cooperation strategies. The size of each node is proportional to the average number of source nodes it serves as cooperation partner to per transmission round (each node is also marked with this number).

the lifetime of the Topology A network presented in Fig. 10.4 is very similar to the distribution of cooperation partner service in Fig. 8.2 from the initial partner selection round. This shows that the overall pattern of ECO-OP partner service does not change substantially throughout the lifetime of the Topology A network. This is confirmed by Fig. 10.5, which shows the number of cooperation partners that each source node in the Topology A network selects throughout its lifetime⁵. Using ECO-OP a source node only reselects its cooperation partner once its existing partner node is about to deplete its batteries. Consequently, Fig. 10.5 shows that nodes reselect their cooperation partner no more than 3, 4, and 6 times throughout their lifetimes using ECO-OP with GKH_1 , GKH_2 , and LKH respectively. This demonstrates that network-wide cooperation using ECO-OP entails a low signalling and organisational overhead throughout the lifetime of the Topology A network. By contrast, using the centralised greedy cooperation algorithm [18], whenever a node depletes its energy each surviving source node in the network is allocated its cooperation partner anew by the central controller, as illustrated in Fig. 10.5.

Finally, Fig. 10.4 shows that the centralised greedy cooperation algorithm [18] results in a very similar partner allocation to ECO-OP with GKH_1 or GKH_2 . Importantly, the distinct underlying approaches of the two cooperation strategies are also illustrated by Fig. 10.4: the centralised greedy cooperation algorithm [18] selects as cooperation partners the nodes that can *most afford to help* (i.e. the nodes closest to the destination receiver with the highest non-cooperative lifetimes are selected most frequently), whereas ECO-OP with GKH_1 or GKH_2 selects as cooperation partners the nodes that can *help the most* (i.e. the partner node midway between the source and the destination receiver which minimises the energy spent over the cooperative link). This distinction between the two cooperation strategies is also reflected in the results of Fig. 10.2, which shows that the centralised greedy cooperation algorithm [18] achieves a more uniform x^{th} node lifetime than ECO-OP with GKH_1 or GKH_2 , at the expense of substantially diminished lifetimes for the last 15% of node deaths.

⁵The number of partner nodes that some source node x cooperates with throughout its lifetime is given by I in terms of the notation presented in Section 7.6.2.

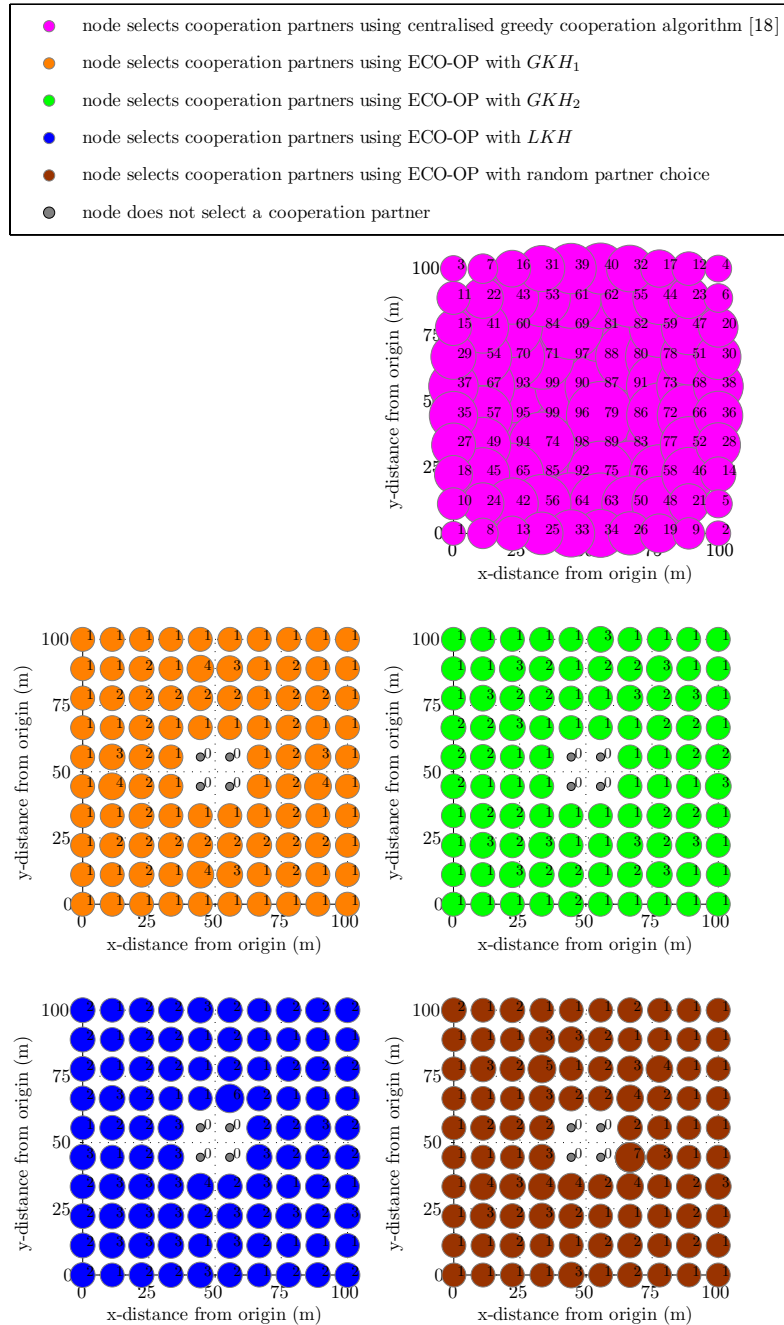


Figure 10.5: Distribution of cooperation partner selection in a Topology A network (central destination receiver) of $M=100$ nodes regularly placed over a 100 m by 100 m network area, using different cooperation strategies. The size of each node is proportional to the number of cooperation partners the source node selects throughout its lifetime (each node is also marked with this number).

10.3 Topology B Network: Remote Destination Receiver

Fig. 10.6 illustrates the relative lifetime of each individual node in the Topology B network, using non-cooperative communication and cooperative communication with different cooperation strategies, $T_{non-coop_node}$ and T_{coop_node} respectively⁶. Fig. 10.7 shows the x^{th} node lifetime versus x , the number of node deaths since network activation, for the Topology B network of Fig. 10.6, using non-cooperative communication and cooperative communication with different cooperation strategies. Fig. 10.8 is an alternative representation of the results in Fig. 10.7, showing the x^{th} node lifetime improvement factor versus x for the Topology B network of Fig. 10.6 using different cooperation strategies. Lastly, Table 10.2 summarises the x^{th} node lifetime improvement results presented in Fig. 10.8 in terms of the average network lifetime improvement factor achieved by each cooperation strategy.

Fig. 10.6 shows that network-wide cooperation significantly extends the lifetime of all of the $M=100$ nodes in the Topology B network, for all considered cooperation strategies. This result is consistent with the significant energy savings achieved by each node in the Topology B network in Fig. 8.5 regardless of cooperation strategy, which is due to all nodes in the Topology B network being within each other's energy efficient partner choice region, as discussed in Section 8.3. Fig. 10.7 confirms that the x^{th} node lifetime achieved by cooperative communication is consistently significantly higher than that resulting from non-cooperative communication for the Topology B network of Fig. 10.6. Specifically, network-wide cooperation in the Topology B network achieves an x^{th} node lifetime improvement factor ranging from 2.5 to 16, as shown by Fig. 10.8.

Importantly, Figs. 10.7 and 10.8 reveal that the distributed ECO-OP cooperation strategy with GKH_1 or GKH_2 overall achieves a comparable x^{th} node lifetime improvement in the Topology B network to the centralised greedy cooperation algorithm proposed in [18]. Specifically, Table 10.2 shows that the centralised greedy cooperation algorithm [18] achieves an average network lifetime improvement factor of 8.8, which is somewhat lower than that achieved by ECO-OP with GKH_1 and GKH_2 , which yield an average network lifetime improvement factor of 9.4 and 9.2 respectively. Table 10.2 also shows that ECO-OP with LKH results in an average network lifetime improvement factor of 7.8, which is 1.2 times lower than that achieved by ECO-OP with GKH_1 .

⁶It should be noted that different scaling factors are employed in Figs. 10.1, 10.6, and 10.11 to represent the relative node lifetimes over the Topology A, B, and C networks. Each network topology is associated with a different absolute node lifetime range, and thus the relative node lifetime values illustrated in these three figures cannot be explicitly compared.

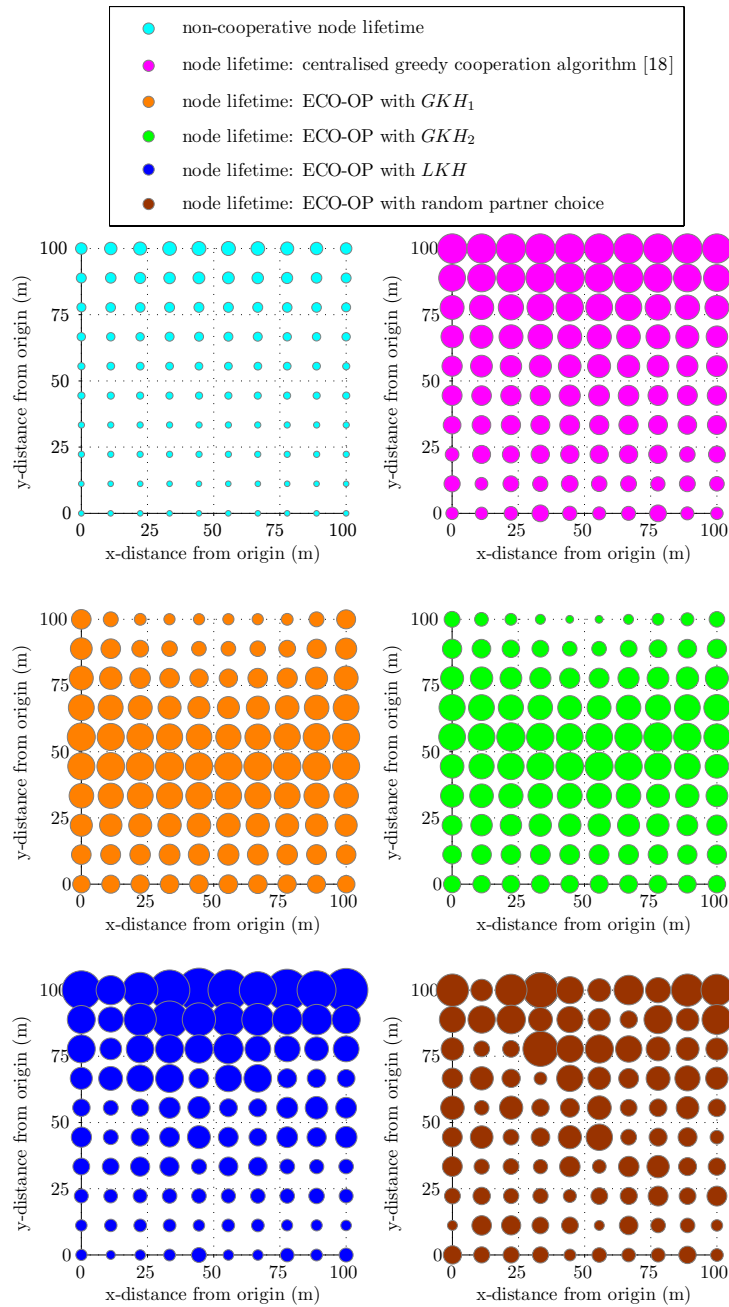


Figure 10.6: Node lifetime in a Topology B network (remote destination receiver) of $M=100$ nodes regularly placed over a 100 m by 100 m network area, using non-cooperative communication and cooperative communication with different cooperation strategies. The size of each node is proportional to its lifetime.

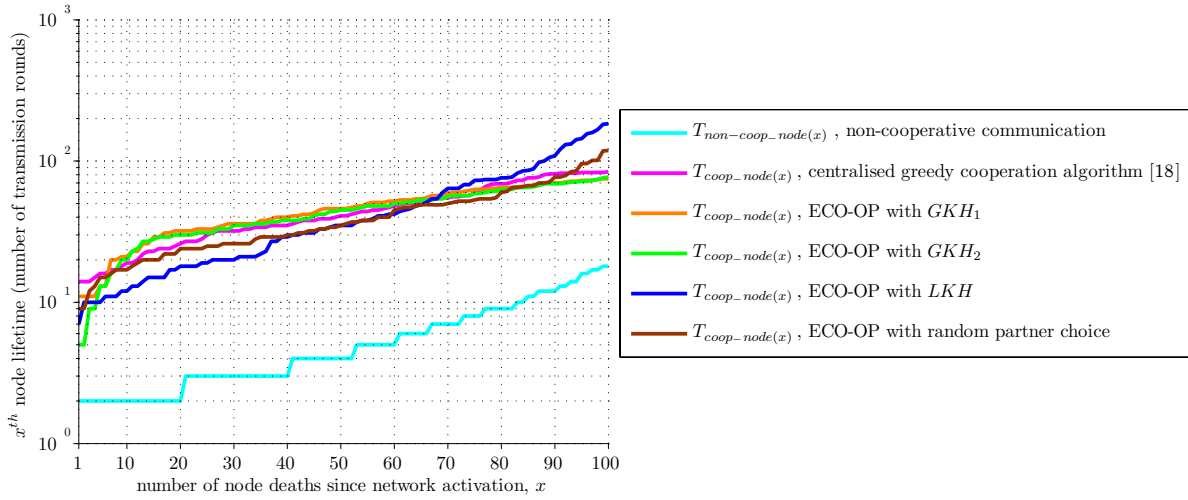


Figure 10.7: Node lifetime vs. number of node deaths since network activation for a Topology B network (remote destination receiver) of $M=100$ nodes regularly placed over a 100 m by 100 m network area, using non-cooperative communication and cooperative communication with different cooperation strategies.

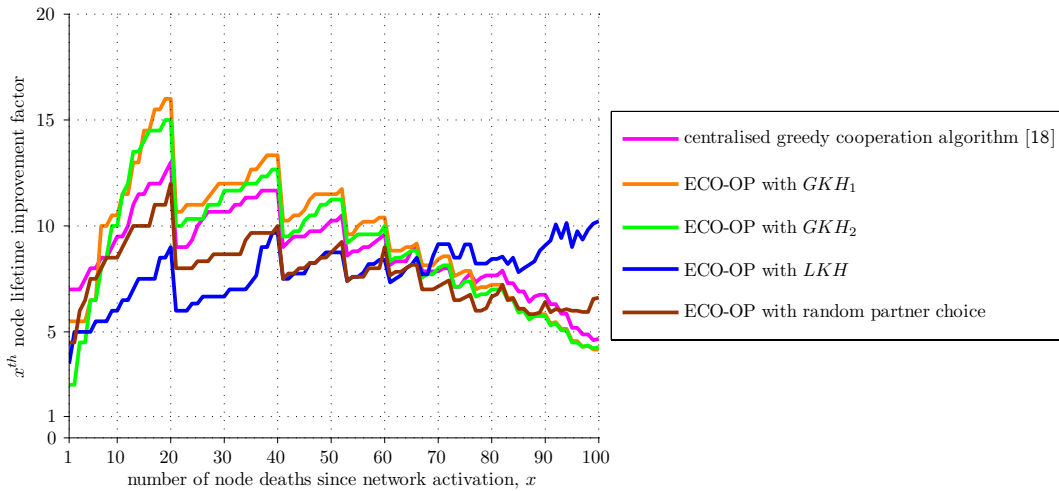


Figure 10.8: x^{th} node lifetime improvement factor vs. x for a Topology B network (remote destination receiver) of $M=100$ nodes regularly placed over a 100 m by 100 m network area, using different cooperation strategies.

Moreover, Table 10.2 shows that ECO-OP with random partner choice yields the same average network lifetime improvement factor in the Topology B network as ECO-OP with *LKH*. This follows from the results presented in Fig. 10.7, which show that ECO-OP with *LKH* generally results in a lower x^{th} node lifetime than ECO-OP with random partner choice for the first 50% of node deaths, and vice versa for the last 50% of node deaths. This trend is due to the fact that the nodes with the lowest non-cooperative lifetimes (i.e. those located in the lower half of the Topology B network, furthest from the remote destination receiver) generally randomly select a partner node located closer to the

Table 10.2: Cooperative network lifetime improvement in a Topology B network (remote destination receiver) of $M=100$ nodes regularly placed over a 100 m by 100 m network area, using different cooperation strategies.

Cooperation strategy	Average network lifetime improvement factor
centralised greedy cooperation algorithm [18]	8.8
ECO-OP with GKH_1	9.4
ECO-OP with GKH_2	9.0
ECO-OP with LKH	7.8
ECO-OP with random partner choice	7.8

neighbouring partner node chosen by LKH , as discussed in Section 8.3. It is interesting to note that the node lifetime results in Fig. 10.6 for ECO-OP with LKH and random partner choice are thus consistent with those predicted by the node energy consumption over the Topology B network in Fig. 8.7 corresponding to the initial partner selection at the time of the network's deployment.

By contrast, the node lifetime results in Fig. 10.7 for ECO-OP with GKH_1 and GKH_2 noticeably differ from those predicted by the node energy consumption over the Topology B network in Fig. 8.7. This is because the overall pattern of GKH_1 and GKH_2 partner service changes considerably throughout the lifetime of the Topology B network. Fig. 10.9 presents the average distribution of cooperation partner service throughout the lifetime of the Topology B network of Fig. 10.6 using different cooperation strategies, in terms of the number of source nodes that each node in the network serves as cooperation partner to per transmission round. Fig. 10.9 clearly illustrates that in the long term GKH_1 and GKH_2 result in a much more even distribution of cooperation partner service than the highly concentrated distribution from the initial partner selection round in Fig. 8.6. Namely, the partner service burden becomes increasingly distributed over the Topology B network as the most popular partner nodes (i.e. those located nearest the middle of the top boundary of the network) deplete their energy. This is confirmed by Fig. 10.10, which shows the number of cooperation partners that each source node in the Topology B network selects throughout its lifetime using different cooperation strategies. Using ECO-OP with GKH_1 and GKH_2 nodes reselect their cooperation partner up to 21 and 29 times respectively. Thus network-wide cooperation using ECO-OP with GKH_1 and GKH_2 entails a higher signalling and organisational overhead throughout the lifetime of the Topology B network compared with the Topology A network, as evidenced by a comparison of Figs. 10.10 and 10.5. By contrast, Fig. 10.10 shows that using ECO-OP with LKH and random partner choice nodes reselect their cooperation partner no more

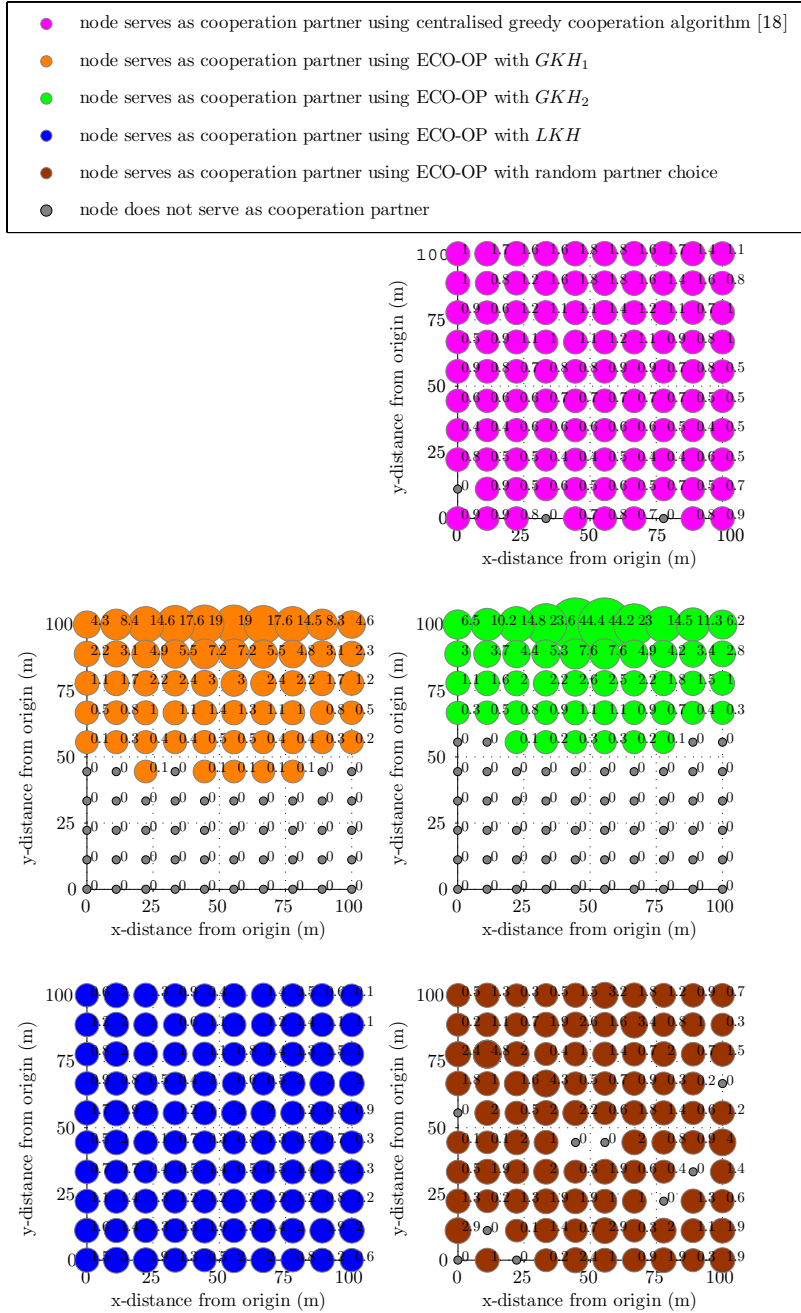


Figure 10.9: Average distribution of cooperation partner service throughout the lifetime of a Topology B network (remote destination receiver) of $M=100$ nodes regularly placed over a 100 m by 100 m network area, using different cooperation strategies. The size of each node is proportional to the average number of source nodes it serves as cooperation partner to per transmission round (each node is also marked with this number).

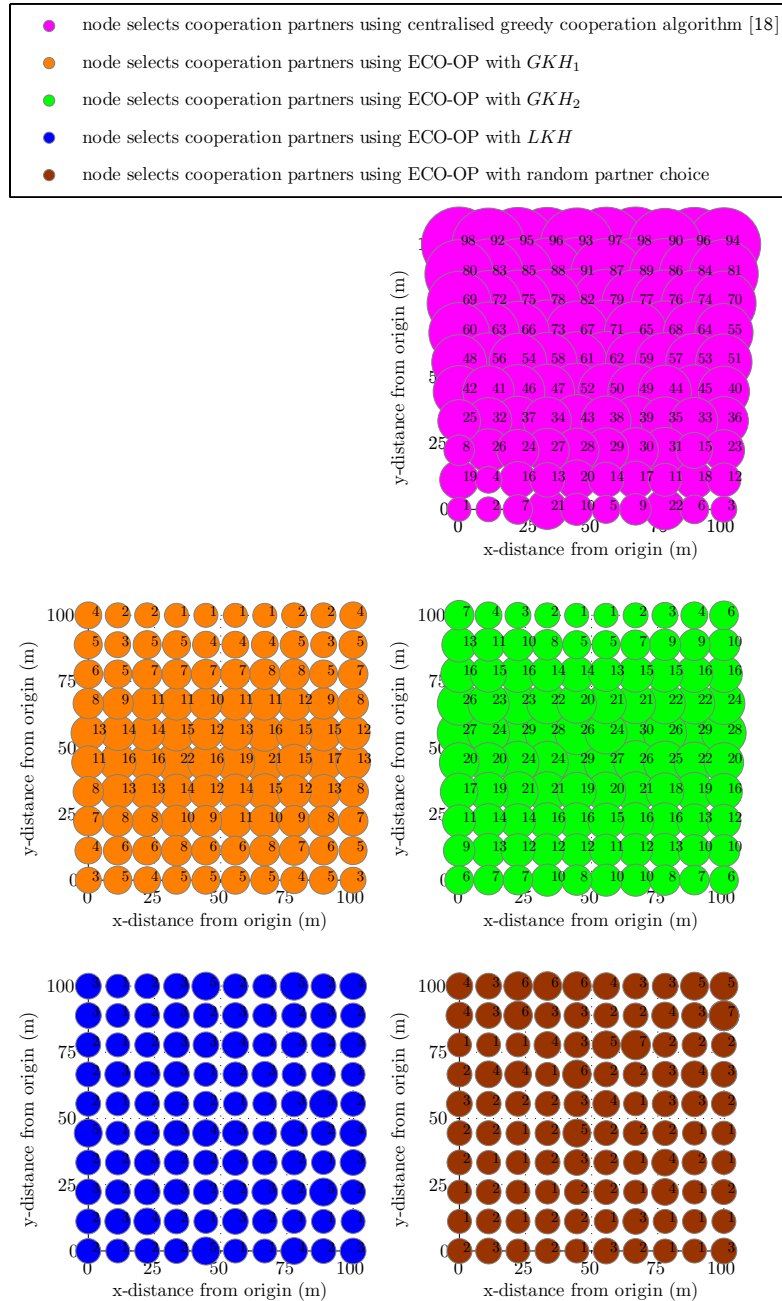


Figure 10.10: Distribution of cooperation partner selection in a Topology B network (remote destination receiver) of $M=100$ nodes regularly placed over a 100 m by 100 m network area, using different cooperation strategies. The size of each node is proportional to the number of cooperation partners the source node selects throughout its lifetime (each node is also marked with this number).

than 5 and 7 times throughout their lifetimes, respectively. Consequently, the average distribution of partner service over the Topology B network exhibited by these two cooperation strategies in Fig. 10.9 is very similar to the initial partner selection distribution in Fig. 8.6.

Furthermore, the pattern of partner service distribution over the lifetime of the Topology B network exhibited by ECO-OP with GKH_1 and GKH_2 in Fig. 10.9 is also reflected in the corresponding x^{th} node lifetime versus x curves in Fig. 10.7. Namely, ECO-OP with GKH_1 and GKH_2 result in substantially lower x^{th} node lifetimes than the other cooperation strategies for about the first 10% of node deaths. This accounts for the nodes located at the top of the Topology B network (as illustrated by Fig. 10.6), which deplete their batteries prematurely as a consequence of the unsustainably large cooperation partner burden placed upon them. However, the subsequent unavailability of these overpopular partner nodes forces a redistribution of partner service over the GKH_1 and GKH_2 Topology B network, producing the more balanced and sustainable partner allocation illustrated by Fig. 10.9. As a result, Fig. 10.7 shows that ECO-OP with GKH_1 and GKH_2 achieve a superior x^{th} node lifetime to the other cooperation strategies between the 10th and 70th percentile of node deaths. Arriving at a more balanced partner service distribution thus enables ECO-OP with GKH_1 and GKH_2 to reallocate the network's combined energy resource to substantially improve the node lifetime fairness across the Topology B network, as illustrated by Fig. 10.6.

Moreover, Figs. 10.7 and 10.6 reveal that ECO-OP with GKH_1 and GKH_2 overall achieve the most uniform distribution of node lifetime over the Topology B network of all the considered cooperation strategies. This is a very interesting result, as it refutes the prediction in Chapters 8 and 9 that GKH_1 and GKH_2 are unsustainable partner choice strategies for long-term cooperation in the Topology B network due to very popular partner nodes prematurely depleting their own batteries by helping numerous other nodes. The results in Fig. 10.7 clearly demonstrate that ECO-OP with GKH_1 and GKH_2 are not unsustainable long-term cooperation strategies; instead, the lifetimes of the first 10% of nodes are sacrificed in order to arrive at a partner service distribution which most benefits the rest of the network, both in terms of increased node lifetime and improved fairness. It is interesting to observe from Figs 10.9 and 10.6 that, as in the Topology A network, ECO-OP with GKH_1 and GKH_2 achieve an overall improved node lifetime fairness by selecting nodes with high non-cooperative lifetimes to serve as partners to nodes with low non-cooperative lifetimes. Conversely, Fig. 10.6 shows that ECO-OP with LKH and random partner choice maintain the uneven node lifetime distribution of the non-cooperative Topology B network, by virtue of nodes serving as cooperation partners regardless of their own non-cooperative lifetime, as illustrated by Fig. 10.9.

Finally, Fig. 10.9 shows that the centralised greedy cooperation algorithm [18] results in a markedly different partner allocation to ECO-OP with GKH_1 or GKH_2 in the Topology B network. Whereas ECO-OP with GKH_1 or GKH_2 selects as cooperation partners the nodes that can *help the most*, such that only the nodes in the top half of the Topology B network serve as cooperation partners, the centralised greedy cooperation algorithm [18] selects as cooperation partners the nodes that can *most afford to help*, such that the nodes at the top of the Topology B network carry only a slightly heavier partner burden than the nodes at the bottom of the network. Interestingly, this node-centric approach of aiming to equalise the projected node lifetimes over the network which underlies the algorithm from [18] turns out to be short-sighted in the Topology B network; as evidenced by Fig. 10.7, the centralised greedy cooperation algorithm [18] actually achieves a less uniform x^{th} node lifetime than ECO-OP with GKH_1 or GKH_2 for all but the first 10% of node deaths, as well as resulting in inferior node lifetimes between the 10th and 75th percentile of node deaths.

10.4 Topology C Network: Node-to-Node Communication

Fig. 10.11 illustrates the relative lifetime of each individual node in the Topology C network, using non-cooperative communication and cooperative communication with different cooperation strategies, $T_{non-coop_node}$ and T_{coop_node} respectively. Fig. 10.12 shows the x^{th} node lifetime versus x , the number of node deaths since network activation, for the Topology C network of Fig. 10.11, using non-cooperative communication and cooperative communication with different cooperation strategies. Fig. 10.13 is an alternative representation of the results Fig. 10.12, showing the x^{th} node lifetime improvement factor versus x for the Topology C network of Fig. 10.11 using different cooperation strategies. Lastly, Table 10.3 summarises the x^{th} node lifetime improvement results presented in Fig. 10.13 in terms of the average network lifetime improvement factor achieved by each cooperation strategy.

Fig. 10.11 shows that network-wide cooperation significantly extends the lifetime of the majority of the $M = 100$ nodes in the Topology C network, for all considered cooperation strategies. In particular, Fig. 10.1 clearly demonstrates that cooperation significantly increases the minimum and median node lifetimes in the Topology C network. Fig. 10.12 confirms that the x^{th} node lifetime achieved by cooperative communication is substantially higher than that resulting from non-cooperative communication for the Topology C network of Fig. 10.11, for all but the last few node deaths. Specifically, network-wide cooperation in the Topology C network achieves an x^{th} node lifetime improvement factor

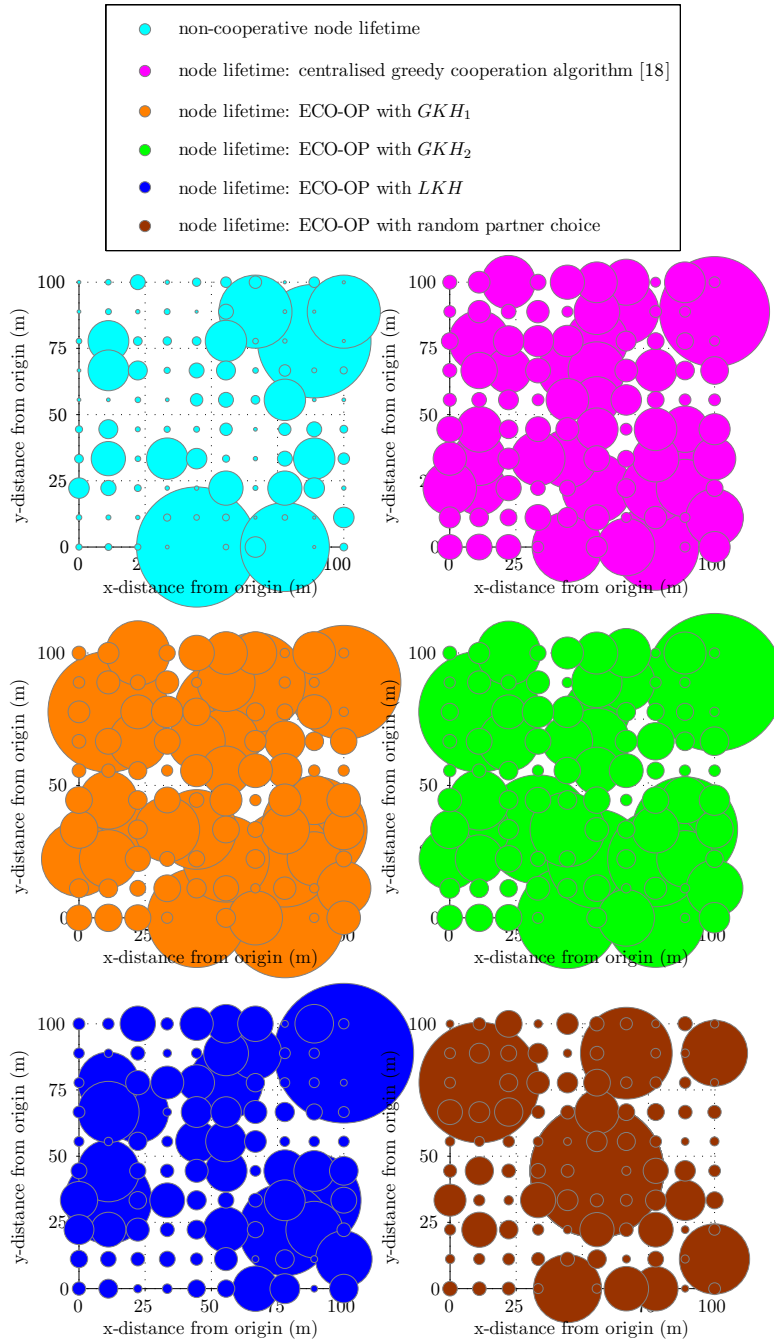


Figure 10.11: Node lifetime in a Topology C network (node-to-node communication) of $M=100$ nodes regularly placed over a 100 m by 100 m network area, using non-cooperative communication and cooperative communication with different cooperation strategies. The size of each node is proportional to its lifetime.

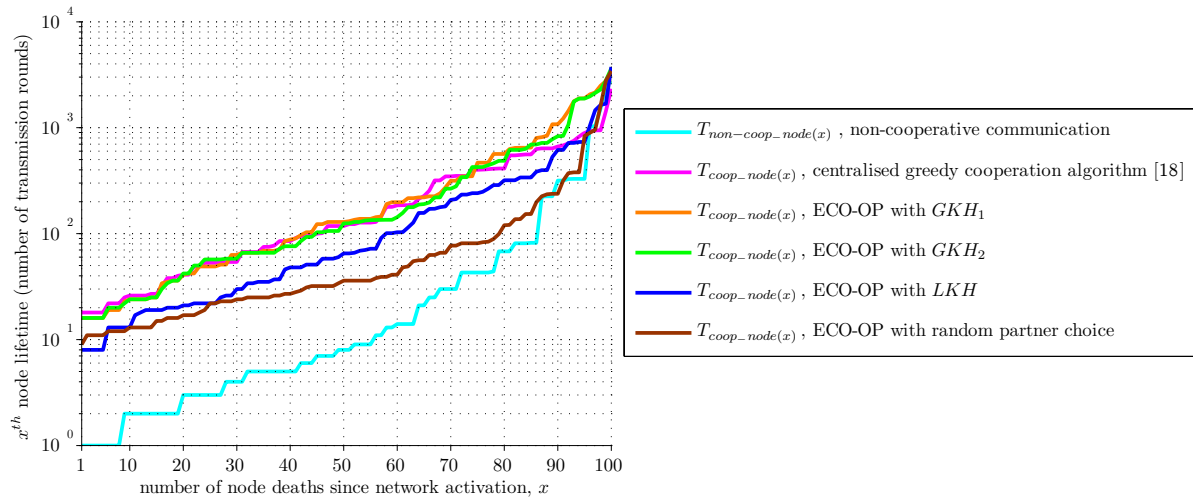


Figure 10.12: Node lifetime vs. number of node deaths since network activation for a Topology C network (node-to-node communication) of $M=100$ nodes regularly placed over a 100 m by 100 m network area, using non-cooperative communication and cooperative communication with different cooperation strategies.

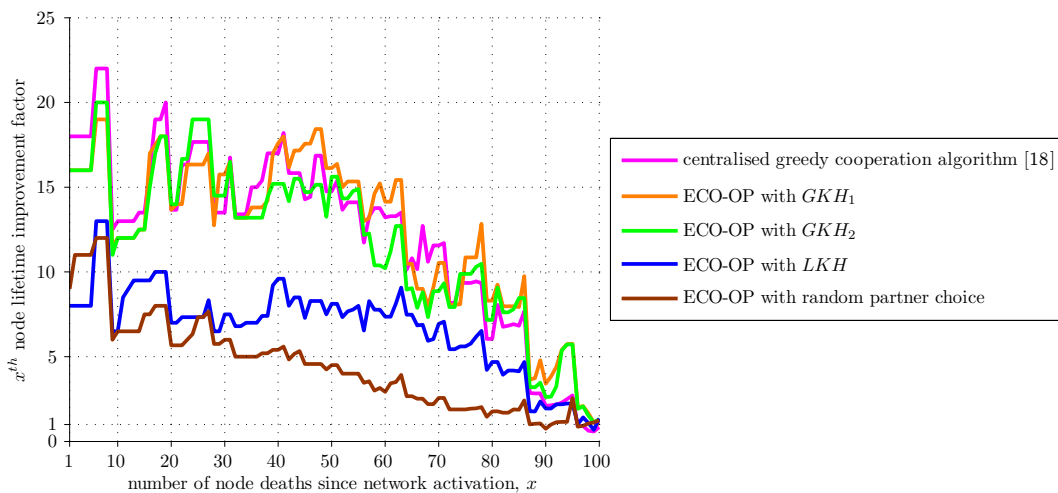


Figure 10.13: x^{th} node lifetime improvement factor vs. x for a Topology C network (node-to-node communication) of $M=100$ nodes regularly placed over a 100 m by 100 m network area, using different cooperation strategies.

Table 10.3: Cooperative network lifetime improvement in a Topology C network (node-to-node communication) of $M=100$ nodes regularly placed over a 100 m by 100 m network area, using different cooperation strategies.

Cooperation strategy	Average network lifetime improvement factor
centralised greedy cooperation algorithm [18]	12.1
ECO-OP with GKH_1	12.3
ECO-OP with GKH_2	11.7
ECO-OP with LKH	6.7
ECO-OP with random partner choice	4.5

ranging from 22.0 to 0.58, as shown by Fig. 10.13. As in the Topology A network, the slightly diminished lifetimes of the (1 to 5) nodes with the highest non-cooperative lifetimes in the Topology C network is due to these nodes being too close to their destination receiver node to benefit from cooperation themselves but nevertheless serving as partners for other source nodes in the network.

Importantly, Figs. 10.12 and 10.13 reveal that the distributed ECO-OP cooperation strategy with GKH_1 or GKH_2 overall achieves a comparable x^{th} node lifetime improvement in the Topology C network to the centralised greedy cooperation algorithm proposed in [18]. This is reflected in Table 10.3, which reveals that the centralised greedy cooperation algorithm [18] yields an average network lifetime improvement factor of 12.1 in the Topology C network of Fig. 10.11, which is slightly lower than the 12.3 factor improvement achieved by ECO-OP with GKH_1 but slightly higher than the 11.7 factor improvement achieved by ECO-OP with GKH_2 . Table 10.3 also shows that ECO-OP with LKH achieves an average network lifetime improvement factor of 6.7, which is 1.8 times lower than that achieved by ECO-OP with GKH_1 . Nonetheless, ECO-OP with LKH yields a very substantial network lifetime improvement which is 1.5 times higher than that achieved by ECO-OP with random partner choice. This is also readily observed in Fig. 10.12, which shows that ECO-OP with LKH generally results in a substantially lower x^{th} node lifetime than ECO-OP with GKH_1 , but generally achieves a higher x^{th} node lifetime than ECO-OP with random partner choice.

Furthermore, it is interesting to observe from Fig. 10.12 that all the considered cooperation strategies exhibit a less steep lifetime curves than that of non-cooperative communication. Fig. 10.11 confirms that cooperative communication always reallocates the network's combined energy resource to achieve a substantially more uniform node lifetime distribution over the Topology C network than non-cooperative communication. It is interesting to note that the ECO-OP node lifetime results in Fig. 10.11 are thus consistent with those predicted by the node energy consumption over the Topology C network in Fig. 8.11 corresponding to the initial partner selection at the time of the network's deployment. Moreover, Figs. 10.11 and 10.12 reveal that the centralised greedy cooperation algorithm [18] overall achieves the most uniform distribution of node lifetimes over the Topology C network of all the considered cooperation strategies, followed by ECO-OP with GKH_1 and GKH_2 . Fig. 10.14 presents the average distribution of cooperation partner service throughout the lifetime of the Topology C network of Fig. 10.11 using different cooperation strategies, in terms of the number of source nodes that each node in the network serves as cooperation partner to per transmission round. Comparing Figs. 10.11 and 10.14 shows that the nodes with the lowest non-cooperative lifetimes at the corners of the Topology C network are generally not selected as cooperation partners

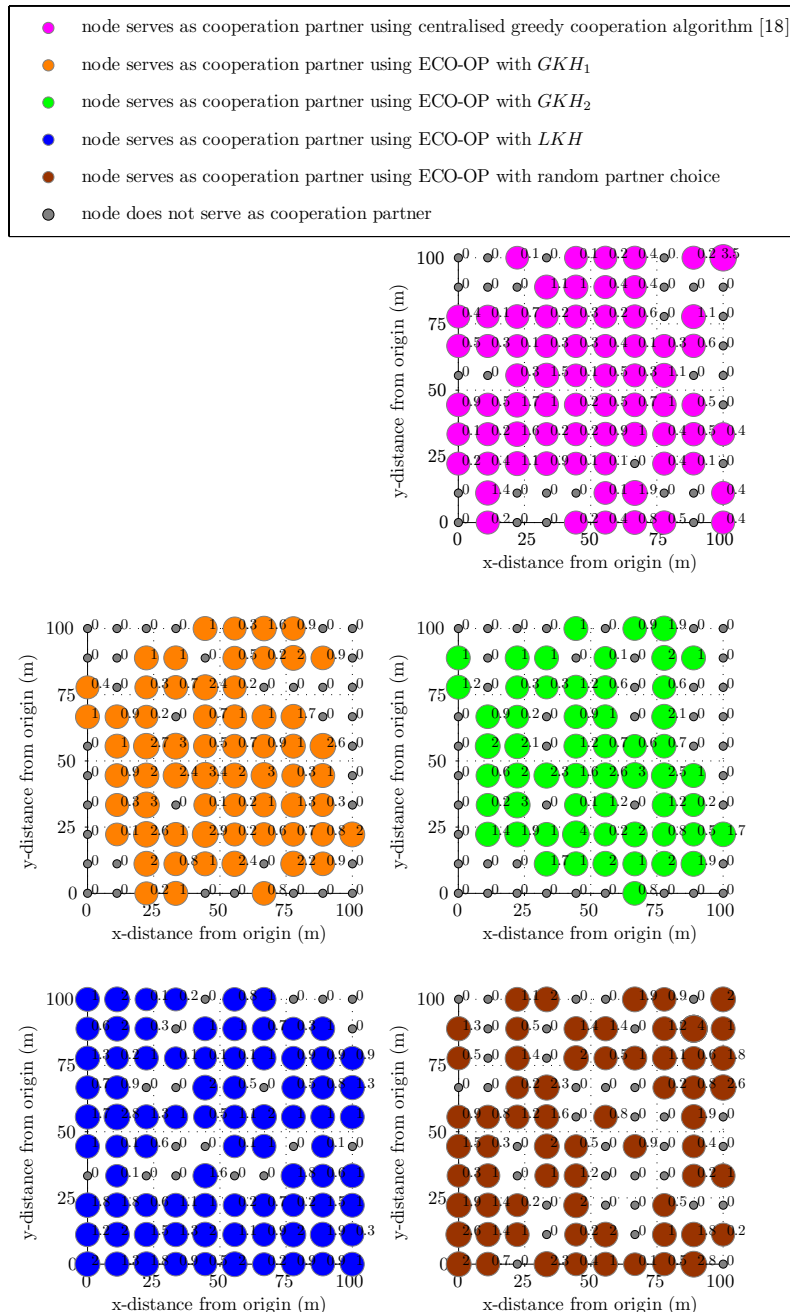


Figure 10.14: Average distribution of cooperation partner service throughout the lifetime of a Topology C network (node-to-node communication) of $M=100$ nodes regularly placed over a 100 m by 100 m network area, using different cooperation strategies. The size of each node is proportional to the average number of source nodes it serves as cooperation partner to per transmission round (each node is also marked with this number).

using the centralised greedy cooperation algorithm [18], ECO-OP with GKH_1 , and ECO-OP with GKH_2 . This is consistent with the finding in Section 8.4 that a weak negative correlation exists between a node's inherent communication energy requirements and its popularity as a cooperation partner in the Topology C network using GKH_1 and GKH_2 . Namely, the aforementioned three cooperation strategies achieve an overall improved node lifetime fairness over the Topology C network by generally selecting nodes with high non-cooperative lifetimes to serve as partners to nodes with low non-cooperative lifetimes. By contrast, Figs. 10.11 and 10.12 demonstrate that ECO-OP with LKH and random partner choice result in a much less even node lifetime distribution over the Topology C network, by virtue of nodes serving as cooperation partners regardless of their own non-cooperative lifetime, as illustrated by Fig. 10.14.

Finally, it is interesting to note that the average distribution of cooperation partner service throughout the lifetime of the Topology C network presented in Fig. 10.14 is very similar to the distribution of cooperation partner service in Fig. 8.10 from the initial partner selection round. This shows that the overall pattern of ECO-OP partner service does not change substantially throughout the lifetime of a Topology C network. This is confirmed by Fig. 10.15, which shows the number of cooperation partners that each source node in the Topology C network selects throughout its lifetime. Fig. 10.15 shows that nodes reselect their cooperation partner no more than 3 times throughout their lifetimes using ECO-OP, regardless of partner choice strategy. This demonstrates that network-wide cooperation using ECO-OP entails a low signalling and organisational overhead throughout the lifetime of the Topology C network. By contrast, using the centralised greedy cooperation algorithm [18], whenever a node depletes its energy each surviving source node in the network is allocated its cooperation partner anew by the central controller, as illustrated in Fig. 10.15. Importantly, this demonstrates that ECO-OP with GKH_1 or GKH_2 achieves a very similar partner allocation as the centralised greedy cooperation algorithm [18] in the Topology C network (as illustrated by Fig. 10.4), at a much lower cost to the network in terms of computational complexity and signalling overhead.

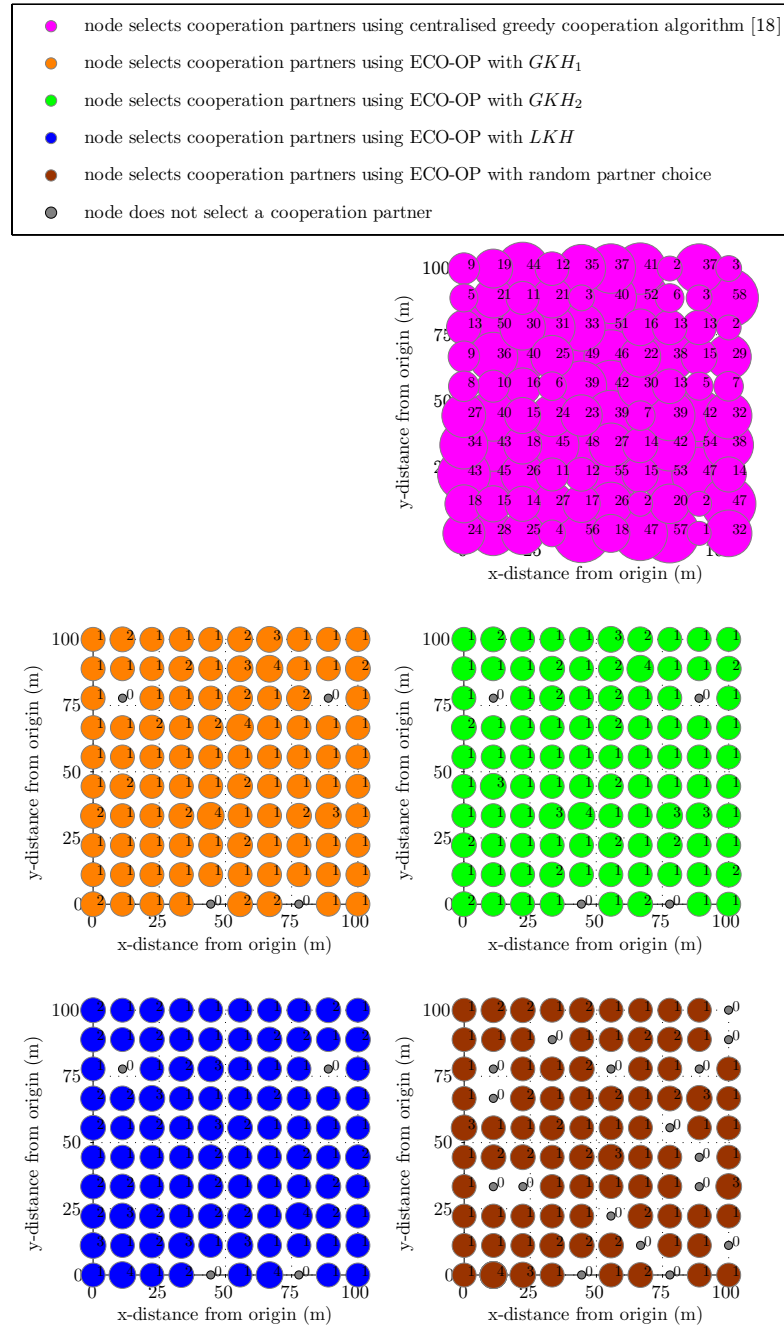


Figure 10.15: Distribution of cooperation partner selection in a Topology C network (node-to-node communication) of $M=100$ nodes regularly placed over a 100 m by 100 m network area, using different cooperation strategies. The size of each node is proportional to the number of cooperation partners the source node selects throughout its lifetime (each node is also marked with this number).

10.5 Summary

In this chapter network-wide cooperation using the ECO-OP cooperation strategy proposed in Chapter 7 has been illustrated throughout the lifetime of the wireless sensor network in three representative network Topologies (A, B, C) by simulating cooperation among 100 nodes regularly placed over a 100 m by 100 m network area. Moreover, the network lifetime extension performance of the low-complexity distributed ECO-OP cooperation strategy with different partner choice rules (GKH_1 , GKH_2 , LKH , and random partner choice) has been compared against that of the computationally intensive centralised greedy cooperation algorithm proposed in [18]. The network lifetime extension performance of each cooperation strategy has been investigated in terms of the x^{th} node lifetime improvement achieved over the lifetime of the wireless sensor network, and summarised overall by the average network lifetime improvement factor achieved. The long-term behaviour of network-wide cooperation using each cooperation strategy has also been illustrated in terms of the distribution of the individual node lifetimes across the cooperative versus the non-cooperative network and the average distribution of cooperation partner service and selection among the network's nodes.

The results presented in this chapter have shown that network-wide cooperation using ECO-OP always significantly extends the lifetime of the regular wireless sensor network under consideration for all three network topologies. Importantly, it has been demonstrated that the distributed ECO-OP cooperation strategy with GKH_1 or GKH_2 consistently overall achieves a comparable cooperative lifetime improvement to the centralised greedy cooperation algorithm [18]. Regardless of network topology, ECO-OP with GKH_1 achieves the highest average network lifetime improvement factor which ranges from 9.4 to 13.0, followed by ECO-OP with GKH_2 and the centralised greedy cooperation algorithm [18] which yield an average network lifetime improvement factor which ranges from 8.8 to 12.1 and from 9.0 to 11.7, respectively. ECO-OP with LKH and random partner choice result in a lower average network lifetime improvement factor which ranges from 6.7 to 7.8 and from 3.8 to 7.8, respectively.

It has been illustrated that the overall pattern of ECO-OP partner service does not change substantially throughout the lifetime of the Topology A and C networks, demonstrating the low signalling and organisational overhead of long-term cooperation using ECO-OP. Consequently, the ECO-OP node lifetime results presented in this chapter are consistent with those predicted by the node energy consumption over the Topology A and C networks in Chapter 8 corresponding to the initial partner selection round at the time of the network's deployment. The same trend has also been observed in the Topology B network using ECO-OP with LKH or random partner choice.

By contrast, the overall pattern of partner service using ECO-OP with GKH_1 or GKH_2 changes considerably throughout the lifetime of the Topology B network, becoming increasingly distributed as the several overpopular partner nodes prematurely deplete their energy. The lifetimes of the first 10% of nodes in the Topology B network are thus sacrificed using ECO-OP with GKH_1 or GKH_2 in order to arrive at a sustainable partner service distribution which improves the lifetimes of the rest of the network's nodes. Importantly, these results thus clearly demonstrate that ECO-OP with GKH_1 or GKH_2 is *not* an unsustainable long-term cooperation strategy in the Topology B network, refuting the prediction made in Chapters 8 and 9.

It has also been shown that ECO-OP with GKH_1 or GKH_2 reallocates the network's combined energy resource among nodes to achieve a substantially more uniform distribution of node lifetimes over network, regardless of network topology. This improved node lifetime fairness is a result of selecting partner nodes with high non-cooperative lifetimes to serve as partners to nodes with low non-cooperative lifetimes. By contrast, ECO-OP with LKH and random partner choice generally maintain the uneven node lifetime distribution of the non-cooperative network, by virtue of nodes serving as cooperation partners regardless of their own non-cooperative lifetime.

Importantly, the analysis in this chapter has served to illustrate the distinct underlying approaches of ECO-OP and the centralised greedy cooperation algorithm [18]. Whereas ECO-OP with GKH_1 or GKH_2 selects as cooperation partners the nodes that can *help the most*, the centralised greedy cooperation algorithm [18] aims to equalise the projected node lifetimes over the network and thus selects as cooperation partners the nodes that can *most afford to help*. Consequently, the centralised greedy cooperation algorithm [18] achieves the most uniform node lifetime distribution in the Topology A and C networks. However, in the Topology B network the node-centric approach of the centralised greedy cooperation algorithm [18] turns out to be short-sighted, overall resulting in both inferior and less uniform node lifetimes than ECO-OP with GKH_1 or GKH_2 .

Having examined and illustrated the fundamental long-term behaviour of ECO-OP in this chapter, the typical network lifetime extension performance of ECO-OP is evaluated in Chapter 11. Specifically, by considering the general case of randomly deployed networks of various node density, the analysis in Chapter 9 serves to establish the general validity of the distributed ECO-OP cooperation strategy as an effective technique for extending the lifetime of a wireless sensor network.

Chapter 11

Network Lifetime Extension Performance of Network-wide Cooperation

11.1 Introduction

In Chapter 10 the fundamental long-term behaviour of ECO-OP, the low-complexity distributed cooperation strategy presented in Chapter 7, was illustrated by considering cooperation among $M=100$ regularly placed nodes over the lifetime of the wireless sensor network. In this chapter the typical network lifetime extension performance of network-wide cooperation using ECO-OP is evaluated for the general case of randomly deployed networks of various node density. Specifically, cooperation among $M=\{2, 3, 4, 5, 6, 10, 30, 100, 300, 1000\}$ nodes¹ randomly placed with a uniform distribution over a 100 m by 100 m network area is simulated in the three representative network topologies (A, B, and C) introduced in Section 7.4. As in Chapter 10, the performance of the proposed low-complexity distributed ECO-OP cooperation strategy with different partner choice rules (GKH_1 , GKH_2 , LKH , and random partner choice) is compared throughout this chapter against that of the computationally intensive centralised greedy cooperation algorithm from the literature [18]. The typical network lifetime extension performance of ECO-OP is thus thoroughly analysed for both sparse and dense networks with both directed and random data flow, serving to establish the general validity of the proposed ECO-OP cooperation strategy as an effective technique for extending the lifetime of a wireless sensor network.

¹The minimum number of nodes considered for a Topology C network is $M=3$, since a node cannot simultaneously serve as another node's destination receiver and cooperation partner.

Firstly, the typical x^{th} node lifetime versus x curve² of each cooperation strategy in a network of $M=100$ randomly placed nodes is presented for each network topology. Whereas the example node lifetime curves presented in Chapter 10 served only to illustrate the fundamental behaviour of different cooperation strategies, the typical node lifetime results presented in this chapter show the characteristic performance of different cooperation strategies in extending the lifetime of a Topology A, B, and C network³. Secondly, the overall network lifetime extension performance of each cooperation strategy as M is varied is quantified for each network topology in terms of the average network lifetime improvement factor, which is defined as the average of the x^{th} node lifetime improvement factors achieved over all values of x , as given by (7.13). In order to represent the typical behaviour of ECO-OP, the results presented throughout this chapter are given by the median of $Q = \left(\frac{10^5}{M}\right)$ simulation runs. It is important to note that the cooperation strategy proposed in [18] is not suitable for practical implementation in a dense network, due to the fact that the computationally intensive centralised greedy cooperation algorithm [18] must be repeated each time a node depletes its energy. Nevertheless, simulation results for the centralised greedy cooperation algorithm [18] are still presented alongside ECO-OP in this chapter for large values of M , albeit based on a smaller number of network realisations due to the extremely long simulation times⁴. The analysis in this chapter thus enables a thorough comparison of the characteristic performance of these two distinct approaches to coordinating cooperative communication in an energy-constrained wireless network.

The results for the central destination receiver Topology A network are presented in Section 11.2, the remote destination receiver Topology B network in Section 11.3, and the node-to-node communication Topology C network in Section 11.4. In Section 11.5 the overall network lifetime extension performance of different cooperation strategies is compared, based on the results presented in the preceding sections. This leads to a recommendation of the best practical cooperation strategy to employ for a given set of network conditions, as well as the best overall cooperation strategy for extending the lifetime of a general energy-constrained wireless sensor network.

The reference cooperative system parameters specified in Table 2.1 are employed throughout the analysis presented in this chapter. As in Chapter 10, a TDMA wireless sensor network with uniform traffic is assumed, whereby every source node in the

²The number of node deaths since network activation is denoted x and the x^{th} node lifetime in a non-cooperative and cooperative wireless sensor network are defined as $T_{non-coop_node(x)}$ and $T_{coop_node(x)}$ as given by (7.14) and (7.17) respectively.

³It should be noted that the typical node lifetime curves for networks of various node density have been intentionally excluded from the results presented in this chapter in the interest of brevity, since they generally exhibit similar trends as a network with $M=100$ nodes.

⁴The results for the centralised greedy cooperation algorithm [18] presented for $M=\{100, 300\}$ are given by the median of $Q=\{350, 15\}$ simulation runs respectively, and no results are presented for $M=1000$. It is also interesting to note that the simulation results (of first node lifetime only) presented in [18] only consider networks of up to $M=50$ nodes.

network in turn sends a message block of $B=100$ bits to its destination receiver in each transmission round. Moreover, it is assumed that prior to network activation all sensor nodes have an initial battery energy of $E_{battery}=10$ J for Topology A and C networks and $E_{battery}=100$ J for Topology B networks, and that each node in the network acts as a source and is eligible to be selected as a cooperation partner by any other source node. It is important to note that the ECO-OP simulation results presented in this chapter are based on an implementation of the overall distributed ECO-OP cooperation strategy employed by each source node in the cooperative network throughout its lifetime, as specified in Fig. 7.2. For further details of the ECO-OP cooperation strategy, the simulation parameters and assumptions related to this investigation, and the node and network lifetime metrics employed in this chapter, please refer to Sections 7.2, 7.4, and 7.6 respectively. For a detailed description of the centralised greedy cooperation algorithm [18] and further details of its implementation in generating the simulation results presented in this chapter, please refer to Appendix A.

11.2 Topology A Network: Central Destination Receiver

Fig. 11.1 shows the typical x^{th} node lifetime versus x curve for a Topology A network of $M=100$ nodes randomly placed over a 100 m by 100 m network area, using non-cooperative communication and cooperative communication with different cooperation strategies. Fig. 11.1 reveals that the centralised greedy cooperation algorithm [18] achieves a 1st node lifetime improvement factor of 14.3 in a Topology A network, whereas ECO-OP with GKH_1 and GKH_2 result in a somewhat higher 1st node lifetime improvement factor of 16.7 and 16.6 respectively. This is a particularly interesting result since the centralised greedy cooperation algorithm [18] is explicitly designed to maximise the minimum (i.e. 1st) node lifetime, yet ECO-OP with GKH_1 or GKH_2 achieves a longer 1st node lifetime simply by striving to minimise the total energy consumption of each individual cooperative link. Fig 11.1 also shows that the x^{th} node lifetime achieved using the centralised greedy cooperation algorithm [18] is slightly lower than that achieved using ECO-OP with GKH_1 and GKH_2 for about the first 30% and 15% of node deaths respectively (by a factor of 1.05 on average) and for about the last 20% of node deaths (by about factor of 1.5 on average). Otherwise, the centralised greedy cooperation algorithm [18] results in a slightly higher x^{th} node lifetime than ECO-OP with GKH_1 and GKH_2 (by a factor of about 1.07, between the 30th and 80th and between the 15th and 80th percentile of node deaths, respectively). Therefore, in a Topology A network the distributed ECO-OP cooperation strategy with

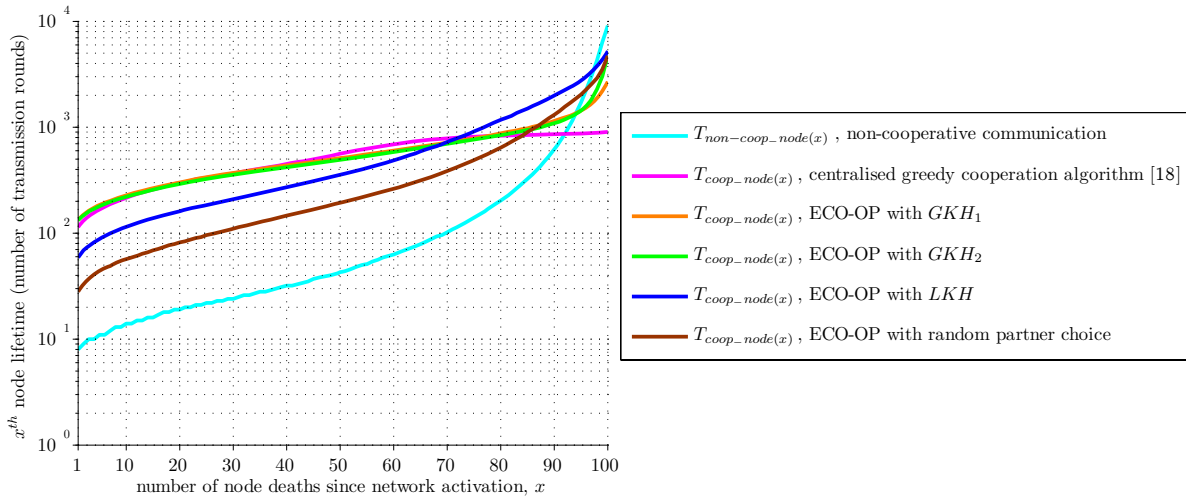


Figure 11.1: Node lifetime vs. number of node deaths since network activation for a Topology A network (central destination receiver), using non-cooperative communication and cooperative communication with different cooperation strategies (median of Q network realisations of $M=100$ nodes randomly placed over a 100 m by 100 m network area).

GKH_1 or GKH_2 overall achieves a comparable x^{th} node lifetime improvement to the centralised greedy cooperation algorithm proposed in [18].

Moreover, Fig 11.1 demonstrates that the centralised greedy cooperation algorithm [18], ECO-OP with GKH_1 , and ECO-OP with GKH_2 exhibit a less steep lifetime curve than that of non-cooperative communication. As discussed in Section 10.2, this indicates that these three cooperation strategies yield a significantly more uniform distribution of node lifetimes over the Topology A network by reallocating the network’s combined energy resource. By contrast, Fig 11.1 shows that ECO-OP with LKH generally maintains the relative node lifetime distribution of the non-cooperative Topology A network. As discussed in Section 10.2, this trend is due to neighbouring nodes with similar non-cooperative lifetimes serving as each other’s cooperation partners using ECO-OP with LKH . Consequently, ECO-OP with LKH results in the highest x^{th} node lifetime of all the cooperation strategies for the last 30% of node deaths in a Topology A network (higher than ECO-OP with GKH_1 by a factor of 1.46 times on average). Conversely, Fig 11.1 shows that for about the first 70% of node deaths ECO-OP with LKH results in a significantly lower x^{th} node lifetime than ECO-OP with GKH_1 (by a factor of 1.65 on average). However, Fig. 11.1 also shows that in a Topology A network ECO-OP with LKH consistently achieves a substantially higher x^{th} node lifetime than ECO-OP with random partner choice (by a factor of 1.82 on average).

Finally, Fig 11.1 demonstrates that the centralised greedy cooperation algorithm [18] achieves an appreciably more uniform x^{th} node lifetime distribution than ECO-OP with GKH_1 or GKH_2 . However, as noted in Section 10.2, this node lifetime fairness improvement achieved by the algorithm from [18] is largely due to the significantly diminished

lifetimes of the last 20% of nodes; thus in a sense it constitutes an artificial advantage over ECO-OP with GKH_1 or GKH_2 . Namely, by aiming to equalise the projected node lifetimes over the network, the centralised greedy cooperation algorithm [18] on average halves the lifetimes of the last 20% of nodes in exchange for a modest 7% increase in the lifetimes of the preceding 50% of nodes compared to ECO-OP with GKH_1 . Similarly, ECO-OP with GKH_1 results in a slightly more uniform distribution of node lifetimes across the Topology A network than ECO-OP with GKH_2 by virtue of diminished lifetimes for about the last 5% of nodes. Specifically, Fig 11.1 shows that ECO-OP with GKH_1 results in a marginally higher (by a factor of 1.03 on average) x^{th} node lifetime than ECO-OP with GKH_2 for all but the last 5% of nodes, whose lifetimes are reduced by a factor of 1.25 on average. However, it is important to note that the lifetimes of the last 5% of nodes are unlikely to be of great practical significance, since the last few remaining nodes are unlikely to constitute a functional network (i.e. as discussed in Section 7.6, specifying a value of x very close to M is almost certainly an overestimate of the useful lifetime of a wireless sensor network)⁵. Therefore, ECO-OP with GKH_2 is the preferable long-term cooperation strategy for practical deployment in a Topology A network, since it results in a virtually identical x^{th} node lifetime as ECO-OP with GKH_1 but entails a lower computational complexity. It is interesting to note that this conclusion is consistent with the preliminary comparison of the performance of GKH_1 and GKH_2 in the Topology A network presented in Chapter 9 based on the node energy consumption over the network following the initial partner selection round.

Fig. 11.2 shows the average network lifetime improvement factor achieved in a Topology A network as the number of nodes in the network M is varied, using different cooperation strategies. Importantly, Fig. 11.2 demonstrates that network-wide cooperation always significantly extends the lifetime of a Topology A wireless sensor network for both sparse and dense networks, by a factor ranging from 3.5 to 10.9. The average network lifetime improvement factor achieved using ECO-OP with GKH_1 and GKH_2 increases with increasing node density, ranging from 3.5 to 10.3 and 10.2 respectively. This trend is due to the increased energy efficiency of partner choice in a larger candidate partner set and is consistent with that exhibited by GKH_1 and GKH_2 in Figs. 9.1 and 9.2. Namely, the larger candidate partner set associated with a more dense network means that good cooperation partners are more likely to exist in the network; this effect has previously been illustrated in Fig. 6.5 for the case of a single source node selecting its cooperation partner from an increasingly large candidate partner set. By contrast, the average network lifetime improvement factor achieved using ECO-OP with LKH increases with increasing

⁵This also suggests that it is not of great engineering relevance that cooperative communication always reduces the lifetimes of the last 3-8% of nodes in a Topology A network (as shown by Fig 11.1).

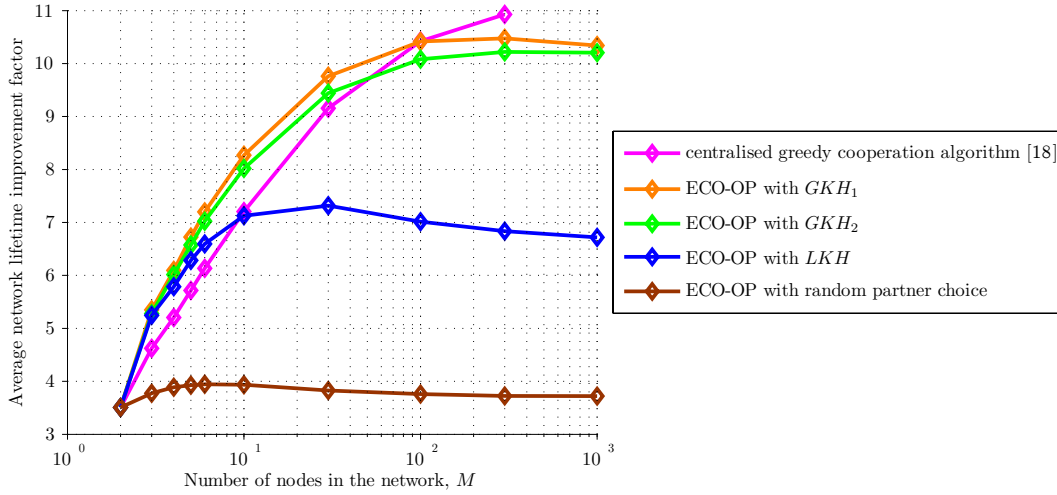


Figure 11.2: Average network lifetime improvement factor, as given by (7.13), vs. number of nodes in the network, for a Topology A network (central destination receiver) using different cooperation strategies (median of Q network realisations of M nodes randomly placed over a 100 m by 100 m network area).

node density for sparse networks (i.e. ranging from 3.5 to 7.3 for $M \leq 30$), but then decreases slightly (to 6.7) for increasingly dense networks. This trend is consistent with that exhibited by LKH in Fig. 9.2 and is due to the fact that a node in an increasingly dense LKH network selects a neighbouring partner node which is increasingly close to itself and thus increasingly far away from the optimal partner location (i.e. midway between the source and the destination receiver). As discussed in Section 9.2, this results in nodes consuming more energy as the source, due to selecting an increasingly sub-optimal cooperation partner, and spending more energy serving as partner, due to being selected by a neighbouring source node with similarly high inherent energy requirements. This increased node energy consumption reduces node lifetimes in dense LKH networks, as reflected in the decreasing average network lifetime improvement exhibited by ECO-OP with LKH in Fig. 11.2. Finally, Fig 11.2 shows that ECO-OP with random partner choice achieves an average network lifetime improvement factor of around 3.8 regardless of node density⁶.

Importantly, Fig. 11.2 demonstrates that in a Topology A network the distributed ECO-OP cooperation strategy with GKH_1 or GKH_2 overall achieves a comparable network lifetime improvement to the centralised greedy cooperation algorithm proposed in [18]. Namely, ECO-OP with GKH_1 and ECO-OP with GKH_2 achieve a slightly higher average network lifetime improvement factor than the centralised greedy cooperation algorithm [18] in sparse Topology A networks and vice versa in dense Topology A networks. Specifically, for $M \leq 30$ ECO-OP with GKH_1 outperforms the centralised greedy coop-

⁶More specifically, the average network lifetime improvement factor decreases slightly with increasing node density for $M > 10$ due to the decreased likelihood of all nodes randomly selecting an energy efficient cooperation partner, as discussed in Section 9.2.

eration algorithm [18] by a factor 1.13 on average, whereas for $M \geq 100$ the centralised greedy cooperation algorithm [18] outperforms ECO-OP with GKH_1 by a factor 1.02 on average. The difference between the performance of ECO-OP and the centralised greedy cooperation algorithm [18] exhibited in Fig. 11.2 is due to the distinct design approaches underlying these two cooperation strategies. As discussed in Section 7.3.2 and demonstrated by Fig.11.1, the greedy cooperation algorithm [18] aims to equalise the projected node lifetimes over the network. However, this node-centric approach typically means that the total energy consumption over the network is increased compared to ECO-OP with GKH_1 or GKH_2 , which is instead designed to minimise the network-wide energy consumption per message. In a sparse network, node lifetimes are inherently more variable across only a few randomly placed nodes and thus the greedy cooperation algorithm [18] wastes more energy attempting to equalise them. Conversely, in a dense network consisting of a high number nodes, the greedy cooperation algorithm [18] is better able to match cooperation partner nodes with “location and energy advantages” [18] to source nodes with high inherent communication energy requirements and low residual battery energy. Consequently, ECO-OP with GKH_1 or GKH_2 slightly outperforms the greedy cooperation algorithm [18] in sparse Topology A networks and vice versa in a dense Topology A networks.

11.3 Topology B Network: Remote Destination Receiver

Fig. 11.3 shows the typical x^{th} node lifetime versus x curve for a Topology B network of $M=100$ nodes randomly placed over a 100 m by 100 m network area, using non-cooperative communication and cooperative communication with different cooperation strategies. Fig. 11.3 demonstrates that the centralised greedy cooperation algorithm [18] achieves a 1st node lifetime improvement factor of 7 in a Topology B network, whereas ECO-OP with GKH_1 and GKH_2 result in a significantly lower 1st node lifetime improvement factor of 1.5 and 2.5 respectively. Fig. 11.3 also shows that the centralised greedy cooperation algorithm [18] achieves a substantially higher x^{th} node lifetime than ECO-OP with GKH_1 and GKH_2 for about the first 10% and 11% of node deaths respectively (by a factor of 1.45 and 1.59 on average respectively). As discussed in Section 10.3, this is due to ECO-OP with GKH_1 or GKH_2 overburdening a handful of popular partner nodes located at the top of the Topology B network, causing them to prematurely deplete their

⁷The authors of [18] refer to nodes that are located close to the destination receiver and thus have low inherent communication energy requirements as having a “location advantage”, whereas nodes that have higher residual battery energy than other nodes in the network before the greedy algorithm performs the network-wide allocation of cooperation partners are referred to as having an “energy advantage”.

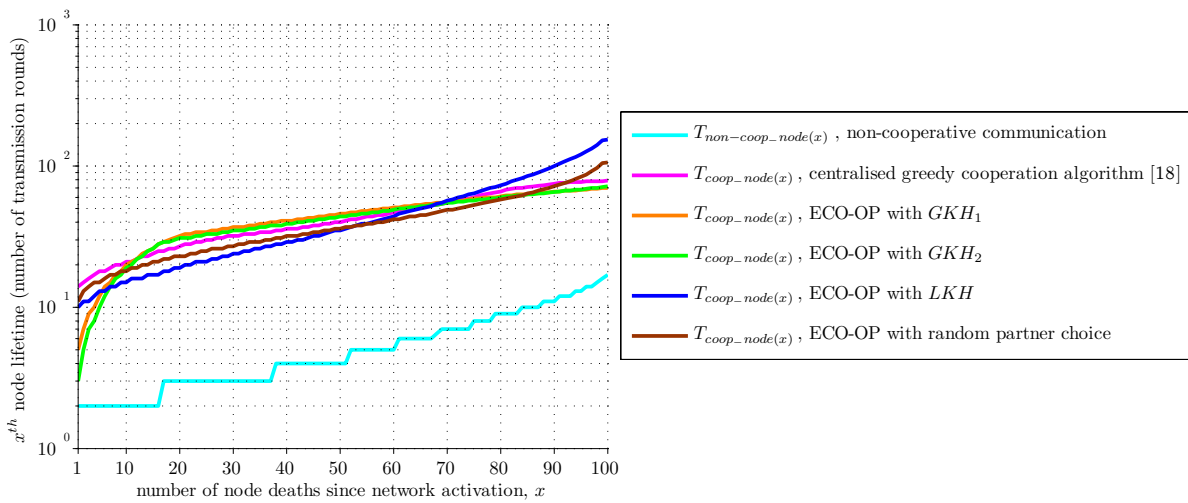


Figure 11.3: Node lifetime vs. number of node deaths since network activation for a Topology B network (remote destination receiver), using non-cooperative communication and cooperative communication with different cooperation strategies (median of Q network realisations of $M=100$ nodes randomly placed over a 100 m by 100 m network area).

batteries in helping numerous other nodes. However, the subsequent unavailability of these overpopular partner nodes forces a redistribution of partner service over the Topology B network. Consequently, Fig 11.3 shows that ECO-OP with GKH_1 and GKH_2 achieve a somewhat higher x^{th} node lifetime than the centralised greedy cooperation algorithm [18] between the 13th and 70th and between the 14th and 65th percentile of node deaths respectively (by a factor of 1.12 and 1.08 on average respectively). Finally, Fig 11.3 shows that the x^{th} node lifetime achieved using the centralised greedy cooperation algorithm [18] is slightly higher than that achieved by ECO-OP with GKH_1 and GKH_2 for the last 28% and 30% of node deaths respectively (by about factor of 1.1 on average). Importantly, the results in Fig 11.3 thus demonstrate that in a Topology B network the distributed ECO-OP cooperation strategy with GKH_1 or GKH_2 overall achieves a comparable x^{th} node lifetime improvement to the centralised greedy cooperation algorithm proposed in [18].

Furthermore, Fig 11.3 reveals that ECO-OP with GKH_1 and GKH_2 overall achieve a somewhat more fair node lifetime distribution over the Topology B network than the centralised greedy cooperation algorithm [18]. This is a particularly interesting result since the centralised greedy cooperation algorithm [18] is essentially designed to equalise the projected node lifetimes over the network, yet ECO-OP with GKH_1 and GKH_2 actually come closer to achieving this aim by selecting as cooperation partners the nodes that can *help the most*, rather than those that can *most afford to help*. This result also clearly demonstrates that ECO-OP with GKH_1 and GKH_2 are *not* unsustainable long-term cooperation strategies, as was previously predicted in Chapters 8 and 9 based on the energy consumption over the Topology B network following the initial partner selection

round. On the contrary, ECO-OP with GKH_1 and GKH_2 sacrifice the lifetimes of the first 10% of nodes in the Topology B network in order to produce a sustainable partner service distribution which is of long-term benefit to the rest of the network. However, it should be noted that the modified partner choice strategy discussed in Chapter 9, whereby a limit is placed on the number of source nodes a partner node can serve, is still likely to be beneficial in the GKH_1 and GKH_2 Topology B network. By restricting the partner burden placed upon a single partner node, this modified strategy might from the outset produce a sustainable distribution of partner service (similar to that illustrated in Fig. 10.9). This would preclude the premature loss of the first 10% of nodes using ECO-OP with GKH_1 and GKH_2 , which only serves to force the eventual redistribution of partner service over the Topology B network. This modification would thus also reduce the signalling overhead of reselecting a cooperation partner every few transmission rounds using ECO-OP with GKH_1 and GKH_2 in the Topology B network (as illustrated by comparing Figs. 10.6 and 10.10), although this must be balanced against the increased signalling overhead inherent in this modified partner choice strategy (as discussed in Chapter 9). Investigating the viability of such a modification to ECO-OP with GKH_1 and GKH_2 in a Topology B network and evaluating the accompanying engineering trade-offs is an interesting direction for future research.

Fig. 11.3 also shows that ECO-OP with GKH_1 results in a significantly higher x^{th} node lifetime than ECO-OP with GKH_2 for the first 5% of nodes (by a factor of 1.36 on average). Fig. 11.3 thus demonstrates that the lifetimes of the first 5% of nodes are sacrificed more using ECO-OP with GKH_2 than using GKH_1 in arriving at a sustainable partner allocation over the Topology B network. Otherwise, ECO-OP with GKH_1 results in a marginally higher x^{th} node lifetime than ECO-OP with GKH_2 (by a factor of 1.03 on average). Moreover, ECO-OP with GKH_2 also results in a slightly less uniform distribution of node lifetimes across the Topology B network than ECO-OP with GKH_1 , mainly by virtue of the diminished lifetimes of the first 5-10% of nodes. The network lifetime extension performance of GKH_2 is thus overall inferior to that of GKH_1 , consistently achieving a lower x^{th} node lifetime improvement and resulting in a slightly less fair node lifetime distribution over the Topology B network. Most importantly, GKH_1 is the preferable long-term cooperation strategy because it wastes less energy in arriving at a sustainable partner distribution over the Topology B network. It is interesting to note that this conclusion is consistent with the preliminary comparison of the performance of GKH_1 and GKH_2 in the Topology B network presented in Chapter 9 based on the node energy consumption over the network following the initial partner selection round.

Lastly, Fig 11.3 demonstrates that ECO-OP with LKH generally maintains the relative node lifetime distribution of the non-cooperative Topology B network. As discussed in Section 10.3, this trend is due to neighbouring nodes with similar non-cooperative

lifetimes serving as each other's cooperation partners using ECO-OP with LKH . By contrast, the centralised greedy cooperation algorithm [18], ECO-OP with GKH_1 , and ECO-OP with GKH_2 reallocate the network's combined energy to substantially improve node lifetime fairness, as evidenced by the lower average gradient of their lifetime curves in Fig 11.3 compared to that of non-cooperative communication. Consequently, ECO-OP with LKH results in the highest x^{th} node lifetime of all the cooperation strategies for the last 30% of node deaths in a Topology B network (higher than ECO-OP with GKH_1 by a factor of 1.37 times on average). Conversely, Fig 11.3 shows that for about the first 70% of node deaths ECO-OP with LKH results in a significantly lower x^{th} node lifetime than ECO-OP with GKH_1 (by a factor of 1.25 on average). Furthermore, Fig. 11.3 shows that ECO-OP with LKH overall only achieves a slightly higher x^{th} node lifetime than ECO-OP with random partner choice in a Topology B network. Specifically, ECO-OP with LKH exhibits a somewhat higher x^{th} node lifetime than ECO-OP with random partner choice in Fig. 11.3 for the last 47% of node deaths (by a factor of 1.24 on average), and vice versa for the first 51% of node deaths (by a factor of 1.15 on average). As discussed in Section 10.3, this trend is due to the fact that, for the source nodes with the lowest non-cooperative lifetimes, random partner choice results in a better cooperation partner than the neighbouring partner node chosen by LKH .

Fig. 11.4 shows the average network lifetime improvement factor achieved in a Topology B network as the number of nodes in the network M is varied, using different cooperation strategies. Importantly, Fig. 11.4 demonstrates that network-wide cooperation always significantly extends the lifetime of a Topology B wireless sensor network for both sparse and dense networks, by a factor ranging from 7.3 to 9.3. The average network lifetime improvement factor achieved using ECO-OP with GKH_1 and GKH_2 increases with increasing node density for sparse networks (ranging from 8.0 to 9.3 for $M \leq 10$ and from 8.0 to 8.9 for $M \leq 6$, respectively) but decreases slightly for increasingly dense networks (to 8.8 and 8.6 respectively). The larger candidate partner set associated with a more dense network results in an increased energy efficiency for each cooperative link in the Topology B network, as demonstrated in Fig. 9.6. However, in the initial partner selection round, only a handful of nodes are selected to serve as cooperation partners to the entire Topology B network (as illustrated in Fig. 8.6). As M increases these partner nodes serve an increasing number of source nodes each. Thus the lifetimes of these most popular partner nodes are increasingly short in increasingly dense Topology B networks (as predicted by the GKH_1 and GKH_2 maximum node energy consumption results in Fig. 9.8). In a sufficiently sparse network the most popular partner nodes are not overburdened since they serve only a small number of other nodes, which is consistent with the trend exhibited by ECO-OP with GKH_1 and GKH_2 in Fig 11.4 for sparse Topology B networks. However, ECO-OP with GKH_1 and GKH_2 result in an increasingly lower

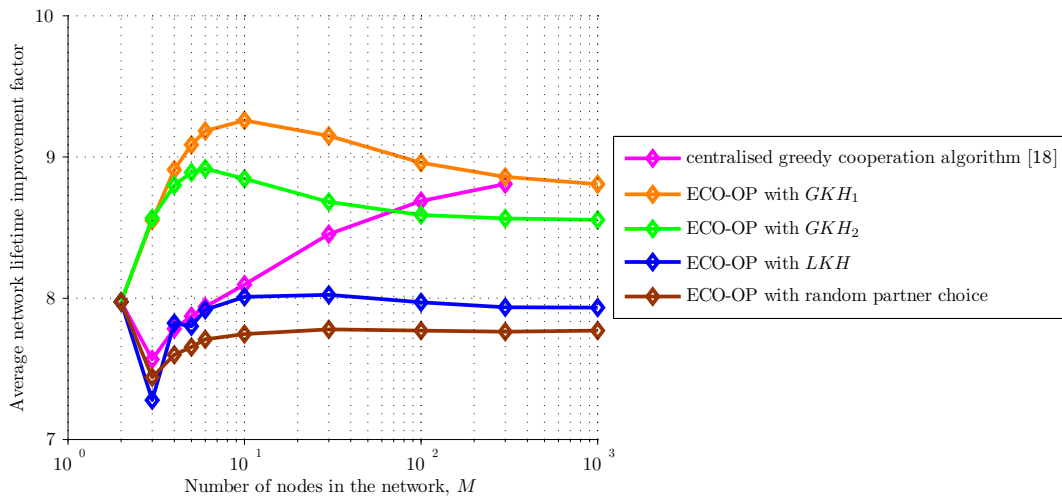


Figure 11.4: Average network lifetime improvement factor, as given by (7.13), vs. number of nodes in the network, for a Topology B network (remote destination receiver) using different cooperation strategies (median of Q network realisations of M nodes randomly placed over a 100 m by 100 m network area).

x^{th} node lifetime improvement for these first few node deaths in increasingly dense Topology B networks, leading to the diminished average network lifetime improvement factor observed in Fig 11.4.

Interestingly, Fig 11.4 shows that ECO-OP with LKH results in an average network lifetime improvement factor of 8.0 for $M = 2$, yet a lower average network lifetime improvement factor of 7.3 in a Topology B network of $M = 3$ nodes. The average network lifetime improvement factor achieved using ECO-OP with LKH then generally increases with increasing node density for sparse Topology B networks (i.e. increasing from 7.3 for $M = 3$ to 8.0 for $M = 30$). This trend may be explained by considering the extent to which cooperation partner service is evenly distributed over the sparse Topology B network. Cooperation partner service is inherently fairly distributed for a Topology B network of $M = 2$ nodes since each node helps the other. However, in a network of $M = 3$ nodes there is only a 25% chance that each node will help exactly one other node; this means that there is a 75% likelihood that one of the three nodes in the network will have a diminished cooperative lifetime due to carrying a heavier partner burdened than its neighbours. As the number of nodes in the Topology B network increases, the typical distribution of LKH partner service over the Topology B network becomes more uniform as the likelihood of each node being the closest neighbour of only one other node increases. Accordingly, Fig 11.4 reveals that in a sufficiently dense network ($M = 30$) the average network lifetime improvement factor achieved using ECO-OP with LKH increases back up to the value of 8.0 corresponding to the ideal uniform partner service distribution inherent in a network of $M = 2$ nodes⁸. For increasingly dense Topology B

⁸It is also interesting to note that this effect is specific to Topology B networks and is not observed for Topology A or C networks. This is because non-cooperative node lifetimes are significantly more

networks the average network lifetime improvement factor achieved using ECO-OP with *LKH* decreases slightly (up to 6.7 for $M = 1000$). This trend is consistent with that observed for a dense Topology A network using ECO-OP with *LKH* in Fig. 11.2 and is due to the same reasons discussed in Section 11.2. Fig 11.4 also shows that ECO-OP with random partner choice exhibits a similar trend as ECO-OP with *LKH* in sparse Topology B networks (due to the same reasons of partner service distribution uniformity), whereas it exhibits an average network lifetime improvement factor of 7.8 in dense Topology B networks. The average network lifetime improvement factor achieved in a Topology B network using ECO-OP with *LKH* is thus somewhat higher than that achieved using ECO-OP with random partner choice, regardless of node density. This is consistent with the results presented in Fig. 11.3, which demonstrate that the x^{th} node lifetime advantage of *LKH* over random partner choice for the second half of node deaths is somewhat higher than the advantage of random partner choice over *LKH* for the first half of node deaths in the Topology B network.

Importantly, Fig. 11.2 demonstrates that in a Topology B network the distributed ECO-OP cooperation strategy with GKH_1 or GKH_2 overall achieves a comparable network lifetime improvement to the centralised greedy cooperation algorithm proposed in [18]. Namely, ECO-OP with GKH_2 achieves a somewhat higher average network lifetime improvement factor than the centralised greedy cooperation algorithm [18] in sparse Topology B networks and vice versa in dense Topology B networks. Specifically, for $M \leq 30$ ECO-OP with GKH_2 outperforms the centralised greedy cooperation algorithm [18] by a factor 1.09 on average, whereas for $M \geq 100$ the centralised greedy cooperation algorithm [18] outperforms ECO-OP with GKH_2 by a factor 1.02 on average. Similarly, the discrepancy between the average network lifetime improvement factor achieved using ECO-OP with GKH_1 and that achieved using the centralised greedy cooperation algorithm [18] decreases as M is increased, although the latter cooperation strategy remains inferior to the former for all considered node density values. Thus the trend exhibited by the centralised greedy cooperation algorithm [18] in Fig. 11.4 for Topology B networks is similar to that in Fig. 11.2 for Topology A networks. As discussed in Section 11.2, the performance of the centralised greedy cooperation algorithm [18] is inferior to that of ECO-OP with GKH_1 or GKH_2 in a sparse network because the algorithm from [18] wastes energy in attempting to equalise the projected node lifetimes of a few randomly placed nodes. As the node density increases, the centralised greedy cooperation algorithm [18] achieves a higher network lifetime improvement since it is better able to

uniform across the Topology B network compared to the Topology A and C networks. Consequently, in a Topology A or C network there exist nodes with high non-cooperative lifetimes which can afford to consume some of their energy in helping other nodes with significantly lower non-cooperative lifetimes. By contrast, any given node in a Topology B network can afford to act as cooperation partner about as much as any other node in the network; thus a uniform partner allocation is essential to ensure that the cooperative lifetimes of individual nodes are not diminished by an unfairly distributed partner burden.

improve the node lifetime fairness over the network without substantially increasing the actual network energy consumption. It is also interesting to note that Fig. 11.4 thus clearly demonstrates that the behaviour of the centralised greedy cooperation algorithm [18] is similar to that of ECO-OP with LKH in sparse networks and becomes increasingly similar to that of ECO-OP with GKH_1 or GKH_2 with increasing node density.

11.4 Topology C Network: Node-to-Node Communication

Fig. 11.5 shows the typical x^{th} node lifetime versus x curve for a Topology C network of $M=100$ nodes randomly placed over a 100 m by 100 m network area, using non-cooperative communication and cooperative communication with different cooperation strategies. Fig 11.5 shows that the x^{th} node lifetime achieved using the centralised greedy cooperation algorithm [18] is somewhat higher than that achieved using ECO-OP with GKH_1 and GKH_2 for about the first 75% and 77% of node deaths respectively (by a factor of 1.08 on average). Conversely, the centralised greedy cooperation algorithm [18] results in a substantially lower x^{th} node lifetime than ECO-OP with GKH_1 and GKH_2 for the last 25% and 23% of node deaths respectively (by a factor of 1.6 on average)⁹. Thus the distributed ECO-OP cooperation strategy with GKH_1 or GKH_2 overall achieves a comparable x^{th} node lifetime improvement in a Topology C network to the centralised greedy cooperation algorithm proposed in [18].

Moreover, Fig 11.5 demonstrates that the centralised greedy cooperation algorithm [18] achieves a more uniform x^{th} node lifetime distribution in a Topology C network than ECO-OP with GKH_1 or GKH_2 . However, this node lifetime fairness improvement achieved by the algorithm from [18] is largely due to the significantly diminished lifetimes of the last 25% of nodes. Nonetheless, the centralised greedy cooperation algorithm [18] sacrifices the lifetimes of the last quarter of nodes to improve the lifetimes of the first three quarters of nodes by a non-negligible 8% on average compared to ECO-OP with GKH_1 or GKH_2 . Fig 11.5 thus very clearly illustrates the mechanism which underlies the algorithm from [18], namely aiming to equalise the projected node lifetimes over the network. Furthermore, comparing Figs. 11.1, 11.3, and 11.5 shows that, compared to ECO-OP with GKH_1 or GKH_2 , the centralised greedy cooperation algorithm [18] performs the best in a Topology C network and the worst in a Topology B network. This

⁹Fig. 11.5 also shows that the centralised greedy cooperation algorithm [18] actually reduces the lifetimes of the last 3% of nodes in a Topology C network (by a factor of 1.76 on average), whereas ECO-OP with GKH_1 and GKH_2 reduce the lifetimes of the last 1% of nodes in a Topology C network by a factor of 1.2. However, the lifetimes of these last few remaining nodes are unlikely to be of great practical engineering significance, as previously discussed in Section 11.2.

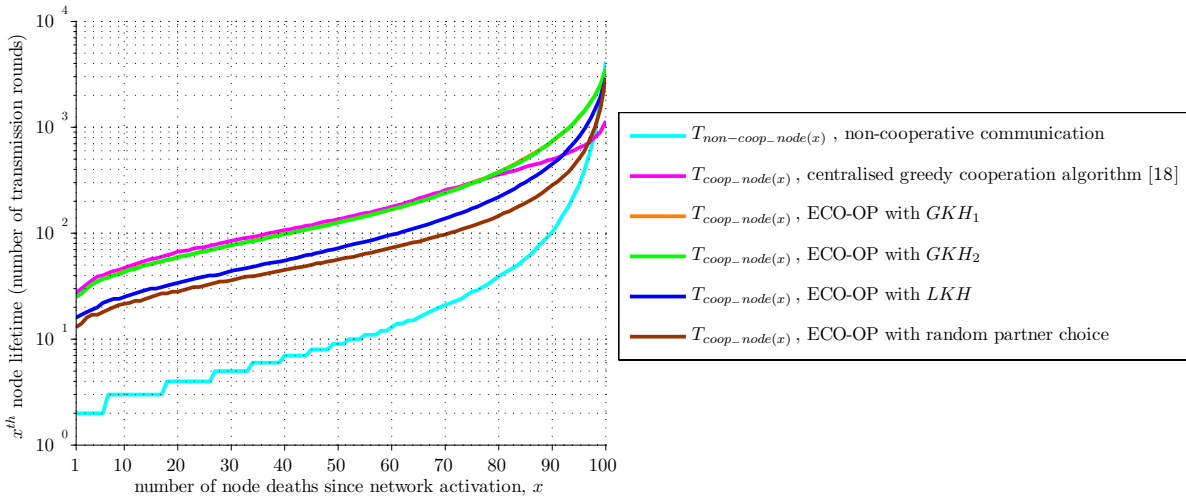


Figure 11.5: Node lifetime vs. number of node deaths since network activation for a Topology C network (node-to-node communication), using non-cooperative communication and cooperative communication with different cooperation strategies (median of Q network realisations of $M=100$ nodes randomly placed over a 100 m by 100 m network area).

is because the approach of selecting cooperation partners which can *most afford to help* works best in a network with a wide range of non-cooperative node lifetimes, allowing the algorithm from [18] to easily reallocate node energy consumption over the network so as to both maximise the x^{th} node lifetime of the majority of nodes and improve node lifetime fairness. Conversely, the non-cooperative lifetimes are significantly more uniform over the Topology B network and consequently the algorithm from [18] generally sacrifices the x^{th} node lifetime by striving to achieve node lifetime fairness, instead of selecting the cooperation partners which can *help the most* as does ECO-OP with GKH_1 or GKH_2 .

Finally, Fig. 11.5 shows that ECO-OP with GKH_1 results in a virtually identical x^{th} node lifetime as ECO-OP with GKH_2 (the discrepancy between the two partner choice rules is 0.5% on average and no more than 3%). Therefore, ECO-OP with GKH_2 is the preferable of the two cooperation strategies for practical long-term deployment in a Topology C network, as it entails a lower computational complexity. It is interesting to note that this conclusion is consistent with the preliminary comparison of the performance of GKH_1 and GKH_2 in the Topology C network presented in Chapter 9 based on the node energy consumption over the network following the initial partner selection round. Moreover, Fig. 11.5 demonstrates that ECO-OP with LKH consistently results in a lower x^{th} node lifetime than ECO-OP with GKH_1 or GKH_2 (lower than ECO-OP with GKH_1 by a factor of 1.7 times on average). However, Fig. 11.5 also shows that in a Topology C network ECO-OP with LKH consistently achieves a higher x^{th} node lifetime than ECO-OP with random partner choice (by a factor of 1.3 on average).

Fig. 11.6 shows the average network lifetime improvement factor achieved in a Topology C network as the number of nodes in the network M is varied, using different co-

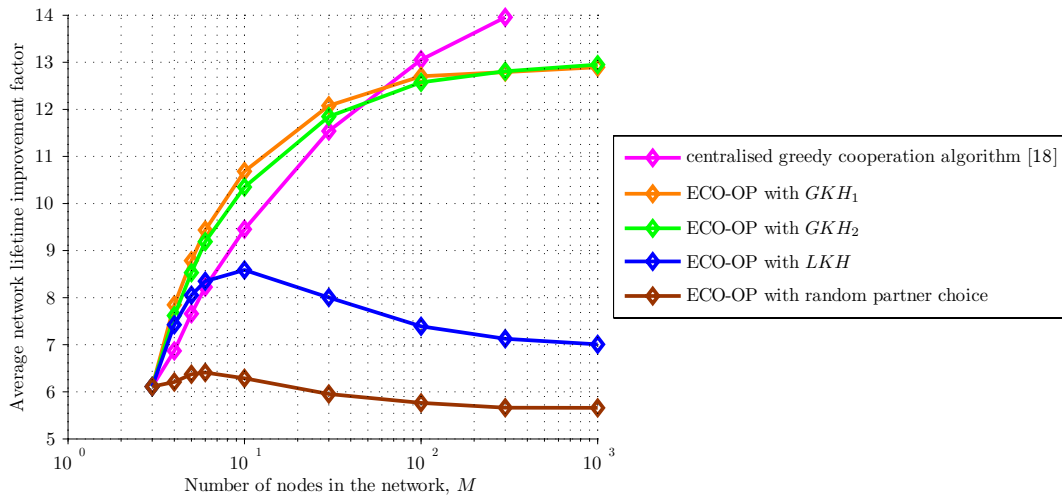


Figure 11.6: Average network lifetime improvement factor, as given by (7.13), vs. number of nodes in the network, for a Topology C network (node-to-node communication) using different cooperation strategies (median of Q network realisations of M nodes randomly placed over a 100 m by 100 m network area).

operation strategies. Importantly, Fig. 11.6 demonstrates that network-wide cooperation always significantly extends the lifetime of a Topology C wireless sensor network for both sparse and dense networks, by a factor ranging from 5.7 to 14.0. The average network lifetime improvement factor achieved using ECO-OP with GKH_1 and GKH_2 increases with increasing node density, ranging from 6.1 to 12.9 and 13.0 respectively. The average network lifetime improvement factor achieved using ECO-OP with LKH increases with increasing node density for sparse networks (i.e. ranging from 6.1 to 8.6 for $M \leq 10$), but then decreases slightly (to 7.0) for increasingly dense networks. Lastly, ECO-OP with random partner choice achieves an average network lifetime improvement factor of 6.0 on average (specifically, for $M > 6$ the improvement factor achieved decreases slightly from 6.4 to 5.7 with increasing node density). These Topology C network trends are consistent with those observed for a Topology A network using ECO-OP, and are due to the same reasons discussed in Section 11.2.

Importantly, Fig. 11.6 demonstrates that in a Topology C network the distributed ECO-OP cooperation strategy with GKH_1 or GKH_2 overall achieves a comparable network lifetime improvement to the centralised greedy cooperation algorithm proposed in [18]. Namely, ECO-OP with GKH_1 and ECO-OP with GKH_2 achieve a slightly higher average network lifetime improvement factor than the centralised greedy cooperation algorithm [18] in sparse Topology C networks and vice versa in dense Topology C networks. Specifically, for $M \leq 30$ ECO-OP with GKH_1 outperforms the centralised greedy cooperation algorithm [18] by a factor 1.10 on average, whereas for $M \geq 100$ the centralised greedy cooperation algorithm [18] outperforms ECO-OP with GKH_1 by a factor 1.06 on average. The difference between the performance of ECO-OP and the

centralised greedy cooperation algorithm [18] exhibited in Fig. 11.6 is thus consistent with that observed in Fig. 11.2 for a Topology A network. As discussed in Section 11.2, these trends are a reflection of the distinct design approaches underlying these two cooperation strategies; the algorithm from [18] selects cooperation partners which can *most afford to help*, whereas ECO-OP with GKH_1 or GKH_2 selects those than can *help the most*. It is furthermore interesting to note by comparing Figs. 11.6 and 11.2 that the centralised greedy cooperation algorithm [18] performs better relative to ECO-OP with GKH_1 or GKH_2 in a Topology C network than a Topology A network. As discussed previously, this is because the Topology C network has a wider range of non-cooperative node lifetimes so that the greedy cooperation algorithm [18] is better able to match cooperation partner nodes with high non-cooperative lifetimes to source nodes with high inherent communication energy requirements and low residual battery energy. Furthermore, in a Topology A network there is a strong correlation between *how much a node can help* and *how much it can afford to help*. Consequently the approaches employed by the two cooperation strategies result in nearly equivalent behaviour. By contrast, there is only a weak correlation between these two node attributes in a Topology C network. It follows that the algorithm from [18] has a greater advantage over ECO-OP with GKH_1 or GKH_2 in a dense Topology C network than in a dense Topology A network.

11.5 Discussion

In this section the overall network lifetime extension performance of ECO-OP with different partner choice rules and the centralised greedy cooperation algorithm [18] are compared based on the results presented in the preceding sections. This analysis serves to determine the recommended cooperation strategy for practical long-term deployment in a wireless sensor network for a given set of network conditions. It should be noted that this analysis is analogous to the preliminary comparison of ECO-OP with different partner choice rules presented in Section 9.5 based on the overall energy conservation performance of ECO-OP following the initial partner selection round.

The results presented in this chapter show that the distributed ECO-OP cooperation strategy with GKH_1 or GKH_2 overall achieves a comparable network lifetime improvement to the centralised greedy cooperation algorithm proposed in [18], regardless of network topology. Specifically, ECO-OP with GKH_1 or GKH_2 achieves a slightly higher average network lifetime improvement factor than the centralised greedy cooperation algorithm [18] for sparse networks and vice versa for dense networks. This is summarised in the third column of Table 11.1, which shows the cooperation strategy which achieves the best network lifetime extension performance under different network conditions. However, as mentioned in Section 11.1 and discussed in Appendix A, the centralised greedy

Table 11.1: Summary of the best cooperation strategy for extending the lifetime of sparse and dense wireless sensor networks of various topology.

Network topology	Network node density	Cooperation approach achieving the best simulation results	Best practical cooperation strategy
A	sparse	ECO-OP with GKH_1 or GKH_2	ECO-OP with GKH_2
	dense	centralised greedy cooperation algorithm [18]	ECO-OP with GKH_2
B	sparse	ECO-OP with GKH_1 or GKH_2	ECO-OP with GKH_1
	dense	centralised greedy cooperation algorithm [18]	ECO-OP with GKH_1
C	sparse	ECO-OP with GKH_1 or GKH_2	ECO-OP with GKH_2
	dense	centralised greedy cooperation algorithm [18]	ECO-OP with GKH_2

cooperation algorithm [18] would be prohibitively computationally expensive for practical implementation in a dense network. Therefore, the cooperation strategy proposed in [18] is not a practical candidate for dense wireless sensor networks from the point of view of engineering implementation, despite achieving the highest lifetime improvement for dense networks in simulation. By contrast, the low-complexity distributed ECO-OP cooperation strategy is inherently scalable and thus suitable for a wireless sensor network of any node density. This also means that ECO-OP with GKH_1 or GKH_2 outperforms the centralised greedy cooperation algorithm [18] in terms of extending the lifetime of a wireless sensor network over the feasible range of node densities.

Moreover, the results presented in this chapter demonstrate that ECO-OP with GKH_1 or GKH_2 always outperforms ECO-OP with LKH in terms of network lifetime improvement and node lifetime fairness, regardless of network topology or node density. These results are thus contrary to the preliminary conclusion in Section 9.5, which predicted that ECO-OP with GKH_1 and GKH_2 would be unsustainable cooperation strategies for a dense Topology B network. The results in this chapter also show that GKH_1 performs only marginally better than the lower computational complexity heuristic GKH_2 in a Topology A or C network. Therefore, ECO-OP with GKH_2 is the best long-term cooperation strategy in a Topology A or C network. This is consistent with the preliminary recommendation presented in Section 9.5. However, in a Topology B network GKH_2 results in significantly shorter lifetimes than GKH_1 for the first 5% of nodes, due to the more heavily concentrated initial partner service distribution of GKH_2 . Therefore, in a Topology B network ECO-OP with GKH_1 is the preferable long-term cooperation strategy, since ECO-OP with GKH_2 more heavily sacrifices the lifetimes of the first few nodes in arriving at a sustainable partner service distribution. It is interesting to note that this

is contrary to the preliminary recommendation of *LKH* or random partner choice for dense Topology B networks in Section 9.5.

The recommendations given above for the best practical long-term cooperation strategy to employ under different network conditions are summarised in the last column of Table 11.1. Additionally, it is important to determine which cooperation strategy works best in general, if these network conditions are unknown. The results in Table 11.1 show that there is no single cooperation strategy which is superior under all network conditions. However, the results presented in this chapter show that the performance of ECO-OP with *GKH₂* is significantly inferior to ECO-OP with *GKH₁* in a Topology B network, whereas the two heuristics are comparable for Topology A and C networks. Therefore, ECO-OP with *GKH₁* is overall the best all-round cooperation strategy for extending the lifetime of a general energy-constrained wireless sensor network of an unknown topology. It is interesting to note that this differs from the preliminary recommendation of *LKH* as the cooperation strategy which best improves the energy efficiency of a general wireless sensor network in Section 9.5. Nevertheless, the results in this chapter have demonstrated that ECO-OP with *LKH* always achieves a very substantial cooperative network lifetime improvement, regardless of network topology or node density. Importantly, *LKH* has the significant practical advantage over *GKH₁* of requiring solely local information and entailing a much lower computational complexity. Therefore, using ECO-OP with *LKH* always enables resource-constrained sensor nodes to substantially extend the lifetime of the wireless sensor network as a whole by making fully autonomous distributed cooperation decisions.

11.6 Summary

In this chapter the network lifetime extension performance of the ECO-OP cooperation strategy proposed in Chapter 7 has been evaluated in three representative network topologies (A, B, C) for the general case of randomly deployed networks of various node density. Moreover, the performance of the low-complexity distributed ECO-OP cooperation strategy with different partner choice rules (*GKH₁*, *GKH₂*, *LKH*, and random partner choice) has been compared against that of the computationally intensive centralised greedy cooperation algorithm proposed in [18].

The results presented in this chapter have shown that ECO-OP always significantly extends the lifetime of a wireless sensor network, for both sparse and dense networks with both random and directed data flow. Specifically, network-wide cooperation using ECO-OP achieves an average network lifetime improvement factor ranging from 3.5 to 10.3 for a Topology A (central destination receiver) network, from 7.3 to 9.3 for a Topology B (remote destination receiver) network, and from 5.7 to 13.0 for a Topology C (node-

to-node communication) network. Therefore, the results in this chapter demonstrate the general validity of network-wide cooperation using ECO-OP as an effective technique for extending the lifetime of a wireless sensor network. Importantly, these results show that altruistic distributed cooperation among autonomous resource-constrained sensor nodes can significantly extend the lifetime of a wireless sensor network as a whole.

Moreover, it has been demonstrated that the distributed ECO-OP cooperation strategy with GKH_1 or GKH_2 overall achieves a comparable network lifetime improvement to the centralised greedy cooperation algorithm [18], regardless of network topology. Specifically, ECO-OP with GKH_1 or GKH_2 achieves a slightly higher average network lifetime improvement factor than the centralised greedy cooperation algorithm [18] for sparse networks and vice versa for dense networks. However, the centralised greedy cooperation algorithm [18] would be prohibitively computationally expensive for practical implementation in a dense network. By contrast, the low-complexity distributed ECO-OP cooperation strategy is inherently scalable and thus suitable for a wireless sensor network of any node density. Therefore, ECO-OP with GKH_1 or GKH_2 outperforms the centralised greedy cooperation algorithm [18] as a practical technique for extending the lifetime of a wireless sensor network over the feasible range of node densities.

The analysis in this chapter has also enabled a through comparison of the characteristic node lifetime curves achieved by these two distinct approaches to coordinating cooperative communication in an energy-constrained wireless sensor network. The algorithm from [18] selects cooperation partners which can *most afford to help*, whereas ECO-OP with GKH_1 or GKH_2 selects those that can *help the most*. Moreover, the centralised greedy cooperation algorithm [18] aims to equalise the projected node lifetimes over the network by matching cooperation partner nodes with high non-cooperative lifetimes to source nodes with low non-cooperative lifetimes and low residual battery energy. In a Topology C network there is a wide range of non-cooperative lifetimes and only a weak correlation between *how much* a node can help and *how much it can afford to help*; consequently the approach from [18] overall achieves a slightly higher node lifetime than ECO-OP as well as a more uniform node lifetime distribution. Conversely, in a Topology B network there is almost no correlation between these two node qualities and a narrow range of non-cooperative lifetimes; therefore the ECO-OP approach works better overall, both in terms of node lifetime improvement and fairness. Finally, in a Topology A network, there is a strong correlation between these two node qualities, and consequently the overall performance of the two approaches is near-equivalent.

Finally, the analysis presented in this chapter has served to determine the best long-term cooperation strategy to employ under different network conditions. The recommended cooperation strategy for practical long-term cooperation among energy-constrained nodes is GKH_2 for a Topology A and C network and GKH_1 for a Topology B network.

Moreover, it has been shown that ECO-OP with GKH_1 is overall the best practical cooperation strategy for extending the lifetime of a general energy-constrained wireless sensor network, as it always achieves the highest network lifetime improvement and node lifetime fairness. However, the results in this chapter have also demonstrated that ECO-OP with LKH always achieves a very substantial cooperative network lifetime improvement, regardless of network topology or node density. Importantly from the point of view of practical implementation, this demonstrates that resource-constrained sensor nodes can cooperate in a fully autonomous and distributed manner using ECO-OP with LKH to substantially extend the lifetime of the wireless sensor network as a whole.

Chapter 12

Conclusions

Wireless sensor networks consist of many resource-constrained distributed nodes, powered by small batteries which are typically never replaced. Consequently, reducing node energy consumption is of central concern to wireless sensor network design. The overall goal of this thesis has been to examine the feasibility of deploying cooperative diversity as a practical energy saving technique for extending the useful lifetime of a wireless sensor network. In order to exploit the energy saving potential of cooperative communication in energy-constrained wireless networks, it is crucial to determine: when cooperation is beneficial and when it is not; how to select the best cooperation partner out of a set of candidate nodes; and how to best allocate transmit power to the cooperating source and partner nodes. Importantly, for a practical deployment of energy efficient cooperative communication to be feasible in a wireless sensor network, resource-constrained sensor nodes must make these cooperation decisions autonomously.

The major outcome of the original research presented in this thesis has been the development of ECO-OP, a novel low-complexity distributed cooperation strategy for coordinating cooperative communication among the nodes in an energy-constrained wireless sensor network. Importantly, it has been demonstrated that altruistic cooperation among autonomous resource-constrained sensor nodes using ECO-OP always significantly extends the lifetime of the wireless sensor network as a whole. Furthermore, it has been shown that the low-complexity distributed ECO-OP cooperation strategy proposed in this thesis overall achieves a comparable network lifetime improvement to a computationally intensive centralised cooperation algorithm from the literature [18].

The original research which has been presented in previous chapters of this thesis is summarised below by highlighting key contributions and analysis results and discussing their significance. Some directions for future research are also suggested.

Energy Efficiency of Cooperative Communication

The energy efficiency of an individual cooperative communication link (consisting of a source node communicating its message to the destination receiver by cooperating with a partner node) has been investigated in this thesis for three major cooperative diversity schemes. The schemes considered are those which have been identified as feasible candidates for practical deployment in wireless sensor networks: virtual-MISO (vMISO), decode-and-forward (DF), and adaptive decode-and-forward (aDF). The problem of transmit power allocation for optimally energy efficient cooperation, subject to a BER constraint, has been studied for each scheme. Moreover, the total communication energy savings achieved by each scheme using optimal transmit power allocation have been illustrated in terms of network geometry for a source node cooperating with a range of potential partners. The resulting *partner choice region* has been used as a tool for evaluating the energy conservation performance of each cooperative diversity scheme and predicting its robustness as a practical energy saving technique in a randomly deployed wireless sensor network with a wide range of potential partner locations.

Optimal Transmit Power Allocation for Energy Efficient Cooperation

The optimal transmit power allocation has been derived analytically for vMISO and DF cooperation. The transmit power allocation problem for energy efficient aDF cooperation has been shown to be non-linear, necessitating the use of a numerical search to obtain the optimum solution. It has been shown that the information exchange between the source and partner dominates the transmit energy consumption of vMISO and DF cooperation. By contrast, it has been demonstrated that optimal transmit power allocation for energy efficient aDF cooperation must achieve a balance between ensuring a good source-partner channel and a good partner-destination channel.

Partner Choice Region for Energy Efficient Cooperation

The problem of best partner choice for energy efficient cooperation has been studied by examining the partner choice region of each cooperative diversity scheme. It has been shown that a non-ideal source-partner channel limits the energy efficiency of vMISO and DF cooperation, such that only a restricted range of partner node locations close the source are beneficial. Therefore, a basic proximity-based partner choice rule for energy efficient vMISO and DF cooperation has been proposed: “*select the partner node closest to the source*”. By contrast, it has been demonstrated that the source-partner and partner-destination channels are both equally important factors in determining the energy efficiency of aDF cooperation. Accordingly, the energy efficiency of aDF cooperation is highest when the partner is located roughly midway between the source and the desti-

nation. Therefore, a basic proximity-based partner choice rule for energy efficient aDF cooperation has been proposed: “*select the partner node closest to the midway point between the source and the destination*”.

Best Cooperative Diversity Scheme for Energy-Constrained Wireless Sensor Networks

The energy conservation performance of vMISO, DF, and aDF cooperation has been thoroughly compared across a wide range of communication system settings and cooperative link configurations, by examining each scheme’s partner choice region as several key system parameters are varied. Specifically, the general energy efficiency of each cooperative diversity scheme has been investigated by analysing the effect of varying the transceiver circuit power consumption, the source-destination separation, the channel path loss exponent, and the target BER. The results have shown that DF always results in a slightly larger energy efficient partner choice region than vMISO. This is due to the additional energy consumption of the explicit source to partner transmission in vMISO, which is avoided in DF. Additionally, in a distributed wireless sensor network it would be difficult to achieve the strict synchronisation between nodes required for vMISO. By contrast, DF has a low implementation complexity. Importantly, the results have consistently demonstrated that aDF results in a significantly larger energy efficient partner choice region than vMISO and DF. This is due to the adaptive nature of aDF, which enables significant energy savings to be achieved despite a non-ideal source-partner channel (unlike in vMISO and DF). This significant energy efficiency advantage of aDF clearly demonstrates the scheme’s superior robustness and flexibility as a practical energy saving technique. Additionally, being a variant of DF, aDF is straightforward to practically implement. Therefore, aDF is the best cooperative diversity scheme to practically deploy in an energy-constrained wireless sensor network.

Distributed Cooperation Strategy for Energy-Constrained Wireless Sensor Networks

A novel low-complexity distributed cooperation strategy for energy-constrained wireless sensor networks has been proposed in this thesis. The proposed cooperation strategy has been named ECO-OP in reference to the energy-conserving cooperation it facilitates among autonomous sensor nodes. ECO-OP is based on simple yet near-optimal power allocation and partner choice heuristics for energy efficient aDF cooperation which have been developed in this thesis. Importantly, ECO-OP thereby enables resource-constrained sensor nodes to cooperate autonomously to extend the lifetime of the wireless sensor network

as a whole. To the best knowledge of the author, ECO-OP is the first distributed cooperation strategy for coordinating cooperative communication in an energy-constrained wireless network. Moreover, ECO-OP is a computationally efficient cooperation strategy with low signalling overhead and is thus suitable for practical implementation on resource-constrained sensor nodes.

Power Allocation Heuristic for Practical Energy Efficient aDF Cooperation

A simple and practical yet near-optimal power allocation heuristic for energy efficient aDF cooperation has been proposed. The development of the heuristic has been informed by the insight gained from examining the nature of the optimal aDF transmit power allocation solution, i.e. that the source-partner and partner-destination channels are both equally important factors in determining the energy efficiency of aDF cooperation. The heuristic has been formulated by considering the individual impact of the source-partner and partner-destination channels on the power allocation for energy efficient aDF; the solutions to these two independent sub-problems have been superimposed to obtain a very good approximation to the optimal aDF power allocation solution. The energy conservation performance of the resulting aDF power allocation heuristic has been thoroughly compared against that of the optimal aDF transmit power allocation solution obtained via numerical search, by examining their respective partner choice regions as several key system parameters are varied. The results have consistently demonstrated that the proposed power allocation heuristic is near-optimal with respect to maximising the energy efficiency of the aDF cooperative communication link. Importantly, the proposed heuristic consists of two straightforward formulae suitable for practical implementation on a resource-constrained sensor node. By contrast, obtaining the optimal aDF power allocation solution via numerical search would be practically infeasible for a sensor node.

Partner Choice Heuristics for Practical Energy Efficient aDF Cooperation

Three simple and robust partner choice heuristics for practical energy efficient aDF cooperation have been proposed: GKH_1 , GKH_2 , and LKH . The heuristics are computationally efficient and based solely on knowledge of average path loss values in the network. This is practically very significant for a wireless sensor network, where nodes can measure average received signal strength but would have to infer the location of other nodes in the network. Importantly, these computationally efficient heuristics enable resource-constrained sensor nodes to independently make energy efficient cooperation decisions. By contrast, it would be prohibitively computationally expensive for a sensor node to select its cooperation partner by explicitly calculating the actual energy saving expected from each candidate partner node. The global knowledge heuristics, GKH_1 and GKH_2 , require the source

node to have knowledge of the source-partner and partner-destination channel quality for each candidate partner node; GKH_1 then involves a simple calculation to determine the ranking of each candidate partner node, whereas GKH_2 requires only a comparison of the two measurements. It has been demonstrated that GKH_1 and GKH_2 achieve near-optimally energy efficient partner selection across a wide range of communication system configurations. The local knowledge heuristic, LKH , ranks each candidate partner by directly using the single measurement of the source-partner channel quality, which the source can obtain autonomously via direct measurement. It has been shown that LKH is suboptimal but nevertheless consistently achieves highly energy efficient partner selection. Thus using LKH simple sensor nodes can cooperate autonomously in a fully distributed and scalable manner to substantially improve the energy efficiency of their cooperative communication link.

The ECO-OP Cooperation Strategy

ECO-OP has been developed based on the power allocation and partner choice heuristics for energy efficient aDF cooperation which have been proposed in this thesis. Using ECO-OP individual source nodes independently make cooperation decisions to minimise the total energy consumed per bit over their own cooperative communication link, ignorant of the cooperation decisions of the other source nodes in the network. Moreover, each sensor node makes its cooperation decisions based solely on measurements of average path loss and is altruistic in the sense that it will unconditionally accept any requests to serve as cooperation partner for other source nodes in the network. Following network activation, each source node in the wireless sensor network selects its preferred cooperation partner. Throughout the lifetime of the cooperative network, a source node only reselects its cooperation partner if its current partner node broadcasts an “ABOUT-TO-EXPIRE” message, indicating it is about to deplete its batteries. Therefore, ECO-OP is a distributed and computationally efficient cooperation strategy with low signalling overhead, suitable for practical implementation on resource-constrained sensor nodes.

Performance of Network-wide Cooperation using ECO-OP

The ultimate aim of the proposed ECO-OP cooperation strategy is to extend the lifetime of a wireless sensor network by coordinating network-wide cooperation among its sensor nodes. However, ECO-OP has been designed to simply maximise the energy efficiency of individual cooperative links in the network, without any regard to the resulting distribution of cooperation partner service, individual node energy consumption, or resulting node lifetimes over the network. This means that ECO-OP is intended to achieve its overall aim of network lifetime extension indirectly. Consequently, the behaviour and

performance of network-wide cooperation using ECO-OP have been thoroughly investigated in this thesis, with respect to the resulting energy conservation and network lifetime extension. This analysis has been based on extensive simulation results of network-wide cooperative communication using ECO-OP with different partner choice rules (GKH_1 , GKH_2 , and LKH) in three representative wireless sensor network topologies: Topology A (central destination receiver), Topology B (remote destination receiver), and Topology C (node-to-node communication). The fundamental behaviour of ECO-OP in these different basic topologies has been illustrated by considering cooperation among 100 nodes regularly placed over the network area. The typical performance of ECO-OP has also been evaluated by considering the general case of randomly deployed networks of various node density for each network topology. Moreover, the network lifetime extension performance of a centralised greedy cooperation algorithm from the literature [18] has been analysed alongside ECO-OP, serving as a benchmark for evaluating the effectiveness of the distributed ECO-OP cooperation strategy proposed in this thesis.

Energy Conservation Performance of ECO-OP

The energy conservation performance of ECO-OP has been investigated by considering the network-wide energy impact of the initial partner selection round at the time of the network's deployment. The results have shown that network-wide cooperation using ECO-OP always significantly reduces the overall network energy expenditure, regardless of network topology or node density. Importantly, this demonstrates that the distributed cooperation decisions made by individual nodes using ECO-OP constitute an effective network-wide cooperation strategy for reducing a wireless sensor network's energy consumption. However, a cooperation strategy which overall conserves energy at the expense of overburdening individual partner nodes is unsustainable. Therefore, the distribution of cooperation partner service and individual node energy consumption over the cooperative network has also been examined to facilitate a preliminary analysis of the general long-term viability of ECO-OP.

It has been shown that using ECO-OP with LKH , partner service is inherently evenly distributed over the network (since nodes cooperate with their nearest neighbour), regardless of network topology. By contrast, using ECO-OP with GKH_1 and GKH_2 partner service is significantly less evenly distributed over the network, with the entire burden of partner service falling on an increasingly smaller number of popular partner nodes the more directed the network's data flow is. Namely, data flow in the remote destination receiver Topology B network is highly directed and consequently the partner service is heavily concentrated on a handful of nodes at the very top of the network. In the central destination receiver Topology A network with moderately directed data flow, the partner service burden is carried by a minority of nodes near the centre of the network, whereas it

is carried by over half of the network's nodes in the node-to-node communication Topology C network with random data flow.

Importantly, it has been demonstrated that popular partner nodes in the GKH_1 and GKH_2 Topology A and C network are not overburdened, despite helping several other nodes. This is because the preferred partner node using GKH_1 or GKH_2 is midway between the source node and the destination receiver. Consequently, the emergent network-wide behaviour of ECO-OP with GKH_1 or GKH_2 is that nodes with relatively low inherent communication energy requirements help source nodes with relatively high inherent energy requirements. The total battery energy resource of the network is thereby reallocated among nodes to produce a more even distribution of energy consumption over the network, which translates into both longer and more uniform predicted node lifetimes. Therefore, ECO-OP with GKH_1 or GKH_2 is always an effective and sustainable cooperation strategy for Topology A and C networks, achieving a significant reduction in overall network energy expenditure without overburdening individual partner nodes.

However, in a dense Topology B network ECO-OP with GKH_1 or GKH_2 achieves the highest overall network energy reduction at the cost of overburdening several partner nodes, to the extent that their energy consumption actually exceeds the maximum non-cooperative node energy consumption in a very dense network. This suggests that ECO-OP with GKH_1 or GKH_2 may be an unsustainable cooperation strategy for a dense Topology B network, as very popular partner nodes would prematurely deplete their own energy supply in helping other nodes.

By contrast, partner nodes are never overburdened in the LKH cooperative network due to an inherently distributed partner service burden. Moreover, ECO-OP with LKH always yields a substantial overall network energy reduction, albeit inferior to ECO-OP with GKH_1 and GKH_2 . Therefore, ECO-OP with LKH is a sustainable energy-conserving cooperation strategy, regardless of network topology or node density. Importantly from the point of view of practical implementation, this demonstrates that resource-constrained sensor nodes can autonomously cooperate in a fully distributed and scalable manner to substantially improve the energy efficiency of the wireless sensor network as a whole.

Network Lifetime Extension Performance of ECO-OP

In order to establish the validity of ECO-OP as an effective technique for extending the lifetime of a wireless sensor network, the long-term benefit of network-wide cooperation using ECO-OP has been explicitly investigated. The long-term performance of ECO-OP has been examined by comparing the node lifetime curves of a non-cooperative and cooperative network (i.e. node lifetime versus the number of node deaths since network activation: x^{th} node lifetime vs. x). The overall network lifetime extension performance of ECO-OP

has been quantified in terms of the average network lifetime improvement achieved (i.e. the average of the cooperative x^{th} node lifetime improvement achieved from network activation through to the last node death). The results have shown that network-wide cooperation using ECO-OP always significantly extends the lifetime of a wireless sensor network, for both sparse and dense networks with both random and directed data flow. Importantly, this demonstrates that altruistic cooperation among independently-acting resource-constrained sensor nodes can significantly extend the lifetime of the wireless sensor network as a whole.

The long-term behaviour of ECO-OP has been further analysed by examining the distribution of the individual node lifetimes across the cooperative network and the average distribution of cooperation partner service and selection throughout the lifetime of the network. It has been shown that the overall pattern of ECO-OP partner service does not change substantially throughout the lifetime of the Topology A and C networks. This demonstrates the low signalling and organisational overhead of long-term cooperation using ECO-OP. The same trend has also been demonstrated for the Topology B network using ECO-OP with *LKH*. By contrast, the overall pattern of partner service using ECO-OP with *GKH₁* or *GKH₂* changes considerably throughout the lifetime of the Topology B network, automatically becoming increasingly distributed as overpopular partner nodes prematurely deplete their energy. Importantly, this clearly demonstrates that ECO-OP with *GKH₁* or *GKH₂* is *not* an unsustainable long-term cooperation strategy for the Topology B network. Rather, the lifetimes of the first 10% of nodes are sacrificed in order to arrive at a sustainable partner service distribution which improves the lifetimes of the rest of the network's nodes.

It has also been shown that ECO-OP with *GKH₁* or *GKH₂* reallocates the network's combined energy resource among nodes to achieve a substantially more uniform distribution of node lifetimes over network, for all three network topologies. An even distribution of node lifetimes across the network is desirable because it means that the network will remain fully functional throughout its operational lifetime. The improved node lifetime fairness achieved by ECO-OP with *GKH₁* or *GKH₂* is a result of generally selecting partner nodes with high non-cooperative lifetimes to serve as partners to nodes with low non-cooperative lifetimes. By contrast, ECO-OP with *LKH* generally maintains the relative node lifetime distribution of the non-cooperative network, by virtue of neighbouring nodes with similar non-cooperative lifetimes serving as each other's cooperation partners.

Recommended Cooperation Strategy for Practical Deployment in a Wireless Sensor Network

The network lifetime extension performance of ECO-OP using different partner choice rules has been extensively compared in this thesis. This analysis has served to determine

the recommended cooperation strategy for practical deployment in an energy-constrained wireless sensor network for a given set of network conditions. The results in this thesis have shown that ECO-OP with GKH_1 or GKH_2 always outperforms ECO-OP with LKH in terms of network lifetime improvement and node lifetime fairness, regardless of network topology or node density. In a Topology A or C network, GKH_1 performs only marginally better than the lower computational complexity heuristic GKH_2 . Therefore, ECO-OP with GKH_2 is the best practical long-term cooperation strategy for a Topology A or C network. However, in a Topology B network, GKH_2 results in significantly shorter lifetimes than GKH_1 for the first 5% of nodes, due to the more heavily concentrated initial partner service distribution of GKH_2 . Therefore, in a Topology B network ECO-OP with GKH_1 is the preferable long-term cooperation strategy, since ECO-OP with GKH_2 more heavily sacrifices the lifetimes of the first few nodes in arriving at a sustainable partner service distribution. It follows that ECO-OP with GKH_1 is the best all-round cooperation strategy for extending the lifetime of a general energy-constrained wireless sensor network (of an unknown topology). However, the results in this thesis have also demonstrated that ECO-OP with LKH always achieves a very substantial cooperative network lifetime improvement, regardless of network topology or node density. Importantly, LKH has the distinct practical advantage of requiring solely local information and entailing a much lower computational complexity than GKH_1 . Therefore, using ECO-OP with LKH always enables resource-constrained sensor nodes to substantially extend the lifetime of the wireless sensor network as a whole, by making fully autonomous distributed cooperation decisions.

Comparison of ECO-OP with a Centralised Greedy Cooperation Algorithm from the Literature

The network lifetime extension performance of the proposed ECO-OP cooperation strategy has been extensively compared against that of the centralised greedy cooperation algorithm from the literature [18]. The results have consistently demonstrated that ECO-OP with GKH_1 or GKH_2 achieves a slightly higher average network lifetime improvement factor than the centralised greedy cooperation algorithm [18] for sparse networks and vice versa for dense networks, regardless of network topology. Importantly, this demonstrates that the low-complexity distributed ECO-OP cooperation strategy proposed in this thesis overall achieves a comparable network lifetime improvement to the computationally intensive centralised cooperation algorithm from the literature. Additionally, the computationally intensive greedy cooperation algorithm [18] must be repeated whenever a node depletes its energy, to reallocate cooperation partners to each surviving node in the network; this renders the algorithm from [18] prohibitively computationally expensive for practical long-term implementation in a dense network. By contrast, the low-complexity

distributed ECO-OP cooperation strategy is inherently scalable and thus suitable for a wireless sensor network of any node density. Therefore, ECO-OP with GKH_1 or GKH_2 outperforms the centralised greedy cooperation algorithm [18] as a practical technique for extending the lifetime of a wireless sensor network over the feasible range of node densities.

The analysis in this thesis has furthermore enabled a thorough comparison of the characteristic node lifetime curves achieved by these two fundamentally distinct approaches to coordinating cooperative communication in an energy-constrained wireless network. It has been shown that the algorithm from [18] selects cooperation partners which can *most afford to help*, whereas ECO-OP with GKH_1 or GKH_2 selects those that can *help the most*. Moreover, the centralised greedy cooperation algorithm [18] aims to equalise the projected node lifetimes over the network by matching cooperation partner nodes with high non-cooperative lifetimes to source nodes with low non-cooperative lifetimes and low residual battery energy. In the random data flow Topology C network there is a wide range of non-cooperative lifetimes and only a weak correlation between *how much* a node can help and *how much it can afford to help*; consequently the approach from [18] overall achieves a slightly higher node lifetime than ECO-OP, as well as a more uniform node lifetime distribution. Conversely, in the remote destination receiver Topology B network there is almost no correlation between these two node qualities and a narrow range of non-cooperative lifetimes; thus the ECO-OP approach performs better overall, both in terms of node lifetime improvement and fairness. Finally, in the central destination receiver Topology A network, there is a strong correlation between these two node qualities, and consequently the overall performance of the two approaches is near-equivalent.

Future Research Directions

This thesis has presented a thorough investigation of the feasibility of deploying cooperative diversity as a practical energy saving technique for extending the useful lifetime of a wireless sensor network. Importantly, it has presented a robust analytical evaluation of the proposed distributed ECO-OP cooperation strategy to demonstrate that altruistic cooperation among independently-acting sensor nodes can significantly prolong the lifetime of the wireless sensor network as a whole. Several possible directions for extending the research presented in this thesis are briefly outlined below.

Modified ECO-OP Cooperation Strategy

Analysis of the performance of ECO-OP in the remote destination receiver Topology B network has shown that ECO-OP with GKH_1 or GKH_2 initially overburdens a handful of very popular partner nodes, causing them to prematurely deplete their batteries.

Subsequently, the lifetimes of the first 10% of nodes are sacrificed in order to arrive at a sustainable partner service distribution which is of long-term benefit to the rest of the network. It would be interesting to instead consider a modified ECO-OP partner selection strategy, whereby a limit is placed on the number of source nodes a partner node can serve (as discussed briefly in Chapters 9 and 11). By restricting the partner burden placed upon a single partner node, this modified strategy might from the outset produce a sustainable distribution of partner service, thus precluding the premature loss of the first 10% of nodes. This modification would thus also reduce the signalling overhead of nodes reselecting a cooperation partner every few transmission rounds, although this would need to be balanced against the increased signalling inherent in implementing the selective acceptance of cooperation requests by nodes. Investigating the viability of such a modification to ECO-OP and evaluating the accompanying engineering trade-offs is an interesting direction for future research.

Robustness of ECO-OP to Channel Measurement Errors

The analysis in this thesis has assumed that nodes can acquire perfect knowledge of average path losses in the network. In practice, nodes would have to measure average received signal strength to estimate channel quality. It would be practically significant to investigate the impact of channel measurement errors on nodes' cooperation decisions and to study the potential associated degradation in ECO-OP's performance.

Impact of Node Mobility on the Performance of ECO-OP

The performance of ECO-OP has been analysed in this thesis solely for static networks. However, ECO-OP is in general valid for energy-constrained networks with low to moderate mobility, which also exhibit slow fading. Examining the implications of node mobility on the operation, performance, and signalling overhead of ECO-OP is an interesting future research direction.

The Role of Altruism for Energy Efficient Cooperation

In this thesis it has been assumed that using ECO-OP all nodes in the network are completely altruistic, in the sense that they unconditionally accept all requests to serve as cooperation partner for other nodes in the network. The ECO-OP strategy has been designed in this manner in accordance with the self-organising and low signalling overhead requirements of wireless sensor networks; using ECO-OP nodes are completely ignorant of each other's cooperation decisions, resulting in a fully self-organising distributed cooperation strategy. However, it would also be interesting to investigate what proportion of the network's nodes *must* be altruistic in order for the network as a whole to benefit from

ECO-OP. Conversely, the question of what proportion of nodes can be selfish (i.e. refusing to serve as cooperation partners) for the network to still benefit from energy efficient cooperation may be of greater practical interest. This would be particularly relevant in the context of deploying energy efficient cooperative diversity for “green communications” in infrastructure-based wireless networks such as cellular networks, where node selfishness is a common assumption.

Appendix A

Description of the Centralised Greedy Cooperation Algorithm from the Literature

A.1 Introduction

This appendix presents a description of the centralised greedy cooperation algorithm which was proposed in [18] to maximise the minimum node lifetime in an energy-constrained wireless network using cooperative communication. It should be noted that the work in [18] is the most relevant in the existing literature to the original research on network-wide cooperation for extending wireless sensor network lifetime presented Chapters 7-11 of this thesis. Consequently, the cooperation algorithm proposed in [18] serves as a benchmark for evaluating the effectiveness of the novel ECO-OP cooperation strategy proposed in this thesis as a technique for extending the lifetime of a wireless sensor network. The network lifetime extension performance of the two distinct cooperation strategies is extensively compared in the simulation results presented in Chapters 10 and 11; an overview of these investigations is presented in Section 7.3.2.

The centralised greedy cooperation algorithm [18] is described in detail in Section A.2, based on the authors' description of the algorithm given in Section III-C of [18]. Section A.3 presents several further notes regarding the implementation of the algorithm proposed in [18] for the purpose of generating the simulation results presented in this thesis.

A.2 Algorithm Description

A central controller performs a computationally intensive offline greedy search in [18] to allocate cooperation partners and transmit power for each node in the network. Specifically, the central controller iteratively allocates a partner node to each source node in the network by maximising the minimum node lifetime over the network at each step, whereby transmit power is allocated to the cooperating source and partner nodes such that their projected lifetimes are equalised. The centralised greedy cooperation algorithm [18] has been summarised in the flowchart of Fig. A.1, which is an adaptation of Fig. 4 and Table I in Section III-C of [18]. It should be noted that the node lifetime notation used in Fig. A.1 is consistent with that presented in Section 7.6.

Fig. A.1 shows how the centralised greedy cooperation algorithm [18] performs network-wide cooperation partner and power allocation. Let us assume a network of M sensor nodes, where \mathbf{M} denotes the set of all nodes in the network. As for the ECO-OP cooperation strategy presented in Section 7.2, it is assumed that each node in the network acts as a source and is eligible to serve as a cooperation partner to any other source node in the network. As shown in Fig. A.1, the central controller firstly initialises the predicted node lifetimes of all nodes in the network by setting $T'_{node(j)}$ equal to the non-cooperative node lifetime $T_{non-coop_node(j)}$, as given by (7.14), for all $j \in \mathbf{M}$. The set of all source nodes yet to be allocated a cooperation partner \mathbf{C} is then initialised as the set \mathbf{M} of all nodes in the network. After this initialisation phase, the central controller iteratively allocates a cooperation partner and transmit power for each source node in set \mathbf{C} . At each step, the central controller selects the source node \hat{j} with the minimum predicted lifetime in the set \mathbf{C} as the current source node to be allocated a cooperation partner. The central controller then selects node \hat{i} (from the set of candidate partner nodes $\varphi_{\hat{j}}$) to serve as cooperation partner for source node \hat{j} , by searching for the candidate partner node which results in the highest minimum predicted node lifetime over the network given that partner allocation. The central controller then allocates the transmit powers $E_{tx_s(\hat{j},\hat{i})}$ and $E_{tx_p(\hat{i},\hat{j})}$ for the cooperative transmission of source node \hat{j} and its allocated partner node \hat{i} , such that the predicted lifetimes of nodes \hat{j} and \hat{i} are equalised. Lastly, the central controller updates the predicted lifetimes of nodes \hat{i} and \hat{j} by setting $T'_{node(\hat{j})}$ and $T'_{node(\hat{i})}$ equal to their cooperative node lifetimes $T'_{coop_node(\hat{j})}$ and $T'_{coop_node(\hat{i})}$ respectively, as given by (7.17). The set \mathbf{C} is then updated by removing node \hat{i} and the iteration loop is repeated by the central controller until all source nodes in the network have been allocated a cooperation partner (i.e. the set \mathbf{C} is empty).

It is important to note that the greedy search performed by the algorithm in [18] to find the best candidate partner node for a given source node \hat{j} is very computationally intensive. Firstly, for each candidate partner node $i \in \varphi_{\hat{j}}$ the central controller must

search for the transmit power allocation $E_{tx-s(\hat{j},i)}$ and $E_{tx-p(i,\hat{j})}$ which will make the predicted lifetimes of nodes \hat{j} are i equal if candidate partner node i was to be selected to serve source node \hat{j} (i.e. $T'_{node(\hat{j})}=T'_{node(i)}$). Here the predicted lifetimes of nodes i and \hat{j} if candidate partner node i was to be selected to serve source node \hat{j} are calculated using the cooperative node lifetime formula given by (7.17), taking into account the energy consumption of nodes i and \hat{j} associated with the potential cooperation between them, as well as any other cooperation partner service hitherto assigned to either node. The central controller must then record the corresponding minimum predicted lifetime over the network if candidate partner node i was to be selected to serve source node \hat{j} , $T'_{MIN(i)} = \min_{j \in \mathbf{M}} \{T'_{node(j)}\}$. Finally, the central controller allocates to source node \hat{j} the candidate partner node \hat{i} which maximises the minimum predicted node lifetime over the network after the partner assignment is made, namely $\hat{i} = \max_{i \in \varphi_{\hat{j}}} \{T'_{MIN(i)}\}$.

It is also important to note that, in generating the simulation results presented in Chapters 10 and 11, the algorithm described in Fig. A.1 was first performed after network activation and then re-run each time a node depletes its energy. In these subsequent runs, all non-surviving nodes are removed from the set \mathbf{M} and the residual energy of each surviving node replaces $E_{battery}$ in calculating $T_{non-coop-node(j)}$ using (7.14) in the first step of the algorithm (as well as in calculating the cooperative node lifetimes using (7.17) in subsequent steps of the algorithm).

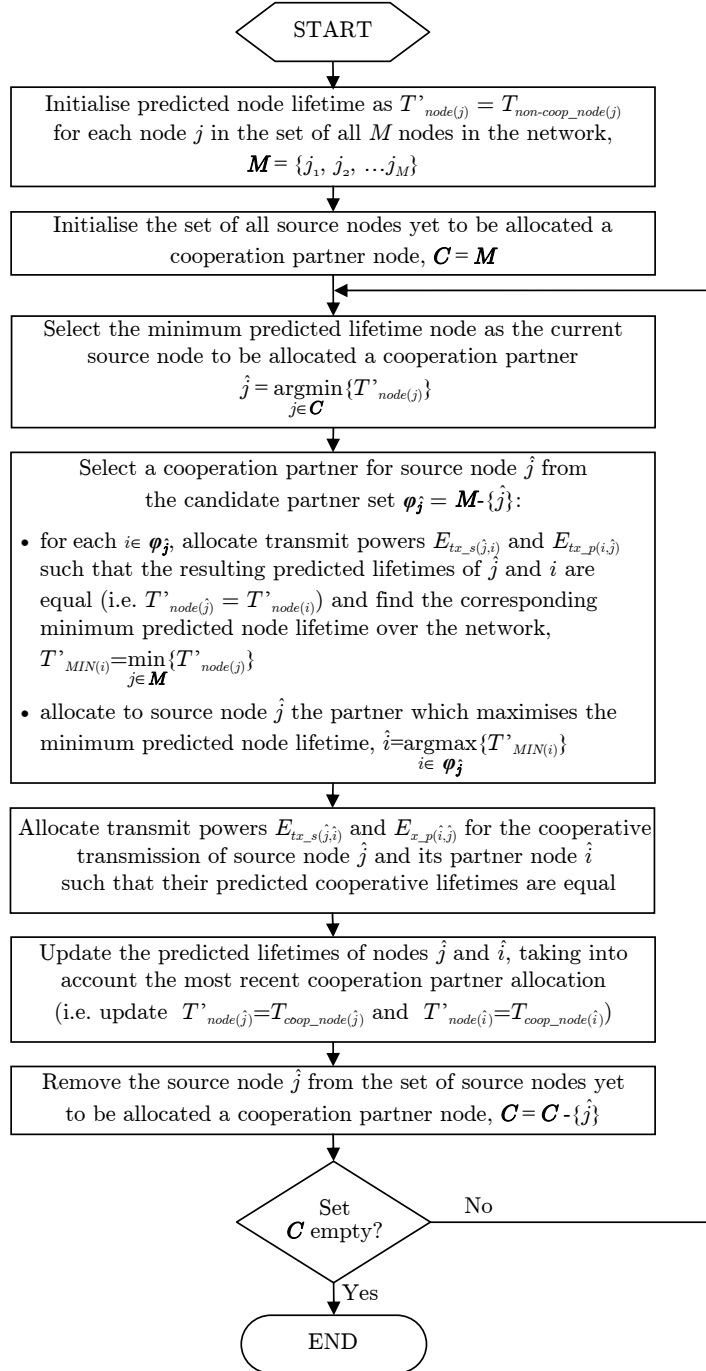


Figure A.1: Flowchart describing the centralised greedy cooperation algorithm proposed in [18]. In generating the simulation results presented in Chapters 10 and 11, this algorithm was first performed after network activation and then re-run each time a node depletes its energy, reallocating cooperation partners to all surviving nodes while taking into account their residual battery energy levels.

A.3 Implementation Notes

The analysis presented in [18] only considered network lifetime in terms of the time until the first node death. Namely, in the results presented in [18], the simulation would have ended when the first node depletes its energy and thus the algorithm in Fig. A.1 is performed only once after network activation. By contrast, the analysis in Chapters 10 and 11 considers the performance of network-wide cooperative communication from network activation through to the last node death. Therefore, in generating the simulation results for the centralised greedy algorithm [18] in Chapters 10 and 11, each surviving source node in the network was allocated its cooperation partner anew as per the algorithm in Fig. A.1 whenever a node would expire. Importantly, this affords the centralised greedy cooperation algorithm [18] the advantage over ECO-OP of continually balancing the projected lifetimes of all remaining nodes based on the distribution of residual energy in the network. However, the fact that the computationally intensive algorithm described in Fig. A.1 is repeated each time a node depletes its energy also effectively renders the cooperation strategy proposed in [18] prohibitively computationally expensive for long-term cooperation in dense wireless networks. By contrast, using the low-complexity distributed ECO-OP cooperation strategy proposed in this thesis, only the source nodes associated with the expired partner node must reselect a partner. Nonetheless, to enable a thorough comparison of these two distinct cooperation strategies, simulation results for the centralised greedy cooperation algorithm [18] are still presented in Chapters 10 and 11 for large values of M , albeit based on a smaller number of network realisations due to the extremely long simulation times. Specifically, the results for the centralised greedy cooperation algorithm [18] presented in Chapter 11 for $M=\{100, 300\}$ are given by the median of $Q=\{350, 15\}$ simulation runs respectively, and no results are presented for $M=1000$. It is also interesting to note that the simulation results (of first node lifetime only) presented in [18] only consider networks of up to $M=50$ nodes.

It should also be noted that the cooperative system model adopted in [18] differs somewhat from that employed throughout this thesis. Therefore, for the sake of a fair comparison with ECO-OP, in generating the simulation results presented in Chapters 10 and 11 the cooperation algorithm proposed in [18] was faithfully implemented based on the authors' description in [18], but based on the energy model, cooperative diversity scheme, reference system parameters, and wireless sensor network model employed throughout this thesis¹ (as specified in Chapters 2 and 7). Moreover, the node and network lifetime definitions presented in reference to ECO-OP in Section 7.6 also apply in the investigation of the lifetime extension performance of the centralised greedy cooperation algorithm [18] in Chapters 10 and 11 (except that the upper bound on the size of the cooperation partner

¹Indeed in [18] the authors comment that “*the proposed greedy ... approach can be applied to any multi-node cooperation strategy*” [18].

sets \mathbf{I} and \mathbf{H}' is different to ECO-OP, due to the network-wide reallocation of cooperation partners after each node death using the algorithm from [18]). Finally, it should be noted that the system model assumed in [18] means that cooperative transmit power allocation is calculated in [18] by solving a cubic equation, whereas it is found via an exhaustive search² in generating the simulation results for the centralised greedy cooperation algorithm [18] presented in Chapters 10 and 11.

²Namely, the transmit power allocation for the centralised greedy cooperation algorithm [18] has been implemented via an exhaustive search so as to equalise the projected lifetimes of the source and its candidate partner node, while satisfying the BER constraint $BER_{coop-ADF} \leq pb$.

References

- [1] I. Akyildiz, W. Su, Y. Sankarasubramaniam, and E. Cayirci, “A survey on sensor networks,” *IEEE Commun. Mag.*, vol. 40, no. 8, pp. 102–114, Aug. 2002.
- [2] K. Holger and A. Willig, *Protocols and Architectures for Wireless Sensor Networks*. Chichester: John Wiley & Sons, 2005.
- [3] G. J. Pottie and W. J. Kaiser, “Wireless integrated network sensors,” *Commun. ACM*, vol. 43, no. 5, pp. 51–58, May 2000.
- [4] V. Raghunathan, C. Schurgers, S. Park, and M. Srivastava, “Energy-aware wireless microsensor networks,” *IEEE Signal Process. Mag.*, vol. 19, no. 2, pp. 40–50, Mar. 2002.
- [5] Y. Chen and Q. Zhao, “On the lifetime of wireless sensor networks,” *IEEE Commun. Lett.*, vol. 9, no. 11, pp. 976–978, Nov. 2005.
- [6] T. S. Rappaport, *Wireless Communications: Principles and Practice*, 2nd ed. Upper Saddle River: Prentice Hall, 2002.
- [7] H. Jafarkhani, *Space-Time Coding: Theory and Practice*. Cambridge: Cambridge University Press, 2005.
- [8] J. G. Proakis, *Digital Communications*, 3rd ed. New York: McGraw-Hill, 1995.
- [9] D. Tse and P. Viswanath, *Fundamentals of Wireless Communication*. Cambridge: Cambridge University Press, 2005.
- [10] B. Vucetic and J. Yuan, *Space-Time Coding*. Chichester: John Wiley & Sons, 2003.
- [11] A. Sendonaris, E. Erkip, and B. Aazhang, “User cooperation diversity - Part I: System description,” *IEEE Trans. Commun.*, vol. 51, no. 11, pp. 1927–1938, Nov. 2003.
- [12] —, “User cooperation diversity - Part II: Implementation aspects and performance analysis,” *IEEE Trans. Commun.*, vol. 51, no. 11, pp. 1939–1948, Nov. 2003.

-
- [13] J. Laneman, D. Tse, and G. Wornell, "Cooperative diversity in wireless networks: Efficient protocols and outage behavior," *IEEE Trans. Inf. Theory*, vol. 50, no. 12, pp. 3062–3080, Dec. 2004.
- [14] A. Nosratinia, T. Hunter, and A. Hedayat, "Cooperative communication in wireless networks," *IEEE Commun. Mag.*, vol. 42, no. 10, pp. 74–80, Oct. 2004.
- [15] T. Hunter and A. Nosratinia, "Diversity through coded cooperation," *IEEE Trans. Wireless Commun.*, vol. 5, no. 2, pp. 283–289, Feb. 2006.
- [16] S. Cui, A. J. Goldsmith, and A. Bahai, "Energy-efficiency of MIMO and cooperative MIMO techniques in sensor networks," *IEEE J. Select. Areas Commun.*, vol. 22, no. 6, pp. 1089–1098, Aug. 2004.
- [17] S. Jayaweera, "Virtual MIMO-based cooperative communication for energy-constrained wireless sensor networks," *IEEE Trans. Wireless Commun.*, vol. 5, no. 5, pp. 984–989, May 2006.
- [18] T. Himsoon, W. P. Siriwongpairat, Z. Han, and K. J. R. Liu, "Lifetime maximization via cooperative nodes and relay deployment in wireless networks," *IEEE J. Select. Areas Commun.*, vol. 25, no. 2, pp. 306–317, Feb. 2007.
- [19] V. Mahinthan, C. Lin, J. Mark, and X. Shen, "Maximizing cooperative diversity energy gain for wireless networks," *IEEE Trans. Wireless Commun.*, vol. 6, no. 7, pp. 2530–2539, July 2007.
- [20] N. Vien, H. Nguyen, and T. Le-Ngoc, "Diversity analysis of smart relaying," *IEEE Trans. Veh. Technol.*, vol. 58, no. 6, pp. 2849–2862, July 2009.
- [21] J. Laneman and G. Wornell, "Distributed space-time-coded protocols for exploiting cooperative diversity in wireless networks," *IEEE Trans. Inf. Theory*, vol. 49, no. 10, pp. 2415–2425, Oct. 2003.
- [22] M. Dohler, A. Gkelias, and A. Aghvami, "Capacity of distributed PHY-layer sensor networks," *IEEE Trans. Veh. Technol.*, vol. 55, no. 2, pp. 622–639, Mar. 2006.
- [23] P. Herhold, E. Zimmermann, and G. Fettweis, "A simple cooperative extension to wireless relaying," in *Proc. International Zurich Seminar on Communications*, Zurich, 2004.
- [24] V. Mahinthan, J. Mark, and X. Shen, "Adaptive regenerate and forward cooperative diversity system based on quadrature signaling," in *Proc. IEEE Global Telecommunications Conference (GLOBECOM 2006)*, San Francisco, 2006.

-
- [25] M. Janani, A. Hedayat, T. Hunter, and A. Nosratinia, "Coded cooperation in wireless communications: space-time transmission and iterative decoding," *IEEE Trans. Signal Process.*, vol. 52, no. 2, pp. 362–371, Feb. 2004.
- [26] A. Stefanov and E. Erkip, "Cooperative coding for wireless networks," *IEEE Trans. Commun.*, vol. 52, no. 9, pp. 1470–1476, Sept. 2004.
- [27] B. Zhao and M. Valenti, "Distributed turbo coded diversity for relay channel," *Electron. Lett.*, vol. 39, no. 10, pp. 786 – 787, May 2003.
- [28] R. Madan, N. Mehta, A. Molisch, and J. Zhang, "Energy-efficient cooperative relaying over fading channels with simple relay selection," *IEEE Trans. Wireless Commun.*, vol. 7, no. 8, pp. 3013–3025, Aug. 2008.
- [29] A. Bletsas, A. Khisti, D. Reed, and A. Lippman, "A simple cooperative diversity method based on network path selection," *IEEE J. Sel. Areas Commun.*, vol. 24, no. 3, pp. 659–672, Mar. 2006.
- [30] B. Zhao and M. Valenti, "Practical relay networks: a generalization of hybrid-ARQ," *IEEE J. Sel. Areas Commun.*, vol. 23, no. 1, pp. 7–18, Jan. 2005.
- [31] C. Lo, S. Vishwanath, and R. Heath, "Relay subset selection in wireless networks using partial decode-and-forward transmission," *IEEE Trans. Veh. Technol.*, vol. 58, no. 2, pp. 692–704, Feb. 2009.
- [32] K. Phan, T. Le-Ngoc, S. Vorobyov, and C. Tellambura, "Power allocation in wireless multi-user relay networks," *IEEE Trans. Wireless Commun.*, vol. 8, no. 5, pp. 2535–2545, May 2009.
- [33] V. Mahinthan, L. Cai, J. Mark, and X. Shen, "Partner selection based on optimal power allocation in cooperative-diversity systems," *IEEE Trans. Veh. Technol.*, vol. 57, no. 1, pp. 511–520, Jan. 2008.
- [34] S. Wei, "Diversity-multiplexing tradeoff of asynchronous cooperative diversity in wireless networks," *IEEE Trans. Inf. Theory*, vol. 53, no. 11, pp. 4150–4172, Nov. 2007.
- [35] L. Simić, S. M. Berber, and K. W. Sowerby, "Partner choice and power allocation for energy efficient cooperation in wireless sensor networks," in *Proc. IEEE International Conference on Communications (ICC 2008)*, Beijing, 2008.
- [36] R. Eaves and A. Levesque, "Probability of block error for very slow Rayleigh fading in Gaussian noise," *IEEE Trans. Commun.*, vol. 25, no. 3, pp. 368–374, Mar. 1977.

- [37] S. Cui, A. Goldsmith, and A. Bahai, "Energy-constrained modulation optimization," *IEEE Trans. Wireless Commun.*, vol. 4, no. 5, pp. 2349–2360, Sept. 2005.
- [38] L. Simić, S. M. Berber, and K. W. Sowerby, "Energy-efficiency of cooperative diversity techniques in wireless sensor networks," in *Proc. 18th Annual IEEE International Symposium on Personal, Indoor and Mobile Radio Communications (PIMRC 2007)*, Athens, 2007.
- [39] X. Li, M. Chen, and W. Liu, "Application of STBC-encoded cooperative transmissions in wireless sensor networks," *IEEE Signal Process. Lett.*, vol. 12, no. 2, pp. 134–137, Feb. 2005.
- [40] Y. Yuan, Z. He, and M. Chen, "Virtual MIMO-based cross-layer design for wireless sensor networks," *IEEE Trans. Veh. Technol.*, vol. 55, no. 3, pp. 856–864, May 2006.
- [41] W. Heinzelman, A. Chandrakasan, and H. Balakrishnan, "Energy-efficient communication protocol for wireless microsensor networks," in *Proc. Hawaii Int. Conf. System Sci.*, Maui, 2000.
- [42] Z. Zhou, S. Zhou, S. Cui, and J.-H. Cui, "Energy-efficient cooperative communication in a clustered wireless sensor network," *IEEE Trans. Veh. Technol.*, vol. 57, no. 6, pp. 3618–3628, Nov. 2008.
- [43] A. Scaglione and Y.-W. Hong, "Opportunistic large arrays: cooperative transmission in wireless multihop ad hoc networks to reach far distances," *IEEE Trans. Signal Process.*, vol. 51, no. 8, pp. 2082–2092, Aug. 2003.
- [44] B. Sirkeci-Mergen and A. Scaglione, "On the power efficiency of cooperative broadcast in dense wireless networks," *IEEE J. Sel. Areas Commun.*, vol. 25, no. 2, pp. 497–507, Feb. 2007.
- [45] A. Kailas and M. Ingram, "Alternating opportunistic large arrays in broadcasting for network lifetime extension," *IEEE Trans. Wireless Commun.*, vol. 8, no. 6, pp. 2831–2835, June 2009.
- [46] L. Lai and H. El Gamal, "On cooperation in energy efficient wireless networks: the role of altruistic nodes," *IEEE Trans. Wireless Commun.*, vol. 7, no. 5, pp. 1868–1878, May 2008.
- [47] J. Luo, R. Blum, L. Cimini, L. Greenstein, and A. Haimovich, "Decode-and-forward cooperative diversity with power allocation in wireless networks," *IEEE Trans. Wireless Commun.*, vol. 6, no. 3, pp. 793–799, Mar. 2007.

- [48] R. Annavajjala, P. C. Cosman, and L. B. Milstein, "Statistical channel knowledge-based optimum power allocation for relaying protocols in the high SNR regime," *IEEE J. Sel. Areas Commun.*, vol. 25, no. 2, pp. 292–305, Feb. 2007.
- [49] Y. Li, B. Vucetic, Z. Zhou, and M. Dohler, "Distributed adaptive power allocation for wireless relay networks," *IEEE Trans. Wireless Commun.*, vol. 6, no. 3, pp. 948–958, Mar. 2007.
- [50] W. Su, A. Sadek, and K. Liu, "SER performance analysis and optimum power allocation for decode-and-forward cooperation protocol in wireless networks," in *Proc. IEEE Wireless Communications and Networking Conference (WCNC 2005)*, New Orleans, 2005.
- [51] A. Ibrahim, A. Sadek, W. Su, and K. Liu, "Cooperative communications with relay-selection: when to cooperate and whom to cooperate with?" *IEEE Trans. Wireless Commun.*, vol. 7, no. 7, pp. 2814–2827, July 2008.
- [52] B. Maham, A. Hjørungnes, and M. Debbah, "Power allocations in minimum-energy SER-constrained cooperative networks," *Annals of Telecommunications*, vol. 64, no. 7-8, pp. 545–555, Aug. 2009.
- [53] Y. Yao, X. Cai, and G. Giannakis, "On energy efficiency and optimum resource allocation of relay transmissions in the low-power regime," *IEEE Trans. Wireless Commun.*, vol. 4, no. 6, pp. 2917–2927, Nov. 2005.
- [54] Z. Lin, E. Erkip, and A. Stefanov, "Cooperative regions and partner choice in coded cooperative systems," *IEEE Trans. Commun.*, vol. 54, no. 7, pp. 1323–1334, July 2006.
- [55] A. Nosratinia and T. E. Hunter, "Grouping and partner selection in cooperative wireless networks," *IEEE J. Select. Areas Commun.*, vol. 25, no. 2, pp. 369–378, Feb. 2007.
- [56] J. Cannons, L. Milstein, and K. Zeger, "An algorithm for wireless relay placement," *IEEE Trans. Wireless Commun.*, vol. 8, no. 11, pp. 5564–5574, Nov. 2009.
- [57] Y. Jing and H. Jafarkhani, "Single and multiple relay selection schemes and their achievable diversity orders," *IEEE Trans. Wireless Commun.*, vol. 8, no. 3, pp. 1414–1423, Mar. 2009.
- [58] L. Simić, S. M. Berber, and K. W. Sowerby, "Distributed partner choice for energy efficient cooperation in a wireless sensor network," in *Proc. IEEE Global Telecommunications Conference (GLOBECOM 2008)*, New Orleans, 2008.

- [59] Z. Han, T. Himsoon, W. Siriwongpairat, and K. Liu, "Resource allocation for multiuser cooperative OFDM networks: Who helps whom and how to cooperate," *IEEE Trans. Veh. Technol.*, vol. 58, no. 5, pp. 2378–2391, June 2009.
- [60] T. C. Wang, S. Y. Chang, and H.-C. Wu, "Optimal energy-efficient pair-wise cooperative transmission scheme for WiMAX mesh networks," *IEEE Sel. Areas Commun.*, vol. 27, no. 2, pp. 191–201, Feb. 2009.
- [61] P. Liu, Z. Tao, S. Narayanan, T. Korakis, and S. S. Panwar, "CoopMAC: A cooperative MAC for wireless LANs," *IEEE J. Sel. Areas Commun.*, vol. 25, no. 2, pp. 340–354, Feb. 2007.
- [62] T. C.-Y. Ng and W. Yu, "Joint optimization of relay strategies and resource allocations in cooperative cellular networks," *IEEE J. Sel. Areas Commun.*, vol. 25, no. 2, pp. 328–339, Feb. 2007.
- [63] W. Chen, L. Dai, K. Ben Letaief, and Z. Cao, "A unified cross-layer framework for resource allocation in cooperative networks," *IEEE Trans. Wireless Commun.*, vol. 7, no. 8, pp. 3000–3012, Aug. 2008.
- [64] T. Guo and R. Carrasco, "CRBAR: Cooperative relay-based auto rate MAC for multirate wireless networks," *IEEE Trans. Wireless Commun.*, vol. 8, no. 12, pp. 5938–5947, Dec. 2009.
- [65] B. Wang, Z. Han, and K. Liu, "Distributed relay selection and power control for multiuser cooperative communication networks using Stackelberg game," *IEEE Trans. Mobile Comput.*, vol. 8, no. 7, pp. 975–990, July 2009.
- [66] Z. Zhou, S. Zhou, J.-H. Cui, and S. Cui, "Energy-efficient cooperative communication based on power control and selective single-relay in wireless sensor networks," *IEEE Trans. Wireless Commun.*, vol. 7, no. 8, pp. 3066–3078, Aug. 2008.
- [67] L. Simić, S. M. Berber, and K. W. Sowerby, "Cooperative communication for energy efficient wireless sensor networks," in *4G Mobile & Wireless Communications Technologies*, S. Kyriazakos, I. Soldatos, and G. Karetsos, Eds. Aalborg: River Publishers, 2008, pp. 97–108.
- [68] ———, "Extending the lifetime of wireless sensor networks via cooperative communication," in *Proc. 19th Virginia Tech Symposium on Wireless Personal Communications*, Blacksburg, 2009.
- [69] A. L. Edwards, *An Introduction to Linear Regression and Correlation*, 2nd ed. New York: W. H. Freeman and Company, 1984.

-
- [70] Q. Dong, "Maximizing system lifetime in wireless sensor networks," in *Proc. 4th International Symposium on Information Processing in Sensor Networks (IPSN '05)*, Los Angeles, 2005.